Development and application of single cell biosensors for the improvement of amino acid production in *Escherichia coli* and *Corynebacterium glutamicum*

Inaugural Dissertation

for the attainment of the title of doctor
in the Faculty of Mathematics and Natural Sciences
at the Heinrich-Heine-Universität Düsseldorf

presented by

Regina Irmgard Mahr

born in Lichtenfels

Jülich, Januar 2016

The thesis in hand has been performed at the Institute of Bio- and Geosciences, IBG-1: Biotechnology, Forschungszentrum Jülich, from November 2012 until January 2016 under the supervision of Juniorprof. Dr. Julia Frunzke.

Published by permission of the Faculty of Mathematics and Natural Sciences of the Heinrich-Heine-Universität Düsseldorf

Supervisor: Juniorprof. Dr. Julia Frunzke

Institute of Bio- and Geosciences, IBG-1: Biotechnology

Population heterogeneity and signal transduction group

Research Center Jülich GmbH

Co-supervisor: Prof. Dr. Johannes Hegemann

Institute for the functional genome research of microorganisms

Heinrich-Heine Universität Düsseldorf

Date of oral examination: 21.03.2016

Bekomme Augen für das Kleine das Dein Fuß so arglos zertreten kann.

Den Wundern begegne, wo sie sich im Alltäglichen verstecken.

Freue Dich an den Kleinigkeiten, die Dir jeden Tag zuwachsen.

Results described in this dissertation have been published in the following articles

Mustafi N., Grünberger A., **Mahr R.**, Helfrich S., Nöh K., Blombach B., Kohlheyer D., Frunzke J. (2014) Application of a genetically encoded biosensor for live cell imaging of L-valine production in pyruvate dehydrogenase complex-deficient *Corynebacterium glutamicum* strains. PLoS ONE 9(1): e85731.

Mahr R., Gätgens C., Gätgens J., Polen T., Kalinowski J., Frunzke J. (2015) Biosensor-driven adaptive laboratory evolution of L-valine production in *Corynebacterium glutamicum.* Metab Eng 32: 184-194.

Mahr R., Gätgens C., Frunzke J. Urease inactivity increases L-valine production in *Corynebacterium glutamicum*. ***To be submitted***

Mahr R., Freiherr von Boeselager, R., Wiechert J., Frunzke J. Screening of an *Escherichia coli* promoter library for a phenylalanine biosensor. ***Submitted to Appl Microbiol Biotechnol***

Mahr R., Frunzke J. (2016) Transcription factor-based biosensors in biotechnology: current state and future prospects. Appl Microbiol Biotechnol. 100(1): 79-90.

Mahr R., Frunzke J. (2013) Transkriptionsregulatoren im Dienste der Biotechnologie. BioSpektrum 07.13: 739-741.

CONTENT

Abbreviations

2D	Two dimensional
AFP	Auto-fluorescent protein
AHAIR	Acetohydroxy acid isomeroreductase
AHAS	Acetohydroxy acid synthase
AK	Acetate kinase
ALE	Adaptive laboratory evolution
ARTP	Atmospheric and room temperature plasma
ATCC	American Type Culture Collection
B. subtilis	*Bacillus subtilis*
BHI(S)	Brain Heart Infusion (+Sorbitol)
C. glutamicum	*Corynebacterium glutamicum*
cDNA	Complementary DNA
CDW	Cell dry weight
CFP	Cyan fluorescent protein
CO_2	Carbon dioxide
CoA	Coenzyme A
CRISPR	Clustered regularly interspaced short palindromic repeats
DAHP	3-deoxy-D-arabinoheptulosonate 7-phosphate
DHAD	Dihydroxy acid dehydratase
DNA	Deoxyribonucleic acid
E. coli	*Escherichia coli*
e.g.	*exempli gratia*
Ery-4-P	Erythrose-4-phosphate
EPSP	5-enolpyruvylshikimate 3-phosphate
et al.	*et alii*
etc.	*et cetera*
eYFP	Enhanced yellow fluorescent protein
FACS	Fluorescence-activated cell sorting
FC	Flow cytometry
FbFP	FMN-based fluorescent protein
FMN	Flavin mononucleotide
FRET	Förster resonance energy transfer
FREP	Feedback-regulated evolution of phenotype
FSC	Forward-scatter characteristics
GC-ToF-MS	Gas chromatography Time-of-flight mass spectrometry
GFP	Green fluorescent protein
GFPmut2	Green fluorescent protein mut2
HCO_3^-	Hydrogen carbonate
HT	High-throughput
(u)HPLC	(ultra-)high performance liquid chromatography
K_d	Rate constant for complex dissociation
LB	Lysogeny broth
LOV-domain	Light oxygen voltage-domain
Lrp	Leucine-responsive protein
MAGE	Multiplex-automated genome engineering
MNNG	N-methyl-N'-nitro-N-nitrosoguanidine
NADPH	Nicotinamide adenine dinucleotide phosphate
NGS	Next generation sequencing
OD_{600}	Optical density at 600 nm
PCR	Polymerase chain reaction
PCx	Pyruvate carboxylase
PEP	Phosphoenolpyruvate
PEPCx	Phosphoenolpyruvate carboxylase
PDHC	Pyruvate dehydrogenase complex
PK	Pyruvate kinase
PQO	Pyruvate:quinone oxidoreductase
PPP	Pentose phosphate pathway
PTA	Phosphotransacetylase
PTS	Phosphoenolpyruvate:sugar phosphotransferase system
RBS	Ribosome binding site
(m)RNA	(messenger) Ribonucleic acid
RNA-seq	RNA sequencing
S. cerevisiae	*Saccharomyces cerevisiae*
SELEX	Systemic evolution of ligands by exponential enrichment
SNPs	Small nucleotide polymorphisms
SSC	Side-scatter characteristics
TA	transaminase
TCA	Tricarboxylic acid cycle
TF	Transcription factor
TR	Transcriptional regulator
US$	United States dollar
UV	Ultraviolet
v/v	Volume per volume
WT	Wild-type
w/v	Weight per volume
YFP	Yellow fluorescent protein
$Y_{P/S}$	Substrate-specific product yield
$Y_{P/X}$	Biomass-specific product yield

Further abbreviations not included in this section are according to international standards, as for example listed in the author guidelines of the *FEBS Journal*.

1 SUMMARY

1.1 English Summary

In the last decade, the application of genetically-encoded biosensors proved successful to establish novel and elaborated strategies for engineering microbial cell factories by enlarging the repertoire of metabolic engineering tools and by enabling unprecedented insights into bioprocesses at single-cell resolution. Especially, biosensors based on bacterial transcriptional regulators translating intracellular metabolite concentration into a measureable output proved to be of high value for a variety of metabolic engineering approaches.

Although nature provides a plethora of transcriptional regulators to sense intrinsic and extrinsic stimuli, only a few regulators and their respective target promoters have been well characterized to date. This hampers the prompt decision for suitable sensor candidates. To this end, an elaborated FACS (fluorescence-activated cell sorting)-based strategy was developed for the rapid identification of effector-responsive promoters as suitable parts for biosensor design. Basically, a library of *Escherichia coli* promoter-auto-fluorescent protein fusions was screened by toggled rounds of positive and negative selection. This approach led to the isolation of the L-phenylalanine-responsive *mtr* promoter. The construction of different biosensors based on the *mtr* promoter revealed a significant influence of the sensor's architecture on the dynamic range and the sensitivity towards effector molecules. Additionally, the *mtr* biosensor was successfully applied to screen a mutant library of *E. coli* cells for cells with increased L-phenylalanine productivity.

Adaptive laboratory evolution (ALE) has widely been applied to adapt microbes to environmental stress or to improve metabolite production. So far, however, the strategy was only applicable to fitness-linked phenotypes. To this end, we established biosensor-driven adaptive laboratory evolution to evolve inconspicuous product formation. Sensor cells with the highest fluorescent output and hence, increased metabolite production, were iteratively isolated by FACS and re-cultivated. This strategy was successfully applied to the pyruvate-dehydrogenase deficient L-valine producer strain *Corynebacterium glutamicum* Δ*aceE* using the Lrp biosensor, which was developed for the detection of branched-chain amino acids and methionine. Evolved clones featured about 25% increased production and 3-4-fold reduced by-product formation. By genome sequencing and the subsequent evaluation of single mutations in the cured Δ*aceE* background, decreased L-alanine production was attributed to a mutation in the global regulator GlxR. Interestingly, a loss-of-function mutation in the urease accessory protein UreD resulted in about 100% increased L-valine formation in CGXII minimal medium. Further studies demonstrated that urea as part of the cultivation medium imposes a central bottleneck for efficient L-valine production: Urea degradation increases the pH by ammonia release, thereby interfering with growth and L-valine production. Likewise, carbon dioxide formation stimulates anaplerosis leading to a reduced pyruvate pool – the precursor for L-valine production.

Altogether, these studies emphasize biosensors as valuable and versatile tools to improve metabolic cell factories with an enormous potential for future applications.

1.2 German Summary

Im letzten Jahrzehnt hat sich die Anwendung genetisch-kodierter Sensoren als erfolgreich erwiesen, um neue und effiziente Strategien für die Entwicklung mikrobieller Zellfabriken zu etablieren. Biosensoren vergrößern zum einen das Repertoire an Werkzeugen für die Stammentwicklung und ermöglichen zum anderen neuartige Einblicke in Bioprozesse auf Einzelzellebene. Vor allem Biosensoren, die auf bakteriellen Transkriptionsregulatoren basieren und so die intrazelluläre Metabolitkonzentration in ein messbares Signal übersetzen, spielen aufgrund ihrer vielseitigen Einsatzmöglichkeiten eine große Rolle im Metabolic Engineering Bereich.

Obwohl die Natur eine große Anzahl an Transkriptionsregulatoren hervorgebracht hat, damit Zellen intrinsische und extrinsische Signale wahrzunehmen können, gibt es bis heute nur wenige gut untersuchte Regulatoren und entsprechende Zielpromotoren. Dies beeinträchtigt allerdings eine schnelle Identifizierung neuer Sensorkandidaten. Zu diesem Zweck wurde eine Methode entwickelt, welche auf der Fluoreszenz-aktivierten Zellsortierung (FACS) basiert und deren Ziel es ist, schnell neue Promotoren, die durch bestimmte Effektoren aktiviert werden, zu identifizieren, um somit neue und geeignete Bausteine für die Sensorentwicklung zu gewinnen. Das Grundprinzip besteht darin aus einer *Escherichia coli* Promoter-Sammlung (Promotoren fusioniert an ein autofluoreszierendes Protein) diejenigen Promotoren durch abwechselnde Runden positiver und negativer Selektion anzureichern, die durch Effektoren aktiviert werden können. Dieser Ansatz führte zur Isolierung des *mtr* Promoters, der durch Phenylalanin aktiviert wird. Die Evaluierung unterschiedlicher *mtr*-basierter Biosensoren ergab, dass die Sensorarchitektur einen signifikanten Einfluss auf den dynamischen Bereich und die Effektormolekül-Sensitivität hat. Zudem wurden mit Hilfe des *mtr* Biosensors erfolgreich Zellen mit erhöhter intrazellulärer Phenylalaninkonzentration mittels FACS aus eine *E. coli* Mutantenbibliothek isoliert.

Im Labor durchgeführte adaptive Evolutionsstrategien werden vielseitig angewendet, um Mikroben an Umweltstress anzupassen oder um deren Produktion zu verbessern. Bisher war diese Strategie jedoch nur für phänotypische Merkmale geeignet, die direkt an die Fitness des Organismus gekoppelt sind. Deshalb haben wir eine Sensor-gesteuerte adaptive Evolutionsmethode entwickelt, um die Produktion unscheinbarer Metabolite zu verbessern. Sensorzellen mit dem höchsten Fluoreszenzsignal, was gleichzeitig auf eine erhöhte Metabolit-Produktion hindeutet, wurden mehrmals mittels FACS isoliert und kultiviert. Diese Methode wurde erfolgreich am Beispiel des Pyruvat-Dehydrogenase-Komplex-defizienten Valin-Produktionsstammes *Corynebacterium glutamicum* Δ*aceE* etabliert. Hier wurde der Lrp Biosensor verwendet, der für die Detektion von verzweigtkettigen Aminosäuren und Methionine entwickelt wurde. Evolvierte Klone zeigten eine um 25% erhöhte Valin-Produktion und gleichzeitige eine drei- bis vierfach reduzierte Nebenproduktbildung. Durch Genomsequenzierung und anschließender Evaluierung von einzelnen Mutationen im nicht-evolvierten Δ*aceE* Stamm wurde gezeigt, dass eine Mutation im globalen Regulator GlxR zu einer verringerten Alanin-Produktion führt. Interessanterweise führte der mutationsbedingte Funktionsverlust des Urease akzessorischen Proteins UreD bei Kultivierung im CGXII Minimalmedium zu einer um 100% erhöhten Valin-Bildung. Weitere Experimente zeigten, dass Harnstoff als Bestandteil des Mediums ein zentrales Problem für eine effiziente Valin-Produktion darstellt: Durch den Abbau von Harnstoff zu Ammonium steigt der pH-Wert, was das Wachstum positiv, aber die Produktion negativ beeinflusst. Ebenso zeigte sich, dass die Bildung von Kohlenstoffdioxid die Anaplerose stimuliert, was zu einer reduzierten Pyruvat-Konzentration als Vorstufe der Valin-Biosynthese führt.

Zusammenfassend haben die durchgeführten Experimente gezeigt, dass die Produktion von Zellfabriken durch den geschickten und vielseitigen Einsatz von Biosensoren verbessert werden kann. Darüber hinaus bieten Sensoren ein enormes Potential für zukünftige Anwendungen.

2 INTRODUCTION

2.1 Microbial cell factories – towards a sustainable bioeconomy

Since Neolithic times, humans have used microbial fermentation for feed and food refinement (Erickson et al., 2012). The awareness of limited fossil resources, untamable industrial waste streams and the climate change are currently driving the efforts for the establishment of a sustainable bioeconomy. Engineering of microorganisms for the production of value-added compounds from renewable feedstocks is one key for the transition from a currently petroleum-dependent and energy-intensive chemical industry towards a sustainable bioeconomy (Becker and Wittmann, 2015; Erickson et al., 2012; Wieschalka et al., 2013). In the last decades, microbial processes have been established to build chemical units for the production of a broad range of products including solvents, polymers, nutrients, biofuels, bioenergy, flavors and pharmaceuticals (Becker and Wittmann, 2015; Woolston et al., 2013). Especially, the market for animal feed products has enormously increased. For 2020, the World Economic Forum expects a market size of about US$95 billion for products generated by microbial fermentation (Erickson et al., 2012).

Nature has equipped organisms with a plethora of pathways, metabolic reactions and enzymes to catalyze the transition of basic carbon sources to complex, high valuable molecules. Superior to chemical synthesis, microbial biosynthesis benefits here from chemo-, stereo- and regioselectivity of enzymatic reactions, which reduces energy and costs for the intensive purification of the desired, enantiopure products (Becker and Wittmann, 2015; Erickson et al., 2012). *Escherichia coli* (Chen et al., 2013; Wendisch et al., 2006), *Corynebacterium glutamicum* (Eggeling and Bott, 2015; Heider and Wendisch, 2015; Wieschalka et al., 2013) and *Saccharomyces cerevisiae* (Liu et al., 2013; Nielsen et al., 2013) are traditionally the most important workhorses. The deep knowledge of their physiology, aerobic as well as anaerobic growth, the availability of a variety of molecular tools and their broad range of metabolic products are of great benefit for metabolic engineering purposes (Becker and Wittmann, 2015; Woo and Park, 2014).

In the last decade, next generation sequencing (NGS) techniques, which deliver the detailed knowledge of the genetic code in short time and allow in turn for the precise manipulation of the genome, revolutionized the field of metabolic engineering. The combination of recombinant

DNA technologies, systems and synthetic engineering approaches contributed to this success e.g. by allowing for the establishment and transfer of artificial or heterologous pathways in production hosts. A broad range of metabolic engineering techniques will be discussed in chapter 2.3 ("Metabolic engineering of microbial cell factories"). The developments of the last decades have pushed the transition from an energy-intensive and fossil oil-dependent chemical industry to a sustainable bioeconomy based on renewable resources. Now, the challenge is to engineer efficient microbial cell factories, which are economically competitive to traditional production processes (Becker and Wittmann, 2015; Erickson et al., 2012).

2.2 Amino acid production using microorganisms

Amino acids represent essential building blocks for the synthesis of proteins and diverse metabolic intermediates (Mitsuhashi, 2014). For commercial applications, the biotechnological production of amino acids nowadays superseded the extraction from protein hydrolysates, which was not efficient enough for large-scale production (Leuchtenberger et al., 2005). In addition, microbial amino acid biosynthesis provides the great advantage of forming the bioactive L-enantiomer (except for the non-chiral glycine and methionine) in contrast to chemical synthesis (Becker and Wittmann, 2012; Bolten et al., 2010). The global amino acid market faces currently an annual microbial production volume of more than 5,000,000 tons (Eggeling and Bott, 2015; Wendisch, 2014). The main drivers are L-glutamate and the animal feed additives L-lysine, L-threonine, L-phenylalanine and D-/L-methionine expecting a market size of US$20.4 billion by 2020 (Global Industry Analysts Inc, 2015). Due to the lack of the respective biosynthesis pathways in humans and animals, all nine essential amino acids (L-histidine, L-isoleucine, L-leucine, L-lysine, L-methionine, L-phenylalanine, L-threonine, L-tryptophan and L-valine) are of high interest for the establishment of microbial production processes (Becker and Wittmann, 2012; Leuchtenberger et al., 2005).

C. glutamicum and *E. coli* are the main platform organisms for the production of amino acids (Becker and Wittmann, 2012; Becker and Wittmann, 2015; Eggeling and Bott, 2015; Leuchtenberger et al., 2005; Mitsuhashi, 2014; Wendisch, 2014). However, both organisms reveal pros and cons for the production of specific amino acids: Although *E. coli* features a higher theoretical yield for methionine biosynthesis, for example, *C. glutamicum* uses a less complex regulatory control for the production of the same amino acid (Krömer et al., 2006; Mitsuhashi, 2014; Tosaka and Takanami, 1986). Furthermore, *C. glutamicum* can utilize several

carbon sources at the same time, while *E. coli* features sequential carbon utilization leading to diauxic growth phenotypes (Wendisch, 2014). In the following, recent efforts for microbial L-phenylalanine production by *E. coli* and L-valine production by *C. glutamicum* are presented in more detail.

Table 2.2: Selected *C. glutamicum* and *E. coli* strains engineered for L-phenylalanine or L-valine production.

Strains	Genotype	Titer ($g\ L^{-1}$)	Comments	References
L-phenylalanine				
E. coli	Not indicated in detail	50.0	Fed batch fermentation on glucose	(Backman et al., 1990)
E. coli F-4/pF81	LJ110 Δ(*pheA tyrA aroF*), pJF119EH $aroF^{wt}$ $pheA^{fbr}$ $aroB^{wt}$ $aroL^{wt}$	38.0	50 $g\ L^{-1}$ during in situ product recovery (ISPR)	(Rüffer et al., 2004)
C. glutamicum	KY10865, pKY1 ($aroII^{fbr}$, csm^{fbr}), pKF1 ($aroII^{fbr}$, csm^{fbr}, $pheA^{fbr}$)	28.0	Jar fermentation on sucrose	(Ikeda and Katsumata, 1992)
E. coli FUS4.11_{kan}	W3110 Δ(*pheA tyrA aroF*), Δ*lacIZYA*::P_{tac}- *aroFBL*, *pykA*::FRT, *pykF*::FRT-Kan-FRT	13.4	Fed batch fermentation on glycerol and ammonia	(Weiner et al., 2014a)
L-valine				
C. glutamicum	ATCC13032 Δ*aceE*, pJC4-*ilvBNCE*	22.8	Fed batch fermentation on glucose and acetate	(Blombach et al., 2007)
C. glutamicum	ATCC13032 Δ*aceE*, Δ*pyc,* Δ*pgi*, pJC4-*ilvBNCE*	48.3	Fed batch fermentation on glucose and acetate	(Blombach et al., 2008)
C. glutamicum	ATCC13032*, aceE* A16, Δ*pqo*, Δ*ppc,* pJC4-*ilvBNCE*	83.6	Fed batch fermentation on glucose	(Buchholz et al., 2013)
C. glutamicum	ATCC13869, Δ*aceE*, Δ*alaT*, Δ*ilvA*, pJYW-4-$ilvBNC_1$-lrp_1-*brnFE*	51.0	Fed batch fermentation on glucose	(Chen et al., 2015)
E. coli	W, Δ*lacI*, Δ*ilvA*, pKBR$ilvBN^{mut}CED$, pTrc184*ygaZHlrp*	60.7	Fed batch fermentation on glucose	(Park et al., 2011)

2.2.1 L-phenylalanine production in *Escherichia coli*

Metabolic engineering of L-phenylalanine production in *E. coli* has been promoted for many years reaching final titers of up to 50 $g\ L^{-1}$ during growth on glucose (Backman et al., 1990; Rüffer et al., 2004) and 13.4 $g\ L^{-1}$ during growth on glycerol (Weiner et al., 2014a) (Tab. 2.2).

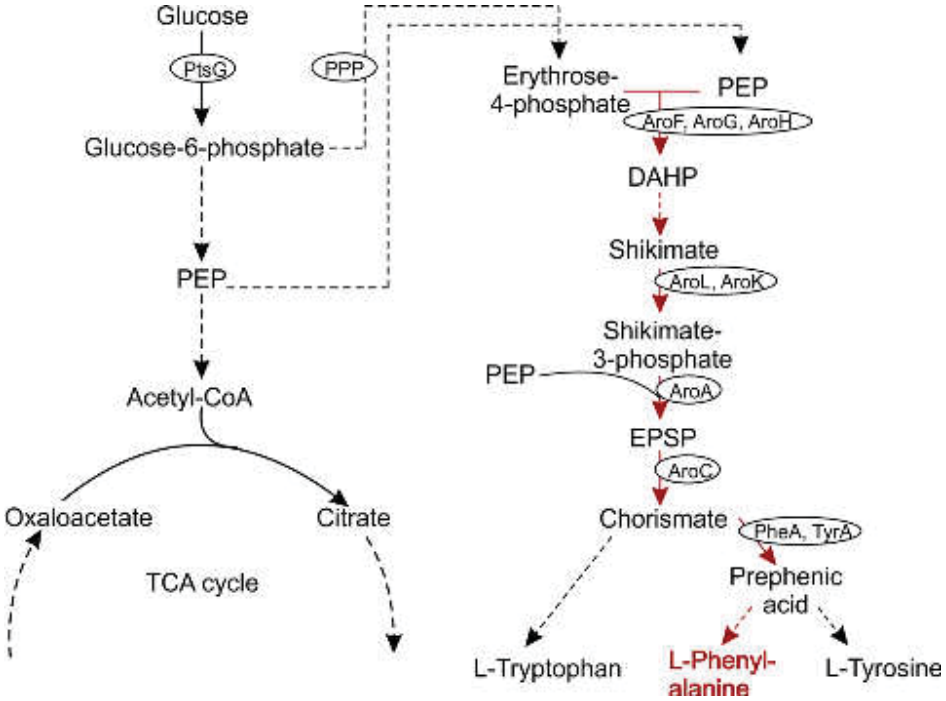

Fig. 2.2.1 Schematic of the biosynthesis of L-phenylalanine by *E. coli*. The precursors phosphoenolpyruvate (PEP) and erythrose-4-phosphate (Ery-4-P) for the general biosynthesis of aromatic amino acids are provided directly by glycolysis or *via* the pentose phosphate pathway (PPP). PEP and Ery-4-P are condensed to 3-deoxy-D-arabino-heptulosonate 7-phosphate (DAHP) by one of the three DAHP synthases AroF, AroG or AroH, which indicates the start point of the shikimate pathway. *Via* several enzymatic steps, the formation of chorismate is catalyzed, which is the shared precursor of all three aromatic amino acids. L-phenylalanine is produced from chorismate via prephenic acid catalyzed by prephenate dehydratase. Abbreviations: tricarboxylic acid cycle (TCA), 5-enolpyruvoylshikimate 3-phosphate (EPSP). Dashed lines indicate the existence of intermediate steps that are not depicted in the figure.

Besides its important role as precursor for the artificial sweetener aspartame or as building block for pharmaceutical products (Sprenger, 2006; Sprenger, 2007), L-phenylalanine became likewise interesting as precursor for various aromatic compounds including pinosylvin, cinnamic and *p*-hydroxycinnamic acid used as flavor enhancer or ingredients of cosmetics (Sariaslani, 2007; van Summeren-Wesenhagen and Marienhagen, 2015; Vargas-Tah et al., 2015). For engineering an efficient L-phenylalanine microbial cell factory, *E. coli* was used as primary workhorse due to its rapid growth, the availability of genetic engineering tools and the well-studied biosynthetic pathway (Backman et al., 1990; Pittard et al., 2005). Recently, efforts were also taken in *C. glutamicum* to push L-phenylalanine production (Zhang et al., 2014a; Zhang et al., 2015a; Zhang et al., 2013). Both organisms produce aromatic amino acids via the shikimate pathway

(Fig. 2.2.1), however, with differences in some involved enzymes (Sprenger, 2006). Key targets during engineering of *E. coli* strains for L-phenylalanine production are i) the generation of feedback-insensitive versions of the 3-deoxy-D-arabino-heptulosonate 7-phosphate (DAHP) synthases AroF, AroG, AroH and chorismate mutase/prephenate dehydratase PheA, ii) the improvement of the supply with the precursors phosphoenolpyruvate (PEP) and erythrose-4-phosphate, and iii) the overproduction of enzymes catalyzing rate limiting steps like the shikimate synthase AroL (Bongaerts et al., 2001; Ikeda, 2006; Sprenger, 2007). Although high L-phenylalanine titers have already been reached during growth on glucose, alternative carbon sources are in demand. For example, glycerol as by-product of biodiesel production may reduce costs and meets the requirements of a sustainable bioeconomy (Weiner et al., 2014a). The negative impact on growth upon high L-phenylalanine concentrations, the delivery of precursors or the central metabolism are still bottlenecks, which need to be addressed during engineering of production strains (Polen et al., 2005; Weiner et al., 2014b).

2.2.2 L-valine production in *Corynebacterium glutamicum*

The biosynthesis pathway of L-valine branches from the glycolytic product pyruvate (Fig. 2.2.2). Hence, the pivotal points for increased L-valine production are the availability of the precursor pyruvate and the overproduction of the L-valine biosynthesis pathway, which have been addressed during engineering L-valine producer strains (Tab. 2.2). To reach high concentrations of pyruvate in *C. glutamicum*, the deletion of *aceE* encoding the E1p subunit of the pyruvate dehydrogenase complex (PDHC) became a central target to inhibit the degradation of pyruvate to acetyl-CoA (Blombach et al., 2007; Schreiner et al., 2005). The drawback of these strains, however, is the growth-decoupled production phenotype. Due to the deficiency of PDHC activity, acetate has to be added to the medium to maintain the acetyl-CoA level for fueling the tricarboxylic acid (TCA) cycle for growth. The presence of acetate, however, abolishes phosphoenolpyruvate:sugar phosphotransferase system (PTS)-mediated glucose uptake via the regulator *sugR* required for L-valine production (Blombach et al., 2009; Engels and Wendisch, 2007). Upon depletion of acetate, L-valine is produced. During fed-batch fermentation, the Δ*aceE* strain produced up to 22.8 g L^{-1} L-valine ($Y_{P/S}$ 0.39 mol L-valine per mol glucose) (Blombach et al., 2007). Based on this strain, the deletion of the pyruvate:quinone oxidoreductase (Δ*pqo*), which inhibits the degradation of pyruvate to acetate, and the deletion of the phosphoglucose isomerase (Δ*pgi*), which pushes carbon flux through the pentose-phosphate

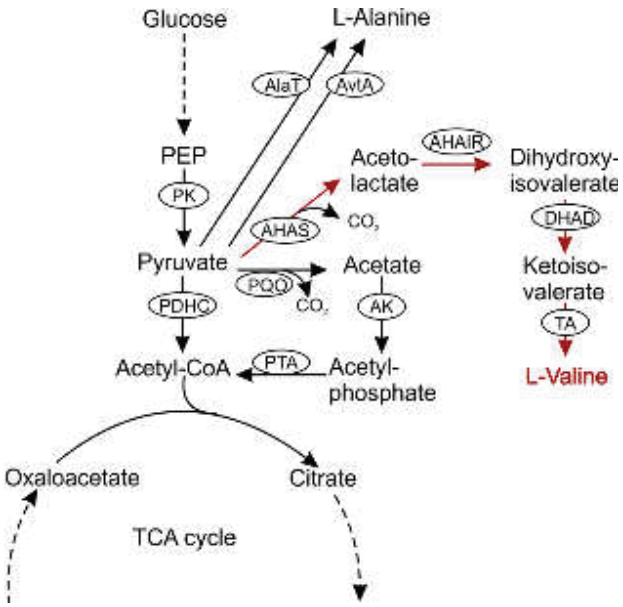

Fig. 2.2.2 Schematic of the biosynthesis of L-valine in *C. glutamicum*. The biosynthesis pathway branches from pyruvate *via* enzymatic steps catalyzed by acetohydroxy acid synthase (AHAS), acetohydroxy acid isomeroreductase (AHAIR), dihydroxy acid dehydratase (DHAD) and transaminase B (TA). Abbreviations: acetate kinase (AK), alanine aminotransferase (AlaT and AvtA), pyruvate dehydrogenase complex (PDHC), pyruvate kinase (PK), phosphoenolpyruvate (PEP), pyruvate:quinone oxidoreductase (PQO), phosphotransacetylase (PTA).

pathway (PPP) to enhance the NADPH availability, resulted in final L-valine titers of up to 48.3 g L^{-1} ($Y_{P/S}$ 0.75 mol L-valine per mol glucose). The additional deletion of the pyruvate carboxylase (*pyc*) preventing the efflux of the precursor pyruvate into the TCA cycle via anaplerosis further enhanced $Y_{P/S}$ to 0.86 mol L-valine per mol glucose (Blombach et al., 2008; Eikmanns and Blombach, 2014). For large-scale industrial production, however, growth-decoupled and auxotrophic phenotypes as well as the cultivation on two carbon sources are costly and laborious. To this end, Buchholz and co-workers reduced the expression of *aceE* by promoter engineering, which allows growth on glucose as single carbon source and resulted in a final L-valine titer of 83.6 g L^{-1} (Buchholz et al., 2013). Alternative approaches for increasing L-valine production relied on i) the additional deletion of by-product synthesis routes (e.g. L-alanine and L-isoleucine), ii) the overexpression of the branched-chain amino acid exporter BrnFE and the transcriptional regulator Lrp or iii) on the inactivation of D-pantothenate synthesis to limit CoA availability for PDHC activity (Chen et al., 2015; Radmacher et al., 2002). Biomass formation, NADPH availability, improved bioprocesses or alternative carbon sources provide certainly targets for increasing L-valine production.

2.3 Metabolic engineering of microbial factories

Microbes are equipped with a plethora of enzymes and metabolic pathways, which enable the conversion of simple carbon sources into highly complex, value-added compounds (Becker and Wittmann, 2015). The natural metabolic activity, however, is stringently controlled and reduced to a minimal level primarily aiming for proliferation and maintenance. For this reason, the

metabolic flux towards product formation is traditionally not maximized to save resources and energy. Although microbial refinement of food and drinks unconsciously accompanied mankind for several thousands of years, the awareness that living organisms are responsible for e.g. lactic acid fermentation discovered by Pasteur in 1857 (Pasteur, 1857), ushered the era of targeted microbial applications.

The first techniques to engineer microbes incorporated the iterative exposition to chemical mutagens or ultraviolet (UV) radiation, which generated random mutations throughout the entire genome (Benigni et al., 1992; Ghribi et al., 2004; Harper and Lee, 2012; Hughes et al., 2012). These mutant libraries were screened for clones with the desired phenotype (Ghribi et al., 2004; Ohnishi et al., 2008). Throughout iterative rounds of mutagenesis, however, several thousand mutations accumulated in the genome including beneficial, non-profitable and silent mutations. Although the resulting strains produced increased amounts of the particular target metabolites, the numerous mutations significantly affected the fitness of the cells, which led to slow growth, low stress tolerance and decreased robustness during bioprocesses (Becker and Wittmann, 2015).

During the last two decades, the increasing knowledge of bacterial physiology, the availability of sequence data as well as the development of recombinant DNA technologies has enabled the targeted deletion and overexpression of endogenous genes as well as the introduction of heterologous sequences (Erickson et al., 2012; Heider and Wendisch, 2015; Wendisch, 2014; Woolston et al., 2013). This rational design concept realizes the local engineering of metabolic pathways with a defined genetic background. Nevertheless, the comprehensive engineering of the complex network of metabolic interactions including efficient co-factor and energy supply as well as potential metabolic bottlenecks requires a deeper knowledge of the microbial physiology (Becker and Wittmann, 2015). Here, systemic analysis provides a novel global and quantitative insight into the microbial cell. Comprehensive *Omics* datasets including valuable quantitative information on genes (genomics), transcripts (transcriptomics), proteins (proteomics), metabolites (metabolomics) and pathway fluxes (fluxomics) provide a powerful basis for the development of mechanisms to control dynamic gene expression, to identify metabolic bottlenecks or to redirect metabolic fluxes (Becker and Wittmann, 2015; Furusawa et al., 2013; Petzold et al., 2015; Woolston et al., 2013). These strategies allow for the system-wide engineering of microbial cell factories. Based on data of *multiomic* platforms, *in silico* models can be derived supporting the simulation of optimal metabolic fluxes through pathways for high yields – which is, however,

still in the early stages of development (Becker and Wittmann, 2015; Kim et al., 2015; Wiechert and Noack, 2011).

Synthetic biology incorporates the full spectrum of genetic engineering possibilities to design cell factories with novel features that have never existed before (Church et al., 2014; Way et al., 2014). Novel synthetic strategies can accelerate the development and commercialization of microbial cell factories by overcoming natural barriers such as gene expression noise, metabolic by-products, crosstalk or broad enzyme activities (Church et al., 2014; Erickson et al., 2012). To this end, a broad range of innovative tools has been developed including CRISPR-Cas9 mediated genome editing and multiplex-automated genome engineering (MAGE) of natural and artificial genomes (Bonde et al., 2014; Jakociunas et al., 2015; Li et al., 2015; Liu and Jiang, 2015; Ronda et al., 2015; Wang et al., 2009), oscillators and genetic switches for the dynamic regulation of gene expression cascades (Church et al., 2014; Liu et al., 2015b; Zhang et al., 2012), optogenetic tools (Binder et al., 2014; Möglich and Hegemann, 2013), and non-invasive quantification of intracellular activities e.g. by biosensors based on native or synthetic transcriptional regulators (Chou and Keasling, 2013; Mahr and Frunzke, 2016; Ng et al., 2015; Tang et al., 2008; Woo and Park, 2014).

Although systemic analysis provides a global and comprehensive view of the metabolic landscape, the high complexity of carbon and energy fluxes has nowadays not been completely understood. There are still many obscured factors including unknown gene activities, regulatory mechanisms or detailed knowledge of certain metabolic pathways. During the last years, adaptive laboratory evolution approaches driven by mutation and selection have drawn the attention for engineering biotechnological interesting strains (Abatemarco et al., 2013; Portnoy et al., 2011; Schmidt-Dannert and Arnold, 1999): By iteratively exposing industrial producer strains to sequentially increasing levels of environmental stress, microbial strains were adapted to e.g. oxidative or thermal stress (Lee et al., 2013; Oide et al., 2015; Sandberg et al., 2014; Tenaillon et al., 2012). Further approaches aimed to improve product formation (Mahr et al., 2015; Raman et al., 2014; Reyes et al., 2014; Xie et al., 2015) or the tolerance towards solvents (Atsumi et al., 2010; Lee et al., 2011; Oide et al., 2015). Most strategies are based on the emergence of natural mutations and the improvement of fitness-linked phenotypes, which are directly exposed to a natural selective pressure. Anyway, an adaptive laboratory evolution approach for inconspicuous

product formation not necessary linked to fitness would beneficially expand the toolbox of metabolic engineering.

Another strategy for the comprehensive engineering of microorganisms is the application of random genomic mutagenesis, which was reinvigorated by the establishment of efficient screening systems based on genetically-encoded biosensors (Delvigne et al., 2015; Dietrich et al., 2010; Eggeling et al., 2015; Mahr and Frunzke, 2016; Schallmey et al., 2014; Zhang et al., 2015b). Due to decreasing prices of genome sequencing by NGS, mutations occurring during adaptive evolution as well as during biosensor-driven selection of mutant libraries can easily be assessed by comparative sequence analysis (Becker and Wittmann, 2015; Harper et al., 2011). These strategies revealed to deliver novel, non-intuitive targets for the establishment and improvement of industrial production strains.

2.4 Genetically-encoded biosensors

Engineering microbes for large-scale production demands efficient tools for the high-throughput (HT) development of novel cell factories as well as approaches for the evaluation of the bioprocess performance. Techniques for single cell analysis, for instance, are required to discover the formation of inefficient subpopulations, which might have a negative impact on the outcome and robustness of bioprocesses (Delvigne and Goffin, 2014; Lieder et al., 2014). Moreover, the screening of vast strain libraries generated by random or transposon mutagenesis presents a HT strategy to identify novel targets for rational engineering approaches. Cases where product formation is directly linked to an easily selectable phenotype, e.g. carotenoid production (An et al., 1991; Ukibe et al., 2008), or the formation of a chromophore as consequence of an enzyme reaction may interface with the development of efficient HT approaches (Santos and Stephanopoulos, 2008). However, the majority of biotech-relevant compounds are inconspicuous small molecules, which do confer a selectable phenotype to the cell, remains laborious without an efficient HT screening tool (Dietrich et al., 2010; Mahr and Frunzke, 2016; Zhang et al., 2015b). Here, the development of genetically-encoded biosensors converting the intracellular metabolite concentration into a measureable, optical output is of high value for diverse biotechnological applications.

Organisms have evolved a broad repertoire of different mechanisms to sense and respond to environmental stimuli including stress, gases, temperature, pH, ions or the availability of

nutrients, in order to control gene expression. This spectrum of natural sensor devices comprising RNA aptamer structures in riboswitches, transcriptional regulators and enzymes provides a valuable repertoire for the construction of biosensors for intracellular metabolite detection.

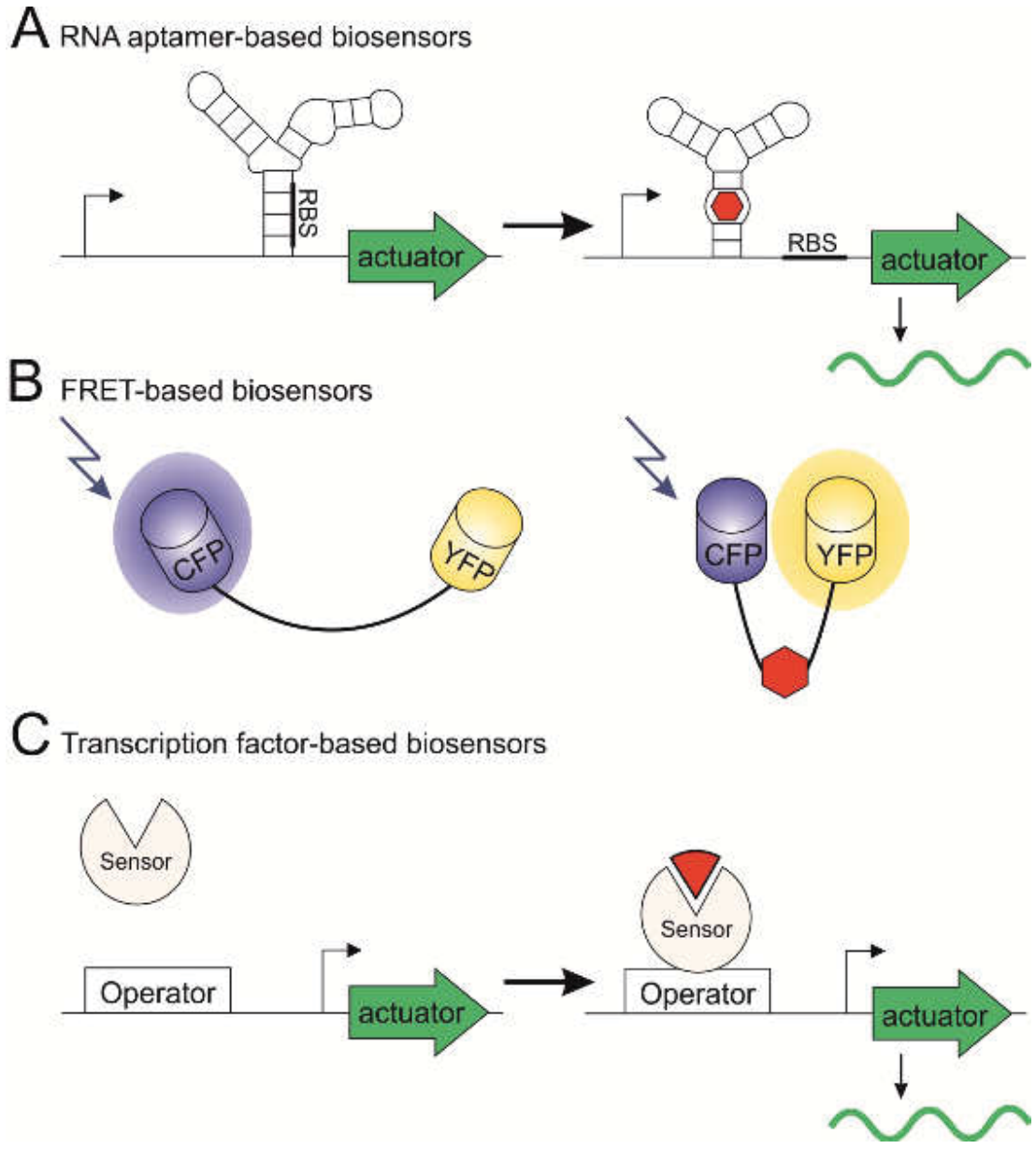

Fig. 2.4 Schematic of biosensors based on A. RNA aptamers, B. FRET and C. transcription factors. The biosensors are shown in their OFF (left) and ON state (right) upon binding of metabolites (red). Abbreviation: ribosome binding site (RBS), cyan (CFP) and yellow fluorescent protein (YFP), Förster (fluorescence) resonance energy transfer (FRET).

2.4.1 RNA aptamer-based biosensors

Riboswitches are non-translated RNA elements, which change their three-dimensional RNA aptamer structure upon binding of effector metabolites triggering the efficiency of the gene expression machinery, RNA stability or the enzymatic activity of RNA molecules – termed ribozymes (Fig. 2.4) (Aboul-Ela et al., 2015; Michener et al., 2012; Serganov and Nudler, 2013). The immense power of riboswitch structures regulating gene expression was first described for the response to thiamine pyrophosphate (Winkler et al., 2002a), flavin mononucleotide (Winkler et al., 2002b) and coenzyme B12 (Nahvi et al., 2002). Nowadays, a wide range of natural metabolite-binding RNAs were identified with the help of algorithms e.g. Riboswitch Finder (http://riboswitch.bioapps.biozentrum.uni-wuerzburg.de/server.html (Bengert and Dandekar, 2004)) or Riboswitch Explorer (http://132.248.32.45:8080/cgi-bin/ribex.cgi (Abreu-Goodger and Merino, 2005)) and archived in different databases including the Aptamer Base (http://aptamerbase.semanticscience.org/ (Cruz-Toledo et al., 2012)). Furthermore, the synthetic architecture by computational methods or methods like the SELEX (systematic evolution of ligands by exponential enrichment) *in vitro* assembly technique theoretically allows engineering of RNA aptamers for the detection of any desired metabolite (Beisel and Smolke, 2009; Ellington and Szostak, 1990). Frequently, the synthetic *in vitro* or *in silico* selection of RNA aptamers revealed rather low compatibility with *in vivo* systems (Kopniczky et al., 2015; Liang et al., 2011; Schallmey et al., 2014). Alternative approaches rely on the step-wise modification of existing RNA aptamers e.g. to alter the specificity (Mannironi et al., 2000). In the last years, RNA aptamer-based biosensors have been constructed for visualization of intracellular xanthine (Win and Smolke, 2007), for screening a library of mutated caffeine demethylases (Michener and Smolke, 2012), as Riboselector for the evolution of L-lysine or L-tryptophan production by the fusion of the RNA-aptamer to a selectable marker gene (Jang et al., 2015; Yang et al., 2013), or for the control of lysine transport in *C. glutamicum* (Zhou and Zeng, 2015). Furthermore, Paige and co-workers connected metabolite-binding aptamers to fluorophore-binding aptamers for sensing S-adenosylmethionine and adenosine 5'-diphosphate (Paige et al., 2012). Recently, this type of sensor was shown to be applicable to study metabolite dynamics at the single cell level (You et al., 2015). The great advantage of RNA-based biosensors is certainly the save of energy and resources as well as the quick response to transient changes during bacterial growth as they do not require, for instance, the pre-existence of a transcription regulator (Kopniczky et al., 2015).

2.4.2 FRET-based biosensors

Another strategy to measure intracellular molecule concentrations is based on Förster (fluorescence) resonance energy transfer (FRET) between two auto-fluorescent proteins (AFPs) (Fig. 2.4). In principle, the excitation energy of an AFP with short wavelength (FRET donor) can be transferred in a radiation-free way to an AFP of high wavelength (FRET acceptor), if both AFPs are in close proximity (<10 nm) and the excitation spectrum of the FRET acceptor overlaps with the emission spectrum of the FRET donor. Both AFPs are linked by a sensory domain, which undergoes a conformational change upon metabolite binding (Constantinou and Polizzi, 2013; Frommer et al., 2009; Michener et al., 2012; Schallmey et al., 2014). Thereupon, both AFPs change their position relatively to each other either inducing or inhibiting FRET. The ratio of the intensity of emitted fluorescence of FRET acceptor and donor even allows the quantitative estimation of the metabolite concentration, which presents one great advantage of this biosensor type (Constantinou and Polizzi, 2013; Frommer et al., 2009). During the last decade, a broad range of FRET-based biosensors has been constructed for sensing sugars (Behjousiar et al., 2012; Bermejo et al., 2011), amino acids (Behjousiar et al., 2012; Gruenwald et al., 2012; Okada et al., 2009), ions (Hessels and Merkx, 2015), redox states (Yano et al., 2010), hydrogen peroxide (Bilan et al., 2013) or oxygen (Potzkei et al., 2012). Helpful platforms for the construction of FRET sensors are the Protein Data Bank (PDB; http://www.rcsb.org/pdb/home/home.do (Berman et al., 2000)) or the FRETView software (http://turroserver.chem.columbia .edu/fretview/index.html (Stevens et al., 2007)). Although the amount of functional FRET-based biosensors promises a high success rate, the low predictability of conformational change of the sensory domain upon metabolite-binding and the resulting change of the FRET ratio render design efforts rather empirical (Constantinou and Polizzi, 2013; Frommer et al., 2009). Furthermore, the pH, ionic strength, temperature, buffer salts and other metabolites can impact the FRET ratio, which have to be considered using this sensor type for quantitative measurements (Moussa et al., 2014; Okumoto et al., 2012). In the last years, FRET-based biosensors have been used to study fundamental questions based on intracellular metabolite concentrations of mammalian, plant or microbial cells (Michener et al., 2012). In addition, they are proposed to be of high value for monitoring biotechnological processes due to their short signal response time (Constantinou and Polizzi, 2013). However, no application during HT strain development has been reported so far. Although binding affinities might be engineered, existing FRET-based

biosensors are highly sensitive and respond mainly to changes in the nM or µM scale, which render these sensors unfeasible for metabolic engineering approaches.

2.4.3 Transcription factor-based biosensors

The allosteric control of transcriptional regulators provides a highly interesting mechanism for metabolite detection, which has widely been exploited for the construction of genetically-encoded biosensors (Mahr and Frunzke, 2016; Schallmey et al., 2014; Zhang et al., 2015b). Metabolite-responsive transcription factors (TFs) change their conformation upon effector binding, which in turn leads to their attachment to the TF-binding site recruiting the RNA polymerase for transcription initiation (Fig. 2.4). Beside small molecule recognition, transcriptional regulators have also been reported to control gene expression in response to ions, physical parameters (temperature, pH), protein-protein interactions or protein modifications (Mahr and Frunzke, 2016). For microorganisms, global databases like DBD (www.transcriptionfactor.org (Wilson et al., 2008)) as well as species-specific platforms such as CMRegNet (http://www.lgcm.icb.ufmg.br/cmregnet/ (Abreu et al., 2015)) for corynebacterial and mycobacterial species exist, which summarize the broad landscape of transcriptional regulators in bacteria and contribute valuable details for the construction of TF-based biosensors (Mahr and Frunzke, 2016).

Transcriptional regulator-based biosensors were first successfully developed for the detection of toxic chemicals or ions as environmental pollutants (Fernandez-Lopez et al., 2015; Merulla et al., 2013; van der Meer and Belkin, 2010). In the last years, their broad applicability was also used to study dynamics in bacterial cells at the single cell level (Kiviet et al., 2014; Mustafi et al., 2014) or for diverse biotechnological applications (Liu et al., 2015a; Mahr and Frunzke, 2016; Schallmey et al., 2014; Zhang et al., 2015b). By linking the metabolite-responsive TF-promoter pair to an easy screenable (e.g. fluorescence) or selectable (e.g. antibiotic or auxotrophic marker) phenotype, HT strain development based on genome-wide random or transposon mutagenesis has become feasible and effective for the isolation of cells with an increased intracellular metabolite concentration. This strategy was successfully applied to improve the production of succinate (Dietrich et al., 2013), branched-chain amino acids (Mustafi et al., 2012), L-lysine (Binder et al., 2012), butanol as well as linear and branched-chain alcohols (Dietrich et al., 2013), benzoic acids (van Sint Fiet et al., 2006) or ß-ketoadipate (Dietrich et al., 2013). Furthermore, TF-based biosensors are also of high interest to screen enzyme libraries for desired characteristics

(Schendzielorz et al., 2014; Siedler et al., 2014a; Siedler et al., 2014b; Uchiyama and Miyazaki, 2010a). Applied in synthetic regulatory circuits, transcriptional regulators proved to be effective tools for the dynamical control and balance of metabolic fluxes for improved product formation. This strategy was efficiently implemented to regulate acyl-CoA and ethanol biosynthesis for the enhanced production of fatty acid ethyl ester (Zhang et al., 2012) or to improve malonyl-CoA levels for malonyl-CoA derived products (Liu et al., 2015b; Xu et al., 2014). The broad applicability of transcriptional regulator-based biosensors features the great success of these valuable sensor devices. However, the low number of well-characterized TF-promoter pairs, the low orthogonality of sensor constructs, the inappropriate characteristics of the biosensor in terms of specificity, sensitivity or dynamic range as well as the requirement to sense non-native and non-natural products requires improvement.

2.5 Aims of this work

Although nature provides a diversity of transcriptional regulator-promoter pairs available for the construction of biosensors, the identification of suitable candidates for the detection of desired metabolites often turns out to be laborious and time-consuming. For this reason, one aim of this work is the development of an efficient HT strategy to screen promoter libraries for appropriate sensor devices. Based on the Alon library, which consists of more than 2000 different *Escherichia coli* promoter-*gfpmut2* fusions and hence, readily available sensor devices, a workflow will be developed using fluorescent-activated cell sorting (FACS) to screen for galactose and L-phenylalanine-responsive promoters, which might be used for the development of biosensors. In the following, selected candidates will be chosen in order to study the influence of the biosensor architecture on the sensor's characteristics. To this end, comparative analysis of different sensor constructs will be performed. Finally, identified L-phenylalanine-responsive biosensors shall be tested for applicability during FACS HT screening of L-phenylalanine producers after random mutagenesis of *E. coli* strains.

Adaptive laboratory evolution (ALE) is an interesting opportunity for the biotechnological improvement of production strains to identify novel and non-intuitive mutations by selecting at the same time against detrimental mutations. So far, however, ALE has only been applied to easy selectable or fitness-linked phenotypes. For this reason, another aim of this work will be the establishment of a biosensor-driven adaptive evolution strategy for improving the production of metabolites not linked to a directly selectable phenotype e.g. amino acids. The novel approach

will be tested using the Lrp biosensor to improve e.g. L-valine production. By iteratively imposing an artificial selective pressure on cells with a high sensor output using FACS, clones with intracellularly increased L-valine levels shall be enriched. Evolved clones will comparatively be analyzed and mutations revealed by whole genome sequencing will then be re-introduced into the non-evolved strain to identify whether they are beneficial for L-valine production. This strategy will also be examined for the production of other biotechnological interesting metabolites.

The application of biosensors for monitoring metabolite production at the single cell level can reveal interesting dynamics as well as inefficient subpopulations. In live cell imaging studies, the Lrp biosensor will be applied to investigate single cell growth and production of *C. glutamicum* Δ*aceE*.

3 RESULTS

The overall topic of this PhD thesis was the development of transcriptional regulator-based biosensors for biotechnological interesting applications. The results were summarized in two published papers, one submitted manuscript and one manuscript that will be submitted in the near future. Furthermore, recent efforts in this research field were summarized in two scientific reviews.

In a first study, the recently developed Lrp biosensor for the visualization of intracellular methionine and branched-chain amino acids was applied to monitor single-cell metabolite production of the L-valine producer strain *C. glutamicum* Δ*aceE* and gradually engineered derivatives. The publication "Application of a genetically encoded biosensor for live cell imaging of L-valine production in pyruvate dehydrogenase complex-deficient *Corynebacterium glutamicum* strains" describes the detection of cell-to-cell variations using the Lrp biosensor, which may occur during bioprocesses. Interestingly, live cell imaging analyses in microfluidic chip devices revealed the formation of different types of non-producing cells as well as the formation of subpopulations in the presence of low amounts of complex medium compounds.

Adaptive laboratory evolution (ALE) has widely been applied to improve diverse characteristics of production strains. The publication "Biosensor-driven adaptive laboratory evolution of L-valine production in *Corynebacterium glutamicum*" describes the application of the Lrp biosensor to improve growth and L-valine production of *C. glutamicum* Δ*aceE* by iteratively cultivating and selecting cells with the highest fluorescent output using FACS. This strategy proved likewise successful to reduce by-product formation. Out of seven emerged mutations, four were reintroduced as single mutations into the non-evolved Δ*aceE* strain and were revealed to increase L-valine production or to reduce by-product formation.

During the biosensor-driven adaptive evolution, one mutation (*ureD*-E188*) arose leading to the formation of a truncated UreD protein, which was revealed to significantly increase L-valine production by about 100%. In previous studies, the lack of the essential accessory protein UreD was described to inactivate urease leading to reduced levels of the urea degradation products carbon dioxide and ammonia. The manuscript "Urease inactivity increases L-valine production in *Corynebacterium glutamicum*" presents a combination of gene deletion studies, batch fermentation with CO_2 aeration and pH shifts, as well as DNA microarray analysis, which

revealed the pH-dependency of growth and production, and the impairment of anaplerosis under reduced CO_2/HCO_3^- levels increasing the pyruvate supply for L-valine production.

The natural abundance of transcriptional regulator sensing metabolites often overwhelms the decision of suitable biosensor candidates. To this end, we developed a HT strategy for the fast and easy detection of novel sensors, which is presented in the manuscript “Screening of an *Escherichia coli* promoter library for a phenylalanine biosensor”. The approach is based on the pooled Alon library consisting of about 2000 different *E. coli* promoter-*gfpmut2* fusions and hence, readily available sensor devices. By toggled rounds of positive and negative selection using FACS, galactose and phenylalanine-responsive promoters were successfully enriched. Based on the enriched phenylalanine-responsive promoter of *mtr*, different biosensor architectures were constructed and characterized. One *mtr* biosensor was successfully applied for FACS HT screening of a randomly mutagenized *E. coli* MG1655 library for phenylalanine producing strains.

Throughout the last years, the development and application of transcription-factor-based biosensors has widely expanded for biotechnological applications. In the review “Transcription factor-based biosensors in biotechnology: current state and future prospects”, the recent process in this research field is summarized. The review provides a detailed overview of biosensors applied in biotechnological strain development and screening approaches. Furthermore, current efforts in the fields of high-throughput screening, dynamic pathway control by regulatory circuits, biosensor-driven adaptive evolution or single-cell analysis are highlighted. In addition, the review describes a broad range of recent studies, which deal with the engineering of biosensors for altered specificities and dynamic ranges, improved or reduced sensitivity as well as achieved orthogonality. Finally, the review emphasizes the integration of *Omics* and NGS techniques to expand the possibilities for biosensor development and future applications.

3.1 Application of a genetically encoded biosensor for live cell imaging of L-valine production in pyruvate dehydrogenase complex-deficient *Corynebacterium glutamicum* strains

Nurije Mustafi[1•], Alexander Grünberger[1•], Regina Mahr[1], Stefan Helfrich[1], Katharina Nöh[1], Bastian Blombach[2], Dietrich Kohlheyer[1], Julia Frunzke[1]*

[1]IBG-1: Biotechnology, Forschungszentrum Jülich, Jülich, Germany

[2]Institute of Biochemical Engineering, University of Stuttgart, Stuttgart, Germany

[•]These authors contributed equally to this work.

*Corresponding author

Name of the Journal: PLoS ONE (Public Library of Science)

Impact Factor: 3.234

Author contributions

Own contribution to the work: 10%

	Name	Contribution
Project planning	Mustafi, N.	30%
	Grünberger, A.	30%
	Nöh, K.	2%
	Blombach, B.	3%
	Kohlheyer, D.	5%
	Frunzke, J.	30%
Writing	Mustafi, N.	40%
	Grünberger, A.	25%
	Mahr, R.	5%
	Kohlheyer, D.	5%
	Frunzke, J.	25%

	Name	Experimental work	Evaluation	Preparation of figure/table
Figure 1	***Mahr, R.***	100%	100%	100%
Figure 2 (Video S1, S2)	Grünberger, A.	100%	100%	100%
Figure 3	Mustafi, N.	10%	10%	10%
	Grünberger, A.	90%	90%	90%
Figure 4	Grünberger, A.	100%	90%	70%
	Helfrich, S.	-	10%	30%
Figure 5 (Video S4)	Grünberger, A.	100%	50%	50%
	Helfrich, S.	-	50%	50%
Table 1	Mustafi, N.	-	-	100%
Figure S1 (Video S5)	Mustafi, N.	10%	-	-
	Grünberger, A.	90%	100%	100%
Figure S2	***Mahr, R.***	10%	-	-
	Grünberger, A.	90%	100%	100%
Figure S3 (Video S3)	Mustafi, N.	10%	-	-
	Grünberger, A.	90%	100%	100%

OPEN ACCESS Freely available online PLOS ONE

Application of a Genetically Encoded Biosensor for Live Cell Imaging of L-Valine Production in Pyruvate Dehydrogenase Complex-Deficient *Corynebacterium glutamicum* Strains

Nurije Mustafi[1☯], Alexander Grünberger[1☯], Regina Mahr[1], Stefan Helfrich[1], Katharina Nöh[1], Bastian Blombach[2], Dietrich Kohlheyer[1], Julia Frunzke[1*]

1 IBG-1: Biotechnology, Forschungszentrum Jülich, Jülich, Germany, **2** Institute of Biochemical Engineering, University of Stuttgart, Stuttgart, Germany

Abstract

The majority of biotechnologically relevant metabolites do not impart a conspicuous phenotype to the producing cell. Consequently, the analysis of microbial metabolite production is still dominated by bulk techniques, which may obscure significant variation at the single-cell level. In this study, we have applied the recently developed Lrp-biosensor for monitoring of amino acid production in single cells of gradually engineered L-valine producing *Corynebacterium glutamicum* strains based on the pyruvate dehydrogenase complex-deficient (PDHC) strain *C. glutamicum ΔaceE*. Online monitoring of the sensor output (eYFP fluorescence) during batch cultivation proved the sensor's suitability for visualizing different production levels. In the following, we conducted live cell imaging studies on *C. glutamicum* sensor strains using microfluidic chip devices. As expected, the sensor output was higher in microcolonies of high-yield producers in comparison to the basic strain *C. glutamicum ΔaceE*. Microfluidic cultivation in minimal medium revealed a typical Gaussian distribution of single cell fluorescence during the production phase. Remarkably, low amounts of complex nutrients completely changed the observed phenotypic pattern of all strains, resulting in a phenotypic split of the population. Whereas some cells stopped growing and initiated L-valine production, others continued to grow or showed a delayed transition to production. Depending on the cultivation conditions, a considerable fraction of non-fluorescent cells was observed, suggesting a loss of metabolic activity. These studies demonstrate that genetically encoded biosensors are a valuable tool for monitoring single cell productivity and to study the phenotypic pattern of microbial production strains.

Citation: Mustafi N, Grünberger A, Mahr R, Helfrich S, Nöh K, et al. (2014) Application of a Genetically Encoded Biosensor for Live Cell Imaging of L-Valine Production in Pyruvate Dehydrogenase Complex-Deficient *Corynebacterium glutamicum* Strains. PLoS ONE 9(1): e85731. doi:10.1371/journal.pone.0085731

Editor: Jérôme Nigou, Centre National de la Recherche Scientifique - Université de Toulouse, France

Received August 7, 2013; **Accepted** November 30, 2013; **Published** January 17, 2014

Funding: This work was funded by grants of the Helmholtz association (VH-NG-716), the German ministry of education and research (0315589A) and the Deutsche Forschungsgemeinschaft (SPP1617). The funders had no role in study design, data collection and analysis, decision to publish, or preparation of the manuscript.

Competing Interests: The authors have declared that no competing interests exist.

* E-mail: j.frunzke@fz-juelich.de

☯ These authors contributed equally to this work.

Introduction

In natural environments, inherent cell-to-cell variation within isogenic populations and resulting formation of subpopulations often bears an overall fitness advantage for the whole population [1]. Variation of phenotypic traits has been reported to promote the division of labor or as "bet-hedging" strategy to enable rapid adaption to sudden environmental changes [1,2,3,4]. In biotechnological processes, however, arising phenotypic variation and the formation of insufficiently producing subpopulations can adversely affect the entire production process [5,6]. Besides its biological origin, heterogeneity within large scale cultivation processes is caused by environmental variations at the micro scale, e.g., of dissolved gases, pH and nutrients caused by insufficient mixing or the formation of biofilms [7,8,9,10].

Nowadays, bioprocess monitoring is still dominated by bulk approaches delivering average values for the whole population. Masking of cell-to-cell variation might consequently result in misleading interpretations of biological phenomena [1]. Analysis of growth and product formation of single microbial cells would provide a detailed insight into the phenotypic structure of the population representing a further, important step towards a systems level understanding of microbial processes. A major drawback of this approach is, however, the limited number of microbially produced metabolites which confer an observable phenotype to the respective cell; among the few exceptions are natural chromophores, such as carotenoids. This challenge demands the development of novel tools and techniques for single-cell quantification and real-time monitoring of inconspicuous, small metabolites [11,12,13]. In this context, genetically encoded biosensors capable of detecting small molecules inside the cell and transforming this information into an optical readout (e.g. fluorescence signal) represent a powerful tool for single-cell analysis of microbial production strains. The implementation of genetically encoded metabolite sensors in live cell imaging studies performed in microfluidic cultivation systems offers the advantage

of long-term observation of single-cell growth and metabolite production with high spatial and temporal resolution [14,15].

Corynebacterium glutamicum represents one of the most important platform organisms in industrial biotechnology; dominating the global, large-scale production of amino acids (e.g., L-glutamate, L-lysine, and L-valine) [16]. Recent studies using multiparameter flow cytometry revealed phenotypic heterogeneity in terms of viability, membrane potential and growth activity of *C. glutamicum* wild type cells grown in shake flasks [17]. However, population heterogeneity during production processes has not been studied in detail for this species, yet. Recently, our group reported on the development of a genetically encoded metabolite sensor (Lrp-sensor), which enables the cytosolic detection of branched-chain amino acids or L-methionine in single *C. glutamicum* cells. The sensor is based on the transcriptional regulator Lrp of *C. glutamicum* which activates expression of the *brnFE* operon, encoding an amino acid export system, upon accumulation of the effector amino acids L-methionine, L-leucine, L-isoleucine, and L-valine [18,19,20,21]. In previous studies, the sensor was successfully applied in flow cytometry-based high-throughput (HT) screenings for the isolation of mutants producing amino acids and in first live cell imaging studies of the L-valine production strain *C. glutamicum ΔaceE* [22].

C. glutamicum was successfully engineered for efficient L-valine production within the last years [23,24,25,26,27]. Strains are based on the deletion of the *aceE* gene, which encodes the E1p subunit of the pyruvate dehydrogenase complex (PDHC) and an additional plasmid-based overexpression of the *ilvBNCE* genes encoding L-valine biosynthesis enzymes. The resulting strain *C. glutamicum ΔaceE* (pJC4-ilvBNCE) was further improved by additional deletion of the genes encoding pyruvate:quinone oxidoreductase (*pqo*), phosphoglucose isomerase (*pgi*), and pyruvate carboxylase (*pyc*). These modifications led to a series of strains, based on the same parental strain (*C. glutamicum ΔaceE*), with a stepwise increasing product yield ($Y_{P/S}$) reaching the theoretical maximal $Y_{P/S}$ of 0.86 mol L-valine *per* mol of glucose in *C. glutamicum ΔaceE Δpqo Δpgi Δpyc* (pJC4-ilvBNCE) [28]. The common and characteristic feature of these PDHC-deficient strains is the onset of the production phase only after a complete consumption of the acetate which is required for growth [23]. Due to these properties the strains represent an ideal testing ground for biosensor performance. In this work, we have successfully applied the genetically encoded Lrp-sensor for live cell imaging studies to monitor amino acid production, growth, and viability in *C. glutamicum* L-valine production strains in a time-resolved manner and at single cell resolution.

Materials and Methods

Bacterial strains, media, and growth conditions

Bacterial strains and plasmids used or constructed in this work are listed in Table 1. Unless stated otherwise, pre-cultures of *C. glutamicum* were inoculated with single colonies from a fresh brain heart infusion (BHI) agar plate containing 51 mM acetate and incubated in 4 ml BHI complex medium with 51 mM acetate for 6 h at 30°C and 170 rpm. This first pre-culture was used to inoculate a 100 ml shake flask containing 20 ml CGXII minimal medium [29] with 222 mM glucose and 154 mM acetate. The cells of the second pre-culture were cultivated overnight at 30°C and 120 rpm, washed twice with 0.9% (w/v) saline and then used to inoculate the main culture to an optical density (OD_{600}) of 1. If not stated differently, cells in the main culture were cultivated under the same conditions as in the pre-culture. Potassium acetate was used in all experiments performed in this study. *Escherichia coli* DH5α was grown aerobically in LB medium on a rotary shaker (120 rpm) or on LB agar plates at 37°C [30]. Where appropriate, the media contained kanamycin (25 μg ml^{-1} for *C. glutamicum* or 50 μg ml^{-1} for *E. coli* DH5α) or isopropyl β-D-1-thiogalactopyranoside (IPTG), as indicated. For online monitoring of growth and fluorescence, cells were cultivated in 48-well flowerplates using the BioLector system (m2p-labs GmbH, Aachen, Germany) [31]. Cultivation conditions have been described previously [22].

Recombinant DNA work

Standard methods like PCR, DNA restriction or ligation were carried out according to standard protocols [30]. Synthesis of oligonucleotides and sequencing analysis were performed by Eurofins MWG Operon (Ebersfeld, Germany). The vector pE2-Crimson was derived by Clontech Laboratories (Mountain View, CA, USA). For the construction of pJC4-ilvBNCE-crimson, *e2-crimson* under transcriptional control of P_{tac} was amplified using oligonucleotides lacI-fw and E2-Crimson-rv [32]. The PCR product was cloned into the vector pJC4-ilvBNCE [25] using the Bst1107I restriction site. For chromosomal integration of the Lrp-sensor, the sensor cassette was inserted into the intergenic region of cg1121-cg1122 using pK18-mobsacB-cg1121, cg1122 [22]. The transfer of the integration plasmid into *C. glutamicum* and selection of the first and second recombination events were performed as described previously [33]. Correct integration at the chromosomal locus was verified by colony PCR using primers Int-cg1121-fw and Int-cg1122-rv.

Quantification of amino acids

For determination of amino acid concentrations in the supernatant, samples of the cultures were centrifuged (13,000 rpm, 10 min, 4°C) and amino acid concentration was quantified by reversed-phase high-pressure liquid chromatography as described before [22].

Microfluidic chip cultivation

Microfluidic PDMS-glass chips were fabricated according to [14,34]. The microfluidic monolayer cultivation system utilized in the present study was designed for microcolony growth and growth-coupled phenotypic studies at the single-cell level [14,35]. The device features 100 arrays of monolayer cultivation chambers (1 μm×40 μm×40 μm; height × width × length) for HT monitoring of microcolony growth under constant environmental conditions. The microfluidic chip connected to 1 ml disposable syringes (Omnifix 40 Duo, B. Braun Melsungen AG, Germany) for continuous media supply was placed inside an in-house manufactured incubator for temperature and atmosphere control. Media flow was controlled with syringe pumps (neMESYS, Cetoni GmbH, Korbussen, Germany). The incubator was mounted onto a fully motorized inverted Nikon Eclipse Ti microscope (Nikon GmbH, Düsseldorf, Germany) suitable for time-lapse live cell imaging. The setup was equipped with a focus assistant (Nikon PFS) compensating for thermal drift during long-term microscopy and a CFI Plan Apo Lambda DM 100X-magnification, 1.45 numeric aperture oil phase contrast objective. Temperature control of the objective was realized using an objective heater (ALA OBJ-Heater, Ala Scientific Instruments, USA). A cell suspension of OD_{600} 0.5-1, transferred from a pre-culture at exponential growth phase, was infused to the system. After successful cell seeding, the growth medium was infused at approximately 100 nl min^{-1} per channel.

Table 1. Bacterial strains, plasmids, and oligonucleotides used in this study.

Strains, plasmids	Relevant characteristics	Reference
Strains		
E. coli DH5α	*supE44, ΔlacU169 (ϕ80lacZDM15), hsdR17, recA1, endA1, gyrA96,thi1,relA1.*	Invitrogen
C. glutamicum ATCC13032	Biotin-auxotrophic wild type.	[48]
ΔaceE	*C. glutamicum* wild type with deletion of the *aceE* gene, coding for the E1p subunit of the pyruvate dehydrogenase-complex (PDHC).	[49]
ΔaceE Δpqo	*C. glutamicum* ΔaceE strain with deletion of the *pqo* gene, coding for pyruvatequinone oxidoreductase.	[50]
ΔaceE Δpqo Δpgi	*C. glutamicum ΔaceE Δpqo* strain with deletion of the *pgi* gene, coding for the phosphoglucose isomerase.	[28]
ΔaceE Δpqo Δpgi Δpyc	*C. glutamicum ΔaceE Δpqo Δpgi* strain with deletion of the *pyc* gene, coding for the pyruvate carboxylase.	[28]
C. glutamicum sensor strain	*C. glutamicum* wild type strain with chromosomally integrated Lrp-sensor (integrated into the intergenic region of cg1121-cg1122) and pJC4-ilvBNCE-crimson plasmid.	This work.
ΔaceE sensor strain	ΔaceE strain with chromosomally integrated Lrp-sensor (cg1121-cg1122) and pJC4-ilvBNCE-crimson plasmid.	This work.
ΔaceE Δpqo sensor strain	ΔaceE *Δpqo* strain with chromosomally integrated Lrp-sensor (cg1121-cg1122) and pJC4-ilvBNCE-crimson plasmid.	This work.
ΔaceE Δpqo *Δpgi* sensor strain	ΔaceE *Δpqo Δpgi* strain chromosomally integrated Lrp-sensor (cg1121-cg1122) and pJC4-ilvBNCE-crimson plasmid.	This work.
ΔaceE Δpqo *Δpgi Δpyc* sensor strain	ΔaceE *Δpqo Δpgi Δpyc* strain with chromosomally integrated Lrp-sensor (cg1121-cg1122) and pJC4-ilvBNCE-crimson plasmid.	This work.
Plasmids		
pJC1	*E. coli-C. glutamicum* shuttle vector, Kan^R, $oriV_{Ec}$, $oriV_{Cg}$.	[51]
pJC1-lrp-bmF'-eyfp	pJC1derivative containing Lrp-sensor cassette, which consists of *lrp* (cg0313), the intergenic region of *lrp bmF* (cg0314) and a transcriptional fusion of *bmF* with *eyfp*.	[22]
pJC4-ilvBNCE	pJC1derivative carrying the *ilvBNCE* genes coding for the L-valine biosynthetic enzymes acetohydroxyacid synthase, isomeroreductase, and transaminase B.	[25]
pJC4-ilvBNCE-crimson	pJC4-ilvBNCE derivative containing *e2-crimson* under transcriptional control of P_{tac}.	This work.
pK18-mobsacB	Vector for allelic exchange in *C. glutamicum*; Kan^R; $oriV_{Ec}$, *sacB*, *lacZα*.	[52]
pK18-mobsacB-cg1121, cg1122-Lrp-sensor	pK18mobsacB derivative for genomic integration of the Lrp-sensor in the intergenic region of cg1121-cg1122 in *C. glutamicum*.	This work.
Oligonucleotides	**Sequence (5′ → 3′)**	
lacI-fw	TCAAGCCTTCGTCACTGGTCC	This work.
E2-Crimson-rv	CTACTGGAACAGGTGGTGGCG	This work.
Int-cg1121-fw	TTGGCGTGTGGTTGGTTAG	This work.
Int-cg1122-rv	CGCATCAAGCAGATCTCTG	This work.

doi:10.1371/journal.pone.0085731.t001

Live cell imaging and image analysis

The microscope was equipped with an ANDOR LUCA R DL604 EMCCD camera (Andor Technology plc., Belfast, UK) for image recording and a 300 W Xenon light source for fluorescence excitation (Lambda DG4, Sutter Instruments, USA). Following fluorescence filters (AHF Analysentechnik, Germany) were applied: i) YFP: HQ 500/20 (excitation filter), Q515 (dichroic), and HQ 535/30 (emission); ii) E2-Crimson: HQ 600/37 (excitation filter), Q630 (dichroic) and Q675/67 (emission). Phase contrast and fluorescence microscopy images of several microcolonies were captured in 15 min time intervals. Growth and fluorescence were recorded for 10–20 isogenic microcolonies during each experiment. Image analysis was performed with the Nikon NIS Elements AR software package. The visualization of lineage tree was realized using our in-house developed Python-based software.

Results

Online monitoring of L-valine production

Previously, we presented the Lrp-biosensor as a convenient tool to discriminate between low levels of L-valine production and wild type level [22]. In the present study, we assessed the performance of the biosensor to monitor the course of L-valine production over time in high-yield and basic *C. glutamicum* L-valine production strains [28]. For this purpose, the Lrp-sensor was chromosomally integrated into the different strains in order to avoid plasmid-based effects, such as a fluctuating copy number or plasmid loss. Strains under study were *ΔaceE*::Lrp-sensor (pJC4-ilvBNCE-crimson), *ΔaceE Δpqo*::Lrp-sensor (pJC4-ilvBNCE-crimson), *ΔaceE Δpqo Δpgi*::Lrp-sensor (pJC4-ilvBNCE-crimson), and *ΔaceE Δpqo Δpgi Δpyc*::Lrp-sensor (pJC4-ilvBNCE-crimson), henceforth referred to as "sensor strains" (Table 1). The sensor strains as well as the wild type *C. glutamicum* ATCC 13032 (pJC4-ilvBNCE-crimson) containing the Lrp-sensor were cultivated in CGXII minimal medium supplied with 154 mM acetate and 222 mM glucose in microtiter

plates (0.75 ml filling volume) in the BioLector cultivation system, enabling online measurement of biomass (backscatter) and eYFP fluorescence [31]. Within the first 10 to 12 hours, the strains grew exponentially while exhibiting a decrease in fluorescence over time (Figure 1A, B). This residual fluorescence and the decrease of the signal in the first hours were also observed in the wild type strain and therefore can likely be ascribed to changes of auto- or background fluorescence during growth. After depletion of the acetate required for growth, the cells entered the stationary phase and an increase in eYFP fluorescence was detected, indicating growth-decoupled L-valine production of the strains (Figure 1B). At the early production phase all strains exhibited a similar sensor signal, but split up in the course of the cultivation. Twelve hours after shifting into the production phase an almost twofold higher sensor output of the high-yield producers (*ΔaceE Δpqo Δpgi* and *ΔaceE Δpqo Δpgi Δpyc* sensor strains) was observed in comparison to the basic producers (*ΔaceE* and *ΔaceE Δpqo* sensor strains) (Figure 1B, C). The fluorescence of the *ΔaceE* and the *ΔaceE Δpqo* sensor strains reached its maximum intensity within five to ten hours, suggesting constant internal L-valine concentrations. In contrast, the fluorescence of the *ΔaceE Δpqo Δpgi* and the *ΔaceE Δpqo Δpgi Δpyc* sensor strains increased for about 15 hours, reflecting the higher potential for L-valine production of these strains. Determination of amino acid concentration in the supernatant confirmed different levels of L-valine production, ranging from 30 mM L-valine in average for the *ΔaceE Δpqo Δpgi* sensor strain and the *ΔaceE Δpqo Δpgi Δpyc* sensor strain to 23 mM in average for the *ΔaceE* sensor strain and the *ΔaceE Δpqo* sensor strain (Figure 1C). These results demonstrate that the Lrp-sensor does not only provide an ON/OFF response (wild type *versus* production strain), but can be applied for online monitoring of production processes in basic as well as high-yield production strains, since (i) information about initiation of the production process is provided, (ii) the course of metabolite production process is displayed over time, and (iii) different levels of productivity are revealed.

Live cell imaging of L-valine production

In the following experiments, we analyzed the applicability of the Lrp-biosensor in live cell imaging studies to investigate growth, physiology, and metabolic activity of single cells in a time-resolved manner. For this purpose, *C. glutamicum* L-valine production stains were cultivated in monolayer microfluidic cultivation chambers under constant environmental conditions (Figure 2A) [14]. After single-cell inoculation into microfluidic chambers, cells were grown in CGXII medium with 154 mM acetate and 222 mM glucose as carbon source. A medium change (after 18.5 hours) to CGXII medium containing 222 mM glucose initiated L-valine production. Figure 2 shows two representative colonies of the *ΔaceE* sensor strain and the *ΔaceE Δpqo Δpgi* sensor strain during growth (t_1, t_2) and L-valine production phase (t_3–t_5) (Video S1, S2). Cells gradually stopped growing and simultaneously exhibited progressively increasing eYFP fluorescence after the medium switch.

The average fluorescence signal of three microcolonies (fluorescence signal *per* colony area) of the *ΔaceE* sensor strain and the *ΔaceE Δpqo Δpgi* sensor strain during growth and production phase is depicted in Figure 2B. In contrast to the *ΔaceE Δpqo Δpgi* sensor strain, colonies of the *ΔaceE* sensor strain already displayed a low eYFP signal during the growth phase. Although starting at different levels, the fluorescence of both strains increased comparably when L-valine production was initiated. In agreement with the results obtained from microtiter plate cultivations (see Figure 1), colonies of the high-yield producer *ΔaceE Δpqo Δpgi*

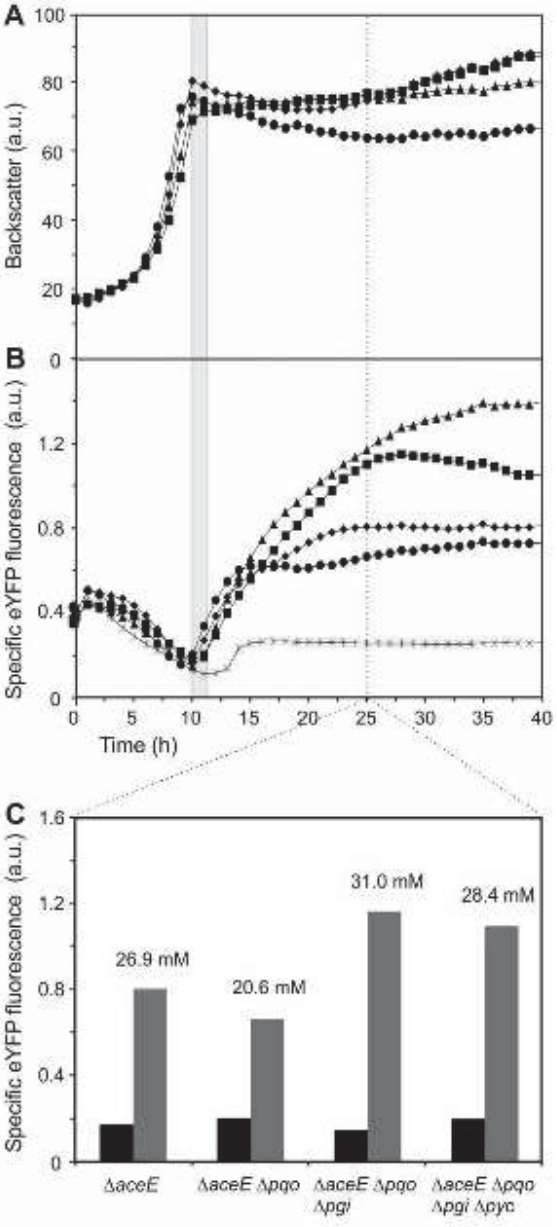

Figure 1. Biosensor-based online monitoring of L-valine production in PDHC-deficient *C. glutamicum* strains. (**A**) Growth and (**B**) Lrp-sensor output (eYFP fluorescence) of the sensor strains *C. glutamicum* ATCC 13032 wild type (stars), *ΔaceE* (diamonds), *ΔaceE Δpqo* (circles), *ΔaceE Δpqo Δpgi* (triangles), and *ΔaceE Δpqo Δpgi Δpyc* (squares) cultivated in CGXII minimal medium containing 222 mM glucose and 154 mM acetate. Data represent average values of three independent cultivations. The transition of the producer strains into the stationary and production phase is highlighted by the grey area. (**C**) EYFP fluorescence of respective strains at the beginning of the production phase (black bars) and twelve hours after the initiation of L-valine production (grey bars). L-valine concentration (mM) in the supernatant of the respective strain 25 h after beginning of cultivation as measured by HPLC is indicated above the grey bars.
doi:10.1371/journal.pone.0085731.g001

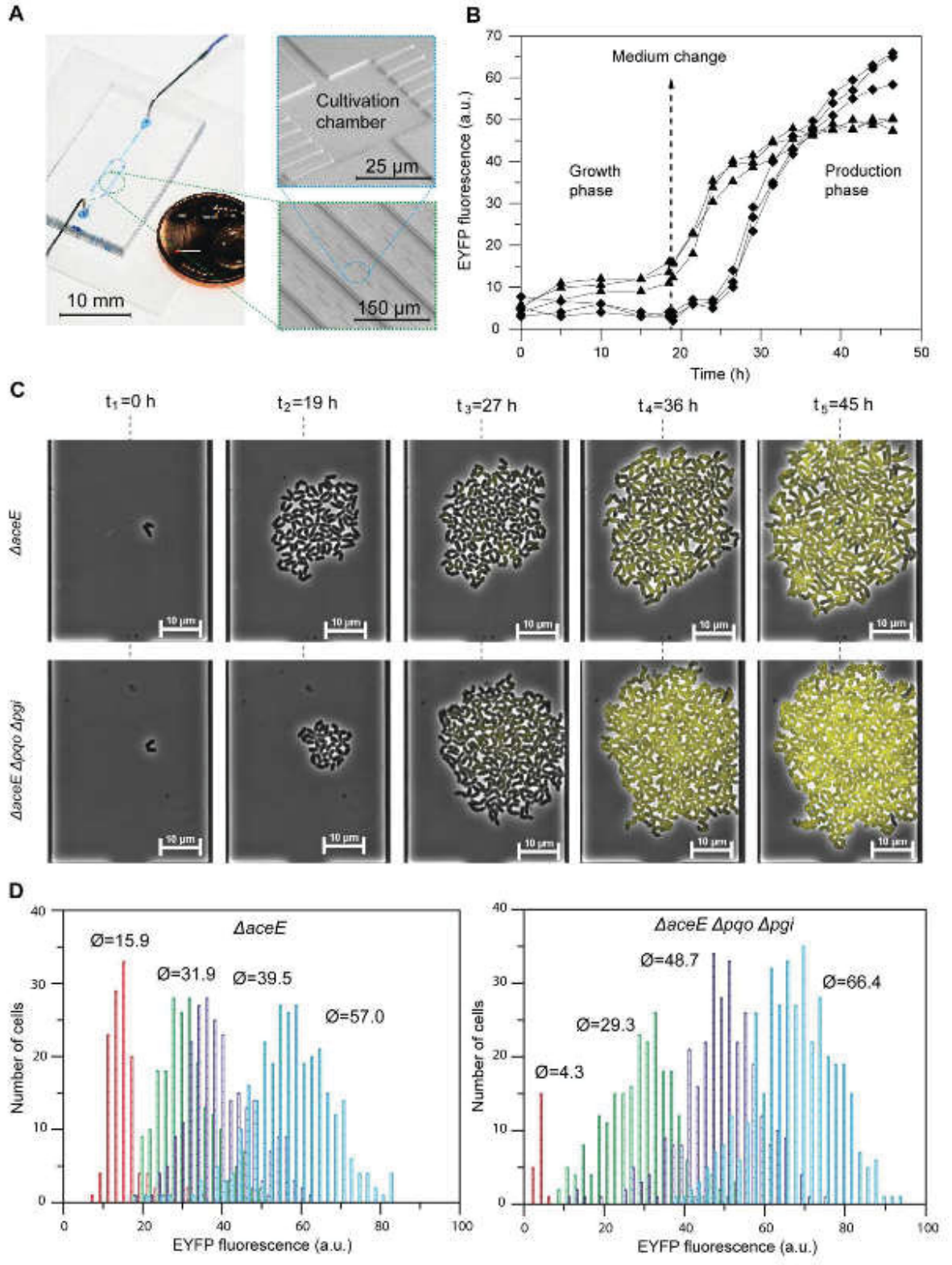
A
Cultivation chamber
25 µm
150 µm
10 mm
B
Medium change
Growth phase
Production phase
EYFP fluorescence (a.u.)
Time (h)
C
t1=0 h
t2=19 h
t3=27 h
t4=36 h
t5=45 h
ΔaceE
ΔaceE Δpqo Δpgi
10 µm
D
ΔaceE
Ø=15.9
Ø=31.9
Ø=39.5
Ø=57.0
ΔaceE Δpqo Δpgi
Ø=4.3
Ø=29.3
Ø=48.7
Ø=66.4
Number of cells
EYFP fluorescence (a.u.)

Figure 2. Live cell imaging of L-valine production strains using microfluidic monolayer cultivation chambers. (**A**) Illustration of the microfluidic cultivation chambers. The system consists of several arrays of picoliter sized monolayer cultivation chambers. (**B**) Fluorescence emission of three entire microcolonies (average eYFP signal *per* colony area) of the *ΔaceE* sensor strain (triangles) and the *ΔaceE Δpqo Δpgi* sensor strain (diamonds) over time. Fluorescence was measured every 2.5 h. (**C**) Growth (t_1–t_2) and production phase (t_3–t_5) of isogenic microcolonies of the *ΔaceE* sensor strain (upper row) and the *ΔaceE Δpqo Δpgi* sensor strain (lower row). (**D**) Histograms illustrating fluorescence distribution within a representative microcolony of the *ΔaceE* sensor strain (left) and the *ΔaceE Δpqo Δpgi* sensor strain (right). The eYFP signal of single cells was measured at t = 19 h (red), t = 26 h (green), t = 34 h (purple), and t = 46 h (blue). Average fluorescence values are indicated above the respective peaks. All cultivations were performed in microfluidic chambers shown in (A) in CGXII minimal medium containing 154 mM acetate and 222 mM glucose during growth phase or CGXII with 222 mM glucose during the production phase, respectively.
doi:10.1371/journal.pone.0085731.g002

sensor strain showed an overall higher final fluorescence in comparison to colonies of the *ΔaceE* sensor strain. This was also reflected by the single-cell fluorescence of the respective strains during the production phase (Figure 2D). Measurement of single-cell fluorescence of both strains revealed a broadening Gaussian distribution in the course of the experiment.

Correlation of sensor output and metabolic activity

In further studies, we intended to validate the correlation of the Lrp-biosensor output and the physiological state of the respective cells. In other words, is a low sensor output an indication for a reduced metabolic activity or even death of the respective cell? To introduce a measure for plasmid stability in L-valine producing sensor strains, *e2-crimson* coding for far-red fluorescence protein E2-Crimson was placed under control of P_{tac} in the vector pJC4-ilvBNCE containing the gene cluster *ilvBNCE* for overexpression of the L-valine biosynthesis genes [32]. The vector with the integrated plasmid marker was transferred into the *ΔaceE Δpqo Δpgi* sensor strain and eYFP (Lrp-biosensor) and E2-Crimson (plasmid marker) fluorescence emission were recorded for microcolonies grown in microfluidic cultivation chambers. Figure 3A shows a representative colony of the *ΔaceE Δpqo Δpgi* sensor strain at the end of the production phase (~46 h). Single-cell eYFP and E2-Crimson fluorescence were recorded and are depicted in a correlation plot, with each dot representing a single cell (Figure 3B). Overall, a strong correlation between eYFP and E2-Crimson signal was observed ($r = 0.73 \pm 0.09$, $n = 1436$). Only a minor amount of cells (<1%) displayed a high E2-Crimson, but low eYFP signal. Metabolically inactive or dead cells (low signal for eYFP and E2-Crimson) were rarely detected. Nevertheless, in a few cases we also observed microcolonies with an increased number of non-fluorescent cells (see section 3.4.). Their frequency, however, strongly depended on the chosen colony and cell density during cultivation.

Occurrence of non-fluorescent cells during the production phase

During the production phase, we always observed the occurrence of some non-fluorescent cells. Live cell imaging studies enable the investigation of this phenomenon in a time-resolved manner and the discrimination between different types of non-fluorescent cells, e.g. lysed, dead cells or dormant forms which resume growth after a while.

Under conditions described in section 3.2, we usually observed colonies showing a typical Gaussian distribution of eYFP intensity, but occasionally colonies with an increased number of non-fluorescing cells were found (<1% of cells) (Figure 4). We tracked different cells in several microcolonies, clustered them and found different types of non-producing cells (Figure 4, Video S3). The majority of cells, however, underwent transition from growth to production and will not be discussed here. The first type of non-producing cells initiated L-valine production, but showed a sudden cell lysis at a later time (Figure 4; I, II and IV). These cells were rarely seen at constant environmental conditions, but were more frequently observed when colony growth exceeded the chamber size, leading to densely packed colonies. A second fraction of cells neither initiated L-valine production nor showed growth after a change of medium. These cells might either represent dead or

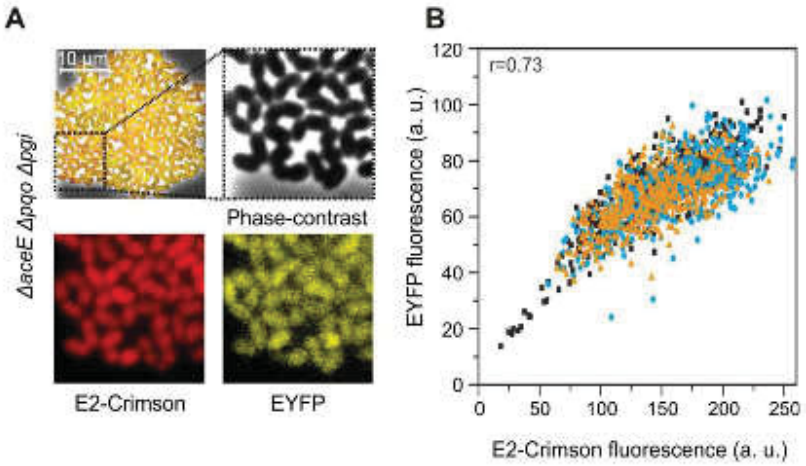

Figure 3. Correlation of the Lrp-sensor output (eYFP) and the plasmid marker E2-Crimson. (**A**) Microscopy overlay plot of phase-contrast, eYFP and E2-Crimson signal of an isogenic microcolony of the *ΔaceE Δpqo Δpgi* sensor strain after 46 h (see Figure 2C). (**B**) Dot plot displaying eYFP and E2-Crimson signal of single cells of three isogenic microcolonies (triangles, circles, and diamonds) of the *ΔaceE Δpqo Δpgi* sensor strain.
doi:10.1371/journal.pone.0085731.g003

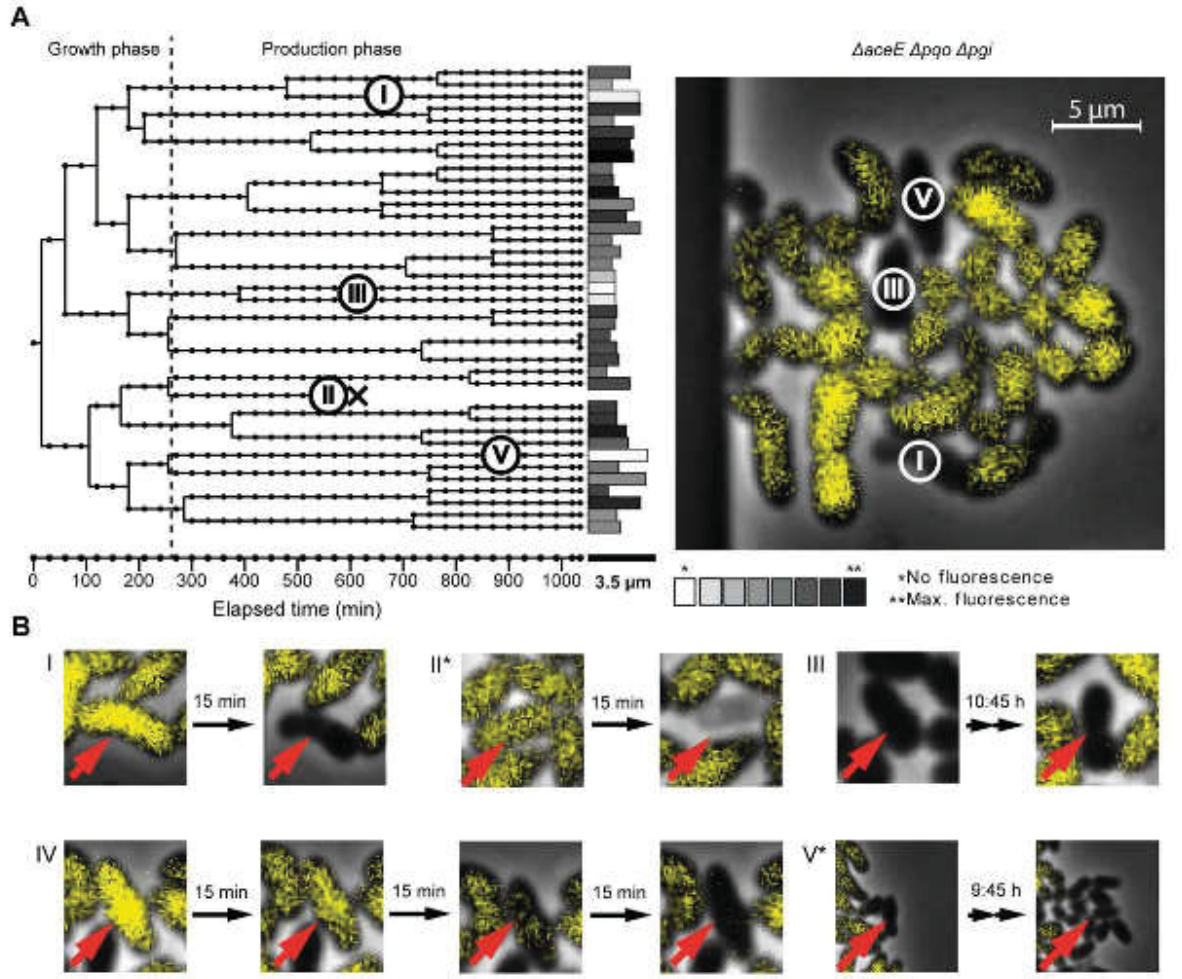

Figure 4. Occurrence of non-fluorescent cells during the production phase. (**A**) Microcolony and lineage tree of the *ΔaceE Δpqo Δpgi* sensor strain. Different types of non-fluorescent cells are illustrated in B. (**B**) **(I-II)** Lysing cells and **(III)** dormant/or dead cell, which do not switch from growth to production. **(IV)** Leaky cell that shows decreasing fluorescence signal over time, potentially caused by a permeabilized cell membrane. **(V*)** Cells showing slow growth, but no production. Images marked with an asterisk show cells of another microcolony of the *ΔaceE Δpqo Δpgi* sensor strain, not shown in this figure.
doi:10.1371/journal.pone.0085731.g004

dormant cells (Figure 4, III). Finally, we also observed non-producing cells which did not enter production phase, but continued to grow (Figure 4, V), although no carbon source, i.e. acetate, was provided in the medium. One possible explanation would be that these cells have adapted their growth to utilizing glucose as carbon source.

Phenotypic heterogeneity of *C. glutamicum* L-valine production strains

In contrast to growth in well-controlled microfluidic devices, cells in typical shake flask or bioreactor cultivations face significant fluctuations with respect to metabolite accumulation and physical parameters (pH, O_2, etc.). Remarkably, when we exchanged the minimal medium used in the abovementioned studies against a non-defined complex medium (CGXII containing low amounts of BHI), we observed a strong impact on the phenotypic pattern with respect to amino acid production in all strains analyzed.

Starting from a single cell, growth of an isogenic microcolony of the *ΔaceE* sensor strain in CGXII medium with 154 mM acetate, 222 mM glucose and 0.5% BHI was monitored in the microfluidic cultivation system. After a primary growth phase, cells were supplemented with 222 mM glucose and 0.5% BHI to trigger L-valine production. Although most of the cells switched from growth to production (Figure 5A, Video S4), in approximately 50% of the recorded colonies one or several single cells continued growing after the medium change. This observed bistability in the decision of switching from growth to production was observed for all L-valine producing strains under study when the cells were grown in the presence of low amounts of BHI (Figure S1 in File S1, Video S5). It was also observed in cells without the Lrp-sensor, which indicates that the observed split in phenotypes is not caused by the sensor itself (Figure S2 in File S1). Figure 5 shows two

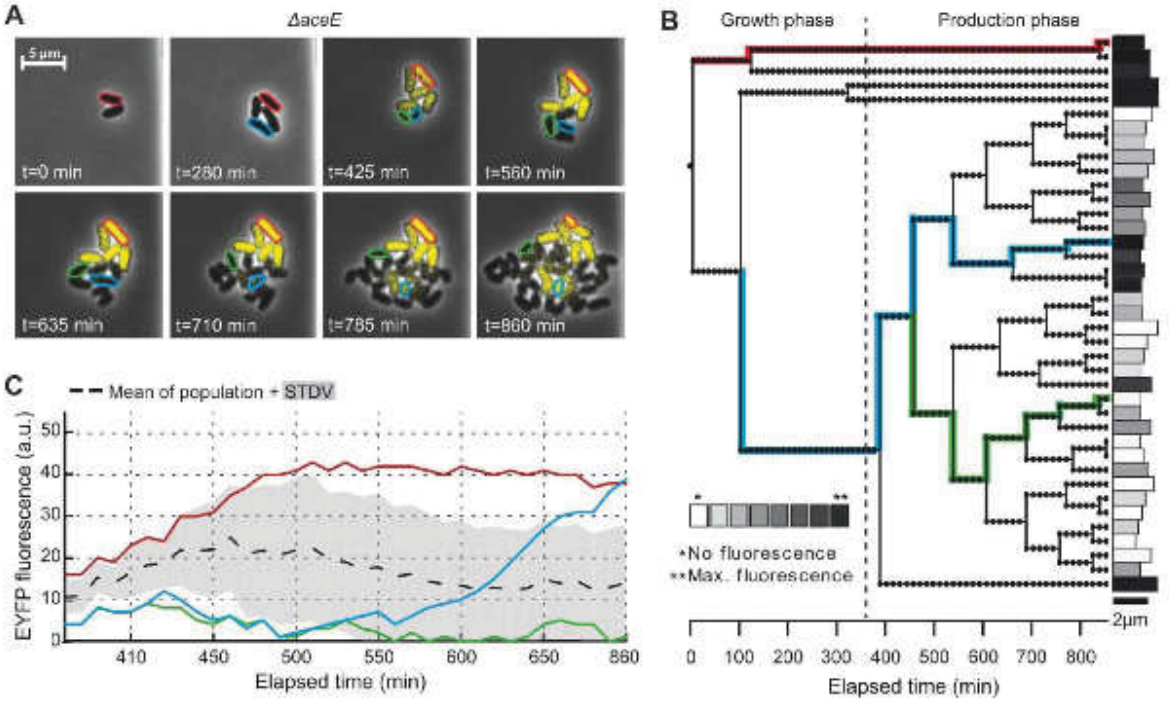

Figure 5. Biosensor-driven analysis of phenotypic heterogeneity. In the presence of low amounts of complex carbon sources, significant cell-to-cell variability in the switch from growth to L-valine production was observed. (**A**) Growth and production phase (initiated after 340 min) of an isogenic microcolony of the *ΔaceE* sensor strain and (**B**) the lineage tree of the respective microcolony highlighting several single cell traces. EYFP fluorescence was quantified in single cells after 860 min. (**C**) Single cell traces of fluorescence output of marked cells (see A and B) and average emission of the whole colony (black, dashed line, SD – grey shading). Cultivation was performed in CGXII minimal medium containing 154 mM acetate, 222 mM glucose and 0.5% BHI during growth phase or 222 mM glucose and 0.5% BHI during production phase, respectively.
doi:10.1371/journal.pone.0085731.g005

exemplary cells, originating from the same mother cell, where one cell (red) divided for the last time and initiated L-valine production directly after the medium switch, while the sister cell continued to grow ($t_D = 105 \pm 21$ min, n = 5). However, some of the descendants later also switched to L-valine production (blue) or continued growth throughout the course of the experiment (green). This experiment illustrated that, depending on the cultivation conditions, recording of the average fluorescent output of the whole population would mask the significant variation at the single-cell level (Figure 5C). In contrast, a uniform switching behavior was observed when only glucose was present in the production medium illustrating the strong impact of slight changes in medium composition on the phenotypic structure of a particular population.

Discussion

Nowadays, multiple physiological parameters in single cells can be analyzed by flow cytometry or fluorescence microscopy using a constantly increasing number of fluorescent dyes and staining protocols [36]. Single-cell productivity is a key performance indicator in biotechnological production processes, which is unfortunately often masked by typical bulk-based analysis. However, technological limitations and a lack of convenient tools for accurate single-cell analysis, prevented in-depth analysis of productivity in microbial bioprocesses. In the present work, the genetically encoded Lrp-biosensor is introduced as a powerful tool for single cell analysis of production strains.

The Lrp sensor cassette was inserted into the genome of different *C. glutamicum* L-valine producing strains in order to avoid the effect of plasmid copy number fluctuations on the sensor output. In first proof of principle experiments, the genomically integrated metabolite sensor proved suitable to visualize different levels of L-valine production in gradually engineered strains [28]. Thus, the sensor is not restricted to provide an ON/OFF response (WT *versus* production strain), but reflects more subtle differences with respect to the metabolic activity of single cells. Remarkably, almost all eYFP-negative cells (>95%) of the L-valine producing sensor strains showed no growth when sorted on agar plates FACS and stained positive for PI, indicating an impaired membrane integrity (data not shown). This is further supported by the high correlation of sensor output (eYFP) and the signal of the integrated plasmid marker (E2-Crimson) shown in Figure 3A, B. Similar correlations were recently described for studies based on a GFP-sensor enabling the detection of carbon-limited conditions in *E. coli* as well as for a reporter system in yeast, in which the expression of *gfp* was set under control of a ribosomal protein promoter [37,38].

C. glutamicum L-valine production strains were analyzed by live cell imaging during growth inside microfluidic chip devices to investigate the phenotypic pattern at the single-cell level [14]. The sensor output of isogenic colonies of the different production strains showed a broad Gaussian distribution suggesting phenotypic heterogeneity with respect to L-valine production. The peak

width increased proportional to the mean fluorescence of the populations, which is also observed when fluorescent reporter genes are set under control of inducible promoters, such as P_{tac} (data not shown). This pattern was obtained in all strains under study and no difference was observed in strains with increased precursor availability (*Δpqo*, *Δpcx*) or increased NADPH supply (*Δpgi*) suggesting that these factors have no impact on the peak width of the sensor output. However, several parameters may influence the distribution of the reporter output of sensor strains, including cofactor supply of the involved biosynthetic enzymes, cell cycle, carbon source uptake or even stochastic effects on gene expression [5].

Individual cell tracking by time-lapse microscopy revealed different types of non-producing cells besides the productive main population. Sudden and progressive cell lysis and cells in a dormant state were observed. Additionally, a complete lack of the switch from growth to production phase was observed, with cells continuing growth at a low rate. These cells might utilize carbon sources, which are low concentrated, but are continuously supplied by the medium flow. For example, protocatechuic acid, required as iron-chelator, can be used as carbon source by *C. glutamicum* [39,40]. Alternatively, cellular metabolism might have adapted to overflow of glucose, bypassing the reactions catalyzed by the PDH complex (deletion of *aceE*) and the pyruvate:quinone oxidoreductase (*pqo*) and providing acetyl-CoA as precursor for TCA-cycle. Studies of Litsanov *et al.* described that in spite of deleting the genes for the known acetate-synthesizing pathways in *C. glutamicum*, residual acetate formation during cultivation in minimal medium was still observed in strains engineered for aerobic succinate production [41].

In the presence of low amounts of complex medium, we observed a bistability in the cells decision to initiate L-valine production or to continue growth (Figure 5, Figure S1 and S3 in File S1, Video S4, S5). Besides the expected transition from growth to production, cells either showed unhampered growth and cell division or a time-delayed switch to production (Figure S3 in File S1). In larger-scale production processes the occurrence of such subpopulations may have a major impact on process efficiency, as these cells might overgrow the entire population in the course of time and, consequently, resources are depleted for biomass formation instead of being converted to the final product. These biosensor-based analysis, again, demonstrate that despite targeted, genetic manipulation on cells to work as efficient, uniform microbial factories, phenotypic variation might lead to the occurrence of drastic differences in cellular productivity even under the well-controlled cultivation conditions present in microfluidic chambers. Continued growth of some cells might be based on different energetic states of the cells or differences in the level of transporter proteins. A low amount of a specific permease is sufficient to induce an autocatalytic positive feedback resulting in a non-uniform induction behavior, as described for lactose uptake and catabolism by Novick and Weiner more than 50 years ago or by Siegele *et al.* for expression driven from the *araBAD* promoter [42,13,44].

Conclusions

In this study, we describe the amino acid sensing Lrp-sensor as a valuable, non-invasive tool to monitor the metabolic activity of PDHC-deficient *C. glutamicum* L-valine producers at single-cell resolution. In recent years, a number of metabolite sensors based on RNA aptamers or transcription factors were reported, increasing the number of accessible metabolites [12,45,46,47]. Future studies will aim at unraveling the underlying molecular mechanisms of the observed phenotypic variation, benchmarking this approach for the analysis and improvement of strains and biotechnological production processes.

Supporting Information

File S1 This file includes Figures S1, S2 and S3. **Figure S1, Phenotypic heterogeneity of the *ΔaceE Δpqo Δpgi Δpyc* sensor strain upon switch from growth to production phase.** **(A)** Microcolony showing transition to producing cells or **(B)** a mixture of growing and producing cells after medium switch (initiated after 240 min). In approximately 50% of the recorded colonies one or several single cells continued growth after medium switch. **(C, D)** Fluorescence histograms depicting single cell fluorescence to selected times during growth (0–240 min) and production phase (0–1200 min) of the microcolonies shown in A **(C)** and B **(D)**. Cultivation was performed in CGXII minimal medium containing 154 mM acetate, 222 mM glucose and 0.5% BHI during growth phase or 222 mM glucose and 0.5% BHI during production phase, respectively. **Figure S2, Phenotypic heterogeneity of *ΔaceE* and *ΔaceE Δpqo Δpgi* upon switch from growth to production phase.** **(A)** *ΔaceE* microcolonies where all cells stopped growth (blue stars) upon transition to the production phase (upper row) or a mixture of growing (red stars) and non-growing cells (lower row) after initiation of the production phase. In approximately 50% of the recorded colonies one or several single cells continued growth after medium switch (initiated after 250 min). **(C)** *ΔaceE Δpqo Δpgi* microcolonies. In the upper row, all cells stopped growth whereas in the lower row a microcolony is shown were some cells continued growth after initiation of the production phase. In approximately 50% of the recorded colonies one or several single cells continued growth after medium switch (initiated after 250 min). These findings confirm that the phenotypic split shown in Figure 5 is not due to the presence of the Lrp-sensor. Cultivation was performed in CGXII minimal medium containing 154 mM acetate, 222 mM glucose and 0.5% BHI during growth phase or 222 mM glucose and 0.5% BHI during production phase, respectively. **Figure S3, Single cell traces of the *ΔaceE Δpqo Δpgi Δpyc* sensor strain upon switch from growth to production phase.** **(A)** Single cell traces showing the switch from growth (cell length = blue line) to production (fluorescence = squares) after several cell divisions during production phase (t = 8.5 h, t = 13.0 h). **(B)** Single cell traces showing no switch from growth to production. Single cell traces are taken from the cultivation of *ΔaceE Δpqo Δpgi Δpyc* sensor strain shown in Figure S1.
(PDF)

Video S1 Growth and production of *C. glutamicum* ATCC 13032 *ΔaceE* sensor strain. Upon the switch to the production phase, cells gradually stopped growing and simultaneously exhibited progressively increasing eYFP fluorescence. Growth phase: CGXII medium with 154 mM acetate and 222 mM glucose; production phase: CGXII medium with 222 mM glucose as carbon source.
(WMV)

Video S2 Growth and production of *C. glutamicum* ATCC 13032 *ΔaceE Δpqo Δpgi* sensor strain. Upon the switch to the production phase, cells gradually stopped growing and simultaneously exhibited progressively increasing eYFP fluorescence. Growth phase: CGXII medium with 154 mM acetate and 222 mM glucose; production phase: CGXII medium with 222 mM glucose as carbon source.
(WMV)

Video S3 Occurrence of non-fluorescent cells during the production phase of the *C. glutamicum* ATCC 13032 *ΔaceE Δpqo Δpgi* sensor strain.
(WMV)

Video S4 Phenotypic heterogeneity of the *C. glutamicum ΔaceE* sensor strain. Cells were grown in CGXII medium with 154 mM acetate, 222 mM glucose and 0.5% BHI. After a primary growth phase, cells were supplemented with 222 mM glucose and 0.5% BHI to trigger L-valine production. Although most of the cells switched from growth to production (Figure 5A), in approximately 50% of the recorded colonies one or several single cells continued growing after the medium change.
(WMV)

Video S5 Microcolonies of the *C. glutamicum ΔaceE Δpqo Δpgi* sensor strain displaying phenotypic heterogeneity. Growth of six microcolonies (CGXII medium with 154 mM acetate, 222 mM glucose and 0.5% BHI) is shown in microfluidic chip devices. After a primary growth phase, cells were supplemented with 222 mM glucose and 0.5% BHI to trigger L-valine production. In the upper three colonies all cells showed a switch from growth to production. In the lower three colonies one or several single cells continued growing after initiation of the production phase.
(WMV)

Acknowledgments

We thank Cornelia Gätgens for technical support and Michael Bott for discussions. This work was performed in parts at the Helmholtz Nanoelectronic Facility (HNF) of Forschungszentrum Jülich. The authors would like to thank all those at HNF for their help and support.

Author Contributions

Conceived and designed the experiments: NM AG JF. Performed the experiments: NM AG RIM. Analyzed the data: NM AG JF. Contributed reagents/materials/analysis tools: BB DK SH KN. Wrote the paper: NM AG JF.

References

1. Lidstrom ME, Konopka MC (2010) The role of physiological heterogeneity in microbial population behavior. Nat Chem Biol 6: 705–712.
2. Kussell E, Leibler S (2005) Phenotypic diversity, population growth, and information in fluctuating environments. Science 309: 2075–2078.
3. Acar M, Mettetal JT, van Oudenaarden A (2008) Stochastic switching as a survival strategy in fluctuating environments. Nature Genetics 40: 471–475.
4. Veening J-W, Smits WK, Kuipers OP (2008) Bistability, epigenetics, and bet-hedging in bacteria. Ann Rev Microbiol 62: 193–210.
5. Müller S, Harms H, Bley T (2010) Origin and analysis of microbial population heterogeneity in bioprocesses. Curr Op Biotechnol 21: 100–113.
6. Lencastre Fernandes R, Nierychlo M, Lundin L, Pedersen AE, Puentes Tellez PE, et al. (2011) Experimental methods and modeling techniques for description of cell population heterogeneity. Biotechnol Adv 29: 575–599.
7. Lara AR, Galindo E, Ramírez OT, Palomares LA (2006) Living with heterogeneities in bioreactors. Mol Biotechnol 34: 355–381.
8. Lüders G (2002) Understanding the bioreactor. Bioprocess and Biosystems Engineering 24: 273–279.
9. Takors R (2012) Scale-up of microbial processes: impacts, tools and open questions. J Biotechnol 160: 3–9.
10. Enfors SO, Jahic M, Rozkov A, Xu B, Hecker M, et al. (2001) Physiological responses to mixing in large scale bioreactors. J Biotechnol 85: 175–185.
11. Heinemann M, Zenobi R (2011) Single cell metabolomics. Curr Op Biotechnol 22: 26–31.
12. Dietrich JA, McKee AE, Keasling JD (2010) High-throughput metabolic engineering: advances in small-molecule screening and selection. Ann Rev Biochem 79: 563–590.
13. Eräsaari DT, Liao J, Zhao H (2013) Protein design for pathway engineering. J Struct Biol doi: 10.1016/j.jsb.2013.03.011.
14. Grünberger A, Paczia N, Probst C, Schendzielorz G, Eggeling L, et al. (2012) A disposable picoliter bioreactor for cultivation and investigation of industrially relevant bacteria on the single cell level. Lab Chip 12: 2060.
15. Locke JCW, Elowitz MB (2009) Using movies to analyse gene circuit dynamics in single cells. Nat Rev Microbiol 7: 383–392.
16. Wendisch VF (2007) Amino acid biosynthesis - pathways, regulation and metabolic engineering: Microbiol Monographs, Springer-Verlag.
17. Neumeyer A, Hübschmann T, Müller S, Frunzke J (2013) Monitoring of population dynamics of *Corynebacterium glutamicum* by multiparameter flow cytometry. Microb Biotechnol 6: 157–167.
18. Kennerknecht N, Sahm H, Yen MR, Patek M, Saier MH, et al. (2002) Export of L-isoleucine from *Corynebacterium glutamicum*: a two-gene-encoded member of a new translocator family. J Bacteriol 184: 3947–3956.
19. Lange C, Mustafi N, Frunzke J, Kennerknecht N, Wessel M, et al. (2012) Lrp of *Corynebacterium glutamicum* controls expression of the *brnFE* operon encoding the export system for L-methionine and branched-chain amino acids. J Biotechnol 158: 231–241.
20. Trötschel C, Deutenberg D, Bathe B, Burkovski A, Krämer R (2005) Characterization of methionine export in *Corynebacterium glutamicum*. J Bacteriol 187: 3786–3794.
21. Yin L, Shi F, Hu X, Chen C, Wang X (2013) Increasing L-isoleucine production in *Corynebacterium glutamicum* by overexpressing global regulator Lrp and two-component export system BrnFE. J Appl Microbiol 114: 1369–1377.
22. Mustafi N, Grünberger A, Kohlheyer D, Bott M, Frunzke J (2012) The development and application of a single-cell biosensor for the detection of L-methionine and branched-chain amino acids. Metab Eng 14: 449–457.
23. Blombach B, Schreiner ME, Holatko J, Bartek T, Oldiges M, et al. (2007) L-Valine production with pyruvate dehydrogenase complex-deficient *Corynebacterium glutamicum*. Appl Environ Microbiol 73: 2079–2084.
24. Bartek T, Blombach B, Lang S, Eikmanns BJ, Wiechert W, et al. (2011) Comparative ^{13}C metabolic flux analysis of pyruvate dehydrogenase complex-deficient, L-valine-producing *Corynebacterium glutamicum*. Appl Environ Microbiol 77: 6644–6652.
25. Radmacher E, Vaitsikova A, Burger U, Krumbach K, Sahm H, et al. (2002) Linking central metabolism with increased pathway flux: L-valine accumulation by *Corynebacterium glutamicum*. Appl Environ Microbiol 68: 2246–2250.
26. Hasegawa S, Suda M, Uematsu K, Natsuma Y, Hiraga K, et al. (2013) Engineering of *Corynebacterium glutamicum* for high-yield L-valine production under oxygen deprivation conditions. Appl Environ Microbiol 79: 1250–1257.
27. Buchholz J, Schwentner A, Brunnenkan B, Gabris C, Grimm S, et al. (2013) Platform engineering of *Corynebacterium glutamicum* with reduced pyruvate dehydrogenase complex activity for improved production of L-lysine, L-valine, and 2-ketoisovalerate. Appl Environ Microbiol 79: 5566–5575.
28. Blombach B, Schreiner ME, Bartek T, Oldiges M, Eikmanns BJ (2008) *Corynebacterium glutamicum* tailored for high-yield L-valine production. Appl Microbiol Biotechnol 79: 471–479.
29. Keilhauer C, Eggeling L, Sahm H (1993) Isoleucine synthesis in *Corynebacterium glutamicum* - molecular analysis of the *ilvB-ilvN-ilvC* operon. J Bacteriol 175: 5595–5603.
30. Sambrook J, MacCallum P, Russell D (2001) Molecular cloning: a laboratory manual: Cold Spring Harbor Laboratory Press, NewYork.
31. Kensy F, Zang E, Faulhammer C, Tan R-K, Büchs J (2009) Validation of a high-throughput fermentation system based on online monitoring of biomass and fluorescence in continuously shaken microtiter plates. Microb Cell Fact 8: doi:10.1186/1475-2859-8188-8131.
32. Strack RL, Hein B, Bhattacharyya D, Hell SW, Keenan RJ, et al. (2009) A rapidly maturing far-red derivative of DsRed-Express2 for whole-cell labeling. Biochemistry 48: 8701–8704.
33. Niebisch A, Bott M (2001) Molecular analysis of the cytochrome bc_1-aa_3 branch of the *Corynebacterium glutamicum* respiratory chain containing an unusual diheme cytochrome c_1. Arch Microbiol 175: 282–294.
34. Grünberger A, Probst C, Heyer A, Wiechert W, Frunzke J, et al. (2013) Microfluidic picoliter bioreactor for microbial single-cell analysis: fabrication, system setup and operation. J Vis Exp, doi:10.3791/50360.
35. Grünberger A, van Ooyen J, Paczia N, Rohe P, Schirrmacher G, et al. (2013) Beyond growth rate 0.6: *Corynebacterium glutamicum* cultivated in highly diluted environments. Biotechnol Bioeng 110: 220–228.
36. Müller S, Nebe-von-Caron G (2010) Functional single-cell analyses: flow cytometry and cell sorting of microbial populations and communities. FEMS Microbiol Rev 34: 554–587.
37. Delvigne F, Baumans A, Francis F, Twizere J-C, Goffet N, et al. (2011) Green fluorescent protein (GFP) leakage from microbial bioreactors provides useful information for the evaluation of the scale-down effect. Biotechnol J 6: 968–978.
38. Carlquist M, Fernandes R, Helmark S, Heins A-L, Lundin L, et al. (2012) Physiological heterogeneities in microbial populations and implications for physical stress tolerance. Microb Cell Fact 11: 94.
39. Haussmann U, Poetsch A (2012) Global proteome survey of protocatechuate- and glucose-grown *Corynebacterium glutamicum* reveals multiple physiological differences. J Proteomics 75: 2649–2659.
40. Unthan S, Grünberger A, van Ooyen J, Gätgens J, Heinrich J, et al. (2013) Beyond growth rate 0.6: What drives *Corynebacterium glutamicum* to higher growth rates in defined medium. Biotechnol Bioeng: doi: 10.1002/bit.25103.

41. Litsanov B, Kabus A, Brocker M, Bott M (2012) Efficient aerobic succinate production from glucose in minimal medium with *Corynebacterium glutamicum*. Microb Biotechnol 5: 116–128.
42. Siegele DA, Hu JC (1997) Gene expression from plasmids containing the *araBAD* promoter at subsaturating inducer concentrations represents mixed populations. Proc Natl Acad Sci U S A 94: 8168–8172.
43. Novick A, Weiner M (1957) Enzyme induction as an all-or-none phenomenon. Proc Natl Acad Sci U S A 43: 553–566.
44. Ozbudak EM, Thattai M, Lim HN, Shraiman BI, van Oudenaarden A (2004) Multistability in the lactose utilization network of *Escherichia coli*. Nature 427: 737–740.
45. Binder S, Schendzielorz G, Stabler N, Krumbach K, Hoffmann K, et al. (2012) A high-throughput approach to identify genomic variants of bacterial metabolite producers at the single-cell level. Genome Biology 13: R40.
46. Zhang F, Keasling J (2011) Biosensors and their applications in microbial metabolic engineering. Trends Microbiol 19: 323–329.
47. Michener JK, Thodey K, Liang JC, Smolke CD (2012) Applications of genetically-encoded biosensors for the construction and control of biosynthetic pathways. Metab Eng 14: 212–222.
48. Kinoshita S, Udaka S, Shimono M (1957) Studies on the amino acid fermentation. I. Production of L-glutamic acid by various microorganisms. J Gen Appl Microbiol 3: 193–205.
49. Schreiner ME, Fiur D, Holatko J, Patek M, Eikmanns BJ (2005) E1 enzyme of the pyruvate dehydrogenase complex in *Corynebacterium glutamicum*: molecular analysis of the gene and phylogenetic aspects. J Bacteriol 187: 6005–6018.
50. Schreiner ME, Riedel C, Holatko J, Patek M, Eikmanns BJ (2006) Pyruvate:quinone oxidoreductase in *Corynebacterium glutamicum*: molecular analysis of the *pqo* gene, significance of the enzyme, and phylogenetic aspects. J Bacteriol 188: 1341–1350.
51. Schäfer A, Tauch A, Droste N, Pühler A, Kalinowski J (1997) The *Corynebacterium glutamicum cglIM* gene encoding a 5-cytosine methyltransferase enzyme confers a specific DNA methylation pattern in an McrBC-deficient *Escherichia coli* strain. Gene 203: 95–101.
52. Schäfer A, Tauch A, Jäger W, Kalinowski J, Thierbach G, et al. (1994) Small mobilizable multipurpose cloning vectors derived from the *Escherichia coli* plasmids pK18 and pK19 – selection of defined deletions in the chromosome of *Corynebacterium glutamicum*. Gene 145: 69–73.

3.2 Biosensor-driven adaptive laboratory evolution of L-valine production in *Corynebacterium glutamicum*

Regina Mahr[1], Cornelia Gätgens[1], Jochem Gätgens[1], Tino Polen[1], Jörn Kalinowski[2], Julia Frunzke[1]*

[1]IBG-1: Biotechnology, Forschungszentrum Jülich, Jülich, Germany

[2]Center for Biotechnology (*CeBiTec*), Bielefeld University, Bielefeld, Germany

*Corresponding author

Name of the Journal: Metabolic Engineering

Impact Factor: 6.767

Author contributions

Own contribution to the work: 80%

	Name	Contribution
Project planning	***Mahr, R.***	50%
	Frunzke, J.	50%
Writing	***Mahr, R.***	90%
	Frunzke, J.	10%

	Name	Experimental work	Evaluation	Preparation of figure/table
Figure 1	***Mahr, R.***	-	-	100%
Figure 2	***Mahr, R.***	100%	100%	100%
Figure 3	***Mahr, R.***	100%	100%	100%
Figure 4	***Mahr, R.***	100%	100%	100%
Figure 5	***Mahr, R.***	50%	80%	95%
	Gätgens, J.	50%	20%	5%
Table 1	***Mahr, R.***	-	-	100%
Table 2	***Mahr, R.***	20%	80%	95%
	Polen, T.	40%	15%	5%
	Kalinowski, J.	40%	5%	-
Figure S1	***Mahr, R.***	100%	100%	100%
Figure S2	***Mahr, R.***	100%	100%	100%
Figure S3	***Mahr, R.***	50%	80%	100%
	Gätgens, J.	50%	20%	-
Figure S4	***Mahr, R.***	100%	100%	100%
Table S1	***Mahr, R.***	100%	95%	100%
	Frunzke, J.	-	5%	-

Metabolic Engineering 32 (2015) 184–194

Contents lists available at ScienceDirect

Metabolic Engineering

journal homepage: www.elsevier.com/locate/ymben

Biosensor-driven adaptive laboratory evolution of L-valine production in *Corynebacterium glutamicum*

Regina Mahr [a], Cornelia Gätgens [a], Jochem Gätgens [a], Tino Polen [a], Jörn Kalinowski [b], Julia Frunzke [a,*]

[a] IBG-1: Biotechnology, Forschungszentrum Jülich GmbH, 52425 Jülich, Germany
[b] Center for Biotechnology (CeBiTec), Bielefeld University, 33615 Bielefeld, Germany

ARTICLE INFO

Article history:
Received 12 June 2015
Received in revised form
1 September 2015
Accepted 21 September 2015
Available online 8 October 2015

Keywords:
Biosensor
Adaptive laboratory evolution
Transcription factor
Corynebacterium glutamicum
L-valine
Metabolic engineering

ABSTRACT

Adaptive laboratory evolution has proven a valuable strategy for metabolic engineering. Here, we established an experimental evolution approach for improving microbial metabolite production by imposing an artificial selective pressure on the fluorescent output of a biosensor using fluorescence-activated cell sorting. Cells showing the highest fluorescent output were iteratively isolated and (re-) cultivated. The L-valine producer *Corynebacterium glutamicum* Δ*aceE* was equipped with an L-valine-responsive sensor based on the transcriptional regulator Lrp of *C. glutamicum*. Evolved strains featured a significantly higher growth rate, increased L-valine titers (~25%) and a 3-4-fold reduction of by-product formation. Genome sequencing resulted in the identification of a loss-of-function mutation (UreD-E188*) in the gene *ureD* (urease accessory protein), which was shown to increase L-valine production by up to 100%. Furthermore, decreased L-alanine formation was attributed to a mutation in the global regulator GlxR. These results emphasize biosensor-driven evolution as a straightforward approach to improve growth and productivity of microbial production strains.

1. Introduction

Mutation and selection are key components of evolution driving adaption and the development of novel traits. Short generation times and a natural mutation frequency of 10^{-10} to 10^{-9} mutations per base pair per replication cycle enable the selection of beneficial phenotypical traits from high genetic diversity (Barrick and Lenski, 2013). During the last few years, laboratory evolution strategies went more and more into the focus to adapt industrial producer strains to detrimental growth conditions such as oxidative and thermal stress (Lee et al., 2013; Oide et al., 2015; Sandberg et al., 2014; Tenaillon et al., 2012), to improve product formation (Raman et al., 2014; Reyes et al., 2014; Xie et al., 2015) or solvent tolerance (Atsumi et al., 2010; Lee et al., 2011; Oide et al., 2015) (for reviews discussing the use of adaptive evolution approaches in metabolic engineering, see Abatemarco et al., 2013; Portnoy et al., 2011).

Due to the high complexity of carbon and energy fluxes in living cells, classical strain engineering based on rational design approaches is often limited by the current knowledge of bacterial physiology. Alternatively, high-throughput engineering approaches based on random mutagenesis followed by an efficient screening strategy are applied to overcome the limits of rational strain development. In this context, the use of biosensors has proven to be a highly valuable tool by translating intracellular product formation into a screenable optical output, such as fluorescence (Dietrich et al., 2010; Eggeling et al., 2015; Schallmey et al., 2014). However, after random mutagenesis strains typically reveal several hundreds of genomic alterations representing a major challenge in identifying those mutations linked to the particular phenotype of interest (Binder et al., 2012; Chou and Keasling, 2013). Here, industrial strain development strongly benefits from adaptive evolution approaches, in which strains typically feature only a few mutations and which enable the enrichment of non-intuitive beneficial mutations by improving growth at the same time (Abatemarco et al., 2013; Portnoy et al., 2011). Up to now, laboratory evolution experiments of mainly fitness-linked phenotypes have been performed by exposing microorganisms to sequentially increasing levels of environmental stress (Eckdahl et al., 2015; Lee et al., 2013; Marietou et al., 2014; Oide et al., 2015; Reyes et al., 2014). Especially in the case of the yeast *Saccharomyces cerevisiae*, adaptation to an improved ethanol tolerance has been proven useful for increasing product formation (Alper et al., 2006; Jiménez and Benítez, 1987; Liu, 2006).

* Correspondence to: Institut für Bio- und Geowissenschaften, IBG-1: Biotechnologie, Forschungszentrum Jülich GmbH, Leo-Brandt-Straße, 52425 Jülich, Germany. Fax: +49 2461 61 2710.
E-mail address: j.frunzke@fz-juelich.de (J. Frunzke).

http://dx.doi.org/10.1016/j.ymben.2015.09.017
1096-7176/

The bottom line of almost all reported adaptive evolution approaches is selection for improved growth and survival, which usually coincides with increased product formation – especially in the case of growth-coupled processes (Feist et al., 2010). To expand the toolbox for metabolic engineering, we here report on a novel strategy capable of evolving the production of inconspicuous metabolites, which are not linked to fitness. This approach involves the implementation of an artificial selective pressure on the fluorescent output of transcription factor-based biosensors by fluorescence-activated cell sorting (FACS). In previous studies, several laboratories have successfully demonstrated the value of synthetic sensor constructs for small molecule detection as well as their application in high-throughput screening approaches and single-cell analysis (Binder et al., 2012; Dietrich et al., 2010, 2013; Mustafi et al., 2012, 2014; Siedler et al., 2014).

Recently, we developed an amino acid biosensor, based on the transcriptional regulator Lrp of *Corynebacterium glutamicum* (Lange et al., 2012), which enables the intracellular detection of L-methionine as well as branched-chain amino acids, and translates this information into a measureable fluorescent output (Mustafi et al., 2012). This biosensor system has already been successfully applied for online monitoring and live cell imaging studies of *C. glutamicum* L-valine production strains at the single-cell level to analyze phenotypic production heterogeneity (Mustafi et al., 2014).

C. glutamicum is an important industrial platform organism used for the large-scale industrial production of amino acids (*e.g.* L-glutamate, L-lysine and L-valine) (Eggeling and Bott, 2005; Wendisch, 2007). L-valine is an essential amino acid for vertebrates and is required for infusion solutions, cosmetics or as precursor for herbicides (Eggeling et al., 2001; Leuchtenberger, 1996). In order to engineer strains for L-valine production, mutants deficient in the E1p subunit (*aceE*) of the pyruvate dehydrogenase complex (PDHC) have been constructed and characterized in several studies (Blombach et al., 2008, 2007; Chen et al., 2015; Eikmanns and Blombach, 2014). Due to the inactivation of the PDHC, pyruvate accumulates in the cell and is channeled as a precursor towards L-valine production (Fig. 1). For cell growth, acetate is supplied to the medium to maintain the acetyl-CoA pool for the tricarboxylic acid (TCA) cycle.

In this study, we successfully established a biosensor-driven adaptive evolution approach to improve L-valine production of *C. glutamicum* Δ*aceE*. Isolated evolved clones exhibited significantly increased product formation and reduced formation of the by-product L-alanine. This approach demonstrates the power of biosensor-driven laboratory evolution approaches to select for beneficial and non-intuitive mutations leading to an improved production phenotype.

2. Materials and methods

2.1. Bacterial strains, media and growth conditions

The bacterial strains and plasmids used in this study are listed in Table 1. Strain *C. glutamicum* ATCC 13032 was used as the wild-type strain (Kalinowski et al., 2003). Unless otherwise specified, *C. glutamicum* Δ*aceE* cells were picked from a brain heart infusion (BHI) agar plate containing 85 mM acetate, inoculated in 4 ml BHI medium with 85 mM acetate and incubated for eight hours at 30 °C and 170 rpm. Subsequently, the cells from the first pre-culture were used to inoculate a second pre-culture in a shake flask containing 20 ml CGXII minimal medium (Keilhauer et al., 1993) with 222 mM glucose and 254 mM acetate. The cells were incubated overnight at 30 °C and 120 rpm. The following day, the cells were washed with 0.9% (w/v) saline, adjusted to an optical density (OD_{600}) of 1 in fresh 50 ml CGXII minimal medium

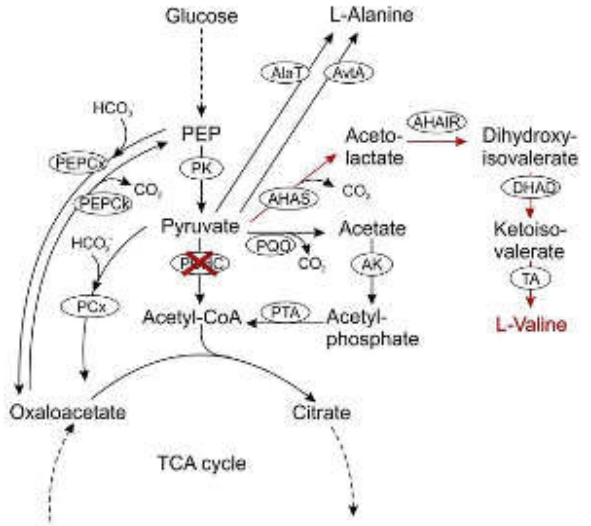

Fig. 1. Schematic of the central metabolism of *C. glutamicum* Δ*aceE* and the L-valine biosynthetic pathway. Due to the deletion of the E1p subunit (Δ*aceE*) of the PDHC, pyruvate is not converted to acetyl-CoA by the activity of the PDHC (red cross). Abbreviations: acetohydroxy acid isomeroreductase (AHAIR), acetohydroxy acid synthase (AHAS), acetate kinase (AK), alanine aminotransferase (AlaT), alanine aminotransferase (AvtA), dihydroxy acid dehydratase (DHAD), pyruvate decarboxylase (PCx), pyruvate dehydrogenase complex (PDHC), pyruvate kinase (PK), phosphoenolpyruvate (PEP), PEP carboxykinase (PEPCk), PEP carboxylase (PEPCx), pyruvate:quinone oxidoreductase (PQO), phosphotransacetylase (PTA), transaminase B (TA).

containing 222 mM glucose and 254 mM acetate, and incubated at 30 °C and 120 rpm. Unless otherwise specified, CGXII minimal medium was prepared without the addition of urea, which is part of the original CGXII recipe (Keilhauer et al., 1993). In this study, acetate was added to the medium as potassium acetate salt. Biomass formation was monitored by measuring OD_{600}, while the cell dry weight (CDW, g L^{-1}) was calculated by following equation: $CDW = OD_{600} \times 0.3\ g\ L^{-1}$ (Buchholz et al., 2013). *Escherichia coli* DH5α cells were incubated in lysogeny broth (LB) medium by agitation at 120 rpm in shake flasks or grown on LB agar plates at 37 °C (Sambrook et al., 2001). If appropriate, kanamycin was added to the media in a final concentration of 25 μg/ml for *C. glutamicum* and 50 μg/ml for *E. coli*.

2.2. Procedure of the biosensor-driven evolution experiment

For the evolution experiment, *C. glutamicum* Δ*aceE* containing the plasmid-encoded Lrp-biosensor was picked from an agar plate and cultivated overnight in 4 ml BHI medium with 85 mM acetate and 25 μg/ml kanamycin. The following day, 2 ml of the preculture was used to inoculate a 200 ml shake flask with 50 ml CGXII minimal medium, 222 mM glucose, 254 mM acetate and 25 μg/ml kanamycin. As the strain *C. glutamicum* Δ*aceE* displays a growth-decoupled production phenotype (Blombach et al., 2007), cells were analyzed and sorted by FACS after 28 h of cultivation. At this time, the cells typically entered the stationary phase and had initiated L-valine production some hours ago. One million cells showing the top 10% sensor output were sorted on MultiScreen HTS filter plates (Millipore, Billerica, USA) to separate cells from the FACSFlow™ buffer (Becton Dickinson, San Jose, USA). We isolated 10^6 cells with the top 10% sensor output to ensure a high genomic variability in the propagated culture. Furthermore, we found that inoculating the culture with a lower number of cells resulted in unstable growth. In parallel, the supernatant of the

Table 1
Bacterial strains, plasmids and oligonucleotides used in this study.

Strains or plasmids Strains	Relevant characteristics	Source or reference
C. glutamicum ATCC 13032	Biotin-auxotrophic wild type	(Kinoshita et al., 2004)
C. glutamicum Δ*aceE*	In-frame deletion of cg2466	(Schreiner et al., 2005)
C. glutamicum Δ*aceE glxR*-T93S	GlxR Thr93 to Ser	This study
C. glutamicum Δ*aceE ureD*-E188*	UreD Glu188 to stop codon	This study
C. glutamicum Δ*aceE prpD*-T201I	PrpD Thr201 to Ile	This study
C. glutamicum Δ*aceE rpsP*-D30D	RpsP with base exchange (*c90t*), silent mutation	This study
E.coli DH5α	*supE44 ΔlacU169* (φ80*lacZDM15*) *hsdR17 recA1 endA1 gyrA96 thi-1 relA1*	Invitrogen
Plasmids		
pJC1-Lrp-sensor	Kan^r; pJC1 derivative containing Lrp-sensor cassette, which consists of *lrp* (cg0313), the intergenic region of *lrp-brnFE* (cg0314/5) and a transcriptional fusion of *brnF* with *eyfp*.	(Mustafi et al., 2012)
pK19-*mobsacB*	Kan^r; plasmid for allelic exchange in *C. glutamicum* (pK18 *oriV$_{E.c.}$ sacB lacZ_*)	(Schäfer et al., 1994)
pK19-*mobsacB-glxR*-T93S	Kan^r; pK19-*mobsacB* derivative for the exchange of Thr93 to Ser in GlxR	This study
pK19-*mobsacB-ureD*-E188*	Kan^r; pK19-*mobsacB* derivative for the exchange of Glu188 to stop codon in UreD	This study
pK19-*mobsacB-prpD*-T201I	Kan^r; pK19-*mobsacB* derivative for the exchange of Thr201 to Ile in PrpD	This study
pK19-*mobsacB-rpsP*-D30D	Kan^r; pK19-*mobsacB* derivative for the exchange of cytosine 90 to thymine, silent mutation	This study
Oligonucleotides	**Sequence (5′–3′)**[a]	
glxR(2)_BamHI_fw	CGCGGATCCGCACTAACATGGTGACCAATTCCATAG (BamHI)	
*glxR*_EcoRI_rev	CCGGAATTCTTATCGAGCGCGACGTGCCAAATG (EcoRI)	
*glxR*_T93S_fw	GGCCCACGCTCCTCCTCTGC	
*glxR*_T93S_rev	GCAGAGGAGGAGCGTGGGCC	
*ureD*_BamHI_fw	CGCGGATCCATGACACAAACCCAACCAGTGGGAAC (BamHI)	
*ureD*_EcoRI_rev	CCGGAATTCCTAGTACTTCCGCAAATTCACCGGTTC (EcoRI)	
*ureD*_E188*_fw	CGGACTCCCGATAGGGAAGTTTTG	
*ureD*_E188*_rev	CAAAACTTCCCTATCGGGAGTCCG	
*prpD*_BamHI_fw	GCCTGCAGGTCGACTCTAGAGGATCCATGATTAACCACGAAGTG CGCACCC (BamHI)	
*prpD*_EcoRI_rev	GTTGTAAAACGACGGCCAGTGAATTCTCAGAACAGTCCTTCCGG AATCACAG (EcoRI)	
*prpD*_T201I_fw	GGCATTGCACATCACCACGCGCGAC	
*prpD*_T201I_rev	GTCGCCGTGGTGATGTGCAATCCC	
rpsP(2)_BamHI_fw	CGCGGATCCCCTATAAACAGTGGTTATTTGACAAGAAG	
rpsP(2)_EcoRI_rev	CCGGAATTCGCCCACGATCACTCGTGTGC	
*rpsP*_D30D_fw	CACCAAGCGCGATGGCAAGGTTATC	
*rpsP*_D30D_rev	GATAACCTTGCCATCGCGCTTGGTG	
*glxR*_genomSeq_fw	TAG ATG CCT CCA GTT AGG TGT CAT C	
*glxR*_genomSeq_rev	CCT GCA GGC TCA GGA AGC TTC	
*prpD*_genomSeq_fw	GGC GTT GAG GTG GTG ATT TTG C	
*prpD*_genomSeq_rev	GCG GGG AGA ATG CAC CAG GC	
*rpsP*_genomSeq_fw	CAC GCG CAG GTT AAA CAA GAA GG	
*rpsP*_genomSeq_rev	CAC TCA GTC AAC CAG GCC TAA C	
*ureD*_genomSeq_fw	CCG CAA GAA CAA ACC ATT CTG CC	
*ureD*_genomSeq_rev	CTG ACC GTT GAA GAA CTC CAC GAT	

[a] Underlined sequences highlight introduced recognition sites for restriction endonucleases (restriction endonucleases indicated in parentheses), while bold letters mark exchanged base pairs during site-directed mutagenesis.

analyzed culture was prepared for uHPLC analysis and a glycerol stock (final conc. 10% (w/v) glycerol) of the evolved culture was stored for further analysis at −80 °C (Fig. 2A). The filter with the cells was excised with single-use scalpels (Braun, Melsungen, Germany), and was inoculated and cultivated overnight in 4 ml BHI medium with 85 mM acetate and kanamycin. The next day, 2 ml of the overnight culture was used to inoculate a new 200 ml shake flask with 50 ml CGXII minimal medium glucose, acetate and kanamycin, as mentioned above. Throughout several evolution steps, cells were analyzed by uHPLC and sorted by FACS after 28 h of cultivation as described above.

2.3. Recombinant DNA work

The standard methods of PCR, DNA restriction and ligation were performed according to standard protocols (Sambrook et al., 2001). Sequencing of DNA fragments and plasmids, as well as the synthesis of the required oligonucleotides (Table 1), were conducted by Eurofins MWG Operon (Ebersfeld, Germany). For the construction of suicide plasmids containing point mutations in *glxR*, *ureD* and *rpsP* the respective wild-type genes were amplified from genomic DNA: *glxR* was amplified using primers *glxR*(2)_BamHI_fw and *glxR*_EcoRI_rev, *ureD* with primers *ureD*_BamHI_fw and *ureD*_EcoRI_rev, and *rpsP* with primers *rpsP*(2)_BamHI_fw and *rpsP*(2)_EcoRI_rev. Amplified products were digested using the restriction enzymes BamHI and EcoRI, and the resulting fragments were ligated into pK19-*mobsacB*, which was digested using the same enzymes. For the construction of pK19-*mobsacB-prpD*, *prpD* was amplified from genomic DNA using primers *prpD*_BamHI_fw and *prpD*_EcoRI_rev, and the resulting fragment was cloned into the BamHI and EcoRI digested vector pK19-*mobsacB* by Gibson assembly (Gibson et al., 2009). *E.coli* DH5α was transformed using the RbCl method (Hanahan, 1983). Preparation of plasmids from *E.coli* was done by using the QIAprep spin miniprep kit (Qiagen, Hilden, Germany). The respective base exchanges were introduced via the QuikChange Lightning Site-Directed Mutagenesis Kit (Agilent, Santa Clara, USA) using primers *glxR*_T93S_fw and *glxR*_T93S_rev, *ureD*_E188*_fw and *ureD* E188* rev, *rpsP* D30D fw and *rpsP* D30D rev, and *prpD* T201I fw and *prpD* T201I rev, respectively. For chromosomal integration, the resulting plasmids pK19-*mobsacB-glxR*-T93S, pK19-*mobsacB-ureD*-E188*, pK19-*mobsacB-rpsP*-D30D (*rpsP-c90t*) and pK19-*mobsacB-prpD*-T201I were transformed in *C. glutamicum* Δ*aceE* by electroporation (van der Rest et al., 1999). First and second recombination events were conducted and verified as previously described (Niebisch and Bott, 2001). Introduced

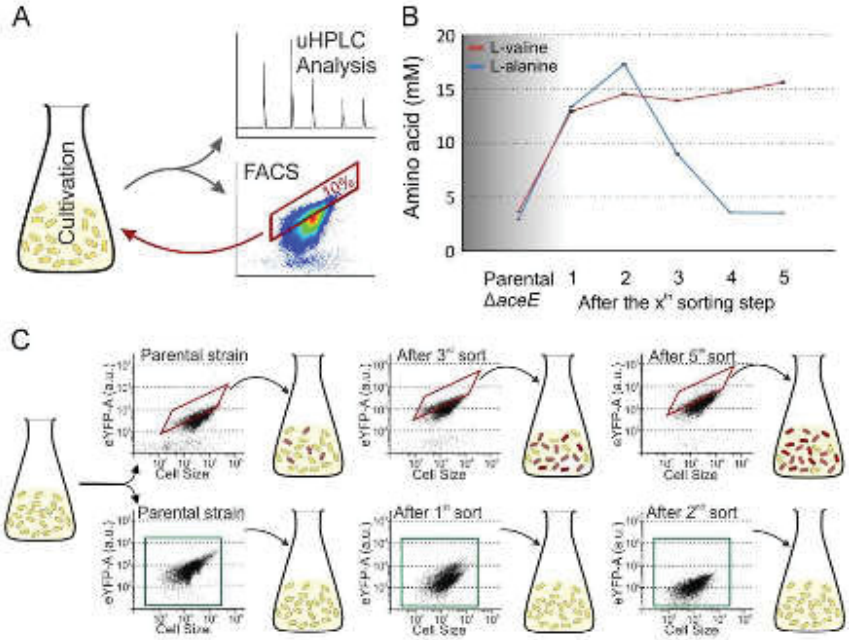

Fig. 2. Biosensor-driven adaptive evolution of L-valine production of *C. glutamicum* Δ*aceE*. (A) Schematic of the experimental approach. Cultivated sensor cells were iteratively analyzed by flow cytometry after 28 h of incubation followed by isolating one million cells by gating on the top 10% fluorescent (sensor) output. Sorted cells were iteratively re-cultivated and re-isolated. L-valine production was monitored throughout the evolution experiment by uHPLC. (B) Development of L-valine (red) and L-alanine (blue) production. The gray zone marks the adaptation of the Δ*aceE* strain to the minimal medium after precultivation in complex medium. The data represent average values from three technical replicates. (C) Development of the biosensor output (eYFP fluorescence) of selected evolution steps analyzed by flow cytometry. Dot plots displaying the eYFP-A (area) fluorescence against the FSC-A signal (cell size). For evolution, one million cells with the highest 10% of the fluorescent output (red gate) were isolated and recultivated. In a control experiment, one million cells were sorted from a gate covering the entire population (green gate).

mutations were reviewed by amplification and sequencing of the respective genome regions using primer pairs *glxR*_genomSeq_fw and *glxR*_genomSeq_rev, *prpD*_genomSeq_fw and *prpD*_genomSeq_rev, *rpsP*_genomSeq_fw and *rpsP*_genomSeq_rev and *ureD*_genomSeq_fw and *ureD*_genomSeq_rev, respectively.

2.4. Flow cytometry

Flow cytometric analyses and cell sorting were performed on a FACSAria II flow cytometer (Becton Dickinson, San Jose, USA) equipped with a blue solid state laser (488 nm excitation). Forward-scatter characteristics (FSC) and side-scatter characteristics (SSC) were detected as small-angle and orthogonal scatters of the 488-nm laser, respectively. EYFP fluorescence was detected using a 502-nm long-pass and a 530/30-nm band-pass filter set. FACS-Diva software 6.0 was used to adjust and record the measurements. All analyses were performed while thresholding on FSC to remove noise. Four-way purity was used as the precision mode for cell sorting with a threshold rate of up to 3000 events/sec. For flow cytometry (FC) analyses, *C. glutamicum* Δ*aceE* culture samples were diluted to an OD_{600} of 0.05 in FACSFlow™ sheath fluid buffer (BD, Heidelberg, Germany). Data were analyzed using FlowJo vX.0.7 analysis software (Tree Star, Ashland, USA).

2.5. DNA microarrays

For transcriptome analysis, 20 µl of the evolved *C. glutamicum* Δ*aceE* glycerol stock frozen after the second and third evolution step was inoculated in 4 ml BHI medium containing 254 mM acetate and kanamycin, and incubated at 30 °C and 170 rpm for eight hours. The second pre-culture and the main culture were prepared as described in 2.1. After 28.5 h of cultivation, the cells were harvested by centrifugation (4256 × *g*, 10 min, 4 °C) at an OD_{600} of 30.4 (culture of second evolution step) and 27.1 (culture of the third evolution step), respectively, the pellet was immediately frozen in liquid nitrogen and stored at −80 °C. RNA preparation, cDNA synthesis and microchip hybridization, scanning and evaluation were performed as previously described (Baumgart et al., 2013).

2.6. Microtiter plate cultivation

Online monitoring of growth and fluorescence was performed in 48-well microtiter FlowerPlates (MFPs) in the BioLector cultivation system (m2p-labs GmbH, Aachen, Germany) (Kensy et al., 2009). Cultivation conditions were adjusted as previously described (Mustafi et al., 2012).

2.7. Quantification of amino acid production

Quantification of amino acids as ortho-phthaldialdehyde derivatives using ultra-high performance liquid chromatography (uHPLC) by automatic pre-column derivatization and separation by reverse-phase chromatography was done on an Agilent 1290 Infinity LC ChemStation (Agilent, Santa Clara, USA) equipped with a fluorescence detector. A gradient of Na-borate buffer (10 mM Na_2HPO_4; 10 mM $Na_2B_4O_7$, pH 8.2; adapted to operator's guide) and methanol was used as the eluent for the Zorbax Eclipse AAA 3.5 µm 4.6 × 7.5 mm column (Agilent, Santa Clara, USA). To measure the amino acid content in the supernatant, samples were taken from the culture, centrifuged for 10 min at 13,000 rpm and 4 °C and diluted 1:100.

2.8. Genome preparation and sequencing

For next-generation sequencing (NGS), genomic DNA was prepared from *C. glutamicum* strains as described (Eikmanns et al., 1994). Extracted DNA was fragmented by sonication and subjected to library preparation and indexing using a TruSeq DNA PCR-free sample preparation kit (Illumina, Chesterford, UK). The resulting libraries were quantified using the KAPA library quant kit (Peqlab, Bonn, Germany).

Sequencing of pooled libraries was performed on a MiSeq (Illumina, Chesterford, UK) using paired-end sequencing with a read-length of 2×250 or 2×300 bases. Data analysis and base calling were undertaken with the Illumina instrument software and stored as fastq output files. Sequencing data of each sample were imported into CLC Genomics Workbench (Version 7.5.1, Qiagen Aarhus A/S, Denmark) for data analysis and variant detection. Sequencing reads were trimmed by adapter and index sequences as well as base quality. Trimmed reads were mapped to accession BX927147 as *C. glutamicum* reference genome (Kalinowski et al., 2003). The resulting mappings were used for the quality-based variant detection of each sample and manually inspected for relevance.

2.9. GC-ToF-MS analysis

Metabolome analyses of supernatants were performed on a 6890N gas chromatograph (Agilent, Santa Clara, USA) coupled to a Micromass GCT Premier high-resolution time-of-flight mass spectrometer (Waters, Milford, USA). Sample preparation, derivatization, MS operation and peak identification were performed as described previously (Paczia et al., 2012).

3. Results

3.1. The biosensor-driven evolution of C. glutamicum ΔaceE

For the proof of concept of the biosensor-driven adaptive evolution approach, the basal L-valine producer strain *C. glutamicum* Δ*aceE* containing the sensor plasmid pJC1-Lrp-sensor was used; herein referred to as the sensor strain (Mustafi et al., 2012). *C. glutamicum* Δ*aceE* served as a basal strain for several metabolic engineering studies and displays a characteristic growth-decoupled production phenotype (Blombach et al., 2008, 2007; Eikmanns and Blombach, 2014). Under the applied experimental conditions, biomass is produced from acetate and L-valine production is initiated in the stationary phase from glucose. Consequently, the cells were analyzed and sorted by FACS after 28 h of cultivation to ensure they had already reached the stationary phase and exhibited an increased intracellular L-valine pool resulting in a measurable output of the Lrp-biosensor. During five iterative evolution steps, one million sensor cells showing the top 10% fluorescent output were iteratively isolated by FACS. Simultaneously, L-valine and L-alanine (by-product) accumulation in the supernatant of the respective cultures was measured by uHPLC (Fig. 2A). Sorted cells were re-cultivated in CGXII containing 222 mM glucose and 254 mM acetate for another 28 h.

After the initial cultivation, the parental sensor strain accumulated 4 mM L-valine and 3 mM of the by-product L-alanine in the supernatant within 28 h of incubation (Fig. 2B). After adaption to CGXII minimal medium, the strain produced 13 mM L-valine and 13 mM L-alanine. Within five evolution steps, the L-valine production of the culture increased by about 25% (from 13 mM to about 16 mM in average, Fig. 2B), while the production of L-alanine decreased by a factor of 3–4 to 3.5 mM after the second sorting step. Throughout the biosensor-driven evolution, the ratio of L-valine to L-alanine increased 3.4-fold.

The iterative sorting of the top 10% of the fluorescent cells resulted in a stepwise increase of the eYFP from a geometric mean of 301 a.u. (parental strain) to 1526 a.u. (after fifth sort) within five sorting steps (red rectangles, Fig. 2C). Meanwhile, Δ*aceE* sensor cells did not split up into several subpopulations suggesting that the increase of fluorescence is a result of genomic modifications and does not reflect phenotypic variability as described previously for derivatives of this strain (Mustafi et al., 2014). In order to verify that the biosensor signal is required for the adaptive evolution approach, the entire population was sorted to escape the selective pressure imposed by the sensor signal and FACS. Applying this sorting strategy, the eYFP signal dropped from a geometric mean of 586 a.u. to 115 a.u. (Fig. 2C). In several independent experiments, no L-valine was determined anymore in the supernatant. Colony PCR revealed contamination with *C. glutamicum* wild-type cells (data not shown) supporting the fact that selection on the sensor signal is crucial for the successful enrichment of adapted clones and to avoid contamination while passing through the non-sterile FACS instrument. Overall, these results suggest that the biosensor-driven evolution is successfully driven by the selectable output of the Lrp-biosensor, which-in combination with FACS-imposes a selective pressure for improved L-valine production.

3.2. Differential expression in evolved cells exhibiting reduced L-alanine production

Comparative transcriptome analysis was performed to assess gene expression changes potentially related to reduced L-alanine production. Since a significant phenotypic change is reflected by the changes in L-alanine production between the second and third evolution step, we conducted a comparative transcriptome experiment. Remarkably, 70 genes exhibited mRNA levels that had been altered more than two-fold (Table S1). Interestingly, *alaT* encoding the L-alanine aminotransferase featured an approximately two-fold decrease in mRNA level after three iterative cultivation and sorting cycles. AlaT is responsible for the conversion of pyruvate to L-alanine (Marienhagen and Eggeling, 2008). Furthermore, a significantly decreased mRNA level of *pyc* encoding the anapleurotic pyruvate carboxylase was observed (Peters-Wendisch et al., 1998). While decreased *alaT* levels are in line with the reduced L-alanine formation, *pyc* downregulation argues for an increased intracellular pyruvate and, thus, improved precursor supply for L-valine production. Remarkably, 21 genes showing an altered mRNA level were reported as being under the control of the global regulator GlxR, which targets more than 180 genes (see Table S1) (Jungwirth et al., 2013; Teramoto et al., 2011). These results suggest that the modified production phenotype after the third evolution step may result from regulatory effects on the transcriptomic level leading to a global reorganization of metabolic fluxes.

3.3. Analysis of isolated clones

The biosensor-driven laboratory evolution approach likely resulted in a highly heterogeneous population in terms of genotype. For further analysis, single *C. glutamicum* Δ*aceE* cells were spotted on BHI agar plates after the fifth evolution step using FACS. The respective growth and production phenotype of isolated strains was analyzed in microtiter plate cultivations. Compared to the non-evolved, parental strain *C. glutamicum* Δ*aceE* ($\mu_{max} = 0.36 \pm 0.007\ h^{-1}$), the evolved cells featured a shortened lag phase and an increased growth rate of $\mu_{max} = 0.41 \pm 0.019\ h^{-1}$ during cultivation in the BioLector system (Fig. 3A). After 30 h of incubation, the isolated evolved strains produced on average about 16% more L-valine than the non-evolved Δ*aceE* strain; a single

isolate, termed M1, even displayed an approximately two-fold increase in product formation (Fig. 3B, Table 2). To verify growth and production of isolated clones, two strains with high (M1) and medium (M2) L-valine accumulation in the supernatant were analyzed in comparison to the parental Δ*aceE* strain by shake flask cultivation (Fig. S2). Here, strain M1 featured 63% (57 mM) and M2 20% (42 mM) increased L-valine production after 48 h compared to the parental Δ*aceE* strain.

The average specific eYFP fluorescence of the Δ*aceE* strain (1.8 ± 0.024 a.u.) increased to 3.4 ± 0.376 a.u. in the evolved strains. Some strains produced the same amount of L-valine by featuring different eYFP sensor signal levels at the same time. As the biosensor signal correlates with the intracellular L-valine level, differences in the extracellular concentration may originate from variability in growth or efficiency of amino acid secretion. To rule out the possibility that this phenotype is linked to mutations within the plasmid pJC1-Lrp-sensor, sensor plasmids of evolved strains were isolated, sequenced and reintroduced into the non-evolved Δ*aceE* strain. However, sequencing showed no mutation within the Lrp-biosensor (data not shown). Reintroduction of plasmids from evolved clones into the parental strain resulted in a basal level of specific eYFP fluorescence (Fig. S1). This suggests that the observed elevated specific fluorescent output of isolated clones reflects specific genomic modifications leading to an increased intracellular L-valine level, but not mutations on the sensor plasmid.

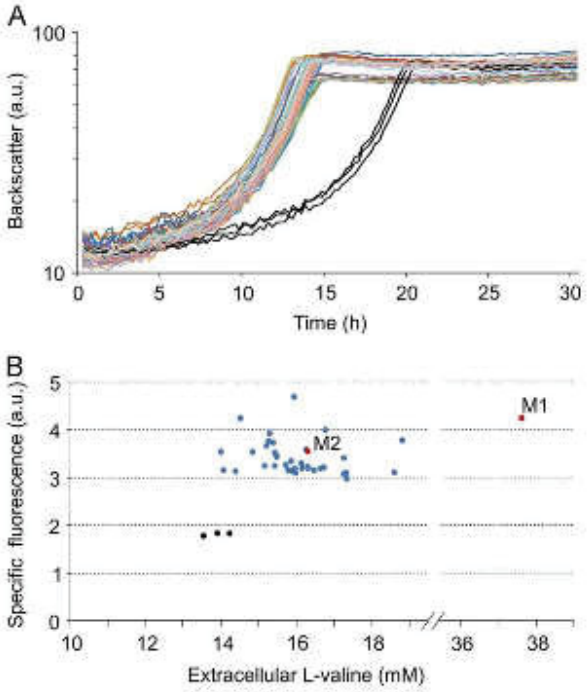

Fig. 3. Growth and production of isolated Δ*aceE* sensor strains after the six evolution steps. (A) Growth of evolved (colored) and non evolved (black) Δ*aceE* sensor strains incubated in microtiter plates in CGXII minimal medium with 222 mM glucose and 254 mM acetate. (B) Specific eYFP fluorescence against L-valine accumulation in the supernatant after 30 h of non-evolved (black dots) and evolved Δ*aceE* strains (blue/red dots). Clones M1 and M2 (red dots) were further analyzed by shake flask incubation (Fig. S2).

3.4. Characterization of accumulated mutations

In order to identify the accumulated mutations in the adaptive evolution experiment, the genomic DNA was isolated from cultures after every evolution step and from two isolated clones (M1 and M2, Fig. S2), and analyzed *via* NGS. Overall, seven mutations were identified in the population after the 5th evolution step (Table 2). Single-nucleotide polymorphisms (SNPs) leading to amino acid exchanges or a stop codon were identified in *glxR* (T93S), encoding a cAMP-dependent global transcriptional regulator, in *prpD2* (T201I), coding for 2-methylcitrate dehydratase, and in *ureD* (E188*), encoding the urease accessory protein UreD. SNPs leading to silent mutations were identified in *rpsP* (*c90t*) encoding the ribosomal protein S16, in *lepA* (*c1045t*) coding for a GTP-binding protein, and in the intergenic region (IGR) of *cg2946* (encoding a putative CarD-like transcriptional regulator) and *cg2947* (*cgtR5*, a two-component response regulator). The deletion of one cytosine in the open reading frame of cg2380, encoding a putative membrane protein, resulted in a frameshift mutation. Sequencing revealed the establishment of most mutations after the third or fourth evolution step (frequency > 80%), whereas the mutation *ureD*-E188* was only identified in one sequenced single mutant (Table 2).

For further analysis, four mutations within annotated genes were introduced into the genome of the non-evolved parental strain *C. glutamicum* Δ*aceE*: *glxR*-T93S (*a277t*), *ureD*-E188* (*g562t*), *prpD*-T201I (*c602t*) and *rpsP*-D30D (*c90t*, silent mutation). The resulting strains were analyzed for growth and production in shake flasks (Fig. 4). Except for Δ*aceE glxR*-T93S, strains showed a similar growth rate of 0.24 to 0.25 h^{-1} (Fig. 4A) and reached a final optical density of 43 after 30 h. Biomass formation of Δ*aceE glxR*-T93S was reduced by about 16%. After 33 h of incubation, *C. glutamicum* Δ*aceE* showed an $Y_{P/X}$ of 1.54 mmol L-valine

Table 2
Accumulated mutations in the biosensor-driven evolution of *C. glutamicum* ATCC13032 Δ*aceE*.

Variant data				*C. glutamicum* ATCC13032 Δ*aceE* (parental strain)[*]	SNP frequency in the last population[*]	Isolated clones[*]	
nt	Gene /IGR	Name	Mutation			M1	M2
G96079T	*cg0719*	*ureD*	E188*	0	0	100	0
T307186A	*cg0350*	*glxR*	T93S	0	100	100	97
C673216T	*cg0759*	*prpD2*	T201I	0	99	100	100
G2135270A	*cg2253*	*rpsP*	D30D (*c90t*)	0	98	100	100
Del C2268302-	*cg2380*	–	G90fs	0	96	93	97
C2455026T	*cg2571*	*lepA*	T348T (*g1044a*)	0	100	100	100
C2803295T	*cg2946-7*	–		0	36	100	0

Genome sequencing was performed for the parental strain *C. glutamicum* Δ*aceE*, the evolved culture after the fifth evolution step as well as for the two clones M1 and M2 isolated after the fifth step. Reads were mapped using accession BX927147 as the reference genome. Abbreviations: absolute nucleotide position with exchange (nt), deletion (Del) given for the plus strand; intergenic region (IGR); frameshift (fs).

[*] The given numbers represent the mapping frequency of the identified genomic alterations.

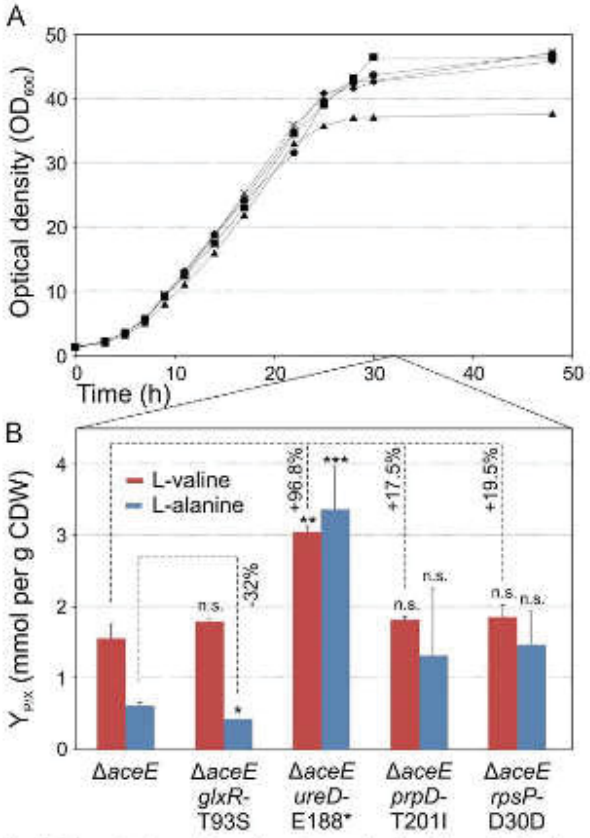

Fig. 4. Characterization of selected mutations reintroduced into *C. glutamicum* Δ*aceE*. (A) Growth of *C. glutamicum* Δ*aceE* (•), Δ*aceE glxR*-T93S (▲), Δ*aceE ureD*-E188* (■), Δ*aceE prpD*-T201I (●) and Δ*aceE*-*rpsP*-D30D (c90t) (×) in CGXII minimal medium containing 222 mM glucose and 254 mM acetate. (B) Biomass yield for L-valine (red) and the by-product L-alanine (blue) as $Y_{P/X}$ in mmol per g CDW after 33 h of incubation. Data represent average values from three independent cultivations. Statistically significantly increased L-valine production and reduced L-alanine production are marked with asterisks, which were calculated by Student's unpaired *t*-test ($n=3$; n.s., not significant; $^*P \le 0.05$; $^{**}P \le 0.01$; $^{***}P \le 0.001$).

per g CDW, while Δ*aceE glxR*-T93S, Δ*aceE prpD*-T201I and Δ*aceE rpsP*-D30D produced about 15–20% more L-valine, respectively (Fig. 4B). Remarkably, L-valine production of Δ*aceE ureD*-E188* was significantly increased by about 100% with a $Y_{P/X}$ of 3.03 ± 0.087 mmol per g CDW (*p*-value 0.004).

Furthermore, the parental strain *C. glutamicum* Δ*aceE* exhibits significant by-product formation (0.6 mmol g^{-1} CDW L-alanine), which is substantially reduced by 32% in Δ*aceE glxR*-T93S (*p*-value 0.03). These results are in line with the expectation that the biosensor-driven adaptive evolution approach selects against detrimental mutations and promotes the accumulation of mutations contributing to the targeted phenotype.

3.5. Loss-of-function in urease activity significantly increases L-valine production

The mutation *ureD*-E188* results in a truncated version of the urease accessory protein UreD. The disruption of *ureD* was shown to disable the function of urease to degrade urea to carbon dioxide and ammonium (Fig. 5A) (Nolden et al., 2000). To test whether the loss-of-function in urease activity leads to similarly increased L-valine levels, *C. glutamicum* Δ*aceE* and Δ*aceE ureD*-E188* were cultivated in CGXII minimal medium with and without 5 g/l urea. After 30 h of cultivation in shake flasks with urea, *C. glutamicum* Δ*aceE* accumulated 20.5 mM L-valine and 9.9 mM L-alanine (Fig. 5B). Without urea, the production of L-valine significantly increased by 75.6% to 36 mM. L-valine levels increased in Δ*aceE ureD*-E188* with urea to 44.2 mM and without urea to 50.5 mM. Without urea and/or in the presence of the *ureD*-E188* mutation, L-alanine production of the Δ*aceE* strain increased about four- to five-fold.

GC-ToF-MS analyses were then performed to further investigate the impact of urea and/or the presence of the *ureD*-E188* mutation on the intracellular metabolite pool. Both the strains cultivated without urea and/or carrying the mutation *ureD*-E188* featured significantly increased levels of the L-valine biosynthesis intermediates 2-acetolactate and dihydroxyisovalerate compared to the Δ*aceE* strain cultivated in the presence of urea (Fig. 5C+D, Fig. S3). Furthermore, the ratio of pyruvate to lactate was 0.24 for the Δ*aceE* strain with urea, and shifted towards pyruvate for Δ*aceE* cultivated without urea (1.22) and for Δ*aceE ureD*-E188* with (1.58) and without urea (2.48). As already measured in the supernatant (Fig. 5B), L-valine and L-alanine levels were strongly increased in strains cultivated without urea and/or with *ureD*-E188*. Whereas significant amounts of urea were left by Δ*aceE ureD*-E188*, urea was metabolized during cultivation of the Δ*aceE* strain in CGXII medium containing urea.

The impact of urea and/or the presence of the *ureD*-E188* mutation was further confirmed in pH-controlled batch fermentations (Fig. S4). Again, the strains Δ*aceE* cultivated without urea or Δ*aceE ureD*-E188* with and without urea exhibited significantly improved product formation (up to 60%). Altogether, these data confirm that urease inactivity (and/or urea deficiency) significantly increases L-valine production, which is reflected by the phenotype of the Δ*aceE ureD*-E188* strain.

4. Discussion

Engineering of bacterial strains for small molecule production remains challenging due to the high complexity of bacterial physiology. Directed evolution of fitness-linked phenotypes has been shown to overcome these limits by selecting against growth defective mutations and by promoting the identification of non-intuitive beneficial mutations (Abatemarco et al., 2013; Portnoy et al., 2011). In most cases, however, phenotypical traits are not directly coupled to bacterial growth. In the present work, we successfully established a biosensor-driven laboratory evolution approach for the improvement of growth and metabolite production of industrially relevant strains by imposing an artificial selective pressure on the fluorescent output of the biosensor using FACS. Within a few iterative rounds, *C. glutamicum* ATCC 13032 Δ*aceE* containing the plasmid-encoded Lrp-biosensor (Blombach et al., 2007; Mustafi et al., 2012) was evolved towards an increased L-valine production, decreased by-product formation (L-valine) and a significantly improved growth behavior (Fig. 2). After the fifth sorting step, L-valine levels remained constant, probably due to the fact that the Lrp-biosensor reached its intracellular detection limit (Mustafi et al., 2012). However, biosensor engineering towards reduced sensitivity and/or increased dynamic range might represent an option for a further improvement of this approach (Mustafi et al., 2015; Tabor et al., 2009). Genome sequencing and insertion of selected SNPs into the parental Δ*aceE* strain background resulted in the identification of novel mutations, which directly affect product (*ureD*-E188*) or by-product (*glxR*-T93S) formation. The observed phenotypes were further confirmed by enhanced batch cultivations in a bioreactor system (Fig. S4). These results prove the general applicability of this approach for strain

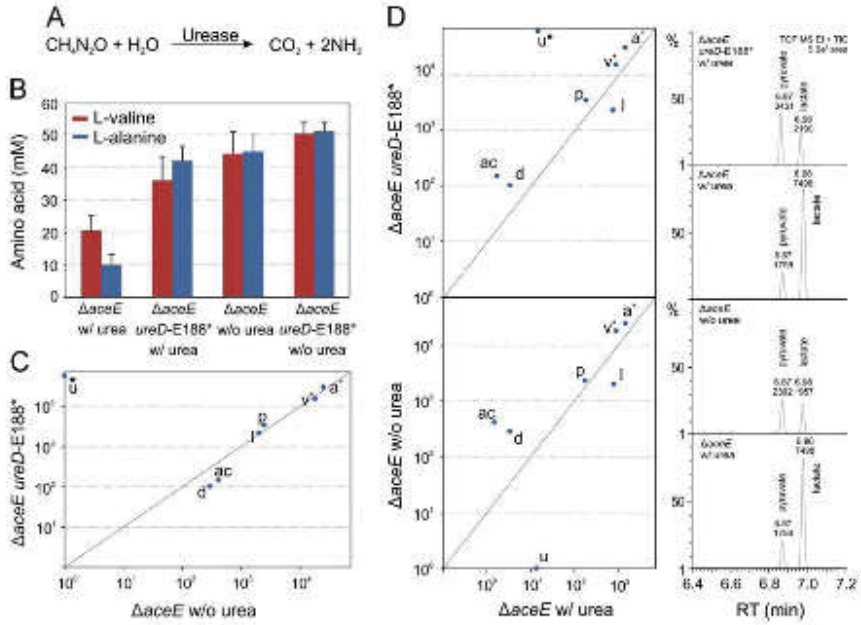

Fig. 5. Influence of urea on the L-valine production of *C. glutamicum* Δ*aceE*. (A) Urea is degraded by urease activity to CO_2 and NH_3. (B–D) *C. glutamicum* Δ*aceE* and *C. glutamicum* Δ*aceE ureD*-E188* were incubated in shake flasks containing CGXII minimal medium prepared with 5 g/l urea or without urea. After 30 h, (B) L-valine (red) and L-alanine (blue) titers were measured by uHPLC and (C+D) the supernatant was analyzed by GC-ToF-MS. Peak areas of MS spectra are plotted against each other. The solid line marks the 45 degree angle line. Abbreviations: alanine (a), 2-aceto-lactate (ac), dihydroxyisovalerate (d), lactate (l), pyruvate (p), urea (u), valine (v). Saturated peak areas are marked with an asterisk (*), while the plus (+) indicates the sum of peak areas of different trimethylsilyl (TMS) derivatives (L-valine 1TMS and L-valine 2TMS; L-alanine 2TMS and L-alanine 3TMS). Integrated cutting of the chromatograms shows relative pyruvate and lactate levels.

engineering and highlight the versatile application of biosensors for the improvement and analysis of production strains.

The generation of genetic diversity is a critical first step in several metabolic engineering approaches. Nowadays, random mutagenesis and screening strategies incorporating the entire genome are widely used for strain development (Derkx et al., 2014; Santos and Stephanopoulos, 2008; Schallmey et al., 2014). Chemical or physical mutagens such as N′-methyl-N′-nitro-N-nitrosoguanidine (MNNG) or UV radiation typically induce several hundred base transitions (Harper and Lee, 2012). Furthermore, mutator strains containing defective DNA repair systems induce up to 5000-fold increased mutation rates (Greener et al., 1997). In a recent study, a mutator phenotype was integrated as an actuator into a synthetic regulatory circuit under the control of a small molecule biosensor. In this way, the mutation rate of the particular strains was flexibly controlled by the concentration of the desired molecule (Chou and Keasling, 2013). All these strategies, however, were shown to generate hundreds of genomic modifications in one strain including single beneficial mutations, which are usually obscured by a high number of neutral and deleterious mutations (Binder et al., 2012; Chou and Keasling, 2013; Derkx et al., 2014). Identification of beneficial mutations, therefore, remains extremely laborious due to the lack of a selective pressure as imposed during biosensor-driven evolution. In contrast to random mutagenesis, adaptive evolution strategies have been shown to lead to a considerably low number of genomic modifications by selecting against detrimental mutations at the same time (Charusanti et al., 2012; Herring et al., 2006). Our biosensor-driven evolution of the Δ*aceE* strain resulted in a total of seven SNPs accumulated within the genome, which enabled the prompt identification of promising candidates for further analysis (Fig. 4; Table 2).

During the evolution of the Δ*aceE* strain, four mutations led to amino acid changes or to a stop codon in annotated genes. When mutations were inserted into the non-evolved Δ*aceE* parental strain, each mutation alone was found to increase the L-valine production. This finding strongly argues that biosensor-based evolution directly selects for strains that accumulate mutations according to the selective pressure. Of these, a mutation in the global regulator GlxR was identified. GlxR represents a central DNA-binding transcriptional regulator of the CRP/FNR protein family in *C. glutamicum*, which binds cAMP and regulates more than 180 genes involved in, amongst others, carbon and nitrogen metabolism, as well as respiration (Kohl et al., 2008; Kohl and Tauch, 2009). During biosensor-based evolution, the amino acid residue threonine at position 93, which is part of the cAMP-binding pocket, was replaced by serine (Townsend et al., 2014). T93 is conserved in *C. glutamicum* and its relative *Mycobacterium tuberculosis*, while this residue is replaced by serine in *E. coli* species (Townsend et al., 2014). We found that this mutation was established in the population after the third sorting step – along with the reduction of L-alanine production. Inserting the SNP into the non-evolved Δ*aceE* strain resulted in a significantly reduced formation of the by-product L-alanine (Fig. 4B). Other tested SNPs did not feature lower L-alanine production thus showing the specificity of the GlxR-T93S effect. Transcriptome analysis revealed the downregulation of several GlxR-activated genes and the upregulation of a set of GlxR-repressed genes after the third evolution step (Table S1). Based on current knowledge, the regulation of the L-alanine aminotransferases AlaT and AvtA is not directly coordinated by the GlxR regulon (Pauling et al., 2012) illustrating that a global reorganization of the regulatory/metabolic networks seems likely to be responsible for the observed production phenotype.

A further mutation beneficial for L-valine production was identified in the gene encoding the urease accessory protein UreD. The urease of *C. glutamicum* is encoded by the *ureABCEFGD* operon encoding structural and accessory proteins catalyzing the degradation of urea to carbon dioxide and ammonium (Nolden et al., 2000).

During biosensor-based evolution, the codon for glutamate residue 188 in the accessory protein UreD was replaced by a stop codon leading to the formation of a truncated protein. Introduction of the UreD-E188* into the parental strain significantly increased the L-valine production of *C. glutamicum* Δ*aceE* by about 100%. This effect was successfully attributed to a strong downregulation of the urease reaction, since a further increase was observed when the CGXII minimal medium was prepared without urea (Fig. 5). In line with this finding, previous studies revealed that the disruption of *ureD* reduces urease activity from 7.8 U (mg protein)$^{-1}$ to 0.1 U (mg protein)$^{-1}$ inhibiting the degradation of urea to carbon dioxide and ammonium (Nolden et al., 2000). Residual urease activity may explain the further increase of L-valine production by cultivation without urea compared to the effect of the *ureD*-E188* mutation in the presence of urea. Consequently, the lack of urea and/or a non-functional urease enzyme are thought to result in reduced intracellular levels of carbon dioxide and ammonium. During fermentation of *C. glutamicum* wild-type cells, Blombach et al. observed an increased level of the by-products L-alanine and L-valine under low CO_2/HCO_3^- concentrations (Blombach et al., 2013). In accordance with their findings, metabolome analysis (using GC-ToF) revealed an increase of the L-valine biosynthesis pathway intermediates 2-aceto-lactate and dihydroxyisovalerate suggesting an increased flux towards L-valine. Furthermore, we observed a shift from lactate to pyruvate overflow in the absence of urea or in the *ureD*-E188* background. As *C. glutamicum* is known to produce increased levels of lactate under oxygen deprivation (Hasegawa et al., 2012), we assume that reduced levels of dissolved carbon dioxide might affect lactate dehydrogenase activity and increase pyruvate availability. In addition, we hypothesize that reduced levels of hydrogen carbonate might impair the activity of the anapleurotic enzymes phosphoenolpyruvate (PEPCx) and pyruvate carboxylases (PCx) *in vivo*, which play the major role of carboxylation reactions in *C. glutamicum*, leading to an increased pool of pyruvate for L-valine production (Peters-Wendisch et al., 1998) (Fig. 1).

Rational engineering approaches of the *C. glutamicum* Δ*aceE* strain yielded final L-valine titers of up to 412 mM or 437 mM during fed-batch fermentation by the overexpression of L-valine biosynthesis genes, deletion of by-product pathways, improvement of precursor and reduction equivalent supply (Blombach et al., 2008; Chen et al., 2015). The great success of the biosensor-driven evolution approach was the identification of alternative, non-intuitive targets, which are obscured by the limited knowledge of the bacterial physiology and which can further improve the production of rationally engineered strains.

In several recent studies, adaptive laboratory evolution approaches served as a complementary strategy for the improvement of production strains (Abatemarco et al., 2013; Portnoy et al., 2011). Simple serial cultivation strategies have been successfully applied to increase the growth rate (Cheng et al., 2014; Fong et al., 2005) as well as tolerance of certain growth substrates (Lee et al., 2013, 2011) or stress conditions immediately linked to product/by-product formation (Reyes et al., 2014). Especially, in the case of growth-linked production processes, an increased growth rate immediately coincides with an improved production rate. For example, by serial transfer of *E. coli* cultures, Fong et al. were able to improve the growth rate along with lactate production (Fong et al., 2005). Furthermore, engineering of *S. cerevisiae* for increased ethanol tolerance was associated with the improvement in ethanol production from glucose (Alper et al., 2006). In the present study, we now successfully applied a metabolite biosensor to exert artificial selective pressure on intracellular product formation in order to specifically enrich mutations leading to an improved production phenotype. The observed phenotype established during the evolution procedure was finally attributed to single SNPs and verified in the parental strain background.

In conclusion, biosensor-driven evolution proved as an efficient strategy to balance metabolic fluxes according to the engineer's purposes without any deep knowledge of the complex bacterial physiology. This approach might also be of great benefit for the establishment of heterologous pathways in order to adapt the organism to changed energy and metabolite fluxes. Thus, biosensor-driven *in vivo* evolution represents a promising complementary strategy to rational metabolic engineering and thereby enlarges the current repertoire of engineering techniques.

Acknowledgments

We thank Jannick Kappelmann and Michael Limberg for fruitful discussions, and Christian Rückert for valuable contribution to sequence data analysis. This work was supported by the German Federal Ministry of Education and Research (BMBF OptoSys grant 031A167B) and the Helmholtz Association (Helmholtz YIG VH-NG-716).

Appendix A. Supplementary material

Supplementary data associated with this article can be found in the online version at http://dx.doi.org/10.1016/j.ymben.2015.09.017.

References

Abatemarco, J., Hill, A., Alper, H.S., 2013. Expanding the metabolic engineering toolbox with directed evolution. Biotechnol. J. 8, 1397–1410.
Alper, H., Moxley, J., Nevoigt, E., Fink, G.R., Stephanopoulos, G., 2006. Engineering yeast transcription machinery for improved ethanol tolerance and production. Science 314, 1565–1568.
Atsumi, S., Wu, T.Y., Machado, I.M., Huang, W.C., Chen, P.Y., Pellegrini, M., Liao, J.C., 2010. Evolution, genomic analysis, and reconstruction of isobutanol tolerance in *Escherichia coli*. Mol. Syst. Biol. 6, 449.
Barrick, J.E., Lenski, R.E., 2013. Genome dynamics during experimental evolution. Nat. Rev. Genet. 14, 827–839.
Baumgart, M., Luder, K., Grover, S., Gätgens, C., Besra, G.S., Frunzke, J., 2013. IpsA, a novel LacI-type regulator, is required for inositol-derived lipid formation in *Corynebacteria* and *Mycobacteria*. BMC Biol. 11, 122.
Binder, S., Schendzielorz, G., Stabler, N., Krumbach, K., Hoffmann, K., Bott, M., Eggeling, L., 2012. A high-throughput approach to identify genomic variants of bacterial metabolite producers at the single-cell level. Genome Biol. 13, R40.
Blombach, B., Buchholz, J., Busche, T., Kalinowski, J., Takors, R., 2013. Impact of different CO_2/HCO_3^- levels on metabolism and regulation in *Corynebacterium glutamicum*. J. Biotechnol. 168, 331–340.
Blombach, B., Schreiner, M.E., Bartek, T., Oldiges, M., Eikmanns, B.J., 2008. *Corynebacterium glutamicum* tailored for high-yield L-valine production. Appl. Microbiol. Biotechnol. 79, 471–479.
Blombach, B., Schreiner, M.E., Holatko, J., Bartek, T., Oldiges, M., Eikmanns, B.J., 2007. L-valine production with pyruvate dehydrogenase complex-deficient *Corynebacterium glutamicum*. Appl. Environ. Microbiol. 73, 2079–2084.
Buchholz, J., Schwentner, A., Brunnenkan, B., Gabris, C., Grimm, S., Gerstmeir, R., Takors, R., Eikmanns, B.J., Blombach, B., 2013. Platform engineering of *Corynebacterium glutamicum* with reduced pyruvate dehydrogenase complex activity for improved production of L-lysine, L-valine, and 2-ketoisovalerate. Appl. Environ. Microbiol. 79, 5566–5575.
Charusanti, P., Fong, N.L., Nagarajan, H., Pereira, A.R., Li, H.J., Abate, E.A., Su, Y., Gerwick, W.H., Palsson, B.O., 2012. Exploiting adaptive laboratory evolution of *Streptomyces clavuligerus* for antibiotic discovery and overproduction. PLoS One 7, e33727.
Chen, C., Li, Y., Hu, J., Dong, X., Wang, X., 2015. Metabolic engineering of *Corynebacterium glutamicum* ATCC13869 for l-valine production. Metab. Eng. 29, 66–75.
Cheng, K.K., Lee, B.S., Masuda, T., Ito, T., Ikeda, K., Hirayama, A., Deng, L., Dong, J., Shimizu, K., Soga, T., Tomita, M., Palsson, B.O., Robert, M., 2014. Global metabolic network reorganization by adaptive mutations allows fast growth of *Escherichia coli* on glycerol. Nat. Commun. 5, 3233.
Chou, H.H., Keasling, J.D., 2013. Programming adaptive control to evolve increased metabolite production. Nat. Commun. 4, 2595.
Derkx, P.M., Janzen, T., Sorensen, K.I., Christensen, J.E., Stuer-Lauridsen, B., Johansen, E., 2014. The art of strain improvement of industrial lactic acid bacteria without the use of recombinant DNA technology. Microb. Cell Fact. 13 (Suppl 1), S5.

Dietrich, J.A., McKee, A.E., Keasling, J.D., 2010. High-throughput metabolic engineering: advances in small-molecule screening and selection. Annu. Rev. Biochem. 79, 563–590.
Dietrich, J.A., Shis, D.L., Alikhani, A., Keasling, J.D., 2013. Transcription factor-based screens and synthetic selections for microbial small-molecule biosynthesis. ACS Synth. Biol. 2, 47–58.
Eckdahl, T.T., Campbell, A.M., Heyer, L.J., Poet, J.L., Blauch, D.N., Snyder, N.L., Atchley, D.T., Baker, E.J., Brown, M., Brunner, E.C., Callen, S.A., Campbell, J.S., Carr, C.J., Carr, D.R., Chadinha, S.A., Chester, G.L., Chester, J., Clarkson, B.R., Cochran, K.E., Doherty, S.E., Doyle, C., Dwyer, S., Edlin, L.M., Evans, K.A., Fluharty, T., Frederick, J., Galeota-Sprung, J., Gammon, B.L., Grieshaber, B., Gronniger, J., Gutteridge, K., Heaningsen, J., Ison, B., Itell, H.L., Keffeler, E.C., Lantz, A.J., Lim, J.N., McGuire, E. P., Moore, A.K., Morton, J., Nakano, M., Pearson, S.A., Perkins, V., Parrish, P., Pierson, C.E., Polpityaarachchige, S., Quaney, M.J., Slattery, A., Smith, K.E., Spell, J., Spencer, M., Taye, T., Trueblood, K., Vrana, C.J., Whitesides, E.T., 2015. Programmed evolution for optimization of orthogonal metabolic output in bacteria. PLoS One 10, e0118322.
Eggeling, L., Bott, M., 2005. Handbook of *Corynebacterium glutamicum*. CRC Press, Boca Raton, FL.
Eggeling, L., Bott, M., Marienhagen, J., 2015. Novel screening methods-biosensors. Curr. Opin. Biotechnol. 35C, 30–36.
Eggeling, L., Pfefferle, W., Sahm, H., (Eds.), 2001. Amino acids. Cambridge University Press London, UK.
Eikmanns, B.J., Blombach, B., 2014. The pyruvate dehydrogenase complex of *Corynebacterium glutamicum*: an attractive target for metabolic engineering. J. Biotechnol. 192 (Pt B), 339–345.
Eikmanns, B.J., Thum-Schmitz, N., Eggeling, L., Ludtke, K.U., Sahm, H., 1994. Nucleotide sequence, expression and transcriptional analysis of the *Corynebacterium glutamicum gltA* gene encoding citrate synthase. Microbiology 140, 1817–1828.
Feist, A.M., Zielinski, D.C., Orth, J.D., Schellenberger, J., Herrgard, M.J., Palsson, B.O., 2010. Model-driven evaluation of the production potential for growth-coupled products of *Escherichia coli*. Metab. Eng. 12, 173–186.
Fong, S.S., Burgard, A.P., Herring, C.D., Knight, E.M., Blattner, F.R., Maranas, C.D., Palsson, B.O., 2005. *In silico* design and adaptive evolution of *Escherichia coli* for production of lactic acid. Biotechnol. Bioeng. 91, 643–648.
Gibson, D.G., Young, L., Chuang, R.Y., Venter, J.C., Hutchison 3rd, C.A., Smith, H.O., 2009. Enzymatic assembly of DNA molecules up to several hundred kilobases. Nat. Methods 6, 343–345.
Greener, A., Callahan, M., Jerpseth, B., 1997. An efficient random mutagenesis technique using an *E. coli* mutator strain. Mol. Biotechnol. 7, 189–195.
Hanahan, D., 1983. Studies on transformation of *Escherichia coli* with plasmids. J. Mol. Biol. 166, 557–580.
Harper, M., Lee, C.J., 2012. Genome-wide analysis of mutagenesis bias and context sensitivity of N-methyl-N′-nitro-N-nitrosoguanidine (NTG). Mutat. Res. 731, 64–67.
Hasegawa, S., Uematsu, K., Natsuma, Y., Suda, M., Hiraga, K., Jojima, T., Inui, M., Yukawa, H., 2012. Improvement of the redox balance increases L-valine production by *Corynebacterium glutamicum* under oxygen deprivation conditions. Appl. Environ. Microbiol. 78, 865–875.
Herring, C.D., Raghunathan, A., Honisch, C., Patel, T., Applebee, M.K., Joyce, A.R., Albert, T.J., Blattner, F.R., van den Boom, D., Cantor, C.R., Palsson, B.O., 2006. Comparative genome sequencing of *Escherichia coli* allows observation of bacterial evolution on a laboratory timescale. Nat. Genet. 38, 1406–1412.
Jiménez, J., Benítez, T., 1987. Adaptation of yeast cell membranes to ethanol. Appl. Environ. Microbiol. 53, 1196–1198.
Jungwirth, B., Sala, C., Kohl, T.A., Uplekar, S., Baumbach, J., Cole, S.T., Pühler, A., Tauch, A., 2013. High-resolution detection of DNA binding sites of the global transcriptional regulator GlxR in *Corynebacterium glutamicum*. Microbiology 159, 12–22.
Kalinowski, J., Bathe, B., Bartels, D., Bischoff, N., Bott, M., Burkovski, A., Dusch, N., Eggeling, L., Eikmanns, B.J., Gaigalat, L., Goesmann, A., Hartmann, M., Huthmacher, K., Kramer, R., Linke, B., McHardy, A.C., Meyer, F., Mockel, B., Pfefferle, W., Pühler, A., Rey, D.A., Rückert, C., Rupp, O., Sahm, H., Wendisch, V.F., Wiegrabe, I., Tauch, A., 2003. The complete *Corynebacterium glutamicum* ATCC 13032 genome sequence and its impact on the production of L-aspartate-derived amino acids and vitamins. J. Biotechnol. 104, 5–25.
Keilhauer, C., Eggeling, L., Sahm, H., 1993. Isoleucine synthesis in *Corynebacterium glutamicum*: molecular analysis of the *ilvB-ilvN-ilvC* operon. J. Bacteriol. 175, 5595–5603.
Kensy, F., Zang, E., Faulhammer, C., Tan, R.K., Buchs, J., 2009. Validation of a high-throughput fermentation system based on online monitoring of biomass and fluorescence in continuously shaken microtiter plates. Microb. Cell Fact. 8, 31.
Kinoshita, S., Udaka, S., Shimono, M., 2004. Studies on the amino acid fermentation. Part 1. Production of L-glutamic acid by various microorganisms. J. Gen. Appl. Microbiol. 50, 331–343.
Kohl, T.A., Baumbach, J., Jungwirth, B., Pühler, A., Tauch, A., 2008. The GlxR regulon of the amino acid producer *Corynebacterium glutamicum*: *in silico* and *in vitro* detection of DNA binding sites of a global transcription regulator. J. Biotechnol. 135, 340–350.
Kohl, T.A., Tauch, A., 2009. The GlxR regulon of the amino acid producer *Corynebacterium glutamicum*: Detection of the corynebacterial core regulon and integration into the transcriptional regulatory network model. J. Biotechnol. 143, 239–246.
Lange, C., Mustafi, N., Frunzke, J., Kennerknecht, N., Wessel, M., Bott, M., Wendisch, V.F., 2012. Lrp of *Corynebacterium glutamicum* controls expression of the *brnFE* operon encoding the export system for L-methionine and branched-chain amino acids. J. Biotechnol. 158, 231–241.
Lee, J.Y., Seo, J., Kim, E.S., Lee, H.S., Kim, P., 2013. Adaptive evolution of *Corynebacterium glutamicum* resistant to oxidative stress and its global gene expression profiling. Biotechnol. Lett. 35, 709–717.
Lee, J.Y., Yang, K.S., Jang, S.A., Sung, B.H., Kim, S.C., 2011. Engineering butanol-tolerance in *Escherichia coli* with artificial transcription factor libraries. Biotechnol. Bioeng. 108, 742–749.
Leuchtenberger, W., (Ed.), 1996. Amino Acids – Technical Production and Use. VCH, Weinheim, Germany.
Liu, Z.L., 2006. Genomic adaptation of ethanologenic yeast to biomass conversion inhibitors. Appl. Microbiol. Biotechnol. 73, 27–36.
Marienhagen, J., Eggeling, L., 2008. Metabolic function of *Corynebacterium glutamicum* aminotransferases AlaT and AvtA and impact on L-valine production. Appl. Environ. Microbiol. 74, 7457–7462.
Marietou, A., Nguyen, A.T., Allen, E.E., Bartlett, D.H., 2014. Adaptive laboratory evolution of *Escherichia coli* K-12 MG1655 for growth at high hydrostatic pressure. Front. Microbiol. 5, 749.
Mustafi, N., Bott, M., Frunzke, J., 2015. Genetically-encoded biosensors for strain development and single cell analysis of *Corynebacterium glutamicum*. In: Burkovski, A. (Ed.), *Corynebacterium glutamicum*: From Systems Biology to Biotechnological Applications. Caister Academic Press, Norfolk, England, p. 190.
Mustafi, N., Grunberger, A., Kohlheyer, D., Bott, M., Frunzke, J., 2012. The development and application of a single-cell biosensor for the detection of L-methionine and branched-chain amino acids. Metab. Eng. 14, 449–457.
Mustafi, N., Grunberger, A., Mahr, R., Helfrich, S., Noh, K., Blombach, B., Kohlheyer, D., Frunzke, J., 2014. Application of a genetically encoded biosensor for live cell imaging of L-valine production in pyruvate dehydrogenase complex-deficient *Corynebacterium glutamicum* strains. PLoS One 9, e85731.
Niebisch, A., Bott, M., 2001. Molecular analysis of the cytochrome bc1-aa3 branch of the *Corynebacterium glutamicum* respiratory chain containing an unusual diheme cytochrome c1. Arch. Microbiol. 175, 282–294.
Nolden, L., Beckers, G., Mockel, B., Pfefferle, W., Nampoothiri, K.M., Krämera, R., Burkovskia, A., 2000. Urease of *Corynebacterium glutamicum*: organization of corresponding genes and investigation of activity. FEMS Microbiol. Lett. 189, 305–310.
Oide, S., Gunji, W., Moteki, Y., Yamamoto, S., Suda, M., Jojima, T., Yukawa, H., Inui, M., 2015. Thermal and solvent stress cross-tolerance conferred to *Corynebacterium glutamicum* by adaptive laboratory evolution. Appl. Environ. Microbiol. 81, 2284–2298.
Paczia, N., Nilgen, A., Lehmann, T., Gätgens, J., Wiechert, W., Noack, S., 2012. Extensive exometabolome analysis reveals extended overflow metabolism in various microorganisms. Microb. Cell Fact. 11, 122.
Pauling, J., Rottger, R., Tauch, A., Azevedo, V., Baumbach, J., 2012. CoryneRegNet 6.0 – Updated database content, new analysis methods and novel features focusing on community demands. Nucleic Acids Res. 40, D610–D614.
Peters-Wendisch, P.G., Kreutzer, C., Kalinowski, J., Patek, M., Sahm, H., Eikmanns, B. J., 1998. Pyruvate carboxylase from *Corynebacterium glutamicum*: characterization, expression and inactivation of the *pyc* gene. Microbiology 144 (Pt 4), 915–927.
Portnoy, V.A., Bezdan, D., Zengler, K., 2011. Adaptive laboratory evolution–harnessing the power of biology for metabolic engineering. Curr. Opin. Biotechnol. 22, 590–594.
Raman, S., Rogers, J.K., Taylor, N.D., Church, G.M., 2014. Evolution-guided optimization of biosynthetic pathways. PNAS 111, 17803–17808.
Reyes, L.H., Gomez, J.M., Kao, K.C., 2014. Improving carotenoids production in yeast via adaptive laboratory evolution. Metab. Eng. 21, 26–33.
Sambrook, J., MacCallum, P., Russell, D., 2001. Molecular Cloning: A Laboratory Manual. Cold Spring Harbor Laboratory Press, New York.
Sandberg, T.E., Pedersen, M., LaCroix, R.A., Ebrahim, A., Bonde, M., Herrgard, M.J., Palsson, B.O., Sommer, M., Feist, A.M., 2014. Evolution of *Escherichia coli* to 42 degrees C and subsequent genetic engineering reveals adaptive mechanisms and novel mutations. Mol. Biol. Evol. 31, 2647–2662.
Santos, C.N., Stephanopoulos, G., 2008. Melanin-based high-throughput screen for L-tyrosine production in *Escherichia coli*. Appl. Environ. Microbiol. 74, 1190–1197.
Schäfer, A., Tauch, A., Jäger, W., Kalinowski, J., Thierbach, G., Pühler, A., 1994. Small mobilizable multi-purpose cloning vectors derived from the *Escherichia coli* plasmids pK18 and pK19: selection of defined deletions in the chromosome of *Corynebacterium glutamicum*. Gene 145, 69–73.
Schallmey, M., Frunzke, J., Eggeling, L., Marienhagen, J., 2014. Looking for the pick of the bunch: high-throughput screening of producing microorganisms with biosensors. Curr. Opin. Biotechnol. 26, 148–154.
Schreiner, M.E., Fiur, D., Holatko, J., Patek, M., Eikmanns, B.J., 2005. E1 enzyme of the pyruvate dehydrogenase complex in *Corynebacterium glutamicum*: molecular analysis of the gene and phylogenetic aspects. J. Bacteriol. 187, 6005–6018.
Siedler, S., Stahlhut, S.G., Malla, S., Maury, J., Neves, A.R., 2014. Novel biosensors based on flavonoid-responsive transcriptional regulators introduced into *Escherichia coli*. Metab. Eng. 21, 2–8.
Tabor, J.J., Groban, E.S., Voigt, C.A., 2009. Performance characteristics for sensors and circuits used to program E.coli. In: Lee, S.Y. (Ed.), Systems Biology and Biotechnology of *Escherichia coli*. Springer Science & Business Media B.V.

Tenaillon, O., Rodriguez-Verdugo, A., Gaut, R.L., McDonald, P., Bennett, A.F., Long, A. D., Gaut, B.S., 2012. The molecular diversity of adaptive convergence. Science 335, 457–461.

Teramoto, H., Inui, M., Yukawa, H., 2011. Transcriptional regulators of multiple genes involved in carbon metabolism in *Corynebacterium glutamicum*. J. Biotechnol. 154, 114–125.

Townsend, P.D., Jungwirth, B., Pojer, F., Bussmann, M., Money, V.A., Cole, S.T., Pohler, A., Tauch, A., Bott, M., Cann, M.J., Pohl, E., 2014. The crystal structures of apo and cAMP-bound GlxR from *Corynebacterium glutamicum* reveal structural and dynamic changes upon cAMP binding in CRP/FNR family transcription factors. PLoS One 9, e113265.

van der Rest, M.E., Lange, C., Molenaar, D., 1999. A heat shock following electroporation induces highly efficient transformation of *Corynebacterium glutamicum* with xenogeneic plasmid DNA. Appl. Microbiol. Biotechnol. 52, 541–545.

Wendisch, V.F., (Ed.), 2007. Amino Acid Biosynthesis – Pathways, Regulation and Metabolic Engineering. Springer-Verlag, Berlin Heidelberg.

Xie, W., Lv, X., Ye, L., Zhou, P., Yu, H., 2015. Construction of lycopene-overproducing *Saccharomyces cerevisiae* by combining directed evolution and metabolic engineering. Metab. Eng. 30, 69–78.

3.3 Urease inactivity increases L-valine production in *Corynebacterium glutamicum*

Regina Mahr and Julia Frunzke*

IBG-1: Biotechnology, Forschungszentrum Jülich, Jülich, Germany

*Corresponding author

Current state: To be submitted

Author contributions

Own contribution to the work: 95%

	Name	Contribution
Project planning	***Mahr, R.***	90%
	Frunzke, J.	10%
Writing	***Mahr, R.***	95%
	Frunzke, J.	5%

	Name	Experimental work	Evaluation	Preparation of figure/table
Figure 1	***Mahr, R.***	100%	100%	100%
Figure 2	***Mahr, R.***	100%	100%	100%
Figure 3	***Mahr, R.***	100%	100%	100%
Figure 4	***Mahr, R.***	100%	100%	100%
Table 1	***Mahr, R.***	-	-	100%
Table 2	***Mahr, R.***	100%	100%	100%
Figure S1	***Mahr, R.***	80%	80%	95%
	Gätgens, J.	20%	20%	5%
Table S1	***Mahr, R.***	100%	100%	100%

Urease inactivity increases L-valine production

Regina Mahr and Julia Frunzke

Institute of Bio-and Geosciences, IBG-1: Biotechnology, Forschungszentrum Jülich, Germany

Abstract

Urea is known as important nitrogen source for the amino acid producer *Corynebacterium glutamicum*. During the biosensor-driven adaptive laboratory evolution of *C. glutamicum* Δ*aceE*, we identified a loss-of-function mutation in UreD (*ureD*-E188*), which increases L-valine production by about 100%. Previously, the disruption of UreD was reported to lead to the formation of an inactive urease enzyme complex, which consequently inhibits the degradation of urea to carbon dioxide and ammonia. Previous metabolome analysis of *C. glutamicum* Δ*aceE* and Δ*aceE ureD*-E188* led to the hypothesis that the reduced level of carbon dioxide might in turn reduce the activity of anaplerotic enzymes phosphoenolpyruvate (PEPCx) and pyruvate carboxylase (PCx). This seems to increase the availability of pyruvate for L-valine biosynthesis. In this study, we analyzed the relationship between L-valine production, anaplerosis, urease activity and CO_2/HCO_3^- availability: By the additional deletion of *pyc* (encoding PCx) in the Δ*aceE* and Δ*aceE ureD*-E188* background, growth was significantly reduced and even inhibited for the urease inactive strain. This fact showed that anaplerosis plays indeed an important role during growth on acetate. The addition of hydrogen carbonate partly complemented the lack of *pyc*, which reveals the impact of CO_2/HCO_3^- availability on the activity of anaplerotic enzymes. Furthermore, batch fermentation by additional CO_2 aeration reduced growth and L-valine production of the Δ*aceE ureD*-E188* to the level of the urease active Δ*aceE* strain. As urea degradation increases the pH by ammonia formation and CO_2 dissociates in water dependent on the pH, batch fermentation was performed at different pH levels. Together with transcriptome analysis of Δ*aceE* and Δ*aceE ureD*-E188*, the increased pH was proposed to enhance the activity of the central metabolism, which contributes to the reduced availability of pyruvate. In conclusion, the beneficial effect of urea deficiency on L-valine production results from a complex interplay between pH and CO_2/HCO_3^- availability.

Introduction

For almost 60 years, *Corynebacterium glutamicum* has been known as an excellent platform organism for large-scale amino acid production (Kinoshita et al., 1957). Due to the lack of biosynthesis enzymes in humans and animals, the nine essential amino acids including L-valine are of central interest for the biotechnological industry (Leuchtenberger et al., 2005; Mitsuhashi, 2014). In *C. glutamicum*, the production of L-valine branches in the glycolysis from pyruvate (Fig. 1A). To increase the pyruvate pool, the E1p subunit (*aceE*) of the pyruvate dehydrogenase complex (PDHC) was deleted, which provided an excellent basal strain for engineering L-valine production strains (Blombach et al., 2008; Blombach et al., 2007; Eikmanns and Blombach, 2014). Due to the inactivation of the PDHC, cells feature growth-decoupled L-valine production in minimal medium containing a mixture of glucose and acetate as carbon source: The Δ*aceE* strain grows on acetate, which provides acetyl-CoA for the tricarboxylic acid (TCA) cycle,

and upon depletion, glucose is metabolized for the production of L-valine (Blombach et al., 2007; Eikmanns and Blombach, 2014; Oldiges et al., 2014).

During biosensor-driven adaptive laboratory evolution of the L-valine producer strain *C. glutamicum* Δ*aceE*, a loss-of-function mutation of urease (*ureD*-E188*) resulting in a truncated protein (aa 1-187) was isolated. The introduction of this point mutation led to significantly increased L-valine production by about two-fold in comparison to the parental strain (Fig. 1 B) (Mahr et al., 2015). Upon the disruption of *ureD*, Nolden and co-workers observed a reduction in urease activity from 7.8 U (mg protein)$^{-1}$ to 0.1 U (mg protein)$^{-1}$, which strongly diminishes the degradation of urea to two molecules ammonia and one molecule carbon dioxide (Fig. 1 C) (Nolden et al., 2000). Urea is a component of the original recipe for CGXII minimal medium (Keilhauer et al., 1993). A further increase of L-valine production was observed when CGXII minimal medium was prepared without urea (Fig. 1 B).

Metabolome analysis (GC-ToF) of *C. glutamicum* Δ*aceE ureD*-E188* revealed increased levels of the L-valine biosynthesis intermediates 2-aceto-lactate and dihydroxyisovalerate in the supernatant suggesting an increased flux towards L-valine compared to the Δ*aceE* strain (Mahr et al., 2015). Furthermore, a shift from lactate to pyruvate in the supernatant was observed for cultures lacking urea or containing the *ureD*-E188* mutation, which indicates intracellular accumulation of the L-valine precursor pyruvate (Mahr et al., 2015).

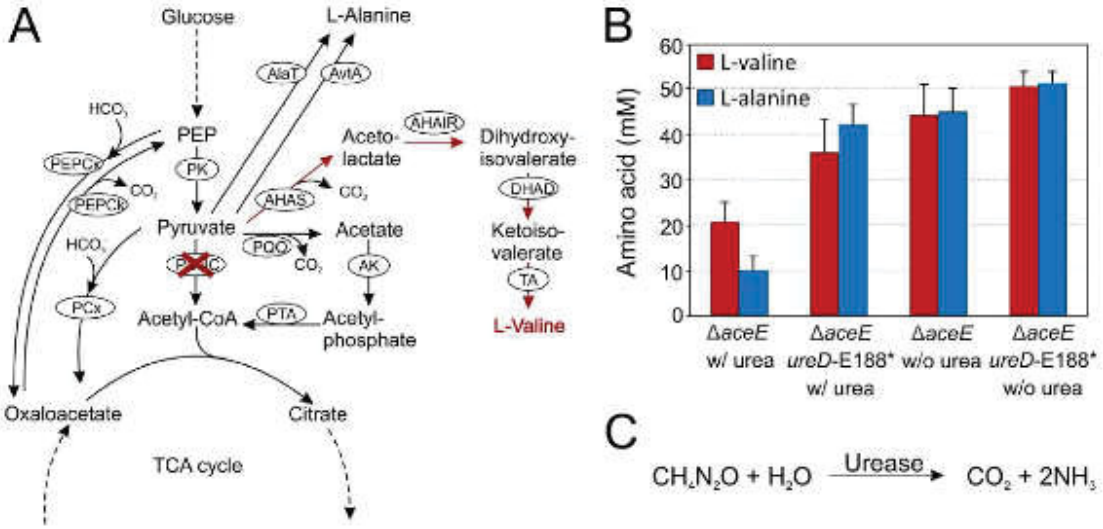

Fig. 1 L-valine production and the influence of urease inactivity. A. Overview of the central metabolism of *C. glutamicum* Δ*aceE* and the L-valine biosynthetic pathway. The Δ*aceE* strain harbors the deletion of the Ep1 subunit (red cross) of the pyruvate dehydrogenase complex (PDHC), which blocks the conversion of pyruvate to acetyl-CoA *via* PDHC activity. Abbreviations: acetohydroxy acid isomeroreductase (AHAIR), acetohydroxy acid synthase (AHAS), acetate kinase (AK), alanine aminotransferase (AlaT), alanine aminotransferase (AvtA), dihydroxy acid dehydratase (DHAD), pyruvate decarboxylase (PCx), pyruvate dehydrogenase complex (PDHC), pyruvate kinase (PK), phosphoenolpyruvate (PEP), PEP carboxykinase (PEPCk), PEP carboxylase (PEPCx), pyruvate:quinone oxidoreductase (PQO), phosphotransacetylase (PTA), transaminase B (TA). B. L-valine (red bars) and L-alanine (blue bars) titers in the supernatant were measured after 30 hours of shake flask cultivation of Δ*aceE* and Δ*aceE ureD*-E188* cells in CGXII minimal medium containing 222 mM glucose and 254 mM acetate prepared with 5 g l^{-1} urea or without urea. Data represent average values from three independent biological replicates. C. 1 mol urea is degraded by urease activity to 1 mol carbon dioxide and 2 mol ammonia.

Urea is an important and easily accessible nitrogen source for *C. glutamicum* besides glutamine, ammonium and creatinine (Nolden et al., 2000; Rehm et al., 2010). Urease presents a key enzyme for the utilization of urea as an alternative nitrogen source. The *ure* gene cluster *ureABCEFGD* encodes the three structural subunits (UreA, UreB, UreC) and the four accessory proteins (UreE, UreF, UreG, UreD) of urease. Thereof, the proteins UreC and UreD were found to be of crucial importance for urease activity and for growth on urea (Nolden et al., 2000).

The lack of urea or urease activity (*ureD*-E188*) was proposed to likewise reduce the availability of ammonia and carbon dioxide (Fig. 1 C). In this context, we hypothesized that the efflux of glycolytic products (phosphoenolpyruvate and pyruvate) into the TCA cycle *via* the hydrogen carbonate-dependent activity of the anaplerotic enzymes phosphoenolpyruvate (PEPCx, *ppc*) and pyruvate carboxylase (PCx, *pyc*) might be reduced under low CO_2/HCO_3^- concentrations (Blombach and Takors, 2015; Mahr et al., 2015). Hence, this might increase the pyruvate pool for L-valine biosynthesis (Fig. 1A). In this study, we demonstrate the influence of anaplerosis during growth on acetate by analyzing the urease-active and –inactive (*ureD*-E188*) *C. glutamicum* Δ*aceE* (±*pyc*) strain in the presence of increased levels of hydrogen carbonate or with CO_2 aeration during batch fermentation. As the degradation of urea impacts the pH and in turn the dissociation of carbon dioxide in water, the dependency of growth and production on pH during batch fermentation is analyzed. Together with transcriptome analysis of the urease-active and –inactive strain, a multilayered influence of urea availability on L-valine production was proposed: the effect of carbon dioxide availability on anaplerosis and the impact on pH-dependent gene regulation and enzymatic activity.

Material and Methods

Bacterial strains, media and growth conditions

All bacterial strains and plasmids used in this study are listed in Table 1. The strains are based on the *C. glutamicum* ATCC13032 wild-type strain (Kalinowski et al., 2003). If not stated differently, *C. glutamicum* Δ*aceE* cells were grown on brain heart infusion (BHI; Becton Dickinson, Heidelberg, Germany) agar plates containing 85 mM acetate at 30°C for two days. Then, one colony was picked and incubated for eight hours at 30°C and 170 rpm in 4 ml BHI medium containing 85 mM acetate. Afterwards, 20 ml of CGXII minimal medium (Keilhauer et al., 1993) containing 222 mM and 254 mM acetate were inoculated with cells from the first pre-culture. Overnight, the culture was incubated at 30°C and 120 rpm. The following day, the cells were washed with 0.9% (w/v) saline and inoculated in a baffled flask with fresh 50 ml CGXII minimal medium containing 222 mM glucose and 254 mM acetate to an optical density (OD_{600}) of 1. The culture was incubated at 30°C and 120 rpm. Where indicated, urea, which is part of the original CGXII recipe (Keilhauer et al., 1993), was not added to the CGXII minimal medium. Acetate and carbonate were provided in the medium as potassium acetate or potassium carbonate salt, respectively. Carbonate was added to the medium after autoclaving at a temperature of 30°C followed by filter sterilizing. The cell dry weight (CDW, g L^{-1}) was calculated from the measured OD_{600} by the following equation: CDW = OD_{600} x 0.3 g L^{-1} (Buchholz et al., 2013). *Escherichia coli* DH5α cells were grown on lysogeny broth (LB) agar plates or incubated in shake flasks with LB medium by agitation at 120 rpm. If necessary, kanamycin was added in a final concentration of 25 µg/ml for *C. glutamicum* or 50 µg/ml for *E. coli* to medium and agar plates.

Table 1: Bacterial strains, plasmids and oligonucleotides used in this study.

Strains or plasmids	Relevant characteristics	Source or reference
Strains		
C. glutamicum ATCC 13032	Biotin-auxotrophic wild type	(Kinoshita et al., 2004)
C. glutamicum Δ*aceE*	In-frame deletion of *cg2466*	(Schreiner et al., 2005)
C. glutamicum Δ*aceE ureD*-E188*	UreD Glu188 to stop codon	(Mahr et al., 2015)
C. glutamicum Δ*aceE* Δ*pyc*	In-frame deletion of *cg2466* and *cg0791*	This study
C. glutamicum Δ*aceE* Δ*pyc ureD*-E188*	In-frame deletion of *cg2466* and *cg0791*; UreD Glu188 to stop codon	This study
E. coli DH5α	*supE44* Δ*lacU169* (ϕ80*lacZ*DM15) *hsdR17 recA1 endA1 gyrA96 thi-1 relA1*	Invitrogen
Plasmids		
pK19mobsacBΔ*pyc*	pK19mobsacB containing the 1 kb fragment of the deleted *pyc* gene	(Peters-Wendisch et al., 1998)
Oligonucleotides	**Sequence (5'-3')**	
151-pyc-fw	GCAGATGCCATTTACCCG	
152-pyc-rv	CGGTGACAGACTCAACG	

Genomic deletion of pyc

The suicide plasmid pK19mobsacBΔ*pyc* was isolated from *E. coli* DH5α cells using the QIAprep spin miniprep kit (Qiagen, Hilden, Germany). The plasmid was transformed in electro-competent *C. glutamicum* Δ*aceE* and Δ*aceE ureD*-E188* cells by electroporation (van der Rest et al., 1999). First and second recombination events were performed and verified as previously described (Niebisch and Bott, 2001). The deletion of *pyc* was reviewed by amplification and sequencing using the primer pair 151-pyc-fw and 152-pyc-rv. Synthesis of required oligonucleotides and the sequencing of DNA fragments were performed in subcontracting with Eurofins MWG Operon (Ebersfeld, Germany).

Microtiter plate cultivation

Online monitoring of bacterial growth was performed in 48-well microtiter FlowerPlates (MFPs) using the BioLector cultivation system (m2p-labs GmbH, Baesweiler, Germany) (Kensy et al., 2009). *C. glutamicum* cells were inoculated from a pre-culture in 48-well MFPs containing 750 µl CGXII minimal medium with 222 mM glucose and 254 mM acetate to an OD_{600} of 1. In the BioLector, cells were incubated at 37°C and 1200 rpm. During cultivation, biomass formation was recorded as the backscattered light intensity (light wavelength 620 nm; signal gain factor of 20).

Batch fermentation

Batch fermentation was performed in the DASbox® Bioreactor system (Eppendorf, Hamburg, Germany). Prior to inoculation of fermenters, cells of an overnight pre-culture (50 ml BHI medium containing 85 mM acetate) were washed with 0.9% (w/v) saline. Initially, the fermenters were filled with 200 ml CGXII minimal medium containing 222 mM glucose and 254 mM

acetate and inoculated to an OD_{600} of 1. The cultures were tempered at 30°C. The bioreactors were sparged with 1 vvm synthetic air. Where indicated, the CO_2 concentration was increased to 10% (v/v). The dissolved oxygen concentration was adjusted to 30% by a stirrer speed cascade from 400 to 1200 rpm and was monitored using a polarimetric oxygen electrode (Oxyferm FDA, Hamilton, Bonaduz, Switzerland). According to the respective experiment, the pH was adjusted using 2 M potassium hydroxide and 2 hydrochloric acid, and measured by a standard pH electrode (Easyferm Plus, Hamilton, Bonaduz, Switzerland). Foam development was suppressed by manual injection of 0.1 ml 25% (v/v) silicon antifoam 204/water suspension when required (Sigma Aldrich, Steinheim, Germany).

Quantification of amino acid production

Using ultra-high performance liquid chromatography (uHPLC), amino acids were quantified as *ortho*-phthaldialdehyde derivatives by automatic pre-column derivatization. Separation of derivatives by reverse-phase chromatography was performed on an Agilent 1290 Infinity LC ChemStation (Agilent, Santa Clara, USA) equipped with a fluorescence detector. As eluent for the Zorbax Eclipse AAA 3.5 micron 4.6 x 7.5 mm column (Agilent, Santa Clara, USA), a gradient of Na-borate buffer (10 mM Na_2HPO_4; 10 mM $Na_2B_4O_7$, pH 8.2; adapted to operater's guide) and methanol was applied. Prior to analysis, samples were centrifuged for 10 min at 13,000 rpm and 4°C and diluted 1:100.

DNA microarrays

For transcriptome analysis, *C. glutamicum* Δ*aceE* and Δ*aceE ureD*-E188* cells were cultivated in 50 ml CGXII minimal medium containing 222 mM glucose and 254 mM acetate at 30°C and 120 rpm. Cells were harvested after 28 hours of cultivation (production phase). The cells were sedimented by centrifugation (4256 x *g*, 10 minutes, 4°C) and the pellet was immediately frozen in liquid nitrogen and stored at -80°C. RNA preparation, cDNA synthesis and microchip hybridization, scanning and evaluation were performed as previously described (Baumgart et al., 2013).

Results and Discussion

Deletion of *pyc* strongly affects the growth of *C. glutamicum* Δ*aceE* and Δ*aceE ureD*-E188*

The pyruvate carboxylase (PCx) encoded by *pyc* is the dominating enzyme in *C. glutamicum* for refueling the TCA cycle via oxaloacetate (Fig. 1 C) (Peters-Wendisch et al., 1998). We deleted *pyc* in the Δ*aceE* and Δ*aceE ureD*-E188* background to examine the influence of anaplerosis on growth and L-valine production. By microtiter cultivation in CGXII minimal medium, the strains Δ*aceE* and Δ*aceE ureD*-E188* featured growth rates of $0.24 \pm 0.006\ h^{-1}$ and $0.27 \pm 0.002\ h^{-1}$, respectively (Fig. 2 A). The additional deletion of *pyc* reduced the growth rate of strain Δ*aceE* Δ*pyc* to $0.15 \pm 0.005\ h^{-1}$ and almost inhibited growth (growth rate: $0.01 \pm 0.001\ h^{-1}$) of this mutant in CGXII minimal medium carrying the loss-of-function mutation in UreD (Δ*aceE* Δ*pyc ureD*-E188*). Moreover, strains with deleted *pyc* featured a significantly increased lag phase of about 20 hours. Peters-Wendisch et al. proposed a very low *in vivo* activity of the second anaplerotic enzyme PEPCx in *C. glutamicum* (Peters-Wendisch et al., 1993; Peters-Wendisch et al., 1998). In accordance with our findings, the lack of PCx activity seems not to be compensated by PEPCx. In addition, the activity of both anaplerotic enzymes is dependent on CO_2/HCO_3^- availability (Fig. 1 C) (Blombach and Takors, 2015; Sauer and Eikmanns, 2005). We hypothesize that urease inactivity evoked by the *ureD*-E188* mutation may result in decreased levels of intracellular carbon dioxide impacting the *in vivo* activity of anaplerotic enzymes. Thus, residual activity of PEPCx might not be sufficient to support growth in the absence of *pyc* in the strain Δ*aceE* Δ*pyc ureD*-E188* strain. The fact that CO_2 deficiency after inoculation induces a long lag phase is well known (Blombach and Takors, 2015; Repaske et al.,

1974). The extended lag phase is traditionally not observed during well-aerated batch fermentation. Under low pCO_2, Blombach and co-workers revealed a three phasic growth behavior with a strongly reduced growth rate (0.09 h^{-1}) of *C. glutamicum* Δ*pyc* in the second phase (Blombach et al., 2013). Furthermore, the additional deletion of *pyc* in a gradually engineered Δ*aceE* strain (Δ*aceE* Δ*pqo* Δ*pgi*) extended the time to reach the stationary phase (growth rate not indicated) (Blombach et al., 2008).

Altogether, these findings suggest that anaplerosis plays indeed an important role during growth of *C. glutamicum* Δ*aceE* and derivatives on acetate. At first sight, this seems surprising as acetate is known to repress phosphoenolpyruvate::sugar phosphotransferase system (PTS)-mediated glucose uptake via the regulator SugR (Blombach et al., 2009; Engels and Wendisch, 2007). However, the lack of glucose significantly impaired growth of the Δ*aceE* strain (Schreiner et al., 2005). For this reason, we suppose here the activity of alternative glucose uptake systems as recently described (Ikeda et al., 2011; Ikeda et al., 2015).

Phenotypic complementation by increased levels of hydrogen carbonate

To reveal whether carbon dioxide deficiency generated by urease inactivity or urea deficiency itself affect anaplerosis reducing indirectly the pyruvate pool for L-valine production, we cultivated the strains by providing hydrogen carbonate to the medium. The addition of 100 mM HCO_3^- had no effect on the growth rate of the Δ*aceE* Δ*pyc* strain itself (0.15 ± 0.002 h^{-1}), but it reduced the lag phase to eight hours. Interestingly, the Δ*aceE* Δ*pyc* *ureD*-E188* strain featured growth at a rate of 0.17 ± 0.002 h^{-1} and a lag-phase of about eight hours by cultivation in presence of 100 mM HCO_3^- (Fig. 2 A). These results indicate that the addition of hydrogen carbonate partly complemented the growth deficiency of the Δ*aceE* Δ*pyc* *ureD*-E188* strain proposing an important role of carbon dioxide delivery by urea for anaplerosis. We propose that full complementation by hydrogen carbonate is not achievable due to the low activity and minor role of PEPCx in *C. glutamicum* (Peters-Wendisch et al., 1998).

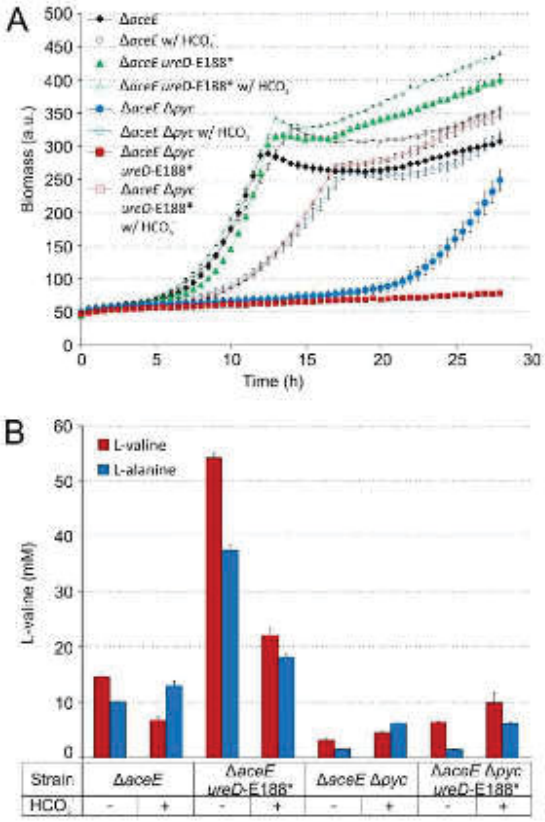

Fig. 2 The influence of carbonate on growth and production of *C. glutamicum* Δ*aceE* derivatives. A. Carbonate improves growth and biomass formation of Δ*aceE* (black, ♦, ◊), Δ*aceE* *ureD*-E188* (green, ▲, Δ), Δ*aceE* Δ*pyc* (blue, ●, ○) and Δ*aceE* Δ*pyc* *ureD*-E188* (red, ■, □) strains. From the first pre-culture in 4 ml BHI medium containing 85 mM acetate, a second pre-culture was inoculated in CGXII minimal medium containing 222 mM glucose and 254 mM acetate without (filled symbols) and with 100 mM carbonate (empty symbols). For online monitoring in the BioLector system, cells were inoculated in 750 µl fresh CGXII minimal medium (with 222 mM glucose, 254 mM acetate; +/-100 mM carbonate) to an OD_{600} of 1 and incubated at 30°C and 1200 rpm for 28 hours. B. L-valine (red bars) and L-alanine titers (blue bars) in the supernatant after 28 hours of cultivation in the BioLector. Data represent average values from three independent biological replicates.

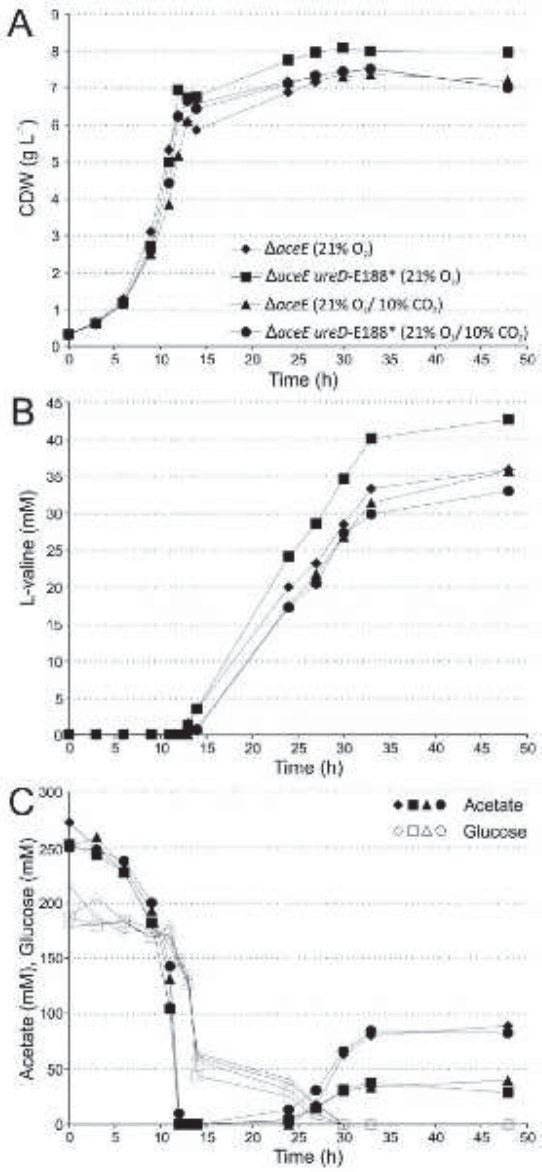

Fig. 3 Carbon dioxide influences A. biomass formation and B. L-valine production of *C. glutamicum* Δ*aceE ureD*-E188* during batch fermentation. *C. glutamicum* Δ*aceE* (♦, ▲) and Δ*aceE ureD*-E188* cells (■, ●) were cultivated CGXII minimal medium containing 222 mM glucose and 254 acetate in presence (▲, ●) and without increased CO_2 levels (♦, ■). For increased CO_2 levels, 10% (v/v) CO_2 was additionally sparged into the bioreactor. Cultivations were performed at 30°C and the pH value was maintained at pH 7. C. Glucose (empty symbols) and acetate (filled symbols) levels were determined throughout batch fermentation.

The production of L-valine and the by-product L-alanine need to be considered as they act as the opponent and desired efflux of glycolysis to contrast to the efflux via anaplerosis. The strains Δ*aceE* and Δ*aceE ureD*-E188* produced 15 mM and 54 mM L-valine, and 10 mM and 38 mM L-alanine within 28 hours of cultivation, respectively (Fig. 2 B). The addition of hydrogen carbonate, however, similarly reduced the L-valine production by 54% (Δ*aceE*) and 59% (Δ*aceE ureD*-E188*); the by-product L-alanine increased by 22% for the Δ*aceE* strain and decreased by 51% for the Δ*aceE ureD*-E188*strain. Although growth was not notably affected, L-valine levels significantly decreased upon cultivation at high hydrogen carbonate levels. In the context of increased L-alanine and L-valine production under low CO_2/HCO_3^- concentrations observed by Blombach and co-workers (Blombach et al., 2013), we suppose an enhanced efflux of glycolysis via anaplerosis under increased CO_2/HCO_3^- level, stimulating PEPCx and PCx activity.

Due to the impaired growth by the deletion of *pyc*, Δ*pyc* mutants entered the stationary and production phase at a later time point. For this reason, the L-valine titers are not directly comparable to those of Δ*aceE* and Δ*aceE ureD*-E188*. The final L-valine concentration of the Δ*aceE* Δ*pyc* strain did not increase significantly in the presence of hydrogen carbonate, but L-alanine production increased 4-fold (Fig. 1 B). Interestingly, *C. glutamicum* Δ*aceE* Δ*pyc ureD*-E188* accumulated 6 mM L-valine without significant growth for unknown reasons. In the presence of hydrogen carbonate; L-valine and L-alanine titers increased by 36% and 76%, respectively.

In an additional experiment, we analyzed the effect of increased CO_2 aeration on growth and production of *C. glutamicum* Δ*aceE ureD*-E188* during batch fermentation. Without additional CO_2 gassing, we observed similar growth rates of 0.26 h^{-1} and 0.27 h^{-1} for *C. glutamicum* Δ*aceE* and Δ*aceE ureD*-E188*, respectively (Fig. 3 A). Aeration with CO_2 only slightly impaired growth

of the Δ*aceE* strain (growth rate 0.23 h^{-1}), but did not significantly affect the growth of Δ*aceE ureD*-E188* strain (0.26 h^{-1}). Without CO_2 aeration, *C. glutamicum* Δ*aceE ureD*-E188* featured an increased biomass formation of 8 g CDW L^{-1} compared to the Δ*aceE* strain with (7.2 g L^{-1}) and without additional CO_2 (7 g L^{-1}) and the Δ*aceE ureD*-E188* strain with CO_2 gassing (7 g L^{-1}). Without CO_2 aeration, *C. glutamicum* Δ*aceE ureD*-E188* produced a final titer of 43 mM L-valine, which was notably reduced by CO_2 gassing to 33 mM L-valine (Fig. 3 B). Compared to the Δ*aceE ureD*-E188* strain, *C. glutamicum* Δ*aceE* featured 16% reduced L-valine production, which did not change significantly under increased CO_2 levels. All strains featured similar acetate and glucose consumption rates (Fig. 1 C). In accordance with the findings during microtiter cultivation, these results indicate once more that carbon dioxide as product of urea degradation affects L-valine production.

Formation of by-products

During batch fermentation with CO_2 aeration, the strains re-accumulated significant amounts of acetate during the L-valine production phase: 89 mM and 40 mM for Δ*aceE* without and with CO_2 aeration, 29 mM and 82 mM for Δ*aceE ureD*-E188* without and with CO_2 aeration, respectively (Fig. 1 C). In addition, metabolome analysis of the supernatant of *C. glutamicum* Δ*aceE* and Δ*aceE ureD*-E188* cultivated in shake flasks revealed increased levels of lactate, succinate and malate for the Δ*aceE*, but not for the Δ*aceE ureD*-E188* strain (Fig. S1). The synthesis of organic acids under aerobic conditions is usually an indicator for glucose excess, the metabolization of which is limited by the maximal enzyme activity and oxygen supply, resulting in substrate-level phosphorylation (overflow metabolism) (Cheng et al., 2014; Paczia et al., 2012). At the same time, *C. glutamicum* – growing as well as non-growing – cells are known to metabolize glucose to organic acids under oxygen deprivation (Okino et al., 2005; Rados et al., 2014; Yamamoto et al., 2012). Furthermore, additional hydrogen carbonate or CO_2 aeration under anaerobic conditions were shown to enhance succinate and acetate yields by enhancing the flux at the pyruvate node towards PEPCx, PCx and PDHC (Okino et al., 2005; Rados et al., 2014). In Δ*aceE* strains, latter can be excluded due to the lack of PDHC activity. At this time, the underlying mechanism for organic acid synthesis of the Δ*aceE* strain in general and the Δ*aceE ureD*-E188* strain under increased CO_2 levels cannot be elucidated completely. Besides the impact of CO_2/HCO_3^- on anaplerosis, the reduced biomass formation might also be an indirect consequence of increased organic acid levels, which are known to inhibit protein activity (Rados et al., 2014) and lead to an elevated loss of carbon.

The impact of the pH on growth and production of *C. glutamicum* Δ*aceE*

The degradation of urea by urease leads to an increase of the pH of a culture by the formation of ammonia. During 28 hours of shake flask cultivation, the initially adjusted pH value of 7 shifted in a culture with *C. glutamicum* Δ*aceE* cells to pH 8, while the pH was not changed for the Δ*aceE ureD*-E188* culture due to urease inactivity. The pH significantly impacts the appearance of carbon dioxide in the medium. Depending on the pH, CO_2 dissociates in water to different ratios of free carbon dioxide, carbonic acid, hydrogen carbonate and carbonate as follows (Bailey and Ollis, 1986; Buytendyk et al., 1927):

$$CO_2 + H_2O \overset{k_1,k_{-1}}{\longleftrightarrow} H_2CO_3 \overset{fast}{\longleftrightarrow} HCO_3^- + H^- \overset{fast}{\longleftrightarrow} CO_3^{2-} + 2H^+$$

According to Bailey and Ollis, a shift from pH 7 to pH 8 results in ten- and 100-fold increased levels of HCO_3^- and CO_3^{2-}, respectively, while a shift to pH 6.5 decreases HCO_3^- four-fold and almost removes CO_3^{2-} species (Bailey and Ollis, 1986; Blombach and Takors, 2015). In contrast, dissolved CO_2 and H_2CO_3 levels are not affected by the pH. Compared to the urease inactive strain, the Δ*aceE* strain generates increased intracellular levels of carbon dioxide.

Table 2: Growth rate, L-valine titers and volumetric productivity of *C. glutamicum* Δ*aceE and* Δ*aceE ureD*-E188* determined during batch fermentation at pH values of 6.5, 7 and 8. The cells were cultivated in CGXII minimal medium containing 222 mM glucose and 254 mM acetate prepared with and without urea.

Strain	Growth rate (μ)			L-valine (mM)			Volumetric productivity (mmol L^{-1} h^{-1})		
	pH 6.5	pH 7	pH 8	pH 6.5	pH 7	pH 8	pH 6.5	pH 7	pH 8
Δ*aceE w/ urea*	0.19	0.26	0.31	32	36	9	0.99	1.67	0.22
Δ*aceE w/o urea*	0.12	n.d.	0.36	27	n.d.	15	0.91	n.d.	0.37
Δ*aceE ureD*-E188* *w/ urea*	0.12	0.27	n.d.	34	43	n.d.	1.41	2.0	n.d.
Δ*aceE ureD*-E188* *w/o urea*	n.d.	n.d.	0.35	n.d.	n.d.	12	n.d.	n.d.	0.30

Thus, in accordance with the pH dependency of dissolved carbon dioxide, these results indicate an increase of HCO_3^- species for the Δ*aceE* strain, in contrast to the Δ*aceE ureD*-E188* strain. Carboxylation reactions as conducted by PEPCx and PCx require HCO_3^-. This argues for in an increased efflux of glycolysis via anaplerosis in the presence of increased HCO_3^- concentrations.

To analyze the influence of different pH levels on growth and production, batch fermentation of *C. glutamicum* Δ*aceE* and Δ*aceE ureD*-E188* was performed by maintaining the pH at 6.5, 7 and 8 (Fig. 4, Tab. 2). Compared to the cultivation at pH 7, the growth rate was significantly reduced at a pH of 6.5, especially by cultivation without urea and with urease inactivity (Tab. 2). Follmann and co-workers observed the formation of H_2O_2 under acidic conditions in *C. glutamicum* wild-type cells, which might lead to oxidative stress. From transcriptomic and proteomic studies at acidic conditions, they concluded that oxidative stress induces iron starvation, which in turn reduces the activity of TCA cycle enzymes and consequently leads to reduced growth (Follmann et al., 2009). The further reduced growth rate by cultivation without urea or urease activity might be explained by decreased oxaloacetate levels as a consequence of reduced anaplerotic activity. At a pH of 8, growth rates were significantly higher compared to pH 7 (Tab. 2). Although *C. glutamicum* is traditionally cultivated at neutral pH, optimal growth is observed up to pH 9 by an increased expression of genes encoding enzymes involved in the TCA, respiration and stress resistance (Barriuso-Iglesias et al., 2006; Barriuso-Iglesias et al., 2008; Follmann et al., 2009). In addition, the increase of HCO_3^- species under elevated pH as mentioned above might contribute to the increase of oxaloacetate supply necessary for enhanced growth (Blombach and Takors, 2015).

During batch fermentation, the volumetric productivity was decreased at pH 6.5 for all strains, and even stronger reduced at a pH of 8. The volumetric productivity and final L-valine production of the Δ*aceE* strain, however, seemed to be more affected by the changed pH level than the Δ*aceE ureD*-E188* strain (Fig. 4, Tab. 2).

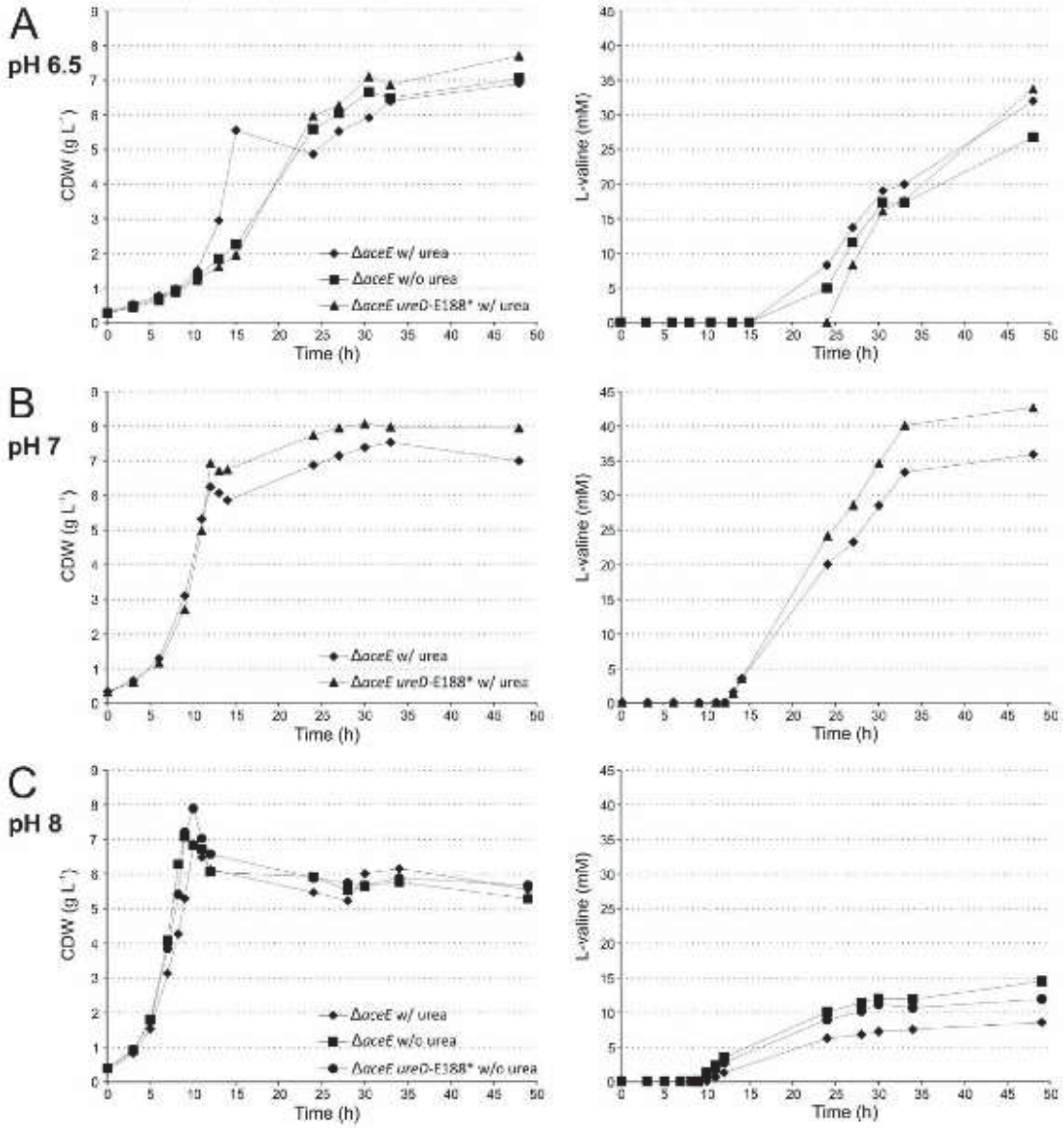

Fig. 4 The pH value influences biomass formation and L-valine production of *C. glutamicum* Δ*aceE* and Δ*aceE ureD*-E188*. Batch fermentation was performed at pH values of A. 6.5, B. 7 and C. 8, which were maintained by titration of 2 M hydrochloric acid and 2 M potassium hydroxide. *C. glutamicum* Δ*aceE* (♦, ■) and Δ*aceE ureD*-E188* (▲, ●) cells were cultivated in CGXII minimal medium containing 222 mM glucose and 254 acetate with (♦, ▲) and without urea (■, ●).

Interestingly, the shift to pH 6.5 had a stronger negative effect on growth than on L-valine production, while at a pH of 8, growth was improved but L-valine production was strongly reduced for so far unidentified reasons.

Comparative transcriptome analysis of *C. glutamicum* Δ*aceE* and Δ*aceE ureD*-E188*

Comparative transcriptome analysis was performed of shake flask cultures to assess changes in gene expression induced by the *ureD*-E188* mutation.

About 120 genes exhibited mRNA levels altered more than 1.5-fold with, however, unexpected high p-values (Tab. S1). Interestingly, the expression of *pyc* encoding the anaplerotic enzyme PCx was downregulated in the Δ*aceE ureD*-E188* strain, which indicates a reduced flux of pyruvate towards oxaloacetate (Mahr et al., 2015; Peters-Wendisch et al., 1998). Interestingly, the expression of *pgi* encoding glucose-6-phosphate isomerase was also downregulated suggesting an increased carbon flux through the pentose-phosphate pathway (PPP), which increases NADPH supply for L-valine production (Tab. S1). During engineering of Δ*aceE* strains, indeed, the deletion of *pgi* significantly increased L-valine production by enhancing NADPH supply via PPP (Blombach et al., 2008; Eikmanns and Blombach, 2014). Similarly, ^{13}C flux analysis revealed an increased flux via PPP by overexpression of genes encoding L-valine biosynthesis enzymes in the Δ*aceE* strain (Bartek et al., 2011), which suggests an increased flux through the PPP as natural consequence of enhanced NADPH demand for L-valine production.

Furthermore, mRNA levels of *ldhA* encoding NAD-dependent L-lactate dehydrogenase, which catalyzes the reduction of pyruvate to lactate, and *lldD* encoding a menaquinone-dependent L-lactate dehydrogenase, which catalyzes the oxidation of lactate, were decreased. This implies a diminished lactate metabolism as already observed during metabolome analysis increasing pyruvate availability for L-valine production (Mahr et al., 2015; Stansen et al., 2005; Toyoda et al., 2009). Moreover, we observed the downregulation of several genes encoding proteins of the respiratory chain (*sdhC*, *lldD*, *qcrB*, *atpE*, *atpG*) and the nitate/nitrite antiporter *narK* in presence of the *ureD*-E188* mutation. Different studies reported on the upregulation of mRNA levels of genes involved in the respiratory chain under alkaline conditions (Barriuso-Iglesias et al., 2006; Barriuso-Iglesias et al., 2008; Follmann et al., 2009). This result agrees with the observed up-shift of the pH during shake flask cultivation of *C. glutamicum* Δ*aceE* in contrast to the Δ*aceE ureD*-E188* culture.

Conclusion

During cultivation of the L-valine producer *C. glutamicum* Δ*aceE*, we observed that the lack of urea in the medium or the inactivity of urease (by the disruption of the accessory protein *ureD*) increased L-valine production by about 100% (Mahr et al., 2015). We hypothesized that carbon dioxide as by-product of urea degradation stimulates the activity of anaplerosis by reducing the availability of pyruvate as precursor for L-valine production. Anaplerosis plays indeed an important role as the additional lack of the anaplerotic enzyme PCx in the Δ*aceE* strain resulted in impaired growth and almost abolished growth in the urease-inactive Δ*aceE* strain. The addition of hydrogen carbonate restored growth of both strains demonstrating that the provision of CO_2 by urease is essential for anaplerotic activity. Furthermore, the beneficial effect of urea deficieny on L-valine production was removed during CO_2-aerated batch fermentation. The degradation of urea increases the pH of a culture by ammonia formation. Batch fermentation at pH 8 showed improved growth, but strongly reduced L-valine formation. Together with transcriptome analysis an increased activity of the central metabolism lowering likewise pyruvate availability was proposed at alkaline conditions. Further studies such as metabolic flux analysis using ^{13}C-labeled urea could elucidate targets of formed CO_2 and its influence on metabolism of *C. glutamicum* Δ*aceE*. Altogether, our efforts revealed the urgent need of considering appropriate environmental conditions e.g. CO_2/HCO_3^-, pH, medium components etc. during metabolic strain engineering and process development besides genomic modifications.

References

Bailey, J. E., Ollis, D. F., 1986. Biochemical engineering fundamentals. McGraw-Hill Science/Engineering/Math, New York.

Barriuso-Iglesias, M., et al., 2006. Transcriptional analysis of the F_0F_1 ATPase operon of *Corynebacterium glutamicum* ATCC 13032 reveals strong induction by alkaline pH. Microbiology. 152, 11-21.

Barriuso-Iglesias, M., et al., 2008. Response of the cytoplasmic and membrane proteome of *Corynebacterium glutamicum* ATCC 13032 to pH changes. BMC Microbiol. 8, 225.

Bartek, T., et al., 2011. Comparative ^{13}C metabolic flux analysis of pyruvate dehydrogenase complex-deficient, L-valine-producing *Corynebacterium glutamicum*. Appl Environ Microbiol. 77, 6644-52.

Baumgart, M., et al., 2013. IpsA, a novel LacI-type regulator, is required for inositol-derived lipid formation in *Corynebacteria* and *Mycobacteria*. BMC Biol. 11, 122.

Blombach, B., et al., 2009. L-valine production during growth of pyruvate dehydrogenase complex-deficient *Corynebacterium glutamicum* in the presence of ethanol or by inactivation of the transcriptional regulator SugR. Appl Environ Microbiol. 75, 1197-200.

Blombach, B., et al., 2013. Impact of different CO_2/HCO_3^- levels on metabolism and regulation in *Corynebacterium glutamicum*. J Biotechnol. 168, 331-40.

Blombach, B., et al., 2008. *Corynebacterium glutamicum* tailored for high-yield L-valine production. Appl Microbiol Biotechnol. 79, 471-9.

Blombach, B., et al., 2007. L-valine production with pyruvate dehydrogenase complex-deficient *Corynebacterium glutamicum*. Appl Environ Microbiol. 73, 2079-84.

Blombach, B., Takors, R., 2015. CO_2 - intrinsic product, essential substrate, and regulatory trigger of microbial and mammalian production processes. Front Bioeng Biotechnol. 3, 108.

Buchholz, J., et al., 2013. Platform engineering of *Corynebacterium glutamicum* with reduced pyruvate dehydrogenase complex activity for improved production of L-lysine, L-valine, and 2-ketoisovalerate. Appl Environ Microbiol. 79, 5566-75.

Buytendyk, F. J., et al., 1927. A Study of the System Carbonic Acid, Carbon Dioxide and Water: Determination of the True Dissociation-constant of Carbonic Acid. Biochem J. 21, 576-84.

Cheng, K. K., et al., 2014. Global metabolic network reorganization by adaptive mutations allows fast growth of *Escherichia coli* on glycerol. Nat Commun. 5, 3233.

Eikmanns, B. J., Blombach, B., 2014. The pyruvate dehydrogenase complex of *Corynebacterium glutamicum*: an attractive target for metabolic engineering. J Biotechnol. 192 Pt B, 339-45.

Engels, V., Wendisch, V. F., 2007. The DeoR-type regulator SugR represses expression of *ptsG* in *Corynebacterium glutamicum*. J Bacteriol. 189, 2955-66.

Follmann, M., et al., 2009. Functional genomics of pH homeostasis in *Corynebacterium glutamicum* revealed novel links between pH response, oxidative stress, iron homeostasis and methionine synthesis. BMC genomics. 10, 621.

Ikeda, M., et al., 2011. Identification and application of a different glucose uptake system that functions as an alternative to the phosphotransferase system in *Corynebacterium glutamicum*. Appl Microbiol Biotechnol. 90, 1443-51.

Ikeda, M., et al., 2015. A third glucose uptake bypass in *Corynebacterium glutamicum* ATCC 31833. Appl Microbiol Biotechnol. 99, 2741-50.

Kalinowski, J., et al., 2003. The complete *Corynebacterium glutamicum* ATCC 13032 genome sequence and its impact on the production of L-aspartate-derived amino acids and vitamins. J Biotechnol. 104, 5-25.

Keilhauer, C., et al., 1993. Isoleucine synthesis in *Corynebacterium glutamicum*: molecular

analysis of the *ilvB-ilvN-ilvC* operon. J Bacteriol. 175, 5595-603.

Kensy, F., et al., 2009. Validation of a high-throughput fermentation system based on online monitoring of biomass and fluorescence in continuously shaken microtiter plates. Microb Cell Fact. 8, 31.

Kinoshita, S., et al., 1957. Studies on the amino acid fermentation part.1. Production of L-glutamic acid by various microorganisms. J Gen Appl Microbiol. 3, 193-205.

Kinoshita, S., et al., 2004. Studies on the amino acid fermentation. Part 1. Production of L-glutamic acid by various microorganisms. J Gen Appl Microbiol. 50, 331-43.

Leuchtenberger, W., et al., 2005. Biotechnological production of amino acids and derivatives: current status and prospects. Appl Microbiol Biotechnol. 69, 1-8.

Mahr, R., et al., 2015. Biosensor-driven adaptive laboratory evolution of l-valine production in *Corynebacterium glutamicum*. Metab Eng. 32, 184-94.

Mitsuhashi, S., 2014. Current topics in the biotechnological production of essential amino acids, functional amino acids, and dipeptides. Curr Opin Biotechnol. 26, 38-44.

Niebisch, A., Bott, M., 2001. Molecular analysis of the cytochrome bc1-aa3 branch of the *Corynebacterium glutamicum* respiratory chain containing an unusual diheme cytochrome c1. Arch Microbiol. 175, 282-94.

Nolden, L., et al., 2000. Urease of *Corynebacterium glutamicum*: organization of corresponding genes and investigation of activity. FEMS Microbiol Lett. 189, 305-10.

Okino, S., et al., 2005. Production of organic acids by *Corynebacterium glutamicum* under oxygen deprivation. Appl Microbiol Biotechnol. 68, 475-80.

Oldiges, M., et al., 2014. Application of metabolic engineering for the biotechnological production of L-valine. Appl Microbiol Biotechnol. 98, 5859-70.

Paczia, N., et al., 2012. Extensive exometabolome analysis reveals extended overflow metabolism in various microorganisms. Microb Cell Fact. 11, 122.

Peters-Wendisch, P. G., et al., 1993. Phosphoenolpyruvate carboxylase in *Corynebacterium glutamicum* is dispensable for growth and lysine production. FEMS Microbiol Lett. 112, 269-274.

Peters-Wendisch, P. G., et al., 1998. Pyruvate carboxylase from *Corynebacterium glutamicum*: characterization, expression and inactivation of the *pyc* gene. Microbiology. 144 (Pt 4), 915-27.

Rados, D., et al., 2014. Carbon flux analysis by ^{13}C nuclear magnetic resonance to determine the effect of CO_2 on anaerobic succinate production by *Corynebacterium glutamicum*. Appl Environ Microbiol. 80, 3015-24.

Rehm, N., et al., 2010. L-Glutamine as a nitrogen source for *Corynebacterium glutamicum*: derepression of the AmtR regulon and implications for nitrogen sensing. Microbiology. 156, 3180-93.

Repaske, R., et al., 1974. Carbon dioxide control of lag period and growth of *Streptococcus sanguis*. J Bacteriol. 117, 652-9.

Sauer, U., Eikmanns, B. J., 2005. The PEP-pyruvate-oxaloacetate node as the switch point for carbon flux distribution in bacteria. FEMS Microbiol Rev. 29, 765-94.

Schreiner, M. E., et al., 2005. E1 enzyme of the pyruvate dehydrogenase complex in *Corynebacterium glutamicum*: molecular analysis of the gene and phylogenetic aspects. J Bacteriol. 187, 6005-18.

Stansen, C., et al., 2005. Characterization of a *Corynebacterium glutamicum* lactate utilization operon induced during temperature-triggered glutamate production. Appl Environ Microbiol. 71, 5920-8.

Toyoda, K., et al., 2009. The *ldhA* gene, encoding fermentative L-lactate dehydrogenase of *Corynebacterium glutamicum*, is under the control of positive feedback regulation mediated by LldR. J Bacteriol. 191, 4251-8.

van der Rest, M. E., et al., 1999. A heat shock following electroporation induces highly efficient transformation of *Corynebacterium glutamicum* with

xenogeneic plasmid DNA. Appl Microbiol Biotechnol. 52, 541-545.

Yamamoto, S., et al., 2012. Overexpression of genes encoding glycolytic enzymes in *Corynebacterium glutamicum* enhances glucose metabolism and alanine production under oxygen deprivation conditions. Appl Environ Microbiol. 78, 4447-57.

3.4 Screening of an *Escherichia coli* promoter library for a phenylalanine biosensor

Regina Mahr, Raphael Freiherr von Boeselager, Johanna Wiechert, Julia Frunzke*

IBG-1: Biotechnology, Forschungszentrum Jülich, Jülich, Germany

*Corresponding author

Current state: Submitted to Applied Microbiology and Biotechnology

Impact Factor: 3.668

Author contributions

Own contribution to the work: 75%

	Name	Contribution
Project planning	***Mahr, R.***	45%
	Frhr.v. Boeselager	10%
	Frunzke, J.	45%
Writing	***Mahr, R.***	90%
	Frunzke, J.	10%

	Name	Experimental work	Evaluation	Preparation of figure/table
Figure 1	***Mahr, R.***	-	20%	100%
	Frhr.v. Boeselager	100%	80%	-
Figure 2	***Mahr, R.***	100%	100%	100%
Figure 3	***Mahr, R.***	100%	100%	100%
Figure 4	***Mahr, R.***	100%	100%	100%
Table 1	***Mahr, R.***	-	-	100%
Figure S1	***Mahr, R.***	60%	90%	100%
	Frhr.v. Boeselager	40%	10%	-
Figure S2	***Mahr, R.***	100%	100%	100%
Figure S3	***Mahr, R.***	100%	100%	100%
Figure S4	***Mahr, R.***	50%	60%	100%
	Wiechert, J.	50%	40%	-

Screening of an *Escherichia coli* promoter library for a phenylalanine biosensor

Regina Mahr, Raphael Freiherr von Boeselager, Johanna Wiechert and Julia Frunzke

Institute of Bio- and Geosciences, IBG-1: Biotechnology, Forschungszentrum Jülich, Germany

Abstract

In recent years, the application of genetically-encoded biosensors for the engineering of microbial production strains and for monitoring metabolite production during fermentation processes opened new opportunities for industrial biotechnology. The construction of transcription factor-based biosensors, however, requires the selection of suitable transcription factor-promoter pairs to convert the concentration of effector molecules into a measureable output signal. Here, we present an efficient strategy to screen promoter libraries for appropriate parts applicable for biosensor design. To this end, we pooled the strains of the Alon library containing about 2000 different *Escherichia coli* promoter-*gfpmut2* fusions, and enriched L-phenylalanine-responsive promoters by toggled rounds of positive and negative selection using fluorescence activated cell sorting (FACS). The promoter of *mtr*, encoding an L-tryptophan-specific transporter, was identified as suitable sensor device for L-phenylalanine detection. Furthermore, we performed a comparative analysis of different biosensor constructs and revealed the strong influence of the biosensor architecture. As proof-of-principle, we successfully applied the *mtr* sensor in a FACS high-throughput (HT) screening of L-phenylalanine producers after random mutagenesis of an *E. coli* MG1655 strain. These results illustrate the utter utility and applicability of the developed screening approach to identify novel sensor candidates.

Introduction

During the last years, genetically-encoded biosensors have revealed their great potential as valuable tools for metabolic strain engineering and for enabling new insights in bioprocesses at single-cell resolution (Delvigne et al., 2014; Liu et al., 2015a; Mahr and Frunzke, 2016; Schallmey et al., 2014). By converting the intracellular effector molecule concentration into a measureable output, biosensors are in demand in cases, in which an easily detectable phenotype is not available. Microorganisms are equipped with a variety of metabolite-sensing mechanisms including transcriptional regulators, riboswitches, enzymes or periplasmic-binding proteins, which can be exploited for the construction of biosensors. Transcription factor (TF)-based biosensors consist of a regulator that binds intracellular effector molecules and in turn activates or represses gradually the expression of target genes. By transcriptionally fusing target promoters to genes encoding auto-fluorescent proteins (AFPs), the intracellular effector concentration can be converted into a measurable optical signal (Mahr and Frunzke, 2016). Biosensors based on bacterial TFs have successfully been implemented in high-throughput (HT) screenings of mutant libraries using fluorescence-activated cell sorting (FACS) (Binder et al., 2012; Mustafi et al., 2012; Siedler et al., 2014) or in biosensor-driven adaptive

laboratory evolution approaches for the improvement of microbial metabolite production (Mahr et al., 2015). Furthermore, the efficient screening of feedback-resistant enzymes (Schendzielorz et al., 2014), dynamic pathway regulation (Dahl et al., 2013; Liu et al., 2015b; Xu et al., 2014; Zhang et al., 2012) and the analysis of population heterogeneity at the single-cell level (Hoffmann et al., 2013; Mustafi et al., 2014) demonstrate the broad applicability of biosensors (Liu et al., 2015a; Mahr and Frunzke, 2016).

Nature has evolved a broad range of these sensor devices. However, only a few regulators and corresponding target genes have been well characterized to date. Frequently, the plethora of targeted promoters hampers the identification of suitable biosensor candidates. Thus, workflows enabling the rapid identification of responsive promoters are required for efficient sensor designs. In this study, we developed a convenient strategy for screening promoter-AFP libraries using FACS. As proof-of-principle, we screened the Alon library consisting of about 2000 different promoter-*gfpmut2* fusions in *Escherichia coli* (Zaslaver et al., 2006) in order to identify biosensor candidates suitable for the detection of L-phenylalanine.

The aromatic amino acid L-phenylalanine is one of the most demanded amino acids besides L-glutamate, L-lysine and L-methionine and faces an increasing commercial interest (Sprenger, 2007). As precursor for the artificial sweetener aspartame or as building block for pharmaceutical products, including infusion fluids or HIV protease inhibitors, L-phenylalanine has played an important role for many years (Sprenger, 2006; Sprenger, 2007). Furthermore, the commercially interesting aromatic compounds pinosylvin (van Summeren-Wesenhagen and Marienhagen, 2015), cinnamic and *p*-hydroxycinnamic acid (Sariaslani, 2007; Vargas-Tah et al., 2015) or phenylpyruvic acid (Hou et al., 2015) are synthesized from the precursor L-phenylalanine and serve as notable flavor enhancers, cosmetical or pharmaceutical building blocks.

Besides chemical synthesis and hydrolytic cleavage of proteins, microbial fermentation has now become the dominating production process (Bongaerts et al., 2001; Leuchtenberger et al., 2005; Sprenger, 2006; Sprenger, 2007). *E. coli* serves as an important platform organism producing L-phenylalanine – as most microorganisms – via the aromatic amino acid biosynthetic pathway (shikimate pathway) (Bentley, 1990; Sprenger, 2007). Rational engineering approaches yielded strains producing final L-phenylalanine titers of up to 50 g L^{-1} from glucose (Backman et al., 1990; Rüffer et al., 2004) and 13.4 g L^{-1} based on glycerol as substrate (Weiner et al., 2014).

In this study, L-phenylalanine-responsive promoters were enriched by toggled rounds of selection and counter-selection from the Alon library. This approach revealed the promoter of *mtr*, encoding an L-tryptophan-specific transporter (Pittard et al., 2005), as an appropriate part for sensor design. Subsequently, biosensors based on the *mtr* promoter were characterized and successfully applied during FACS HT-screening of a mutant *E. coli* K-12 MG1655 library for strains with increased phenylalanine production.

Material and Methods

Bacterial strains, media and growth conditions

In this study, the *E. coli* wild-type strains K-12 MG1655 and DH5α were used (Blattner et al., 1997; Hayashi et al., 2006). All bacterial strains used in this study are listed in Table 1. Unless indicated otherwise, *E. coli* cells were grown on lysogeny broth (LB) agar plates at 37°C or pre-cultivated in LB medium for eight hours at 37°C and 170 rpm (Sambrook et al., 2001).

Table 1: Bacterial strains, plasmids and oligonucleotides used in this study.

Strains or plasmids	Relevant characteristics	Source or reference
Strains		
***E.coli* DH5α**	*supE44 ΔlacU169* (ϕ80*lacZ*DM15) *hsdR17 recA1 endA1 gyrA96 thi-1 relA1*	Invitrogen
***E. coli* K-12 MG1655**	F⁻ lambda⁻ *ilvG⁻ rfb*-50 *rph*-1	(Blattner et al., 1997; Hayashi et al., 2006)
Plasmids		
pEKEx2	Kan^R, Amp^R ; $oriV_{C.g.}$, $oriV_{E.c.}$, P_{tac}, $lacI^q$, pBL1, pUC18 (*E. coli-C. glutamicum* shuttle vector)	(Eikmanns et al., 1994)
pJC1	Kan^R, Amp^R ; $oriV_{C.g.}$, $oriV_{E.c.}$ (*E. coli-C. glutamicum* shuttle vector)	(Cremer et al., 1990)
pJC1-venus-term-BS	pJC1 derivative containing a terminator sequence of *Bacillus subtilis* behind *venus*	Heyer, unpublished
pJC1-*mtr* sensor-type1	pJC1-P_{mtr}-*venus*	This study
pJC1-*mtr* sensor-type2	pJC1-*lacI*-P_{tac}-*tyrR*-P_{mtr}-*venus*	This study
pJC1-*mtr* sensor-type3	pJC1-P_{tac}-*tyrR*-P_{mtr}-*venus*	This study
pJC1-*mtr* sensor-type4	pJC1-P_{tyrR}-*tyrR*-P_{mtr}-*venus*	This study
Oligonucleotides	**Sequence (5'-3')**[a]	
BamHI_lacI_fw	CGATCAGCGACGCCGCAGGGGGATCCGCGTTGCGCTCACTGCCC (BamHI)	
EcoRV_lacI_rv	GATATCGTCTGAATCTGGTGTATATGGCGAG (EcoRV)	
TyrR_inv_fw	CATATACACCAGATTCAGACGATATCCATATTCGCGCTTACTCTTCG TTC	
OL_TyrR_inv_rv	CATCGGCTCGTATAATGTGTGGAGTTCCCATGCGTCTGGAAGTC	
Ptac_fw	GCGAAAGGTTTTGCACCATTCGATGG	
Ptac_rv	TCCACACATTATACGAGCCGATGATTAATTGTC	
OL_200bp_Pmtr_fw	CGAATGGTGCAAAACCTTTCGCGCAGTTACTGGGCGATGCAC	
Pmtr_rv	ATATCTCCTTCTTAAAGTCTATGCATTGCACTGTACCAGTACAC	
STOP_RBS_venus_fw	TAGACTTTAAGAAGGAGATATATGGTGAGCAAGGGCGAG	
Venus_OL_rv	AAAACGACGGCCAGTACTAGTTACTTGTACAGCTCGTCCATGC (SpeI)	
tyrR_OL(BamHI,pJC1)_fw	AGGGCGATCAGCGACGCCGCAGGGGGATCCTTACTCTTCGTTCTTCT TCTGACTCAGAC (BamHI)	
Pmtr_OL(BamHI,pJC1)_fw	AGGGCGATCAGCGACGCCGCAGGGGGATCCGCAGTTACTGGGCGAT GCACAG (BamHI)	
PtyrR_OL(Pmtr)_rv	GCGGCTGTGCATCGCCCAGTAACTGCGGGGATTTCCGTCGTCAGCTT ATC	
GFP_int_rv	CAAGAATTGGGACAACTCCAGTG	

[a]Underlined sequences highlight introduced recognition sites for restriction endonucleases (restriction endonucleases indicated in parentheses).

Subsequently, a second pre-culture was inoculated in a shake flask containing 20 ml M9 minimal or phenylalanine production medium with 0.5% glucose and cells were incubated overnight at 37°C and 120 rpm. The following day, cells were washed with 0.9% (w/v) NaCl solution and adjusted to an optical density (OD_{600}) of 0.5 in 50 ml fresh minimal medium. Further incubation was done at 37°C and 120 rpm. As minimal medium, M9 medium (6 g/L Na_2HPO_4, 3 g/L KH_2PO_4, 0.5 g/L NaCl, 1 g/L NH_4Cl, 1 mM $MgSO_4$, 0.1 mM $CaCl_2$, 1 ml/L trace element solution [3 µM ammonium molybdate, 400 µM H_3BO_3, 30 µM $CoCl_3$, 10 µM $CuSO_4$, 800 µM $MnCl_2$ and 10 µM $ZnSO_4$; filter sterilized]; adjusted to a pH of 7) or an adapted phenylalanine production medium (0.3 g/L $MgSO_4$ x 7 H_2O, 0.015 g/L $CaCl_2$ x 2 H_2O, 3 g/L KH_2PO_4, 12 g/L K_2HPO_4, 0.1 g/L NaCl, 5 g/L $(NH_4)_2SO_4$, 0.075/1.0 g/L $FeSO_4$ x 7 H_2O/ Na-citrate, 1.5 ml/L trace element solution [2 g/L $Al_2(SO_4)_3$ x 18 H_2O, 0.75 g/L $CoSO_4$ x 7 H_2O, 2.5 g/L $CuSO_4$ x 5 H_2O, 0.5 g/L H_3BO_3, 24 g/L $MnSO_4$ x H_2O, 3 g/L Na_2MoO_4 x 2 H_2O, 2.5 g/L $NiSO_4$ x 6 H_2O, 15 g/L $ZnSO_4$ x 7 H_2O; dissolved in ddH_2O at pH 1-2], 0.0075 g/L thiamine/HCl; ingredients were dissolved in ddH_2O [pH ~ 7.2] and filter sterilized) were used (Gerigk et al., 2002; Miller, 1972). When necessary, 50 µg/ml kanamycin was added to the medium. All dipeptide stocks were dissolved in the respective minimal medium and stored at -20°C.

Recombinant DNA work

Cloning techniques including PCR, DNA restriction and ligation were performed according to standard protocols (Sambrook et al., 2001). Synthesis of oligonucleotides and sequencing of plasmids was performed in subcontracting with Eurofins MWG Operon (Ebersfeld, Germany). All plasmids and oligonucleotides are listed in Table 1. Plasmids were isolated from *E. coli* using the GeneJET Plasmid Miniprep Kit (Thermo Fisher Scientific, Waltham, Massachusetts, USA).

For the construction of the pJC1-*mtr* sensor-type2, the *lacI* fragment was amplified from the pEKEx2 vector using primers BamHI_lacI_fw and EcoRV_lacI_rv, the *tyrR* fragment was amplified with primers TyrR_inv_fw and OL_TyrR_inv_rv from genomic DNA of *E. coli* K-12 MG1655, the P_{tac} promoter was amplified from the pEKEx2 vector with primers Ptac_fw and Ptac_rv, 331 bp upstream of the transcriptional start site of the P_{mtr} promoter was amplified from genomic DNA of *E. coli* K-12 MG1655 using primers OL_200bp_Pmtr_fw and Pmtr_rv, and *venus* was amplified from pJC1-venus-term-BS with primers STOP_RBS_venus_fw and Venus_OL_rv. All fragments were pooled to an equimolar concentration and cloned into the BamHI and SpeI digested vector pJC1-venus-term-BS by Gibson assembly (Gibson et al., 2009). For the construction of pJC1-*mtr* sensor-type3, the biosensor construct was amplified without *lacI* from the pJC1-*mtr* sensor-type2 vector using primers tyrR_OL(BamHI,pJC1)_fw and Venus_OL_rv. For the assembly of pJC1-*mtr* sensor-type4, the fragment P_{tyrR}-*tyrR* was amplified from genomic DNA of *E. coli* using primers tyrR_OL(BamHI,pJC1)_fw and PtyrR_OL(Pmtr)_rv, and P_{mtr} and *venus* were amplified from pJC1- sensor-type2 using primers Pmtr_fw and Venus_OL_rv. The plasmid pJC1-*mtr* sensor-type1 was constructed by amplifying P_{mtr} and *venus* from the pJC1-*mtr* sensor-type2 vector using primers Pmtr_OL(BamHI,pJC1)_fw and Venus_OL_rv. The respective fragments were cloned into the BamHI and SpeI digested pJC1-venus-term-BS vector via Gibson assembly (Gibson et al., 2009).

For cloning purposes, *E. coli* DH5α was transformed using the RbCl method (Hanahan, 1983). All other *E. coli* strains were transformed using the transformation and storage solution (TSS) procedure (Chung et al., 1989).

Flow cytometry

Flow cytometric (FC) analyses and cell sorting were performed using a FACSAria II flow

cytometer (Becton Dickinson, San Jose, USA) equipped with a blue solid state laser (488 nm excitation). Forward-scatter characteristics (FSC) and side-scatter characteristics (SSC) were detected as small-angle and orthogonal scatters of the 488-nm laser, respectively. EYFP fluorescence was detected using a 502-nm long-pass and a 530/30-nm band-pass filter set. FACS-Diva software 6.0 was used to record the measurements. During analyses, thresholding on FSC was applied to remove background noise. As precision mode, four-way purity was used for cell sorting with a threshold rate up to 10,000 events per second. If not stated differently, cells were sorted on agar plates or on MultiScreen HTS 96-well filter plates (Millipore, Billerica, USA) to separate cells from the FACSFlow™ buffer (Becton Dickinson, San Jose, USA) as already described in (Mahr et al., 2015). The filter containing the sorted cells was excised with single-use scalpels (Braun, Melsungen, Germany) and inoculated in fresh medium. For FC analyses, *E. coli* culture samples were diluted to an OD_{600} of 0.05 in FACSFlow™ sheath fluid buffer (BD, Heidelberg, Germany). The analysis software FlowJo V.10.0.8 was used to visualize and evaluate the data (Tree Star, Ashland, USA).

Microtiter plate cultivation

Online monitoring of growth and fluorescence was performed in 48-well microtiter FlowerPlates (MFPs) using the BioLector cultivation system (m2p-labs GmbH, Baesweiler, Germany) (Kensy et al., 2009). If not stated differently, 48-well MPFs were inoculated with *E. coli* cells from a pre-culture to an OD_{600} of 0.5 in a total volume of 750 µl. In the BioLector instrument, cells were incubated at 37°C and agitation of 1200 rpm. While biomass production was recorded as the backscattered light intensity (light wavelength 620 nm; signal gain factor of 20), eYFP fluorescence was measured at an excitation of 510 nm and an emission of 532 nm (signal gain factor of 60). The specific fluorescence for the cells is defined as the eYFP fluorescence per backscattered light intensity (given in arbitrary units, a.u.).

Screening of the Alon library for phenylalanine-responsive promoters

Initially, all strains of the Alon promoter library consisting of about 2000 different promoter-*gfpmut2* fusions in *E. coli* K-12 MG1655 were pooled (Fig. 1a) (Zaslaver et al., 2006). To this end, the single clones stored in 96-well plates (Nunc™ MicroWell™ Plates, Thermo Fisher Scientific, Waltham, Massachusetts, USA) were transferred to agar plates (Nunc™ OmniTray™ Single-Well Plates, Thermo Fisher Scientific, Waltham, Massachusetts, USA) containing LB with 50 µM kanamycin using a 96-well plate replicator stamp (LabArt, Waldbüttelbrunn, Germany) and incubated at 37°C for 18 hours. The colonies were washed from the agar plates using 10 ml LB and kanamycin and a Drigalski spatula, and collected in a 1 L shake flask. Then, cells were incubated for one hour at 37°C and 120 rpm, washed in 1x PBS and 2 ml of the mixed library were transferred to 100 ml M9 minimal medium containing 0.5% (w/v) glucose and kanamycin. The culture was incubated overnight at 37°C and 120 rpm. The following day, aliquots were prepared of a glycerol cryo-stock containing a final glycerol concentration of 25% (v/v) and stored at -80°C.

For screening, 500 µl of the glycerol stock containing the pooled Alon library were used to inoculate 20 ml M9 minimal medium containing 0.5% (w/v) glucose and kanamycin, and incubated at 37°C and 120 rpm (Fig. 1a). While the desired effector was added to one culture for induction, a second culture without effector was prepared as negative control. Prior to sorting, the cultures were incubated for three hours. To screen for induced ("ON") promoters, 0.5-1 x 10^6 of the top 35% cells were sorted on filter plates and the excised filter was incubated in 4 ml LB with kanamycin overnight (Fig. 1a). The following day, cells of 1 ml pre-culture were pelleted, washed with 1x

PBS and used to inoculate 20 ml M9 minimal medium containing 0.5% (w/v) glucose and kanamycin. To screen for effector-responsive promoters, which do not show a fluorescent signal under non-induced conditions ("OFF" promoters), the cells were incubated without effector for four hours (Fig.1a). Subsequently, 0.5-1 x 10^6 cells from the bottom 35% gate, which was pre-defined during the first sorting step, were sorted on filter plates and incubated in 4 ml LB with kanamycin. After two toggled rounds of selection, cells were spotted as single clones on agar plates and were re-cultivated in the BioLector system for verification of effector responsiveness and determination of the dynamic range (Fig. 1a). From positive clones, plasmid DNA was prepared and sequenced using primer GFP_int_rv to identify isolated promoters.

Fluorescence microscopy

Fluorescence microscopy was performed on a Zeiss Axioplan 2 imaging microscope equipped with an AxioCam MRm camera and a Plan-Apochromat 100x, 1.40 Oil DIC oil-immersion objective. The AxioVision 4.8 software was used to acquire and analyze the images (Zeiss, Göttingen, Germany). Samples were spread on a microscope slide coated with a thin layer of 400 µl 1% agarose and covered by a cover glass.

Random mutagenesis and FACS screening

Random mutagenesis using the mutagen N'-methyl-N'-nitro-N-nitrosoguanidine (MNNG) was adapted from the protocol of (Harper et al., 2011). Prior to mutagenesis, a pre-culture of *E. coli*/pJC1-*mtr* sensor-type1 cells in LB medium was diluted 1:50 in 20 ml fresh LB medium containing kanamycin. At an OD_{600} of 2, 5 ml of this culture were harvested and washed twice in 2.5 ml 0.1 M citrate buffer (pH 5.5) (two-fold concentration of the cells). Subsequently, the cells were incubated with 50 µg/ml MNNG (dissolved in DMSO) for 30 minutes at 37°C and 60 rpm. As control, a second culture was incubated containing the same amount of DMSO. Then, the cells were washed twice with 5 ml 0.9% (w/v) saline and cultivated in falcons for two hours in LB medium containing 4% glucose at 37°C and 170 rpm. Mutagenized cells were stored as cryo-stocks in LB medium containing 40% glycerol (w/v) at -30°C for up to one week.

For screening, two LB pre-cultures were inoculated with 1 ml of the cryo-stock containing mutagenized and non-mutagenized cells, respectively. The following day, the pre-cultures were used to inoculate 20 ml phenylalanine production medium containing 0.5% glucose and kanamycin to an OD_{600} of 0.5. Cells were incubated for six hours at 37°C and 120 rpm. Subsequently, 2.5 x 10^5 cells with a significantly increased fluorescent output compared to the control were sorted on filter plates as already described above (section "Flow cytometry"). The filter with the cells was inoculated in LB medium with kanamycin overnight, and two further enrichment steps sorting 1 x 10^6 high fluorescent cells using FACS were performed to avoid false positive isolates. Finally, enriched cells were spotted as single cells on agar plates (Nunc™ OmniTray™ Single-Well Plates, Thermo Fisher Scientific, Waltham, Massachusetts, USA) containing LB agar with kanamycin. Single cells were picked using a 96-well plate replicator stamp (LabArt, Waldbüttelbrunn, Germany) inoculated in 96-well plates (Nunc™ MicroWell™ Plates, Thermo Fisher Scientific, Waltham, Massachusetts, USA) containing LB medium and antibiotic, and incubated in the Microtron Pro (Infors HT, Bottmingen, Switzerland) for eight hours. For storage, glycerol at a final concentration of 20% was added and plates were frozen at -80°C.

Verification of isolated mutants after FACS HT-screening

Isolated mutants were first inoculated in 48-well MPFs containing 725 µl LB medium and kanamycin plus 25 µl of the thawed glycerol stock, and incubated at 37°C overnight reaching the stationary phase. Subsequently, 25 µl of this pre-culture were used to inoculate 48-well MFPs containing 725 µl phenylalanine production medium. Incubation and online monitoring of

backscatter and fluorescence were performed in the BioLector system. After 28 hours of incubation, the supernatant was analyzed for amino acid production using ultra-high performance liquid chromatography (uHPLC).

Quantification of amino acid production

Using uHPLC, amino acids were quantified as *ortho*-phthaldialdehyde derivatives by automatic pre-column derivatization and separation by reverse-phase chromatography on an Agilent 1290 Infinity LC ChemStation (Agilent, Santa Clara, USA) equipped with a fluorescence detector. As eluent for the Zorbax Eclipse AAA 3.5 micron 4.6 x 7.5 mm column (Agilent, Santa Clara, USA), a gradient of Na-borate buffer (10 mM Na_2HPO_4; 10 mM $Na_2B_4O_7$, pH 8.2; adapted to operator's guide) was applied. To determine the concentration of amino acids in the supernatant, culture samples were centrifuged for 10 min at 13,000 rpm and 4°C and diluted according to the expected concentration.

Results

Proof-of-principle: Screening for galactose-responsive promoters

For the straightforward development of novel biosensors with desired sensor properties, HT approaches are required for the efficient and rapid identification of suitable parts. Here, we pooled all *E. coli* K-12 MG1655 strains of the Alon library containing about 2000 different promoter-*gfpmut2* fusions on the plasmids pUA66 or pUA139 (Fig. 1a) (Zaslaver et al., 2006). Toggled rounds of selection and counter-selection were conducted to enrich promoters responsive to the desired effector metabolite (for a detailed description of this workflow, the reader is referred to the material and methods section). Initially, cells were incubated in the presence of an effector molecule to activate *gfpmut2* expression from inducible promoters (Fig. 1a). Subsequently, 0.5-1 x 10^6 cells of the top 35% fluorescent cells were isolated using FACS. To get rid of constitutively activated promoters, isolated cells were cultivated without the effector molecule followed by sorting of 0.5-1 x 10^6 cells from a pre-defined bottom 35% gate. The toggled selection procedure was repeated twice to reduce the amount of false positive clones and to enrich desired promoter-AFP fusions. Finally, selected clones were isolated and verified by monitoring growth and fluorescence using microscale cultivation system. Plasmid DNA from cells containing metabolite-responsive promoter-*gfpmut2* fusions was prepared and sequenced to identify isolated promoter fusions (Fig. 1a).

In a first set of experiments, we screened for the well-characterized promoters activated by the effector galactose (Fig. S1a). In a first step, the Alon library cultivated without effector molecules was split by FACS in fractions containing cells with high and low fluorescence to reduce the amount of constitutively active or repressible promoters. To induce responsive promoters of the pooled Alon library, we cultivated the cells in 20 ml M9 minimal containing 0.5% (w/v) galactose and kanamycin. For counter-selection and as reference culture (for FACS gating), cells were cultivated in M9 medium with 0.5% (w/v) glucose. Prior to sorting, the cells were grown for six hours at 37°C and 120 rpm. We enriched cells with a high fluorescent output in the presence of galactose from 3% to 78% within five steps of toggled selection (the gating strategy is depicted in Fig. S1a). Within two counter-selection steps, constitutively activated or false positive cells were reduced from 25% to 4%. While 78% of the cells were induced in presence of galactose, only 9% of the cells showed an increased fluorescent signal in presence of glucose after five selection steps (Fig. S1a). The plasmid DNA of nine clones showing the strongest activation in presence of galactose was sequenced: eight clones harbored the P_{galS}-*gfpmut2* fusion and one clone contained the P_{lacZ}-*gfpmut2* fusion. During cultivation in microtiter plates, both promoter-*gfpmut2*-fusions revealed a minimal dynamic range of 2.1 defining the maximum fold change of the reporter output in

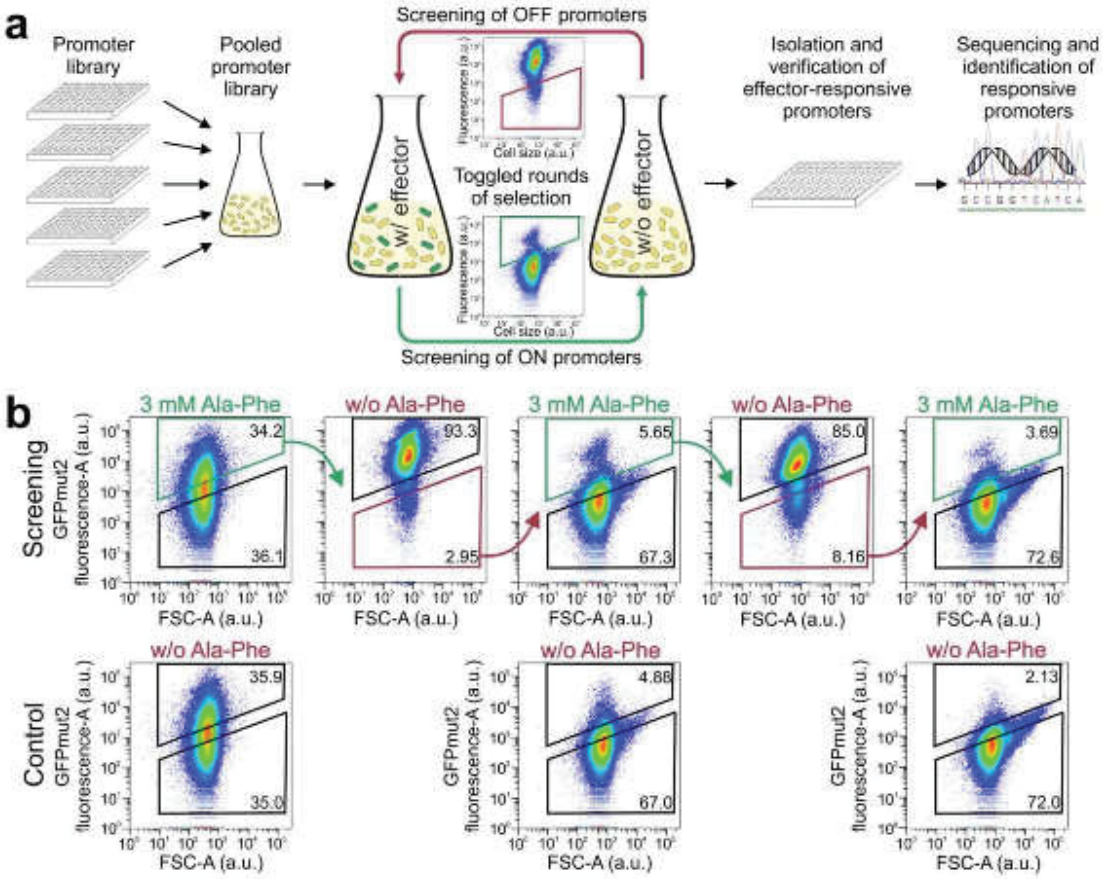

Fig. 1 Screening of L-phenylalanine-responsive promoters. **a** Schematic overview of the screening process. Initially, the Alon library consisting of about 2000 promoter-*gfpmut2* fusions of *E. coli* K-12 MG1655 was pooled and incubated in the presence of a desired effector molecule to induce responsive promoters. In the first step, the top 35% fluorescent cells were sorted to isolate induced ("ON") promoters (green gate). In the second step, the cells were incubated without effector molecules to separate constitutive "ON" promoters from responsive promoters (this time called "OFF" promoters) by sorting the bottom 35% fluorescent cells (red gate). After two rounds of toggled selection, effector-responsive promoters were isolated via FACS and cultivated in microtiter plates to verify the screening outcome. Plasmid DNA of positive clones was prepared and sequenced to identify isolated promoters. **b** Screening of the Alon library for L-phenylalanine-responsive promoters. For induction, 3 mM of the dipeptide L-alanyl-L-phenylalanine (Ala-Phe) were added to the culture. The rounds of toggled selection are marked by the alternation of green ("ON" promoters) and red gates ("OFF" promoters), from which cells were sorted (green and red arrows). The initially defined 35% "ON" and "OFF" gates were maintained throughout the screening process for sorting. The numbers indicate the percentage of the entire population covered by the respective gate

the presence of 0.5% galactose (Fig. S1b). Both isolated promoters regulate the expression of well-known genes. While *galS* encodes the galactose isorepressor which represses the transcription of genes involved in the transport and catabolism of galactose in presence of high galactose concentrations and under glucose limitation (Semsey et al., 2007; Weickert and Adhya, 1992), *lacZ* encodes the ß-galactosidase representing first structural gene of the *lac* operon, which was reported to be weakly induced by galactose (Williams and Paigen, 1968).

Screening for L-phenylalanine-responsive promoters

In the next step, we screened for L-phenylalanine-responsive promoters. Therefore, the pooled Alon libray was cultivated in 20 ml M9 minimal medium containing 0.5% (w/v) glucose and kanamycin (Fig. 1b). After one hour of incubation, the dipeptide L-alanyl-L-phenylalanine (Ala-Phe, final conc. 3 mM) was added as effector molecule. After three hours of induction, activated cells falling within an upper 35% gate were sorted using FACS (Fig. 1b). For counter-selection, the screening medium was prepared without Ala-Phe. We used dipeptides for screening, as previous characterizations of biosensors featured an improved uptake of short peptides – the intracellular hydrolysis of which leads to an increase of the respective amino acids in the cytoplasm (Mustafi et al., 2012; Payne, 1977; Simmonds and Griffith, 1961). Within five steps of toggled selection, no significant enrichment of strains falling within the respective gate was observed. However, a distinct subpopulation of cells displaying an increased reporter output became visible in the second and third round of induction. This population was not detected in the non-induced control sample. After five toggled selection steps, the fraction of cells in the induced state was about two-fold higher in comparison to the control sample 3.7% and 2.1%, respectively (Fig. 1b). Plasmid DNA of 23 isolated strains (from gate P1) was sequenced and the following promoter fusions were identified: *mtr* (12 clones; L-tryptophan/indole:H^+ symporter), *lacZ* (three clones; ß-galactosidase), *prpR* (one clone; 2-methylcitrate DNA-binding transcriptional regulator), *artP* (one clone; L-arginine ABC transporter-ATP binding subunit), *yciT* (one clone; DNA-binding transcriptional regulator), *nupG* (one clone; nucleoside:H^+ symporter), *gadA* (one clone; glutamate decarboxylase A), *fadB* (one clone; fatty acid oxidation complex, α component), *yihU* (one clone; 3-sulfolactaldehyde reductase) and *dinJ* (one clone; antitoxin of YafQ-DinJ toxin-antitoxin system and DNA-binding transcriptional repressor). Verification of the isolated strains *via* microscale cultivation revealed a significant response to Ala-Phe for the *mtr* promoter (minimal dynamic range 2.9), the *gadA* promoter (minimal dynamic range 1.6) and the *artP* promoter (minimal dynamic range 1.3) (Fig. S1c).

Characterization of the *mtr* promoter fusion

The *mtr* gene encodes an L-tryptophan-specific transporter, whose expression is regulated by the two transcriptional regulators TrpR (tryptophan repressor) and TyrR (tyrosine repressor) (Fig. 2a) (Heatwole and Somerville, 1991; Pittard et al., 2005; Whipp and Pittard, 1977). As reported in previous studies, the expression of *mtr* is induced in the presence of phenylalanine and tyrosine and fully repressed in presence of tryptophan (Whipp and Pittard, 1977). In order to verify the *mtr* promoter as suitable part for biosensor design, the respective promoter region (including 331 bp upstream of the transcriptional start site) was transcriptionally fused to the yellow fluorescent protein encoding gene *venus* by adding AAGAAG as ribosomal binding site (RBS) seven base pairs upstream of the start codon and cloned into the vector pJC1 (termed pJC1-*mtr* sensor-type1) (Fig. 3a). In presence of the effector amino acids containing dipeptides Ala-Tyr and Ala-Phe, the biosensor featured minimal dynamic ranges of 3.7 and 7.8, respectively (Fig. 2b). In presence of Ala-Ala, Ala-Trp or without dipeptides, the strains exhibited a low basal fluorescent signal. This result was confirmed by fluorescence microscopy showing low Venus fluorescence after cultivation without dipeptides and a strong signal in the presence of 3 mM Ala-Phe (Fig. 2d). Additionally, mixtures of dipeptides containing aromatic amino acids (overall concentration of 3 mM) were added to the cells during microtiter cultivation (Fig. 2c). While the combination of Ala-Tyr and Ala-Phe featured a minimal dynamic range of 8.2, induction was counteracted by the addition of Ala-Trp to the dipeptide mixture. This confirms the previous findings that repression by TrpR in the presence of

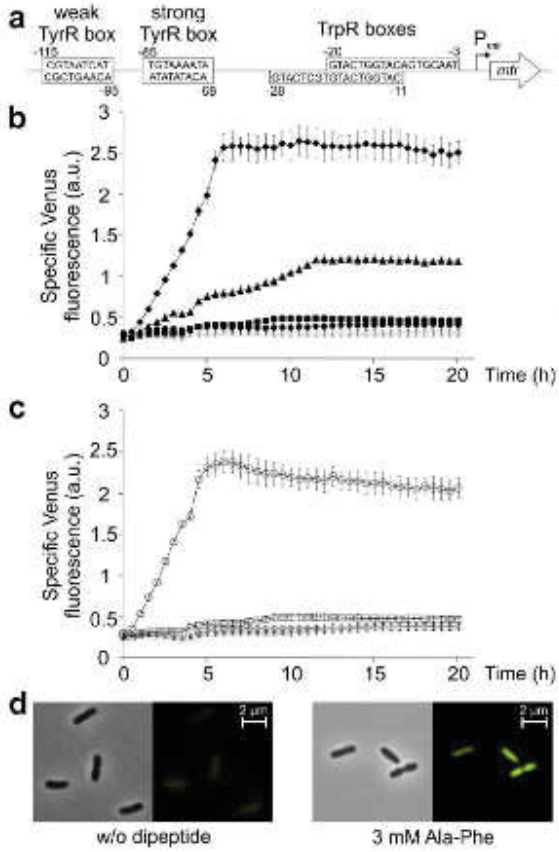

Fig. 2 Native architecture of the *mtr* promoter and characterization. **a** The *mtr* promoter consists of a weak TyrR box (located -98 to -115 bps relative to the transcriptional start site) and a strong TyrR box (located between -68 and -85 bps) as well as two TrpR binding sites located between -3 and -20bp, and between -11 and -28 bps downstream of the transcriptional start site (arrow) (http://ecocyc.org) (Keseler et al., 2013; Pittard, 1996; Pittard et al., 2005). Phenylalanine-dependent gene expression is promoted by binding of TyrR to the strong TyrR box and to the C-terminal domain of the α-subunit of RNA polymerase, while for tyrosine-mediated expression additional binding of TyrR to the weak TyrR box is required. The transcription is completely blocked by binding of the TrpR repressor in presence of L-tryptophan. **b** Specific Venus fluorescence of *E. coli* K-12 MG1655/pJC1-*mtr* sensor-type1 cultivated without dipeptides (■) and in presence of 3 mM Ala-Ala (●), Ala-Phe (♦), Ala-Trp (x) and Ala-Tyr (▲). **c** Specific Venus fluorescence of the same strain cultivated without dipeptides (□) and in presence of equal mixtures of Ala-Phe and Ala-Tyr (○), Ala-Phe and Ala-Trp (◊), Ala-Trp and Ala-Tyr (Δ) and Ala-Phe, Ala-Tyr and Ala-Trp (x) with an overall concentration of 3 mM. Cultivation was performed in the microtiter scale at 37°C and 1200 rpm in M9 minimal medium containing 0.5% (w/v) glucose and kanamycin. The data represent average values from three independent biological replicates. **d** Phase contrast and fluorescence microscope images of *E. coli* K-12 MG1655/pJC1-*mtr* sensor-type1 without (left panels) and in presence of 3 mM Ala-Phe (right panels).

L-tryptophan dominates the regulation of *mtr* expression.

Quantitative characterization of different biosensor designs based on the promoter of *mtr*

In the following, we aimed to analyze the impact of variation in the biosensor design on functionality. Therefore, four different biosensors designs based on the *mtr* promoter were constructed and characterized (Fig. 3a and b). All biosensors consist of the transcriptional fusion of the *mtr* promoter and *venus* as described above (Fig. 3a). Additionally, biosensor types two to four include *tyrR* under the control of P_{tac} (types two and three) or the native promoter (type four), respectively. To control the expression of P_{tac}, we included the *lacI* gene in sensor construct type two (Fig. 3a). The application of biosensors for FACS HT-screenings requires a detailed quantitative characterization of the biosensor response in terms of specificity, sensitivity, dynamic range and the applicability using FACS. Here, referring to Mustafi and coworkers, a competitive dipeptide feeding strategy was used to describe the relationship between effector input concentrations and the biosensor output (Mustafi et al., 2012). More precisely, different ratios of effector containing dipeptides (Ala-Phe) and non-effector dipeptides (Ala-Ala) competitive for dipeptide uptake systems were added to adjust the intracellular concentration of effector molecules (Payne, 1977; Vrljic et al., 1996). Biosensor types two and four, including the *tyrR* gene, featured minimal dynamic ranges of 4.3 and 4.5. Both

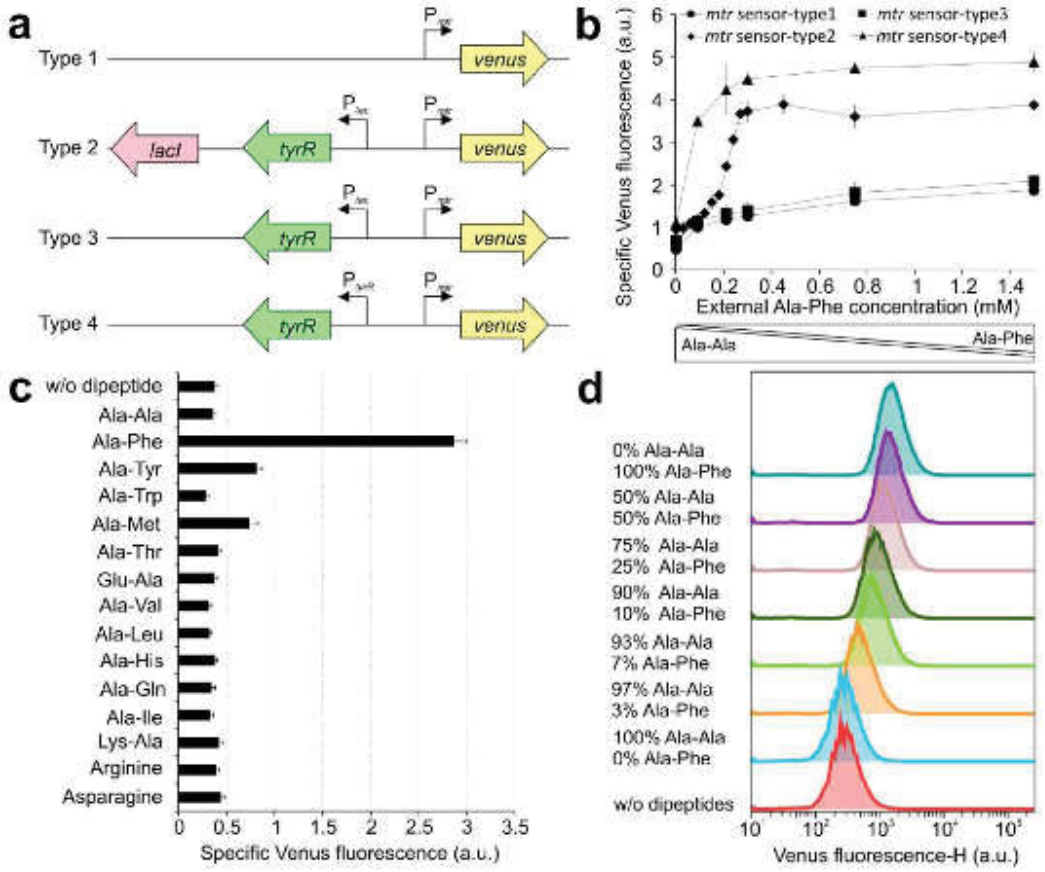

Fig. 3 Quantitative characterization of different promoter designs. **a** For all *mtr* biosensor constructs, the *venus* encoding a yellow fluorescent protein was cloned under the control of the *mtr* promoter. Sensor types two to four encode additionally *tyrR* under the P_{mtr} (types two and three) or the native P_{tyrR} promoter (type four). For the regulation of P_{lacI}, *lacI* was cloned on the construct of biosensor type two. **b** Relationship between the added extracellular concentration of L-phenylalanine and the specific Venus fluorescent output of the *mtr* biosensor types one (●), two (♦), three (■) and four (▲) in *E. coli* K-12 MG1655 on the pJC1 vector. 25 µM IPTG was additionally added to *mtr* biosensor type two. **c** The specificity of the *mtr* biosensor was tested in the BioLector using *E. coli* K-12 MG1655/pJC1-*mtr* sensor-type1 cells. The different amino acids and dipeptides were added in a final concentration of 3 mM. The specific Venus fluorescence was recorded after six hours of cultivation. **d** FACS histograms showing the Venus fluorescent signal of *E. coli* pJC1-*mtr* sensor-type1 after seven hours of cultivation in the BioLector in presence of different dipeptide ratios. **b** and **d** To adjust the intracellular amino acid, different ratios of the dipeptide containing the effector amino acid and the competing neutral dipeptide Ala-Ala were added to an overall dipeptide concentration of 3 mM. Represented data show average values from three independent biological replicates

constructs displayed considerable high basal specific fluorescent outputs without effector molecules or in the presence of 3 mM Ala-Ala (Fig. 3b). Biosensor types one and three displayed minimal dynamic ranges of 3.2 and 4.1 showing also a lower level of basal specific fluorescence. Biosensors expressing *tyrR* featured a saturated signal at extracellular concentrations above 0.3 µM Ala-Phe, while the lack of *tyrR* expression resulted in a saturated signal at 1.5 mM (Fig. 3b).

To verify the specificity of the *mtr* sensor for aromatic amino acids, *E. coli* K-12 MG1655/pJC1-*mtr* sensor-type1 cells were cultivated in the

presence of 13 different dipeptides and two amino acids (Fig. 3c). We observed a significant response to dipeptides containing the aromatic amino acids L-phenylalanine and L-tyrosine. However, we observed that the biosensor responds to 3 mM Ala-Met with a minimal dynamic range of 1.9. To our knowledge, the activation of the *mtr* promoter in the presence of L-methionine has not been described previously.

For testing the suitability of the biosensors for FACS HT-screening, *E. coli* K-12 MG1655/pJC1-*mtr* sensor-type1 cells were incubated in presence of different ratios of Ala-Ala and Ala-Phe and analyzed via flow cytometry (Fig. 3d, Fig. S2). We determined an increasing fluorescent signal in the presence of increasing levels of Ala-Phe proving the applicability of the biosensor for FC analyses and screening.

Biosensor-based high throughput screening of randomly mutagenized strains

To verify the applicability of the *mtr* biosensor for FACS HT-screening of phenylalanine producing cells, the strain *E. coli* K-12 MG1655/pJC1-*mtr* sensor-type1 was chemically mutagenized using N'-methyl-N'-nitro-N-nitrosoguanidine (MNNG) (Fig. 4a). Mutant cells exhibiting an increased biosensor output were spotted on agar plates using FACS.

Notably, also the analysis of non-mutagenized sensor cells revealed about 0.6% high fluorescent cells under all tested conditions (Fig. S4). This observed phenotypic heterogeneity was either evoked spontaneously by the expression of the biosensor, or reflects variability of the metabolic state of bacterial cells within the population. To discriminate between phenotypic heterogeneity and the risc of spontaneous (sensor) mutations, we isolated 2×10^5 spontaneously fluorescent cells (gate P1, 0.66%) and cells from the entire population as control (gate P2) using FACS (Fig. S4). Isolated cells were re-analyzed by FC after eight hours of cultivation in minimal medium. Remarkably, both cultures showed a comparable fraction of spontaneously fluorescent cells (0.6% of gate P1, 0.84% of gate P2) suggesting that the observed spontaneous fluorescence did not originate from genomic modifications or contaminations, but might reflect phenotypic heterogeneity in terms of the intracellular amino acid level (Fig. S4). Furthermore, cells from the entire population (gate P2) and spontaneous cells (gate P1) were spotted as single cells on agar plates. While about 96.7% of sorted cells from the entire population (population P2) formed colonies, only 48.1% of the sorted spontaneous cells (population P1) regrew as colonies on agar plates.

To get rid of these spontaneous cells and in order to enrich positive mutants, we followed a selection strategy: mutant cells were twice sorted and re-cultivated between the two sorting steps (Fig. 4b) (Mahr et al., 2015). The two enrichment steps resulted in an increase of top fluorescent cells from 2% (gate P1) to 53.8% (gate P2, Fig. 4b). As control, the entire population of non-mutagenized cells was sorted without revealing an increase in the fluorescent output. From gate P2, 480 single cells exhibiting a significantly increased fluorescent output were spotted on agar plates (viability 72.3%) (Fig. 4b). Thereof, 90 randomly selected mutants were cultivated in microtiter plates and the supernatant was analyzed after 28 hours for amino acid production using uHPLC (Fig. 4c, Fig. S3). The majority of clones displayed increased biomass formation and significantly increased specific fluorescent signals compared to the non-mutagenized control strain (Fig. S3). Out of 90 randomly selected clones, 71 featured higher L-phenylalanine production than the wild-type strain *E. coli* K-12 MG1655/pJC1-*mtr* sensor-type1 (40 µM ±1.7). 27% of the analyzed mutants depicted two-fold increased L-phenylalanine production. The best mutant produced 4.3-fold increased L-phenylalanine levels (160 µM) compared to the wild-type strain (Fig. 4c).

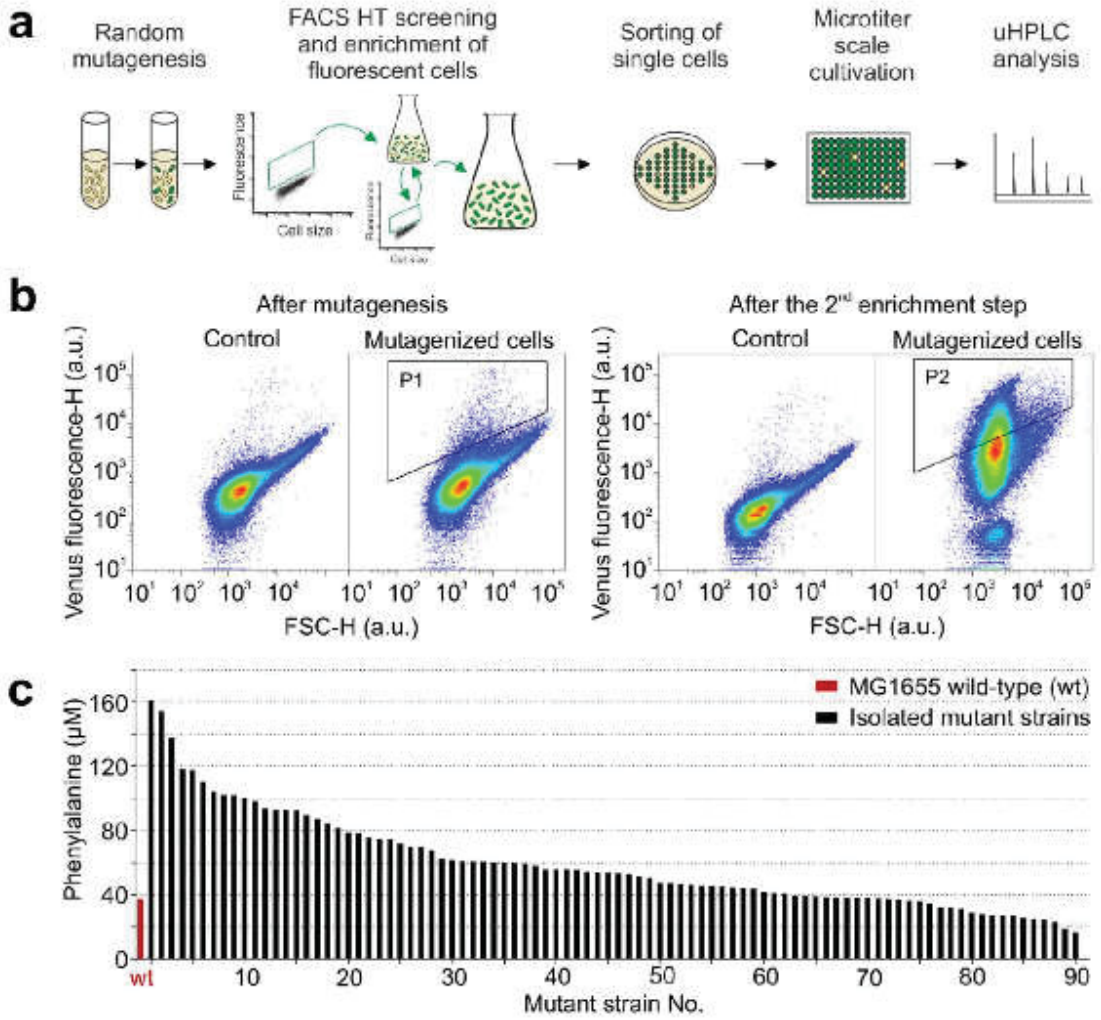

Fig. 4 Biosensor-based FACS HT-screening. **a** Schematic overview of the screening process. Initially, E. coli K-12 MG1655/pJC1-mtr sensor-type1 cells were mutagenized using the chemical mutagen MNNG. Mutagenized cells were analyzed by flow cytometry (FC), and 2.5 x 10^5 to 1 x 10^6 mutants with the top fluorescent output were sorted and re-cultivated. To enrich positive mutants, this step was repeated twice. Subsequently, single cells were spotted on agar plates, re-cultivated as isolated clones in the BioLector for 28 hours in phenylalanine production medium and amino acid production in the supernatant was determined by uHPLC. **b** The dot plots display the Venus fluorescent signal against the forward scatter (FSC) of control (non-mutagenized) and mutagenized cells after mutagenesis and after two enrichment steps. Mutagenized cells were sorted from gates P1 and P2, respectively. As control, cells of the entire population were sorted. **c** L-phenylalanine production of 90 isolated mutant clones (black bars) in comparison to the non-mutagenized E. coli K-12 MG1655/pJC1-mtr sensor-type1 strain (red bars). The cells were cultivated in the BioLector in phenylalanine production medium containing 0.5% (w/v) glucose and kanamycin at 37°C and 1200 rpm. Production was determined by uHPLC after 28 hours of incubation.

Some mutants displayed an increased dynamic range of the sensor output (Fig. S3). To identify whether mutations within the biosensor are responsible, the mtr sensor-type1 fragment of eleven clones with the highest dynamic range was sequenced. Interestingly, only one mutant displayed a base exchange (-54 bp downstream of transcriptional start site; cytosine exchanged to

thymine) in the *mtr* promoter region of the plasmid-encoded biosensor.

Discussion

In this study, we developed an elaborated strategy to use FACS for the screening of promoter libraries for metabolite-responsive promoters, which can be applied as suitable parts for the construction of biosensors. For this purpose, the Alon library presents an excellent source as it consists of about 2000 different promoter-*gfpmut2* fusions (more than 75% of all *E. coli* promoters) and hence, readily available parts for sensor design (Zaslaver et al., 2006). For screening, we pooled all strains of the Alon library and by toggled rounds of selection under induced and non-induced conditions using FACS, metabolite-responsive promoters were enriched (Fig. 1, Fig. S1). For proof-of-principle, we screened for galactose- and phenylalanine-responsive promoters. During the enrichment of galactose-responsive promoters, we successfully enriched *galS* and *lacZ* promoter-*gfpmut2* fusions whereof the regulation by galactose is well-studied (Fig. S1) (Williams and Paigen, 1968).

In a second step, we tested the screening approach for the identification of L-phenylalanine-responsive promoters. The control of biosynthesis and transport of aromatic amino acids underlies a complex hierarchy of regulatory processes (Sprenger, 2007) including feedback-inhibition of pacemaker enzymes (Ogino et al., 1982), transcriptional control by the regulators TyrR and TrpR (Herrmann and Weaver, 1999; Pittard, 1996) as well as attenuation mechanisms at the transcriptional/translational interface (Chen and Yanofsky, 2003). This challenges a well-considered screening strategy, which is an important prerequisite for the final output corresponding to the quotation "You get what you screen for" (Schmidt-Dannert and Arnold, 1999). As promoters respond to effector amino acids at different speed and rate, the time point of screening and for sorting is of crucial importance. Due to the underlying mechanisms including the adaption to growth medium, the uptake and processing of effector molecules (Luo et al., 2014; Payne, 1977), the activation of the gene expression machinery (Bintu et al., 2005b; Carey et al., 2013; Fritz et al., 2014; Mäkelä et al., 2013) and the maturation of fluorescent proteins (Craggs, 2009; Iizuka et al., 2011), we decided to sort L-phenylalanine-(amino acid)-induced cells after four hours and galactose-(carbon-source)-induced cells after six hours of cultivation. Moreover, the impact of the medium composition on e.g. carbon/nitrogen starvation or stress-response needs to be considered. We used M9 minimal medium due to its lack of other amino acids and carbon source and due to its very low auto-fluorescence (Miller, 1972). Furthermore, promoters show different strength of activation and FACS analyses feature a certain variance in the observed signal due to technical artifacts. For these reasons, the choice of the appropriate sorting gate is essential for the final outcome of the screening. We have chosen an upper and lower 35% gate for the entire library which excludes 30% of the cells with a mean fluorescent output (Fig. 1 B). The clearly separated sorting gates eliminate cells with a constitutively mean fluorescent output. To get rid of constitutively activated promoters, we established the toggled rounds of selecting promoters with a high fluorescent output under induced conditions and promoters with a low fluorescent output under non-induced conditions. Using this strategy, we successfully enriched galactose- and L-phenylalanine-responsive promoters (Fig.1, Fig. S1). Our screening process was developed in a way that promoters activated in response to effector molecules were enriched. The selection of negatively-regulated promoters is proposed to be achieved by selecting low fluorescent promoters in presence of the effector of interest (EOI) and by selecting high fluorescent promoters in the absence of an EOI. By coupling the responsive promoter to a strong repressor, which in turn controls the expression of an AFP encoding gene via a tightly regulated promoter, for instance, the output of the

negatively-regulated promoter can be inverted into a positive visible signal, which might be as well suitable for the application as biosensor (Mustafi et al., 2015; Ohlendorf et al., 2012). Alternative approaches for screening promoter libraries mostly rely on the cultivation and characterization of single clones one by one, which appears cost-intensive and laborious (Bjarnason et al., 2003; Keren et al., 2013; Robijns et al., 2014; Zaslaver et al., 2006; Zeevi et al., 2011). Here, the implementation of FACS pre-screening using toggled rounds of selection as described can surely reduce the time-consuming screening process.

During screening for L-phenylalanine-responsive promoters, the promoter of *mtr* encoding a high-affinity L-tryptophan-specific permease (Heatwole and Somerville, 1991; Hiraga et al., 1968) was enriched. Heatwole and Somerville described the activation of *mtr* gene expression by phenylalanine and tyrosine via the TyrR repressor and the superior repression of same by L-tryptophan via TrpR. The regulatory control enables the cell to increase the cellular level of L-tryptophan in presence of high L-phenylalanine and L-tyrosine concentrations or to reduce the uptake by inhibiting the expression of *mtr* in presence of high L-tryptophan levels. This allows modulating the intracellular ratio of the three aromatic amino acids (Heatwole and Somerville, 1991; Sarsero and Pittard, 1991). At the molecular level, TyrR dimerizes in presence of L-phenylalanine, binds to the strong TyrR box and promotes the recruitment of RNA-polymerase, while hexamerization of TyrR and the additional binding to the weak TyrR box in presence of L-tyrosine is required for tyrosine-mediated gene expression (Fig. 2A) (Pittard, 1996; Pittard et al., 2005). L-tryptophan-mediated attachment of TrpR to the TrpR binding sites completely hinders RNA polymerase recruitment (Heatwole and Somerville, 1991; Pittard et al., 2005). This differential expression of the *mtr* gene was likewise observed during biosensor characterization (Fig. 2). For the construction of the *mtr* biosensor, the promoter includes both TrpR and TyrR binding sites. The presence of the TrpR boxes, however, implies consequently the disturbance of biosensor signaling under increased L-tryptophan concentrations. Hence, high intracellular concentrations of L-phenylalanine and L-tyrosine would be masked by high L-tryptophan concentrations. Here, the sensitivity of the biosensor could be reduced by screening an error-prone library of the TrpR boxes for candidates with reduced sensitivity towards tryptophan (Schendzielorz et al., 2014; Wise and Kuske, 2000).

The analysis of different biosensor designs (Fig. 3 A and B) revealed a significant influence on biosensor characteristics in terms of sensitivity and dynamic range in presence and absence of additional copies of the transcriptional repressor TyrR encoded on the plasmid. The additional *tyrR* expression evoked a high basal fluorescence and a saturated biosensor signal at already low L-phenylalanine concentrations (up to 0.21 mM external Ala-Phe). In contrast, native TyrR levels led to similar dynamic ranges, but a reduced basal fluorescence and decreased sensitivity towards L-phenylalanine (Fig. 3 B and D). Plasmid-based expression of *tyrR* results in significantly increased levels of the transcriptional regulator TyrR compared to native expression. Conventional gene expression analyses usually rely on simple promoter-reporter fusions (Keren et al., 2013; Robijns et al., 2014; Zaslaver et al., 2006). For the construction of biosensors, however, the corresponding TF is traditionally added not only to express heterologous genes, but also to avoid titration effects of the native regulator. For single target regulators like Lrp of *Corynebacterium glutamicum* (Lrp biosensor), which controls as solely target the expression of the BrnFE exporter (Lange et al., 2012; Mustafi et al., 2012), an increased number of TF binding sites (due to plasmid-based expression) generates titration effects due to the naturally tight regulation of the transcription factor to a low number of binding

sites (Brewster et al., 2014). Global regulators like TyrR controlling a complex regulon with multiple binding sites, however, are not necessarily affected by a few additional TF binding sites due to their natural high protein abundance. Here, the additional expression of the transcriptional regulator might significantly influence the global regulation. Furthermore, the rate of occupation of a promoter by transcription factors recruiting the RNA polymerase through protein-protein interaction determines the rate of gene expression - hence, the sensitivity and dynamic range of the biosensor (Bintu et al., 2005a; Bintu et al., 2005b; Tabor et al., 2009). Thus, the higher the level of the transcriptional regulator is, the more effector molecules can bind simultaneously resulting in a highly sensitive response and saturated operator sites at low concentrations. Likewise, the introduction of a second operator site or the modification of transcription factors were used to increase the sensitivity and dynamic range of sensor constructs in different studies (Lutz and Bujard, 1997; Mahr and Frunzke, 2015; Silva-Rocha and de Lorenzo, 2012; Tabor et al., 2009). Our studies revealed that the architecture of a biosensor can significantly influence the sensor's output characteristics. For this reason, it is worth to compare different biosensor designs before application.

Based on the observed biosensor performance characteristics, we chose the *mtr* sensor type 1 for the application during FACS HT-screening of *E. coli* K-12 MG1655 chemically mutagenized cells (Fig. 4). All biosensor types featured about 0.6% cells with a strongly increased fluorescent output under induced and non-induced conditions (data not shown, Fig. S4). Sorting and re-cultivation of these spontaneously induced cells did not result in their enrichment, which suggests phenotypic heterogeneity as origin for high fluorescent cells. Furthermore, only half of these cells sorted on agar plates formed colonies. Due to these results, we included additionally two enrichment steps into the FACS HT-screening to reduce the amount of false positive isolates (Fig. 4 A). About 30% of 90 isolated and characterized mutant strains showed at least two-fold up to 4.3-fold increased L-phenylalanine titers (Fig. 4 C), which falls within the scope of success of similar studies (Binder et al., 2012; Mustafi et al., 2012; Santos and Stephanopoulos, 2008). One great disadvantage of L-phenylalanine is its growth limiting effect (Grinter, 1998). At external L-phenylalanine concentrations of 5 g L^{-1}, growth rate of *E. coli* wild-type cells was found to be reduced by half (Polen et al., 2005). In this case, the iterative enrichment of high fluorescent cells selects against false-positive but also growth defective cells at the same time. This might reduce growth-defective mutants with high L-phenylalanine production.

Genetically-encoded biosensors have enlarged the repertoire of tools for engineering and monitoring industrially-relevant production strains. Although nature provides a plethora of sensor devices, the identification of suitable candidates requires the deep knowledge of underlying regulatory mechanisms and intensive research. Efficient and automatized workflows are required, which enable the rapid identification of novel and suitable sensor devices. Here, the screening of a promoter-AFP library using FACS has shown to contribute to the rapid and easy detection of novel biosensors for engineering and improving strains for biotechnological purposes. Furthermore, we were able to demonstrate the significant influence of the biosensor design on the sensor's performance characteristics. Taken together, these efforts contribute to the exploitation and development of custom-made biosensors according to the researcher's purpose.

References

Backman, K., O'Connor, M. J., Maruya, A., Rudd, E., McKay, D., Balakrishnan, R., Radjai, M., DiPasquantonio, V., Shoda, D., Hatch, R., et al., 1990. Genetic engineering of metabolic pathways applied to the production of phenylalanine. Ann NY Acad Sci 589, 16-24.

Bentley, R., 1990. The shikimate pathway - a metabolic tree with many branches. CRC Crit Rev Biochem Mol Biol. 25, 307-84.

Binder, S., Schendzielorz, G., Stäbler, N., Krumbach, K., Hoffmann, K., Bott, M., Eggeling, L., 2012. A high-throughput approach to identify genomic variants of bacterial metabolite producers at the single-cell level. Genome Biol. 13, R40.

Bintu, L., Buchler, N. E., Garcia, H. G., Gerland, U., Hwa, T., Kondev, J., Kuhlman, T., Phillips, R., 2005a. Transcriptional regulation by the numbers: applications. Curr Opin Genet Dev. 15, 125-35.

Bintu, L., Buchler, N. E., Garcia, H. G., Gerland, U., Hwa, T., Kondev, J., Phillips, R., 2005b. Transcriptional regulation by the numbers: models. Curr Opin Genet Dev. 15, 116-24.

Bjarnason, J., Southward, C. M., Surette, M. G., 2003. Genomic profiling of iron-responsive genes in *Salmonella enterica* serovar *typhimurium* by high-throughput screening of a random promoter library. J Bacteriol. 185, 4973-82.

Blattner, F. R., Plunkett, G., 3rd, Bloch, C. A., Perna, N. T., Burland, V., Riley, M., Collado-Vides, J., Glasner, J. D., Rode, C. K., Mayhew, G. F., Gregor, J., Davis, N. W., Kirkpatrick, H. A., Goeden, M. A., Rose, D. J., Mau, B., Shao, Y., 1997. The complete genome sequence of *Escherichia coli* K-12. Science. 277, 1453-62.

Bongaerts, J., Krämer, M., Müller, U., Raeven, L., Wubbolts, M., 2001. Metabolic engineering for microbial production of aromatic amino acids and derived compounds. Metab Eng. 3, 289-300.

Brewster, R. C., Weinert, F. M., Garcia, H. G., Song, D., Rydenfelt, M., Phillips, R., 2014. The transcription factor titration effect dictates level of gene expression. Cell. 156, 1312-23.

Carey, L. B., van Dijk, D., Sloot, P. M., Kaandorp, J. A., Segal, E., 2013. Promoter sequence determines the relationship between expression level and noise. PLoS Biol. 11, e1001528.

Chen, G., Yanofsky, C., 2003. Tandem transcription and translation regulatory sensing of uncharged tryptophan tRNA. Science. 301, 211-3.

Chung, C. T., Niemela, S. L., Miller, R. H., 1989. One-step preparation of competent *Escherichia coli*: transformation and storage of bacterial cells in the same solution. Proc Natl Acad Sci U S A 86, 2172-5.

Craggs, T. D., 2009. Green fluorescent protein: structure, folding and chromophore maturation. Chem Soc Rev. 38, 2865-75.

Cremer, J., Eggeling, L., Sahm, H., 1990. Cloning the *dapA dapB* cluster of the lysine-secreting bacterium *Corynebacterium glutamicum*. MGG Mol Gen Genet. 220, 478-480.

Dahl, R. H., Zhang, F., Alonso-Gutierrez, J., Baidoo, E., Batth, T. S., Redding-Johanson, A. M., Petzold, C. J., Mukhopadhyay, A., Lee, T. S., Adams, P. D., Keasling, J. D., 2013. Engineering dynamic pathway regulation using stress-response promoters. Nat Biotechnol. 31, 1039-46.

Delvigne, F., Zune, Q., Lara, A. R., Al-Soud, W., Sorensen, S. J., 2014. Metabolic variability in bioprocessing:

implications of microbial phenotypic heterogeneity. Trends Biotechnol. 32, 608-16.

Eikmanns, B. J., Thum-Schmitz, N., Eggeling, L., Ludtke, K. U., Sahm, H., 1994. Nucleotide sequence, expression and transcriptional analysis of the *Corynebacterium glutamicum gltA* gene encoding citrate synthase. Microbiology. 140 (Pt 8), 1817-28.

Fritz, G., Megerle, J. A., Westermayer, S. A., Brick, D., Heermann, R., Jung, K., Radler, J. O., Gerland, U., 2014. Single cell kinetics of phenotypic switching in the arabinose utilization system of *E. coli*. PloS ONE. 9, e89532.

Gerigk, M., Bujnicki, R., Ganpo-Nkwenkwa, E., Bongaerts, J., Sprenger, G., Takors, R., 2002. Process control for enhanced L-phenylalanine production using different recombinant *Escherichia coli* strains. Biotechnol Bioeng. 80, 746-54.

Gibson, D. G., Young, L., Chuang, R. Y., Venter, J. C., Hutchison, C. A., 3rd, Smith, H. O., 2009. Enzymatic assembly of DNA molecules up to several hundred kilobases. Nat Methods. 6, 343-5.

Grinter, N. J., 1998. Developing an L-phenylalanine process. Chem Tech. 33-35.

Hanahan, D., 1983. Studies on transformation of *Escherichia coli* with plasmids. J Mol Biol. 166, 557-80.

Harper, M. A., Chen, Z., Toy, T., Machado, I. M., Nelson, S. F., Liao, J. C., Lee, C. J., 2011. Phenotype sequencing: identifying the genes that cause a phenotype directly from pooled sequencing of independent mutants. PloS one. 6, e16517.

Hayashi, K., Morooka, N., Yamamoto, Y., Fujita, K., Isono, K., Choi, S., Ohtsubo, E., Baba, T., Wanner, B. L., Mori, H., Horiuchi, T., 2006. Highly accurate genome sequences of *Escherichia coli* K-12 strains MG1655 and W3110. Mol Syst Biol. 2, 2006 0007.

Heatwole, V. M., Somerville, R. L., 1991. The tryptophan-specific permease gene, *mtr*, is differentially regulated by the tryptophan and tyrosine repressors in *Escherichia coli* K-12. J Bacteriol. 173, 3601-4.

Herrmann, K. M., Weaver, L. M., 1999. The Shikimate Pathway. Annu Rev Plant Physiol Plant Mol Biol. 50, 473-503.

Hiraga, S., Ito, K., Matsuyama, T., Ozaki, H., Yura, T., 1968. 5-methyltryptophan-resistant mutations linked with the arginine G marker in *Escherichia coli*. J Bacteriol. 96, 1880-1.

Hoffmann, K., Grünberger, A., Lausberg, F., Bott, M., Eggeling, L., 2013. Visualization of imbalances in sulfur assimilation and synthesis of sulfur-containing amino acids at the single-cell level. Appl Environ Microbiol. 79, 6730-6.

Hou, Y., Hossain, G. S., Li, J., Shin, H. D., Liu, L., Du, G., 2015. Production of phenylpyruvic acid from L-phenylalanine using an L-amino acid deaminase from *Proteus mirabilis*: comparison of enzymatic and whole-cell biotransformation approaches. Appl Microbiol Biotechnol. 99, 8391-402.

Iizuka, R., Yamagishi-Shirasaki, M., Funatsu, T., 2011. Kinetic study of *de novo* chromophore maturation of fluorescent proteins. Anal Biochem. 414, 173-8.

Kensy, F., Zang, E., Faulhammer, C., Tan, R. K., Büchs, J., 2009. Validation of a high-throughput fermentation system based on online monitoring of biomass and fluorescence in continuously shaken microtiter plates. Microb Cell Fact. 8, 31.

Keren, L., Zackay, O., Lotan-Pompan, M., Barenholz, U., Dekel, E., Sasson, V., Aidelberg, G., Bren, A., Zeevi, D., Weinberger, A., Alon, U., Milo, R.,

Segal, E., 2013. Promoters maintain their relative activity levels under different growth conditions. Mol Syst Biol. 9, 701.

Keseler, I. M., Mackie, A., Peralta-Gil, M., Santos-Zavaleta, A., Gama-Castro, S., Bonavides-Martinez, C., Fulcher, C., Huerta, A. M., Kothari, A., Krummenacker, M., Latendresse, M., Muniz-Rascado, L., Ong, Q., Paley, S., Schroder, I., Shearer, A. G., Subhraveti, P., Travers, M., Weerasinghe, D., Weiss, V., Collado-Vides, J., Gunsalus, R. P., Paulsen, I., Karp, P. D., 2013. EcoCyc: fusing model organism databases with systems biology. Nucleic Acids Res. 41, D605-12.

Lange, C., Mustafi, N., Frunzke, J., Kennerknecht, N., Wessel, M., Bott, M., Wendisch, V. F., 2012. Lrp of *Corynebacterium glutamicum* controls expression of the *brnFE* operon encoding the export system for L-methionine and branched-chain amino acids. J Biotechnol. 158, 231-41.

Leuchtenberger, W., Huthmacher, K., Drauz, K., 2005. Biotechnological production of amino acids and derivatives: current status and prospects. Appl Microbiol Biotechnol. 69, 1-8.

Liu, D., Evans, T., Zhang, F., 2015a. Applications and advances of metabolite biosensors for metabolic engineering. Metab Eng. 31, 35-43.

Liu, D., Xiao, Y., Evans, B. S., Zhang, F., 2015b. Negative feedback regulation of fatty acid production based on a malonyl-CoA sensor-actuator. ACS Synth Biol. 4, 132-40.

Luo, Y., Zhang, T., Wu, H., 2014. The transport and mediation mechanisms of the common sugars in *Escherichia coli*. Biotechnol Adv. 32, 905-19.

Lutz, R., Bujard, H., 1997. Independent and tight regulation of transcriptional units in *Escherichia coli* via the LacR/O, the TetR/O and AraC/I1-I2 regulatory elements. Nucleic Acids Res. 25, 1203-10.

Mahr, R., Frunzke, J., 2016. Transcription factor-based biosensors in biotechnology: current state and future prospects. Appl Microbiol Biotechnol. 100, 79-90.

Mahr, R., Gätgens, C., Gätgens, J., Polen, T., Kalinowski, J., Frunzke, J., 2015. Biosensor-driven adaptive laboratory evolution of L-valine production in *Corynebacterium glutamicum*. Metab Eng. 32, 184-194.

Mäkelä, J., Kandhavelu, M., Oliveira, S. M., Chandraseelan, J. G., Lloyd-Price, J., Peltonen, J., Yli-Harja, O., Ribeiro, A. S., 2013. *In vivo* single-molecule kinetics of activation and subsequent activity of the arabinose promoter. Nucleic Acids Res. 41, 6544-52.

Miller, J. H., 1972. Experiments in molecular genetics. Cold Spring Harbor Laboratory.

Mustafi, N., Bott, M., Frunzke, J., 2015. Genetically-encoded biosensors for strain development and single cell analysis of *Corynebacterium glutamicum*. In: Burkovski, A., (Ed.), *Corynebacterium glutamicum*: From Systems Biology to Biotechnological Applications. Caister Academic Press, Norfolk, England, pp. 190.

Mustafi, N., Grünberger, A., Kohlheyer, D., Bott, M., Frunzke, J., 2012. The development and application of a single-cell biosensor for the detection of L-methionine and branched-chain amino acids. Metab Eng. 14, 449-57.

Mustafi, N., Grünberger, A., Mahr, R., Helfrich, S., Noh, K., Blombach, B., Kohlheyer, D., Frunzke, J., 2014. Application of a genetically encoded biosensor for live cell imaging of L-valine production in pyruvate dehydrogenase complex-deficient

Corynebacterium glutamicum strains. PloS ONE. 9, e85731.

Ogino, T., Garner, C., Markley, J. L., Herrmann, K. M., 1982. Biosynthesis of aromatic compounds: ^{13}C NMR spectroscopy of whole *Escherichia coli* cells. Proc Natl Acad Sci USA. 79, 5828-32.

Ohlendorf, R., Vidavski, R. R., Eldar, A., Moffat, K., Möglich, A., 2012. From dusk till dawn: one-plasmid systems for light-regulated gene expression. J Mol Biol. 416, 534-42.

Payne, J. W., 1977. Transport and hydrolysis of peptides by microorganisms. Ciba Found Symp. 305-34.

Pittard, J., 1996. The various strategies within the TyrR regulation of *Escherichia coli* to modulate gene expression. Genes Cells. 1, 717-25.

Pittard, J., Camakaris, H., Yang, J., 2005. The TyrR regulon. Mol Microbiol. 55, 16-26.

Polen, T., Krämer, M., Bongaerts, J., Wubbolts, M., Wendisch, V. F., 2005. The global gene expression response of *Escherichia coli* to L-phenylalanine. J Biotechnol. 115, 221-37.

Robijns, S. C., Roberfroid, S., Van Puyvelde, S., De Pauw, B., Uceda Santamaria, E., De Weerdt, A., De Coster, D., Hermans, K., De Keersmaecker, S. C., Vanderleyden, J., Steenackers, H. P., 2014. A GFP promoter fusion library for the study of *Salmonella* biofilm formation and the mode of action of biofilm inhibitors. Biofouling. 30, 605-25.

Rüffer, N., Heidersdorf, U., Kretzers, I., Sprenger, G. A., Raeven, L., Takors, R., 2004. Fully integrated L-phenylalanine separation and concentration using reactive-extraction with liquid-liquid centrifuges in a fed-batch process with *E. coli*. Bioprocess Biosyst Eng. 26, 239-48.

Sambrook, J., MacCallum, P., Russell, D., 2001. Molecular cloning: a laboratory manual. Cold Spring Harbor Laboratory Press, New York.

Santos, C. N., Stephanopoulos, G., 2008. Melanin-based high-throughput screen for L-tyrosine production in *Escherichia coli*. Appl Environ Microbiol. 74, 1190-7.

Sariaslani, F. S., 2007. Development of a combined biological and chemical process for production of industrial aromatics from renewable resources. Annu Rev Microbiol. 61, 51-69.

Sarsero, J. P., Pittard, A. J., 1991. Molecular analysis of the TyrR protein-mediated activation of *mtr* gene expression in *Escherichia coli* K-12. J Bacteriol. 173, 7701-4.

Schallmey, M., Frunzke, J., Eggeling, L., Marienhagen, J., 2014. Looking for the pick of the bunch: high-throughput screening of producing microorganisms with biosensors. Curr Opin Biotechnol. 26, 148-54.

Schendzielorz, G., Dippong, M., Grünberger, A., Kohlheyer, D., Yoshida, A., Binder, S., Nishiyama, C., Nishiyama, M., Bott, M., Eggeling, L., 2014. Taking control over control: use of product sensing in single cells to remove flux control at key enzymes in biosynthesis pathways. ACS Synth Biol. 3, 21-9.

Schmidt-Dannert, C., Arnold, F. H., 1999. Directed evolution of industrial enzymes. Trends Biotechnol. 17, 135-6.

Semsey, S., Krishna, S., Sneppen, K., Adhya, S., 2007. Signal integration in the galactose network of *Escherichia coli*. Mol Microbiol. 65, 465-76.

Siedler, S., Stahlhut, S. G., Malla, S., Maury, J., Neves, A. R., 2014. Novel biosensors based on flavonoid-responsive transcriptional regulators

introduced into *Escherichia coli*. Metab Eng. 21, 2-8.

Silva-Rocha, R., de Lorenzo, V., 2012. Broadening the signal specificity of prokaryotic promoters by modifying cis-regulatory elements associated with a single transcription factor. Mol BioSyst. 8, 1950-7.

Simmonds, S., Griffith, D. D., 1961. Metabolism of phenylalanine-containing peptide amides in *Escherichia coli*. J Bacteriol. 83, 256-263.

Sprenger, G. A., 2006. Aromatic Amino Acids. In: Steinbüchel, A., (Ed.), Microbiology Monographs. vol. Amino Acid Biosynthesis - Pathways, Regulation and Metabolic Engineering. Springer-Verlag, Berlin Heidelberg.

Sprenger, G. A., 2007. From scratch to value: engineering *Escherichia coli* wild type cells to the production of L-phenylalanine and other fine chemicals derived from chorismate. Appl Microbiol Biotechnol. 75, 739-49.

Tabor, J. J., Groban, E. S., Voigt, C. A., Performance characteristics for sensors and circuits used to program *E. coli*. In: Lee, S. Y., (Ed.), Systems biology and biotechnology of *Escherichia coli*. Springer Science & Business Media B.V., 2009.

van Summeren-Wesenhagen, P. V., Marienhagen, J., 2015. Metabolic engineering of *Escherichia coli* for the synthesis of the plant polyphenol pinosylvin. Appl Environ Microbiol. 81, 840-9.

Vargas-Tah, A., Martinez, L. M., Hernandez-Chavez, G., Rocha, M., Martinez, A., Bolivar, F., Gosset, G., 2015. Production of cinnamic and p-hydroxycinnamic acid from sugar mixtures with engineered *Escherichia coli*. Microb Cell Fact. 14, 6.

Vrljic, M., Sahm, H., Eggeling, L., 1996. A new type of transporter with a new type of cellular function: L-lysine export from *Corynebacterium glutamicum*. Mol Microbiol. 22, 815-26.

Weickert, M. J., Adhya, S., 1992. Isorepressor of the *gal* regulon in *Escherichia coli*. J Mol Biol. 226, 69-83.

Weiner, M., Albermann, C., Gottlieb, K., Sprenger, G. A., Weuster-Botz, D., 2014. Fed-batch production of L-phenylalanine from glycerol and ammonia with recombinant *Escherichia coli*. Biochem Eng J. 83, 62-69.

Whipp, M. J., Pittard, A. J., 1977. Regulation of aromatic amino acid transport systems in *Escherichia coli* K-12. J Bacteriol. 132, 453-61.

Williams, B., Paigen, K., 1968. Paradoxical effect of weak inducers on the *lac* operon of *Escherichia coli*. J Bacteriol. 96, 1774-82.

Wise, A. A., Kuske, C. R., 2000. Generation of novel bacterial regulatory proteins that detect priority pollutant phenols. Appl Environ Microbiol. 66, 163-9.

Xu, P., Li, L., Zhang, F., Stephanopoulos, G., Koffas, M., 2014. Improving fatty acids production by engineering dynamic pathway regulation and metabolic control. Proc Natl Acad Sci U S A. 111, 11299-304.

Zaslaver, A., Bren, A., Ronen, M., Itzkovitz, S., Kikoin, I., Shavit, S., Liebermeister, W., Surette, M. G., Alon, U., 2006. A comprehensive library of fluorescent transcriptional reporters for *Escherichia coli*. Nat Methods. 3, 623-8.

Zeevi, D., Sharon, E., Lotan-Pompan, M., Lubling, Y., Shipony, Z., Raveh-Sadka, T., Keren, L., Levo, M., Weinberger, A., Segal, E., 2011. Compensation for differences in gene copy number among yeast ribosomal proteins is encoded within their promoters. Genome Res. 21, 2114-28.

Zhang, F., Carothers, J. M., Keasling, J. D., 2012. Design of a dynamic sensor-regulator system for production of chemicals and fuels derived from fatty acids. Nat Biotechnol. 30, 354-9.

3.5 Transcription factor-based biosensors in biotechnology: current state and future prospects

Regina Mahr, Julia Frunzke*

IBG-1: Biotechnology, Forschungszentrum Jülich, Jülich, Germany

*Corresponding author

Name of Journal: Applied Microbiology and Biotechnology

Impact Factor: 3.668

Author contributions

Own contribution to the work: 60%

	Name	Contribution
Draft of the manuscript	***Mahr, R.***	50%
	Frunzke, J.	50%
<u>Writing</u>		
Introduction	***Mahr, R.***	50%
	Frunzke, J.	50%
Exploiting nature's toolbox	***Mahr, R.***	10%
	Frunzke, J.	90%
High-throughput screening	***Mahr, R.***	10%
	Frunzke, J.	90%
Dynamic pathway control	***Mahr, R.***	10%
	Frunzke, J.	90%
Biosensor-driven adaptive evolution	***Mahr, R.***	90%
	Frunzke, J.	10%
Single-cell analysis	***Mahr, R.***	90%
	Frunzke, J.	10%
Biosensor Engineering	***Mahr, R.***	90%
	Frunzke, J.	10%
Future prospects	***Mahr, R.***	10%
	Frunzke, J.	90%
<u>Figures/Tables</u>		
Figure 1	***Mahr, R.***	90%
	Frunzke, J.	10%
Figure 2	***Mahr, R.***	90%
	Frunzke, J.	10%
Figure 3	***Mahr, R.***	90%
	Frunzke, J.	10%
Table 1	***Mahr, R.***	70%
	Frunzke, J.	30%
Table 2	***Mahr, R.***	70%
	Frunzke, J.	30%

Appl Microbiol Biotechnol
DOI 10.1007/s00253-015-7090-3

MINI-REVIEW

Transcription factor-based biosensors in biotechnology: current state and future prospects

Regina Mahr[1] · **Julia Frunzke**[1]

Received: 8 August 2015 / Revised: 8 October 2015 / Accepted: 13 October 2015

Abstract Living organisms have evolved a plethora of sensing systems for the intra- and extracellular detection of small molecules, ions or physical parameters. Several recent studies have demonstrated that these principles can be exploited to devise synthetic regulatory circuits for metabolic engineering strategies. In this context, transcription factors (TFs) controlling microbial physiology at the level of transcription play a major role in biosensor design, since they can be implemented in synthetic circuits controlling gene expression in dependency of, for example, small molecule production. Here, we review recent progress on the utilization of TF-based biosensors in microbial biotechnology highlighting different areas of application. Recent advances in metabolic engineering reveal TF-based sensors to be versatile tools for strain and enzyme development using high-throughput (HT) screening strategies and adaptive laboratory evolution, the optimization of heterologous pathways via the implementation of dynamic control circuits and for the monitoring of single-cell productivity in live cell imaging studies. These examples underline the immense potential of TF-based biosensor circuits but also identify limitations and room for further optimization.

Keywords Transcriptional regulator · Biosensor · Metabolic engineering · Screening · Evolution · Single-cell analysis

✉ Julia Frunzke
j.frunzke@fz-juelich.de

[1] Institute of Bio- and Geosciences, IBG-1: Biotechnology, Forschungszentrum Jülich GmbH, 52425 Jülich, Germany

Introduction

In the last century, the era of metabolic engineering resulted in an enormous increase in microbial processes for the production of value-added compounds, such as proteins, amino acids, biofuels, organic acids and polymer precursors. Based on renewable feedstocks, the efficient establishment and optimization of bioprocesses is the key to a transition from the currently petroleum-dependent and energy-intensive chemical industry towards a sustainable bioeconomy.

Exploiting microorganisms for large-scale production requires, on the one hand, elaborated high-throughput (HT) tools for strain engineering, and, on the other hand, techniques for analyzing the performance of producer strains and the efficiency of bioprocesses. Recent studies using metabolic flux analysis and in silico modelling approaches enable new insights into the bacterial physiology during fermentation (Wiechert and Noack 2011); however, the formation of inefficient subpopulations affecting the outcome of the bioprocess is often neglected (Delvigne and Goffin 2014; Lieder et al. 2014). While rational strain engineering is limited by the high physiological complexity of microbes, traditional random mutagenesis strategies are restricted by the selection and screening capacity, which requires a readily accessible phenotype linked to product formation (Dietrich et al. 2010; Schallmey et al. 2014). During the past decade, advances in synthetic biology significantly contributed to the establishment of novel metabolic engineering tools (Ng et al. 2015; Wendisch 2014). For example, genetically encoded biosensors have proven to be of high value for various applications in strain engineering, dynamic pathway control and single-cell analysis. The basic principle is based on metabolite-sensing proteins (e.g. transcription factors, enzymes or periplasmic-binding proteins) or RNAs (e.g. riboswitches and ribozymes) which are activated upon binding of effector molecules and control in turn the

Published online: 31 October 2015

expression of an actuator part (e.g. fluorescent reporters, regulatory switches or selection markers). This biosensor architecture enables the intracellular detection of metabolite production by converting it into a measureable output (Fig. 1).

In the following sections, we will review recent progress regarding the design of biosensor circuits based on transcription factors (TFs) and their application in metabolic engineering strategies including HT screening approaches, dynamic pathway control, biosensor-driven evolution and single-cell analysis (Fig. 2). We will not include the application of TF-based biosensors for the detection of environmental pollutants, which is reviewed elsewhere (Fernandez-Lopez et al. 2015; van der Meer and Belkin 2010). For recent review articles on RNA- and FRET-based biosensors, see Frommer et al. (2009), Liang et al. (2011), Michener et al. (2012), Schallmey et al. (2014) and Zhang et al. (2015).

Exploiting nature's toolbox—transcription factor-based biosensors

Living organisms have evolved a variety of different sensor principles to monitor the intra- or extracellular accumulation of small molecules, ions or changes in physical parameters. In prokaryotes, TFs play a major role in physiological adaptation by controlling gene expression at the level of transcription—typically by interfering with the binding of the RNA polymerase to DNA. The activity of TFs can be affected by the interaction with small (effector) molecules, ions, physical parameters (e.g. temperature or pH), protein-protein interaction or protein modification. In several recent studies, researchers have demonstrated that these mechanisms provide a versatile toolbox for applications in metabolic engineering and single-cell analysis of production strains (Table 1) (Liu et al. 2015a; Michener et al. 2012; Schallmey et al. 2014).

Especially, metabolite-responsive TFs have proven to be valuable tools for biotechnological applications and have been integrated into a diverse set of synthetic regulatory circuits enabling the detection of, for example, amino acids (Binder et al. 2012; Mustafi et al. 2012), succinate (Dietrich et al. 2013), butanol (Dietrich et al. 2013), malonyl-CoA (Xu et al. 2014a, b) and secondary metabolites (Siedler et al. 2014b). These circuits are typically based on a previously well-characterized TF which limits the rapid access to novel metabolite sensors to a small set of known TFs. However, the principle of substrate-induced gene expression (SIGEX), where fragments of a metagenomic library can be ligated into an operon-trap vector in front of a suitable reporter gene (e.g. *gfp*), might represent an option to overcome this limitation (Uchiyama and Miyazaki 2010b; Uchiyama and Watanabe 2008). Originally developed for the screening of novel enzymes and biosynthetic operons, this design can in principle also be exploited to screen metagenomic libraries for effector-

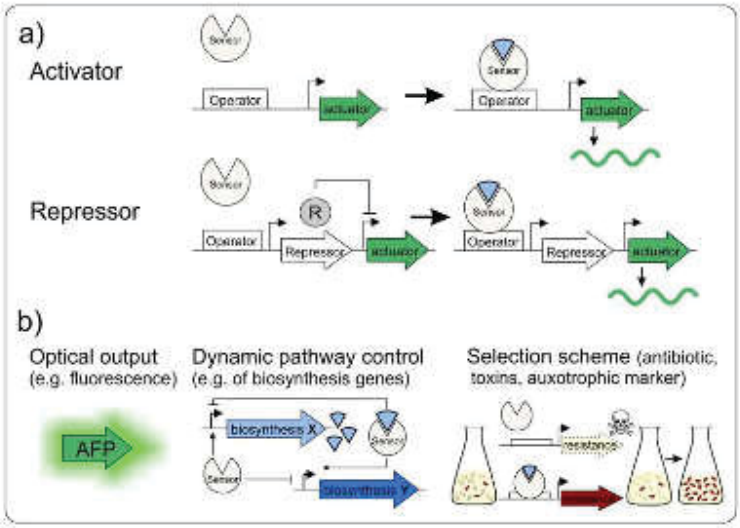

Fig. 1 Principles for the architecture of transcription factor-based biosensors. **a** A transcriptional activator may be used to activate expression of an actuator gene (circuit) in response to effector molecules. In contrast, repressors block the expression of actuators. By setting the expression of a second repressor under the control of the TF-biosensor repressor, the signalling can be inverted, resulting in a positive output of the actuator module. **b** Depending on the final function, different actuators are available as biosensor readout. The expression of e.g. autofluorescent proteins (AFP) results in an optical output, while the insertion of the biosensor into regulatory circuits can trigger and dynamically control biosynthetic pathways. Sensors can further be used to generate an artificial selection scheme by the choice of a suitable actuator (e.g. antibiotics, toxins or auxotrophy) controlling the survival of strains with desired traits

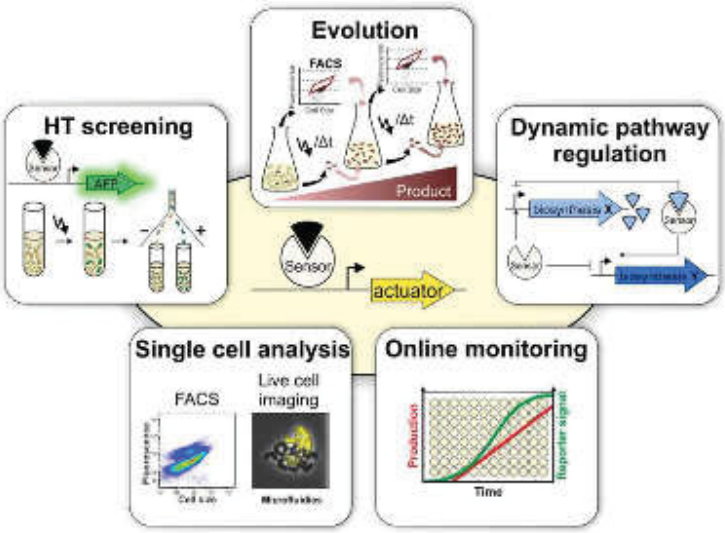

Fig. 2 Versatile applications of TF-based biosensors. Biosensors with an optical readout, e.g. production of an autofluorescent protein (*AFP*), are efficient tools for the high-throughput (*HT*) screening of large mutant libraries using fluorescence-activated cell sorting (*FACS*). Biosensor-driven evolution has proven a convenient strategy to increase production by iteratively imposing an artificial selective pressure on the fluorescent output of a biosensor using FACS or selection schemes. Integrated into synthetic regulatory circuits, biosensors can be used for the dynamic control of biosynthetic pathways in order to avoid, for example, the accumulation of toxic intermediates. Finally, biosensors are convenient tools for non-invasive online monitoring of production processes and for analysis at single-cell resolution using FACS and live cell imaging in microfluidic chip devices

responsive TF-promoter pairs. Furthermore, global databases like DBD (www.transcriptionfactor.org; (Wilson et al. 2008)), RegPrecise (http://regprecise.lbl.gov/RegPrecise; (Novichkov et al. 2013)) or PRODORIC (www.prodoric.de; (Münch et al. 2003)) are useful tools to gain information on prokaryotic transcription factors and regulons. Finally, plenty of species-specific databases are available, including RegulonDB (http://regulondb.ccg.unam.mx; (Salgado et al. 2006)) and EcoCyc (http://ecocyc.org; (Keseler et al. 2013)) for *Escherichia coli* or CMRegNet (www.lgcm.icb.ufmg.br/cmregnet; (Abreu et al. 2015)) for corynebacterial and mycobacterial species which also provide valuable information regarding regulatory circuits for the development of novel sensor devices.

Besides classical one-component TFs, the principle of two-component signalling (TCS) represents a promising mode for the extracellular detection of small molecules in production strains or synthetic communities. Previous studies have already demonstrated that the modular design of TCS can be exploited to create sensor kinases with novel effector specificities and to transduce the information to the level of gene expression (Ohlendorf et al. 2012). In a recent study, Ganesh and co-workers reported on the construction of a chimeric, malate-responsive TCS by fusing the sensor domain of MalK (*Bacillus subtilis*) to the kinase domain of EnvZ (*Escherichia coli*) thereby controlling the activity of the *ompC* promoter in response to external malate accumulation (Ganesh et al. 2015). To ensure specific signal transduction and to avoid detrimental cross-talk to host TCSs, the stoichiometry, the expression level of the protein components, as well as the potential phosphatase activity of the sensor kinase remain critical aspects to be considered for the design of TCS-based biosensors (Podgornaia and Laub 2013).

An alternative principle for intra- or extracellular sensing is represented by extracytoplasmic function (ECF) sigma factors (Mascher 2013). The orthogonality of ECF-based switches has recently been demonstrated by a proof-of-principle study describing the construction of a bistable switch in *E. coli* (Chen and Arkin 2012) and was further developed by Rhodius et al., who characterized ECF sigma factor families in bacteria using bioinformatics. The authors reported on 20 highly orthogonal combinations of sigma factors and their cognate promoters (Rhodius et al. 2013). These studies provide a promising basis for the design of synthetic circuits in metabolic engineering.

High-throughput screening

Genetically encoded biosensors enable the specific translation of intracellular product accumulation into a screenable (e.g. fluorescence) or selectable (e.g. antibiotic resistance) output by driving the production of a reporter protein (Fig. 1b). Consequently, an important field of biosensor application is

Table 1 Overview of TF-based biosensors applied in biotechnological strain development and screening approaches

TF	Analyte	Host chassis	Output	Application
AraC-Idi$_{synth}$ based on AraC of *E. coli*	Isopentenyl diphosphate (lycopene)	*E. coli*	MutD5-mCherry	Improvement of isopentenyl diphosphate production of *E. coli* using a biosensor-controlled mutator strategy. Visualization of the production by the biosensor output (Chou and Keasling 2013)
BenR of *P. putida*	Benzoate	*E. coli*	GFP	Screening of a metagenomics library for improved amidase activities (Uchiyama and Miyazaki 2010a)
BmoR of *Thauera butanivorans*	1-Butanol (response to linear and branched-chain alcohols)	*E. coli*	TetA-GFP	Improvement of 1-butanol production of *E. coli* by a biosensor-based selection scheme. Simultaneous monitoring of growth and fluorescence as measure of the biosensor output (Dietrich et al. 2013)
CysR of *C. glutamicum*	O-acetyl (homo-) serine	*C.glutamicum*	eYFP	Visualization of sulphur limitation at the single cell level (Hoffmann et al. 2013)
DcuR of *E. coli*	Succinate	*E. coli*	TetA	Proof-of-concept study: linking dicarboxylic acid production to bacterial growth (Dietrich et al. 2013)
FadR of *E. coli*	Fatty acid/acyl-CoA	*E. coli*	RFP/regulatory circuit	Implementation of a synthetic circuit for dynamic pathway control of the production of fatty acid ethyl ester in *E. coli* (Zhang et al. 2012)
FapR of *B. subtilis*	Malonyl-CoA	*E. coli*	eGFP/regulatory circuit	• Design and kinetic analysis of a malonyl-CoA sensor in *E. coli* (Xu et al. 2014b) • TF-based negative feedback loop for the dynamic control of fatty acid biosynthesis in dependency of the intracellular malonyl-CoA level (Liu et al. 2015b)
LacI of *E. coli*	IPTG, lactose	*E. coli*	GFP	Live cell imaging study of the correlation between growth rate fluctuations and metabolic stochasticity (Kiviet et al. 2014)
Lrp of *C. glutamicum*	L-valine L-leucine L-isoleucine L-methionine	*C.glutamicum*	eYFP	• HT FACS screening of a chemically mutagenized *C. glutamicum* wt library (Mustafi et al. 2012) • Live cell imaging of L-valine production of PDHC-deficient *C. glutamicum* strains (Mustafi et al. 2014) • Biosensor-driven evolution of L-valine production (Muhr et al. 2015)
LysG of *C. glutamicum*	L-lysine L-arginine L-histidine	*C.glutamicum*	eYFP	• HT FACS screening of a chemically mutagenized *C. glutamicum* wt library (Binder et al. 2012) • Screening of enzyme libraries for feedback-resistant variants of key enzymes for amino acid production (Schendzielorz et al. 2014)
NahR of *P. putida*	Benzoic acids	*E. coli*	TetA	Proof-of-concept study: selection of biocatalysts by the implementation of a TF-based selection scheme (van Sint Fiet et al. 2006)
PcaR of *P. putida*	ß-ketoadipate	*E. coli*	TetA	Proof-of-concept study: linking ß-ketoadipate production to bacterial growth (Dietrich et al. 2013)
SoxR of *E. coli*	NADPH	*E. coli*	eYFP	HT FACS screening of a mutant library of the NADPH-dependent alcohol dehydrogenase of *Lactobacillus brevis* for improved 4-methyl-2-pentanone (Siedler et al. 2014a)
TyrR of *E. coli*	L-tyrosine	*E. coli*	MutD5-mCherry	Improvement of L-tyrosine production of *E. coli* using a biosensor-controlled mutator strategy. Visualization of the production by the biosensor output (Chou and Keasling 2013)

implementation in HT screening approaches for the selection of novel or improved biocatalysts (Fig. 2) (Eggeling et al. 2015; Schallmey et al. 2014). Fluorescence-activated cell sorting (FACS) was applied in several recent studies as a particularly suitable HT technique. For example, the transcriptional regulator Lrp of *Corynebacterium glutamicum* was recently implemented in a FACS HT screening approach for the isolation of mutant strains producing branched-chain amino acids (L-valine, L-leucine and L-isoleucine) from a mutant library after chemical mutagenesis (Mustafi et al. 2012). The native function of Lrp is to sense the intracellular accumulation of branched-chain amino acids and methionine, and in turn to activate the amino acid export system BmFE in order to avoid high intracellular levels and toxic effects of these amino acids (Lange et al. 2012). These characteristics provide an optimal basis for the construction of biosensors featuring an appropriate dynamic range and sensitivity for the improvement of production strains. In addition, they have a significant advantage in comparison to the use of sensors based on transcriptional (biosynthesis) repressors or periplasmic-binding proteins, which typically display a very high effector affinity. The successful application of a similar activator protein has also been demonstrated by a study using the LysG TF for the isolation of L-lysine-producing strains of *C. glutamicum* via FACS (Binder et al. 2012).

Furthermore, TF-based sensors were successfully exploited in enzyme screenings. For example, the abovementioned LysG sensor was used to screen enzyme libraries for feedback-resistant enzyme variants for the overproduction of the effector amino acids L-arginine (N-acetyl-L-glutamate kinase), L-histidine (ATP phosphoribosyl transferase) and L-lysine (aspartate kinase) (Schendzielorz et al. 2014). An engineered AraC variant was used by Tang and co-workers for the directed evolution of 2-pyrone synthase activity (from *Gerbera hybrida*) in *E. coli*. Two iterative rounds of mutagenesis and selection led to the isolation of enzyme variants displaying roughly 20-fold increased triacetic acid lactone production (Tang et al. 2013). The considerable plasticity of the AraC protein for the engineering of new effector specificities was already previously demonstrated in a study where a mevalonate-responsive AraC variant was used for the screening of ribosome binding site (RBS) variants in front of a hydroxymethylglutaryl-CoA reductase (Tang and Cirino 2011). A promising alternative to the sensing of product formation was recently demonstrated by the application of an NADPH-responsive biosensor based on *E. coli* SoxR. This sensor provides a broadly applicable tool for the screening of NADPH-dependent enzymes, as exemplified by screening a dehydrogenase library for enzymes exhibiting improved catalytic activity for the substrate 4-methyl-2-pentanone (Siedler et al. 2014a).

As an alternative to screening strategies, TF-based biosensors can also be integrated in circuits to establish a product-dependent selection scheme driving the expression of, for example, an antibiotic resistance or toxin gene (Fig. 1b) (Dietrich et al. 2013; Raman et al. 2014; van Sint Fiet et al. 2006). The proof-of-principle was provided by a study of van Sint Fiet et al., who used the transcriptional activator NahR which responds to benzoate and 2-hydroxybenzaldehyde by the activation of *tetA* (or *lacZ*) expression (van Sint Fiet et al. 2006). The authors suggested that this design enables the efficient selection of novel or improved biocatalysts for chemical synthesis. Suitability of such a circuit design was later, for instance, demonstrated by the improvement of 1-butanol production of engineered *E. coli* by using the putative σ^{54}-transcriptional activator BmoR and a σ^{54}-dependent, alcohol-regulated promoter (P_{BMO}) from *Pseudomonas butanovora* driving the expression of a *tetA-gfp* gene fusion (Dietrich et al. 2013). This setup allowed the simultaneous monitoring of growth and fluorescence as a measure of the biosensor output.

Dynamic pathway control

In microorganisms, small molecule biosynthesis is typically controlled by a complex regulatory network which optimizes metabolic flux according to the requirements of the host and counteracts the accumulation of toxic intermediates. Consequently, the simple integration of heterologous biosynthetic pathways or enzymes may lead to unbalanced flux and detrimental interference with the host metabolism. In this context, TF-based biosensors can be used to construct synthetic regulatory switches to dynamically regulate metabolic fluxes (Figs. 1b and 2). This has, for example, been achieved by using the fatty acyl-CoA biosensor FadR to coordinate the biosynthesis of acyl-CoA and ethanol as well as the expression of a wax-ester synthase in an *E. coli* strain producing fatty acid ethyl ester (FAEE) (Zhang et al. 2012). Upon accumulation of acyl-CoA, the repressor FadR dissociates from its target promoters, leading to the activation of ethanol biosynthesis and the expression of wax-ester synthase, which converts ethanol and acyl-CoA to FAEE. Similarly, Xu and co-workers designed a hybrid promoter-regulator system based on the malonyl-CoA-responsive TF FapR in *E. coli* (Xu et al. 2014b). This regulator was further used to devise different negative feedback loops for the dynamic control of the enzymes acetyl-CoA carboxylase and fatty acid synthase for improved fatty acid biosynthesis as a function of intracellular malonyl-CoA levels (Liu et al. 2015b; Xu et al. 2014a).

The fact that accumulation of toxic intermediates may lead to a complex cellular stress response can also be exploited for the design of synthetic circuits balancing the pathway flux. In contrast to the choice of a well-known TF for circuit design, transcriptome analysis by DNA microarrays or RNA-Seq may be applied to uncover genes whose expression is altered upon

accumulation of a certain pathway intermediate. For instance, exploiting the cellular response of *E. coli* to the accumulation of farnesyl pyrophosphate was used to balance terpenoid production (Dahl et al. 2013). However, transcriptome analysis provides a snapshot view of the cellular response to metabolite accumulation and, thus, the dynamic behaviour of the particular transcriptional response can hardly be estimated. Furthermore, complex regulatory hierarchies will likely hinder the exact description of the sensor transfer curve and its application for the dynamic control of heterologous pathways.

Biosensor-driven adaptive evolution

Due to the high physiological complexity of living organisms and the limited knowledge of their underlying mechanisms, alternative approaches are in demand to efficiently engineer bacterial strains for biotechnological applications. Random mutagenesis strategies, however, lead to several hundred undirected small nucleotide polymorphisms (SNPs) genome-wide (Harper and Lee 2012), which makes it difficult to identify mutations contributing to the desired phenotypic trait. Evolution approaches driven by mutation and selection have proven a valuable tool to adapt microorganisms to stress conditions (Lee et al. 2013; Oide et al. 2015) or to improve product formation (Reyes et al. 2014; Xie et al. 2015). In several recent strategies, biosensors were successfully implemented to expand adaptive laboratory evolution to include production phenotypes which are not naturally linked to bacterial growth or fitness (Fig. 2) (Chou and Keasling 2013; Dietrich et al. 2013; Mahr et al. 2015; Yang et al. 2013).

Using feedback-regulated evolution of phenotype (FREP), Chou and Keasling dynamically regulated the mutation rate of a strain defective in the DNA repair machinery by controlling the mutator gene (*mutD5*) as the actuator of a small molecule biosensor (Chou and Keasling 2013). The FREP strategy was successfully applied in *E. coli* to increase tyrosine production up to fivefold. Using the same strategy, the propagation of high lycopene producer cells for a total cultivation of 432 h yielded up to 6800 μg lycopene g^{-1} dry cell weight. The application of FREP, however, resulted in several hundred SNPs throughout the entire genome (Chou and Keasling 2013). To reduce the number of mutations, we recently established a biosensor-driven adaptive evolution strategy, which is based on the natural mutation frequency of 10^{-10} to 10^{-9} mutations per base pair per replication cycle (Mahr et al. 2015). Using FACS, cells exhibiting a high biosensor output (eYFP fluorescence) were iteratively isolated and recultivated. Within five rounds of evolution, growth and the L-valine product formation of a pyruvate-dehydrogenase-deficient *C. glutamicum* strain were significantly improved, while at the same time a three- to fourfold reduction in by-product (L-alanine) formation was achieved. Four out of seven identified SNPs were reintroduced into the parental strain and were found to significantly increase L-valine production or to reduce by-product formation (Mahr et al. 2015).

Since artificial selection schemes may result in the enrichment of (false positive) cheaters, Raman et al. devised a combination of a positive and negative selection strategy based on the TolC selector (positive selection: sodium dodecyl-sulphate; negative selection: using colicin E1, (DeVito 2008)). This elegant design enabled the performance of multiple toggled rounds of selection to improve the production of naringenin and glucaric acid (Raman et al. 2014). Altogether, these examples demonstrate that biosensor-driven evolution represents a suitable strategy to complement rational approaches for the engineering of production strains.

Single-cell analysis

Microbial metabolism is typically analyzed using bulk techniques neglecting single-cell behaviour and the formation of complex phenotypic patterns (Huang 2009; Vasdekis and Stephanopoulos 2015). However, even clonal groups of microorganisms may display significant phenotypic variation which can significantly contribute to the fitness of the whole population in its natural ecological niche (Ackermann 2015). Cell-to-cell variability caused by intrinsic or extrinsic factors may, however, strongly influence bioprocess performance and stability (Delvigne et al. 2014; Müller et al. 2010). The formation of inefficient subpopulations has, for example, been observed in the production of solvent by endospore-forming *Clostridia* (Tracy et al. 2008), the production of lactobionic acid in *Pseudomonas taetrolens* (Alonso et al. 2012) and the production of heterologous proteins by *E. coli* (Want et al. 2009), *Bacillus megaterium* (Münch et al. 2015) and yeast (Carlquist et al. 2012; Newman et al. 2006). However, only a limited number of studies implemented TF-based biosensors for single-cell analysis of production strains, so far (Delvigne et al. 2009; Hoffmann et al. 2013; Mustafi et al. 2014).

Recent advances in live cell imaging approaches using microfluidic chip devices and flow cytometry (FC) have significantly contributed to the analysis and monitoring of microbial populations at single-cell resolution (Fig. 2) (Delvigne and Goffin 2014; Grünberger et al. 2014; Vasdekis and Stephanopoulos 2015). To address the variety of biological questions, different microfluidic chips have recently been developed for the spatiotemporal analysis of microbial populations, including two-dimensional picolitre bioreactor chambers (Grünberger et al. 2012, 2014) as well as one-dimensional designs (e.g. the mother machine (Long et al. 2013; Wang et al. 2010)) for the long-term study of bacterial growth and fluorescence. The mother machine structure was, for instance, applied to analyze the correlation of growth rate fluctuations and metabolic stochasticity using a LacI-sensor

(Kiviet et al. 2014). In this study, Kiviet and co-workers demonstrated how gene expression noise can affect growth rate fluctuations and vice versa, leading to cellular heterogeneity (Kiviet et al. 2014). Recently, the abovementioned Lrp biosensor was applied to monitor L-valine production of pyruvate-dehydrogenase-deficient *C. glutamicum* strains grown in 2D microfluidic chip devices (Mustafi et al. 2014). Interestingly, the addition of small amounts of complex medium compounds, as often used during production processes, resulted in phenotypic heterogeneity during the production phase (Mustafi et al. 2014).

Complementing live cell imaging studies, FC allows the convenient analysis of populations grown in large volumes such as shake flasks or bioreactors by HT processes (Huang 2009; Vasdekis and Stephanopoulos 2015). Combined with biosensors, FC has the potential to identify the formation of subpopulations with respect to metabolic activity, co-factor supply or cell cycle state and to use this information for the optimization of bioprocesses. For example, Delvigne and co-workers revealed subpopulations differing in *rpoS* expression applying oscillating feed control during fermentation using a transcriptional *rpoS-gfpmut2* sensor construct (Delvigne et al. 2009). Furthermore, recent advances in the establishment of downstream analytical methods bring the analysis of isolated subpopulations within reach. Jehmlich and co-workers established a workflow to analyze the proteome of FACS-isolated subpopulations by mass spectrometry (Jahn et al. 2013; Jehmlich et al. 2010). This protocol was successfully applied to analyze subpopulations occurring during the growth of *Pseudomonas putida* KT2440 in bioprocesses (Lieder et al. 2014). Altogether, these examples highlight the recent advances in single-cell analysis of microbial production strains. Combined with TF-based biosensors, these technological advances will significantly increase the resolution of bioprocess monitoring.

Biosensor engineering

Although nature has evolved a variety of TF-promoter pairs, these sensor devices only exist for a limited number of cellular metabolites (Mustafi et al. 2015; Tang and Cirino 2011). As organisms tightly regulate their transcriptional machinery, endogenous promoter activity and its control are adapted to the organism's purposes. For this reason, biosensors based on native transcription factors and promoters are often limited in sensitivity as well as the dynamic range, and are incompatible with non-native hosts (Blazeck and Alper 2013; Umeyama et al. 2013; Zhang et al. 2012, 2015). Furthermore, many biotechnological applications require the extension of promiscuous transcriptional regulators for specific or non-natural ligands (Looger et al. 2003; Schallmey et al. 2014). Due to the modular architecture of promoter regions (Blazeck and Alper 2013) and TFs (Galvao et al. 2007), engineering of biosensors for suitable performance characteristics becomes feasible (Fig. 3, Table 2). For example, Zhang and co-workers increased the dynamic range of a sensor system based on the fatty acid-sensing transcriptional regulator FadR about 1000-fold by the introduction of two copies of the FadR-DNA binding sequence into the strong phage lambda (P_L) and phage T7 promoters (P_{A1}) (Lutz and Bujard 1997; Zhang et al. 2012). By combining the FadR binding sites with a LacI operator site in the synthetic promoter, a tight regulation and induction by IPTG and fatty acids was accomplished, yielding a dynamic sensor-regulator system which enabled fatty acid ethyl ester production to be increased threefold (Fig. 3a) (Zhang et al. 2012).

The modulation of the affinity and amount of TF binding sites can likewise contribute to the development of altered effector specificities and sensitivities (de Las Heras et al. 2012; Silva-Rocha and de Lorenzo 2012). For example, the TF BenR (AraC/XylS family) of *P. putida* KT2440 regulates P_b promoter activity by binding to the *Om-p* operator site in response to benzoate and with less efficiency to 3-methylbenzoate (3MBz) (Silva-Rocha and de Lorenzo 2012). Interestingly, the completion of a second truncated operator motif upstream of the *Om-p* site enhanced sensitivity of the sensor construct to 3MBz four- to fivefold (Fig. 3b) (Bintu et al. 2005a, b; Silva-Rocha and de Lorenzo 2012).

The modular architecture of regulators responding to effector molecules theoretically allows the development of any specificity and sensitivity (Fig. 3c) (Galvao and de Lorenzo 2006). Techniques generating genetic diversity, such as error-prone PCR (Wise and Kuske 2000), chemical and saturation mutagenesis (Tang and Cirino 2011; Tang et al. 2008, 2013) or computational modelling based on crystal structure data sets (Looger et al. 2003; Mandell and Kortemme 2009) contributed to the development of effector-molecule binding sites with altered or novel specificities (Galvao and de Lorenzo 2006). For example, the L-arabinose-response transcriptional regulator AraC was engineered by saturation mutagenesis to specifically respond to D-arabinose (Tang et al. 2008), to mevalonate (Tang and Cirino 2011) and to triacetic acid lactone (Tang et al. 2013). The de novo design of TF exhibiting the desired effector specificity was, furthermore, reported in a study by Chou and Keasling, who assembled the ligand binding domain of enzymes with the AraC DNA binding domains, yielding a synthetic transcription factor for the sensing of isopentenyl diphosphate (Chou and Keasling 2013). However, complex conformational changes occurring upon ligand binding and inter-domain interactions required for signal transduction make it more difficult to apply this strategy as a ubiquitous design approach.

The orthogonality of functional biological parts (e.g. promoters, coding sequences or terminators) still represents a major objective in the field of synthetic biology

Table 2 Examples for biosensor engineering

TF; source	Analyte	Host	Output	Characteristics/architecture
AraC-Idi$_{Synth}$; *E. coli*	Isopentenyl diphosphate (lycopene)	*E. coli*	MutD5-mCherry	Sensor based on a synthetic TF composed of a isoprenoid binding domain and the DNA binding domain of AraC (Chou and Keasling 2013)
AraC-mev; *E. coli*	Mevalonate	*E. coli*	GFPuv	Screening of an AraC mutant library for a TF with a specific response towards mevalonate (mutated ligand binding site) (Tang and Cirino 2011)
AraC-Mut; *E. coli*	D-arabinose	*E. coli*	GFP	Screening of an AraC mutant library for a TF with a specific response towards D-arabinose (mutated ligand binding site) (Tang et al. 2008)
AraC-TAL; *E. coli*	Triacetic acid lactone	*E. coli*	GFP, LacZ	Screening of an AraC mutant library for a TF with a specific response towards triacetic acid lactone (mutated ligand binding site) (Tang et al. 2013)
BenR; *P. putida*	Benzoate, 3-methylbenzoate	*P. putida*	LuxCDABE	Introduction of a second operator motif into the promoter region increased specificity of the biosensor towards 3-methylbenzoate (Silva-Rocha and de Lorenzo 2012)
DcuS/EnvZ chimeric TCS; *E. coli*	Fumarate	*E. coli*	GFP	Chimeric TCS-based sensor for the extracellular sensing of fumarate (Ganesh et al. 2013)
GAL4-Idi$_{Synth}$; *S. cerevisiae*/*E. coli*	Isopentenyl diphosphate (isoprenoids)	*E. coli*	Citrine	Sensor based on a synthetic TF composed of a isoprenoid binding domain and the DNA binding domain of GAL4 (Chou and Keasling 2013)
MalK/EnvZ chimeric TCS; *B. subtilis*/*E. coli*	Malate	*E. coli*	GFP	Sensor based on a chimeric TCS enabling the extracellular detection of malate by *E. coli* (Ganesh et al. 2015)
MetJ-B42; *E. coli*	S-adenosyl-methionine	*S. cerevisiae*	Venus, *HIS3*	Equipment of the *E. coli* TF MetJ with the transcriptional activation domain B42 results in the functional expression in *S. cerevisiae* (Umeyama et al. 2013)
PhlF; *E. coli*	2,4-Diacetylphloroglucinol	HEK293 cells	YFP	Equipment of the *E. coli* TF PhlF with eukaryotic-specific signals results in 2,4-diacetylphloroglucinol recognition in eukaryotic HEK293 cells (Stanton et al. 2014)
XylR; *P. putida*	3-Methyl-benzylalcohol m-xylene	*P. putida*	LuxCDABE	Equipment of the biosensor with a positive feedback loop and an attenuation mechanism shifted the specificity towards m-xylene (de Las Heras et al. 2012)

TFs for biosensor designs. However, accessibility to novel biosensor circuits and sensor components with altered effector specificities (e.g. to non-natural compounds) is key to a broad application in a wide variety of studies. As demonstrated by a number of studies, the modular design of TFs and their respective target promoters make a rapid design of novel circuits feasible (Fig. 3, Table 2). Despite this modularity and in-depth knowledge of the molecular basis, however, the design of synthetic regulatory circuits is not yet like a Lego set. To this end, future attempts must focus on the precise definition of highly orthogonal parts for sensor design and on the efficient generation of custom-made sensor domains with novel specificities and suitable characteristics (sensor transfer curves). Here, the combination of rational design and HT screening of mutant TF libraries appears most promising for efficient sensor design. Furthermore, the integration of synthetic biosensor circuits involves a metabolic burden for the host system which may affect productivity. Especially in the case of integral dynamic control circuits, the expression level of sensor components should be optimized to a minimum level, ensuring sensor functionality but minimizing interference with the host system.

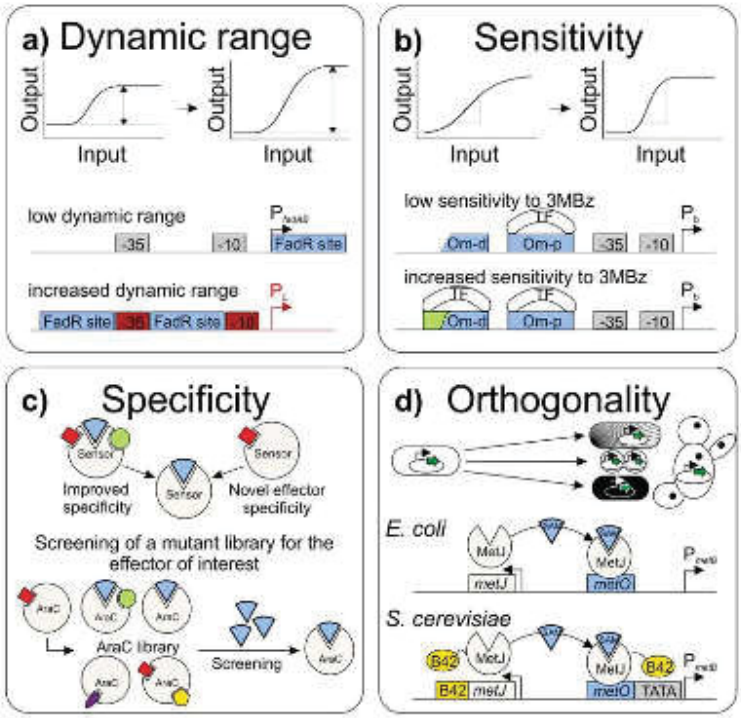

Fig. 3 Examples of biosensor engineering for altered performance characteristics or orthogonal applications. **a** The dynamic range, describing the maximum fold change of a reporter output to a given input signal (Mustafi et al. 2015), was increased by introducing two FadR binding sites from the *fadAB* promoter into the strong lambda phage promoter P_L (Zhang et al. 2012). **b** To increase the sensitivity as rate of increase in reporter output (depicted by the slope of the transfer curve) to 3-methylbenzoate (*3MBz*), the truncated operator site *Omp-d* upstream of the operator site *Omp-p* in the P_b promoter was completed enabling the binding of two benzoate-binding transcription factors (*TF*) (Silva-Rocha and de Lorenzo 2012). **c** Furthermore, screening of an AraC mutein library for effectors of interest resulted in the identification of transcription factors with altered specificities (Tang and Cirino 2011; Tang et al. 2013). **d** The orthogonal transfer of biosensors to host organisms is challenging. Umeyama and co-workers equipped the S-adenosylmethionine (*SAM*)-responsive transcription factor MetJ of *E. coli* with the transcriptional activator domain B42 resulting in SAM detection in *S. cerevisiae* (Umeyama et al. 2013)

(Fig. 3d). Libraries of standardized modules (also designated as BioBricks) may contribute to facilitate the engineering of sensor devices. The functional transfer between organisms, however, still remains challenging. In an interesting study, Umeyama and co-workers fused the transcriptional regulator MetJ of *E. coli* to the transcriptional activation domain B42, yielding the synthetic TF MetJ-B42 which allows S-adenosylmethionine (SAM) sensing in the yeast *Saccharomyces cerevisiae* (Umeyama et al. 2013). Due to the extremely low diversity of regulatory proteins in mammalian cells, Stanton and co-workers supplied the PhlF repressor of *E. coli* with eukaryotic-specific signals (including a nuclear localization signal) and equipped regulated promoters with multiple operator sites resulting in 2,4-diacetylphloroglucinol recognition in HEK293 cells (Stanton et al. 2014). Although orthogonality still remains problematic, these examples show, however, that the transfer of sensor elements is feasible even across kingdom borders.

Future prospects

TF-based biosensors have significantly contributed to a number of recent metabolic engineering approaches by improving production strains or by identifying non-producing subpopulations during bioprocesses (Fig. 2). However, a detailed molecular understanding of the observed phenotypic patterns during fermentation requires the establishment of highly sensitive *Omics* techniques interfacing with live cell imaging (e.g. in microfluidic chips) and cytometry analysis and cell sorting. Here, the combination of biosensors with next generation sequencing (e.g. RNA-seq) or high-resolution proteomics appears promising to reveal new insights into subpopulations and may support the identification of bottlenecks during bioprocesses.

Most biosensors reported to date are based on a small number of well-characterized TFs (Table 1). At this point, the screening of promoter libraries or transcriptome analysis using RNA-seq might contribute to harness still uncharacterized

TF-based biosensors have the potential to revolutionize recent strategies in biotechnological strain development. However, several studies still remain at the level of sensor construction and proof-of-principle applications. To enhance the availability of sensors with appropriate characteristics, more studies are required to establish efficient workflows for biosensor design. Altogether, these efforts should aim to enable an application-oriented construction of biosensors to allow the rapid engineering of required circuits meeting the needs of the particular metabolic engineering purpose.

Compliance with ethical standards

Funding This work was supported by the German Federal Ministry of Education and Research (BMBF OptoSys grant 031A167B) and the Helmholtz Association (Helmholtz YIG VH-NG-716).

Conflict of interest The authors declare that they have no competing interests.

Ethical approval This article does not contain any studies with human participants or animals performed by any of the authors.

References

Abreu VA, Almeida S, Tiwari S, Hassan SS, Mariano D, Silva A, Baumbach J, Azevedo V, Rottger R (2015) CMRegNet-An interspecies reference database for corynebacterial and mycobacterial regulatory networks. BMC Genomics 16:452. doi:10.1186/s12864-015-1631-0

Ackermann M (2015) A functional perspective on phenotypic heterogeneity in microorganisms. Nat Rev Microbiol 13(8):497–508. doi:10.1038/nrmicro3491

Alonso S, Rendueles M, Diaz M (2012) Physiological heterogeneity of *Pseudomonas taetrolens* during lactobionic acid production. Appl Microbiol Biotechnol 96(6):1465–1477. doi:10.1007/s00253-012-4254-2

Binder S, Schendzielorz G, Stäbler N, Krumbach K, Hoffmann K, Bott M, Eggeling L (2012) A high-throughput approach to identify genomic variants of bacterial metabolite producers at the single-cell level. Genome Biol 13(5):R40. doi:10.1186/gb-2012-13-5-r40

Bintu L, Buchler NE, Garcia HG, Gerland U, Hwa T, Kondev J, Kuhlman T, Phillips R (2005a) Transcriptional regulation by the numbers: applications. Curr Opin Genet Dev 15(2):125–135. doi:10.1016/j.gde.2005.02.006

Bintu L, Buchler NE, Garcia HG, Gerland U, Hwa T, Kondev J, Phillips R (2005b) Transcriptional regulation by the numbers: models. Curr Opin Genet Dev 15(2):116–124. doi:10.1016/j.gde.2005.02.007

Blazeck J, Alper HS (2013) Promoter engineering: recent advances in controlling transcription at the most fundamental level. Biotechnol J 8(1):46–58. doi:10.1002/biot.201200120

Carlquist M, Fernandes RL, Helmark S, Heins AL, Lundin L, Sorensen SJ, Gernaey KV, Lantz AE (2012) Physiological heterogeneities in microbial populations and implications for physical stress tolerance. Microb Cell Factories 11:94. doi:10.1186/1475-2859-11-94

Chen D, Arkin AP (2012) Sequestration-based bistability enables tuning of the switching boundaries and design of a latch. Mol Syst Biol 8:620. doi:10.1038/msb.2012.52

Chou HH, Keasling JD (2013) Programming adaptive control to evolve increased metabolite production. Nat Commun 4:2595. doi:10.1038/ncomms3595

Dahl RH, Zhang F, Alonso-Gutierrez J, Baidoo E, Batth TS, Redding-Johanson AM, Petzold CJ, Mukhopadhyay A, Lee TS, Adams PD, Keasling JD (2013) Engineering dynamic pathway regulation using stress-response promoters. Nat Biotechnol 31(11):1039–1046. doi:10.1038/nbt.2689

de Las Heras A, Fraile S, de Lorenzo V (2012) Increasing signal specificity of the TOL network of *Pseudomonas putida* mt-2 by rewiring the connectivity of the master regulator XylR. PLoS Genet 8(10):e1002963. doi:10.1371/journal.pgen.1002963

Delvigne F, Goffin P (2014) Microbial heterogeneity affects bioprocess robustness: dynamic single-cell analysis contributes to understanding of microbial populations. Biotechnol J 9(1):61–72. doi:10.1002/biot.201300119

Delvigne F, Boxus M, Ingels S, Thonart P (2009) Bioreactor mixing efficiency modulates the activity of a P*rpoS*::GFP reporter gene in *E. coli*. Microb Cell Factories 8:15. doi:10.1186/1475-2859-8-15

Delvigne F, Zune Q, Lara AR, Al-Soud W, Sorensen SJ (2014) Metabolic variability in bioprocessing: implications of microbial phenotypic heterogeneity. Trends Biotechnol 32(12):608–616. doi:10.1016/j.tibtech.2014.10.002

DeVito JA (2008) Recombineering with *tolC* as a selectable/counter-selectable marker: remodeling the rRNA operons of *Escherichia coli*. Nucleic Acids Res 36(1):e4. doi:10.1093/nar/gkm1084

Dietrich JA, McKee AE, Keasling JD (2010) High-throughput metabolic engineering: advances in small-molecule screening and selection. Annu Rev Biochem 79:563–590. doi:10.1146/annurev-biochem-062608-095938

Dietrich JA, Shis DL, Alikhani A, Keasling JD (2013) Transcription factor-based screens and synthetic selections for microbial small-molecule biosynthesis. ACS Synth Biol 2(1):47–58. doi:10.1021/sb300091d

Eggeling L, Bott M, Marienhagen J (2015) Novel screening methods—biosensors. Curr Opin Biotechnol 35C:30–36. doi:10.1016/j.copbio.2014.12.021

Fernandez-Lopez R, Ruiz R, de la Cruz F, Moncalian G (2015) Transcription factor-based biosensors enlightened by the analyte. Front Microbiol 6:648. doi:10.3389/fmicb.2015.00648

Frommer WB, Davidson MW, Campbell RE (2009) Genetically-encoded biosensors based on engineered fluorescent proteins. Chem Soc Rev 38(10):2833–2841. doi:10.1039/b907749a

Galvao TC, de Lorenzo V (2006) Transcriptional regulators à la carte: engineering new effector specificities in bacterial regulatory proteins. Curr Opin Biotechnol 17(1):34–42. doi:10.1016/j.copbio.2005.12.002

Galvao TC, Mencia M, de Lorenzo V (2007) Emergence of novel functions in transcriptional regulators by regression to stem protein types. Mol Microbiol 65(4):907–919. doi:10.1111/j.1365-2958.2007.05832.x

Ganesh I, Ravikumar S, Lee SH, Park SJ, Hong SH (2013) Engineered fumarate sensing *Escherichia coli* based on novel chimeric two-component system. J Biotechnol 168(4):560–566. doi:10.1016/j.jbiotec.2013.09.003

Ganesh I, Ravikumar S, Yoo IK, Hong SH (2015) Construction of malate-sensing *Escherichia coli* by introduction of a novel chimeric

two-component system. Bioprocess Biosyst Eng 38(4):797–804. doi:10.1007/s00449-014-1321-3

Grünberger A, Paczia N, Probst C, Schendzielorz G, Eggeling L, Noack S, Wiechert W, Kohlheyer D (2012) A disposable picolitre bioreactor for cultivation and investigation of industrially relevant bacteria on the single cell level. Lab Chip 12(11):2060–2068. doi:10.1039/c2lc40156h

Grünberger A, Wiechert W, Kohlheyer D (2014) Single-cell microfluidics: opportunity for bioprocess development. Curr Opin Biotechnol 29:15–23. doi:10.1016/j.copbio.2014.02.008

Harper M, Lee CJ (2012) Genome-wide analysis of mutagenesis bias and context sensitivity of N-methyl-N'-nitro-N-nitrosoguanidine (NTG). Mutat Res 731(1-2):64–67. doi:10.1016/j.mrfmmm.2011.10.011

Hoffmann K, Grünberger A, Lausberg F, Bott M, Eggeling L (2013) Visualization of imbalances in sulfur assimilation and synthesis of sulfur-containing amino acids at the single-cell level. Appl Environ Microbiol 79(21):6730–6736. doi:10.1128/AEM.01804-13

Huang S (2009) Non-genetic heterogeneity of cells in development: more than just noise. Development 136(23):3853–3862. doi:10.1242/dev.035139

Jahn M, Seifert J, von Bergen M, Schmid A, Buhler B, Müller S (2013) Subpopulation-proteomics in prokaryotic populations. Curr Opin Biotechnol 24(1):79–87. doi:10.1016/j.copbio.2012.10.017

Jehmlich N, Hübschmann T, Gesell Salazar M, Volker U, Benndorf D, Müller S, von Bergen M, Schmidt F (2010) Advanced tool for characterization of microbial cultures by combining cytomics and proteomics. Appl Microbiol Biotechnol 88(2):575–584. doi:10.1007/s00253-010-2753-6

Keseler IM, Mackie A, Peralta-Gil M, Santos-Zavaleta A, Gama-Castro S, Bonavides-Martinez C, Fulcher C, Huerta AM, Kothari A, Krummenacker M, Latendresse M, Muniz-Rascado L, Ong Q, Paley S, Schroder I, Shearer AG, Subhraveti P, Travers M, Weerasinghe D, Weiss V, Collado-Vides J, Gunsalus RP, Paulsen I, Karp PD (2013) EcoCyc: fusing model organism databases with systems biology. Nucleic Acids Res 41(Database issue):D605–D612. doi:10.1093/nar/gks1027

Kiviet DJ, Nghe P, Walker N, Boulineau S, Sunderlikova V, Tans SJ (2014) Stochasticity of metabolism and growth at the single-cell level. Nature 514(7522):376–379. doi:10.1038/nature13582

Lange C, Mustafi N, Frunzke J, Kennerknecht N, Wessel M, Bott M, Wendisch VF (2012) Lrp of *Corynebacterium glutamicum* controls expression of the *brnFE* operon encoding the export system for L-methionine and branched-chain amino acids. J Biotechnol 158(4):231–241. doi:10.1016/j.jbiotec.2011.06.003

Lee JY, Seo J, Kim ES, Lee HS, Kim P (2013) Adaptive evolution of *Corynebacterium glutamicum* resistant to oxidative stress and its global gene expression profiling. Biotechnol Lett 35(5):709–717. doi:10.1007/s10529-012-1135-9

Liang JC, Bloom RJ, Smolke CD (2011) Engineering biological systems with synthetic RNA molecules. Mol Cell 43(6):915–926. doi:10.1016/j.molcel.2011.08.023

Lieder S, Jahn M, Seifert J, von Bergen M, Müller S, Takors R (2014) Subpopulation-proteomics reveal growth rate, but not cell cycling, as a major impact on protein composition in *Pseudomonas putida* KT2440. AMB Express 4:71. doi:10.1186/s13568-014-0071-6

Liu D, Evans T, Zhang F (2015a) Applications and advances of metabolite biosensors for metabolic engineering. Metab Eng. doi:10.1016/j.ymben.2015.06.008

Liu D, Xiao Y, Evans BS, Zhang F (2015b) Negative feedback regulation of fatty acid production based on a malonyl-CoA sensor-actuator. ACS Synth Biol 4(2):132–140. doi:10.1021/sb400158w

Long Z, Nugent E, Javer A, Cicuta P, Sclavi B, Cosentino Lagomarsino M, Dorfman KD (2013) Microfluidic chemostat for measuring single cell dynamics in bacteria. Lab Chip 13(5):947–954. doi:10.1039/c2lc41196b

Looger LL, Dwyer MA, Smith JJ, Hellinga HW (2003) Computational design of receptor and sensor proteins with novel functions. Nature 423(6936):185–190. doi:10.1038/nature01556

Lutz R, Bujard H (1997) Independent and tight regulation of transcriptional units in *Escherichia coli* via the LacR/O, the TetR/O and AraC/I1-I2 regulatory elements. Nucleic Acids Res 25(6):1203–1210

Mahr R, Gätgens C, Gätgens J, Polen T, Kalinowski J, Frunzke J (2015) Biosensor-driven adaptive evolution of L-valine production of *Corynebacterium glutamicum*. Metab Eng 32:184–194. doi:10.1016/j.ymben.2015.09.017

Mandell DJ, Kortemme T (2009) Computer-aided design of functional protein interactions. Nat Chem Biol 5(11):797–807. doi:10.1038/nchembio.251

Mascher T (2013) Signaling diversity and evolution of extracytoplasmic function (ECF) sigma factors. Curr Opin Microbiol 16(2):148–155. doi:10.1016/j.mib.2013.02.001

Michener JK, Thodey K, Liang JC, Smolke CD (2012) Applications of genetically-encoded biosensors for the construction and control of biosynthetic pathways. Metab Eng 14(3):212–222. doi:10.1016/j.ymben.2011.09.004

Müller S, Harms H, Bley T (2010) Origin and analysis of microbial population heterogeneity in bioprocesses. Curr Opin Biotechnol 21(1):100–113. doi:10.1016/j.copbio.2010.01.002

Münch R, Hiller K, Barg H, Heldt D, Linz S, Wingender E, Jahn D (2003) PRODORIC: prokaryotic database of gene regulation. Nucleic Acids Res 31(1):266–269

Münch KM, Müller J, Wienecke S, Bergmann S, Heyber S, Biedendieck R, Münch R, Jahn D (2015) Polar fixation of plasmids during recombinant protein production in *Bacillus megaterium* results in population heterogeneity. Appl Environ Microbiol. doi:10.1128/AEM.00807-15

Mustafi N, Grünberger A, Kohlheyer D, Bott M, Frunzke J (2012) The development and application of a single-cell biosensor for the detection of l-methionine and branched-chain amino acids. Metab Eng 14(4):449–457. doi:10.1016/j.ymben.2012.02.002

Mustafi N, Grünberger A, Mahr R, Helfrich S, Nöh K, Blombach B, Kohlheyer D, Frunzke J (2014) Application of a genetically encoded biosensor for live cell imaging of L-valine production in pyruvate dehydrogenase complex-deficient *Corynebacterium glutamicum* strains. PLoS One 9(1):e85731. doi:10.1371/journal.pone.0085731

Mustafi N, Bott M, Frunzke J (2015) Genetically-encoded biosensors for strain development and single cell analysis of *Corynebacterium glutamicum*. In: Burkovski A (ed) *Corynebacterium glutamicum*: from systems biology to biotechnological applications. Caister Academic Press, Norfolk, p 190

Newman JR, Ghaemmaghami S, Ihmels J, Breslow DK, Noble M, DeRisi JL, Weissman JS (2006) Single-cell proteomic analysis of *S. cerevisiae* reveals the architecture of biological noise. Nature 441(7095):840–846. doi:10.1038/nature04785

Ng CY, Khodayari A, Chowdhury A, Maranas CD (2015) Advances in *de novo* strain design using integrated systems and synthetic biology tools. Curr Opin Chem Biol 28:105–114. doi:10.1016/j.cbpa.2015.06.026

Novichkov PS, Kazakov AE, Ravcheev DA, Leyn SA, Kovaleva GY, Sutormin RA, Kazanov MD, Riehl W, Arkin AP, Dubchak I, Rodionov DA (2013) RegPrecise 3.0—a resource for genome-scale exploration of transcriptional regulation in bacteria. BMC Genomics 14:745. doi:10.1186/1471-2164-14-745

Ohlendorf R, Vidavski RR, Eldar A, Moffat K, Möglich A (2012) From dusk till dawn: one-plasmid systems for light-regulated gene expression. J Mol Biol 416(4):534–542. doi:10.1016/j.jmb.2012.01.001

Oide S, Gunji W, Moteki Y, Yamamoto S, Suda M, Jojima T, Yukawa H, Inui M (2015) Thermal and solvent stress cross-tolerance conferred to *Corynebacterium glutamicum* by adaptive laboratory evolution.

Appl Environ Microbiol 81(7):2284–2298. doi:10.1128/AEM.03973-14

Podgornaia AI, Laub MT (2013) Determinants of specificity in two-component signal transduction. Curr Opin Microbiol 16(2):156–162. doi:10.1016/j.mib.2013.01.004

Raman S, Rogers JK, Taylor ND, Church GM (2014) Evolution-guided optimization of biosynthetic pathways. Proc Natl Acad Sci U S A 111(50):17803–17808. doi:10.1073/pnas.1409523111

Reyes LH, Gomez JM, Kao KC (2014) Improving carotenoids production in yeast via adaptive laboratory evolution. Metab Eng 21:26–33. doi:10.1016/j.ymben.2013.11.002

Rhodius VA, Segall-Shapiro TH, Sharon BD, Ghodasara A, Orlova E, Tabakh H, Burkhardt DH, Clancy K, Peterson TC, Gross CA, Voigt CA (2013) Design of orthogonal genetic switches based on a crosstalk map of sigmas, anti-sigmas, and promoters. Mol Syst Biol 9:702. doi:10.1038/msb.2013.58

Salgado H, Gama-Castro S, Peralta-Gil M, Diaz-Peredo E, Sanchez-Solano F, Santos-Zavaleta A, Martinez-Flores I, Jimenez-Jacinto V, Bonavides-Martinez C, Segura-Salazar J, Martinez-Antonio A, Collado-Vides J (2006) RegulonDB (version 5.0): *Escherichia coli* K-12 transcriptional regulatory network, operon organization, and growth conditions. Nucleic Acids Res 34(Database issue):D394–D397. doi:10.1093/nar/gkj156

Schallmey M, Frunzke J, Eggeling L, Marienhagen J (2014) Looking for the pick of the bunch: high-throughput screening of producing microorganisms with biosensors. Curr Opin Biotechnol 26:148–154. doi:10.1016/j.copbio.2014.01.005

Schendzielorz G, Dippong M, Grünberger A, Kohlheyer D, Yoshida A, Binder S, Nishiyama C, Nishiyama M, Bott M, Eggeling L (2014) Taking control over control: use of product sensing in single cells to remove flux control at key enzymes in biosynthesis pathways. ACS Synth Biol 3(1):21–29. doi:10.1021/sb400059y

Siedler S, Schendzielorz G, Binder S, Eggeling L, Bringer S, Bott M (2014a) SoxR as a single-cell biosensor for NADPH-consuming enzymes in *Escherichia coli*. ACS Synth Biol 3(1):41–47. doi:10.1021/sb400110j

Siedler S, Stahlhut SG, Malla S, Maury J, Neves AR (2014b) Novel biosensors based on flavonoid-responsive transcriptional regulators introduced into *Escherichia coli*. Metab Eng 21:2–8. doi:10.1016/j.ymben.2013.10.011

Silva-Rocha R, de Lorenzo V (2012) Broadening the signal specificity of prokaryotic promoters by modifying *cis*-regulatory elements associated with a single transcription factor. Mol BioSyst 8(7):1950–1957. doi:10.1039/c2mb25030f

Stanton BC, Siciliano V, Ghodasara A, Wroblewska L, Clancy K, Trefzer AC, Chesnut JD, Weiss R, Voigt CA (2014) Systematic transfer of prokaryotic sensors and circuits to mammalian cells. ACS Synth Biol 3(12):880–891. doi:10.1021/sb5002856

Tang SY, Cirino PC (2011) Design and application of a mevalonate-responsive regulatory protein. Angew Chem Int Ed 50(5):1084–1086. doi:10.1002/anie.201006083

Tang SY, Fazelinia H, Cirino PC (2008) AraC regulatory protein mutants with altered effector specificity. J Am Chem Soc 130(15):5267–5271. doi:10.1021/ja7109053

Tang SY, Qian S, Akinterinwa O, Frei CS, Gredell JA, Cirino PC (2013) Screening for enhanced triacetic acid lactone production by recombinant *Escherichia coli* expressing a designed triacetic acid lactone reporter. J Am Chem Soc 135(27):10099–10103. doi:10.1021/ja402654z

Tracy BP, Gaida SM, Papoutsakis ET (2008) Development and application of flow-cytometric techniques for analyzing and sorting endospore-forming *clostridia*. Appl Environ Microbiol 74(24):7497–7506. doi:10.1128/AEM.01626-08

Uchiyama T, Miyazaki K (2010a) Product-induced gene expression, a product-responsive reporter assay used to screen metagenomic libraries for enzyme-encoding genes. Appl Environ Microbiol 76(21):7029–7035. doi:10.1128/AEM.00464-10

Uchiyama T, Miyazaki K (2010b) Substrate-induced gene expression screening: a method for high-throughput screening of metagenome libraries. Methods Mol Biol 668:153–168. doi:10.1007/978-1-60761-823-2_10

Uchiyama T, Watanabe K (2008) Substrate-induced gene expression (SIGEX) screening of metagenome libraries. Nat Protoc 3(7):1202–1212. doi:10.1038/nprot.2008.96

Umeyama T, Okada S, Ito T (2013) Synthetic gene circuit-mediated monitoring of endogenous metabolites: identification of GAL11 as a novel multicopy enhancer of s-adenosylmethionine level in yeast. ACS Synth Biol 2(8):425–430. doi:10.1021/sb300115n

van der Meer JR, Belkin S (2010) Where microbiology meets microengineering: design and applications of reporter bacteria. Nat Rev Microbiol 8(7):511–522. doi:10.1038/nrmicro2392

van Sint Fiet S, van Beilen JB, Witholt B (2006) Selection of biocatalysts for chemical synthesis. Proc Natl Acad Sci U S A 103(6):1693–1698. doi:10.1073/pnas.0504733102

Vasdekis AE, Stephanopoulos G (2015) Review of methods to probe single cell metabolism and bioenergetics. Metab Eng 27:115–135. doi:10.1016/j.ymben.2014.09.007

Wang P, Robert L, Pelletier J, Dang WL, Taddei F, Wright A, Jun S (2010) Robust growth of *Escherichia coli*. Curr Biol 20(12):1099–1103. doi:10.1016/j.cub.2010.04.045

Want A, Thomas OR, Kara B, Liddell J, Hewitt CJ (2009) Studies related to antibody fragment (Fab) production in *Escherichia coli* W3110 fed-batch fermentation processes using multiparameter flow cytometry. Cytometry A 75(2):148–154. doi:10.1002/cyto.a.20683

Wendisch VF (2014) Microbial production of amino acids and derived chemicals: synthetic biology approaches to strain development. Curr Opin Biotechnol 30:51–58. doi:10.1016/j.copbio.2014.05.004

Wiechert W, Noack S (2011) Mechanistic pathway modeling for industrial biotechnology: challenging but worthwhile. Curr Opin Biotechnol 22(5):604–610. doi:10.1016/j.copbio.2011.01.001

Wilson D, Charoensawan V, Kummerfeld SK, Teichmann SA (2008) DBD-taxonomically broad transcription factor predictions: new content and functionality. Nucleic Acids Res 36(Database issue):D88–D92. doi:10.1093/nar/gkm964

Wise AA, Kuske CR (2000) Generation of novel bacterial regulatory proteins that detect priority pollutant phenols. Appl Environ Microbiol 66(1):163–169

Xie W, Lv X, Ye L, Zhou P, Yu H (2015) Construction of lycopene-overproducing *Saccharomyces cerevisiae* by combining directed evolution and metabolic engineering. Metab Eng 30:69–78. doi:10.1016/j.ymben.2015.04.009

Xu P, Li L, Zhang F, Stephanopoulos G, Koffas M (2014a) Improving fatty acids production by engineering dynamic pathway regulation and metabolic control. Proc Natl Acad Sci U S A 111(31):11299–11304. doi:10.1073/pnas.1406401111

Xu P, Wang W, Li L, Bhan N, Zhang F, Koffas MA (2014b) Design and kinetic analysis of a hybrid promoter-regulator system for malonyl-CoA sensing in *Escherichia coli*. ACS Chem Biol 9(2):451–458. doi:10.1021/cb400623m

Yang J, Seo SW, Jang S, Shin SI, Lim CH, Roh TY, Jung GY (2013) Synthetic RNA devices to expedite the evolution of metabolite-producing microbes. Nat Commun 4:1413. doi:10.1038/ncomms2404

Zhang F, Carothers JM, Keasling JD (2012) Design of a dynamic sensor-regulator system for production of chemicals and fuels derived from fatty acids. Nat Biotechnol 30(4):354–359. doi:10.1038/nbt.2149

Zhang J, Jensen MK, Keasling JD (2015) Development of biosensors and their application in metabolic engineering. Curr Opin Chem Biol 28:1–8. doi:10.1016/j.cbpa.2015.05.013

4 DISCUSSION

4.1 Biosensors – valuable tools for biotechnology

4.1.1 Screening of nature's toolbox for novel sensor candidates

Microorganisms possess a plethora of natural sensor devices (e.g. transcriptional regulators, riboswitches or enzymes) for sensing the broad range of intrinsic and extrinsic stimuli. This ability allows for a quick adaption to the changing availability of nutrients and other cellular requirements, or to altered physical and environmental conditions. The principle of sensing metabolites by transcriptional regulators has been proven to be of high value for a variety of biotechnological applications including the visualization of inconspicuous metabolites during bioprocesses, the control of biosynthetic pathways as regulatory circuits, and the development of production strains (Liu et al., 2015a; Mahr and Frunzke, 2016; Zhang et al., 2015b). To date, however, only a few regulators and their corresponding target promoters have been well characterized, which constitutes an important prerequisite to choose a suitable sensor candidate for the desired application. Hence, efficient strategies are in demand for the fast identification of appropriate effector-responsive transcriptional regulators and target promoters. To this end, an elaborated FACS-based workflow was developed in this study to screen libraries of promoters fused to genes encoding auto-fluorescent proteins (chapter 3.4). The Alon library consisting of about 2000 different promoter-*gfpmut2* fusions in *E. coli* presents a valuable tool with readily available sensor devices (Zaslaver et al., 2006). Using FACS, metabolite-responsive promoters were enriched from the pooled library by toggled rounds of positive and negative selection. This novel strategy was successfully applied to screen for galactose- and L-phenylalanine-responsive promoter-*gfpmut2* fusions.

According to the statement "You get what you screen for" (Schmidt-Dannert and Arnold, 1999), the efficient screening for metabolite-responsive promoters by FACS requires a well-considered protocol. Here, the eventual application of the biosensor plays an important role: Due to the diverse underlying dynamics of gene regulatory mechanisms in response to effector molecules, the time point for sorting of cells as well as the composition of the cultivation medium may strongly impact the outcome of the screening process. Furthermore, the choice of the sorting gate may decide about the characteristics of the enriched promoters in terms of background activity and the dynamic range. Beyond that, the toggled rounds of positive and negative selection turned

out to be efficient to get rid of constitutively active promoters of e.g. house-keeping genes. Likewise, this FACS-based strategy is proposed to enable screening for transcriptional repressors by inverting the toggled rounds of selection.

Besides FACS, automated robotic platforms allow for the HT screening of strain libraries clone by clone to identify variants with the desired phenotype or function. Screening clone by clone avoids on the one hand the loss of appropriate strains, which is more probable during FACS screening. One the other hand, the high screening capacity of about 80.000 cells per second and the potential to sort 10.000 cells within the same time argue strongly for the application of FACS reducing likewise costs and time (Dietrich et al., 2010). Furthermore, the outcome of screening promoter libraries depends strongly on the pre-adjusted conditions (e.g. medium, time, etc.). Here, FACS allows for the fast and easy screening of libraries under different conditions within a few minutes in contrast to screening clone by clone. One limitation of the FACS-based strategy is the availability of a suitable and easily accessible library of promoter fusions. Considering biotechnological applications, appropriate and comprehensive collections exist for the biotechnological interesting microbes *E. coli* (Zaslaver et al., 2006) and *S. cerevisiae* (Newman et al., 2006). Nevertheless, the decreasing costs of gene synthesis and robot-based production lines allow for the generation of such libraries in a manageable manner. Furthermore, the integration of promoter libraries in different organisms might also enable the screening for orthogonal sensor devices.

A similar strategy was developed by Uchiyama and co-workers in order to identify catabolic genes from environmental metagenomes (Uchiyama and Miyazaki, 2010b; Uchiyama and Watanabe, 2008). By fusing fragments of a metagenomic library to a reporter gene (e.g. *gfp*) in an operon-trap vector, HT screening for metabolically-relevant fragments using FACS became possible. This strategy might likewise be exploited to screen metagenomic libraries for effector-responsive transcriptional regulator-promoter pairs. Furthermore, comparative transcriptome analysis like DNA microarrays or RNA sequencing may also contribute to the identification of, so far, uncharacterized metabolite-responsive genes, of which the regulatory mechanism might be exploited as biosensor devices (Dahl et al., 2013; Mahr and Frunzke, 2016).

4.1.2 The application of biosensors for single cell studies

Besides their valuable application for metabolic engineering purposes, genetically-encoded biosensors are excellent tools to visualize the development of cell-to-cell heterogeneity e.g. in bioprocesses (Delvigne et al., 2009; Mustafi et al., 2014; Vasdekis and Stephanopoulos, 2015). Typically, the development of phenotypic pattern such as inefficient subpopulations, which may affect the performance and stability of bioprocesses, is neglected by the use of bulk analyses (Delvigne and Goffin, 2014; Delvigne et al., 2014; Müller et al., 2010). In this study, the Lrp biosensor was applied to study phenotypic pattern of the L-valine producer *C. glutamicum* Δ*aceE* and derivatives by live cell imaging (chapter 3.1, (Mustafi et al., 2014)). In contrast to large-scale cultivations, 2D microfluidic chip devices offer the great advantage to analyze single cells in a monolayer with high spatial and temporal resolution and enable likewise the cultivation at environmental constant and defined conditions (Grünberger et al., 2012; Grünberger et al., 2014). Interestingly, the analysis of the growth-decoupled L-valine producer strain Δ*aceE* and derivatives revealed the formation of non-producing subpopulations in the production phase upon addition of small amounts of complex medium compounds as often used during production processes. While most cells switched from growth to production (depicted by the fluorescent signal of the biosensor), single cells continued growing and/or switched to production at a later time point (Fig. 5 in chapter 3.1, (Mustafi et al., 2014)). A similar phenotypic pattern of fluorescent and non-fluorescent sensor Δ*aceE* cells was observed during flow cytometric analysis of shake flask cultures (data not shown). Although the origin for phenotypic heterogeneity was ascribed to the used complex medium compounds, the responsible triggers as well as the underlying physiological and molecular basis remain unknown due to the lack of readily available single cell analysis tools interfacing with FACS or microfluidics.

So far, different staining techniques interfacing with FACS proved efficient to discriminate between living, lysed or dead cells, or may detect variations in the DNA content or membrane potential of cellular populations (Langemann et al., 2016; Neumeyer et al., 2013). Furthermore, workflows have been established to analyze the proteome of FACS-isolated subpopulations by mass spectrometry (Jahn et al., 2013; Jehmlich et al., 2010). Even mass-spectrometric measurements of various metabolites in single cells are nowadays possible (Amantonico et al., 2008; Heinemann and Zenobi, 2011; Rubakhin et al., 2013). In the future, the interplay of biosensors with next generation sequencing techniques (e.g. RNA-seq) and high-resolution

proteomics or metabolomics might provide novel and profitable insights into the formation of subpopulation.

4.1.3 Limitations of transcriptional regulator-based biosensors

Within recent years, biosensors based on transcriptional regulators have proven to be of great benefit for the establishment of efficient microbial cell factories by improving production strains or by identifying inefficient subpopulations in bioprocesses (Binder et al., 2012; Chou and Keasling, 2013; Delvigne et al., 2009; Dietrich et al., 2013; Mahr et al., 2015; Mustafi et al., 2012; Mustafi et al., 2014; Zhang et al., 2012). The drawbacks and limits of genetically-encoded biosensors, however, are often neglected during application, but have to be considered for the correct interpretation of the obtained results.

The mechanism of transcriptional regulators to transfer the intracellular presence of effector metabolites into the expression of target genes is based on a complex hierarchy of molecular interactions and biochemical reactions. This includes metabolite sensing, transcriptional and translational processes, and the interference between different regulatory networks. In *E. coli*, transcription typically runs with a speed of 40-80 base pairs per second, while translation proceeds at about 20 amino acids per second (Dennis and Bremer, 1974; Young and Bremer, 1976). For this reason, the information on a defined amount of effector metabolites at a defined time-point is transmitted as time-delayed response. Moreover, the metabolite-dependent expression of a gene encoding a fluorescent protein results in a further delayed optical response due to protein folding and the maturation of the chromophore. In the case of eYFP, the maturation requires about seven minutes in *E. coli* at 37°C, while the maturation of Venus was measured to proceed within two minutes under the same conditions (Iizuka et al., 2011; Nagai et al., 2002). In comparison, FRET-based biosensors or engineered riboswitches, binding fluorophores upon metabolite recognition, reveal an improved temporal resolution of effector metabolites as ligand-binding directly results in the transmission of fluorescence as consequence of a conformational change (Michener et al., 2012; Mohsin and Ahmad, 2014; Potzkei et al., 2012; Schallmey et al., 2014; You et al., 2015; Zhang et al., 2015b).

For quantitative intracellular measurements, fastidious calibration and characterization of the biosensor's performance are required to describe the relationship between input concentration and output signal under highly defined conditions (Dietrich et al., 2010). To this end, the effector

molecule must enter the cell. This, however, is often not possible due to the lack of uptake systems or inappropriate physical characteristics of the effector to cross the membrane (e.g. high hydrophilicity). In contrast to TF-based biosensors, FRET-based biosensors allow for quantitative analyses upon intensive calibration and definition of assay conditions. This is difficult to achieve for TF-based biosensors due to the high number of mechanisms involved in the expression of target genes upon metabolite sensing (Constantinou and Polizzi, 2013; Michener et al., 2012). In theory, quantitative intracellular analysis would need the incorporation of any intrinsic and extrinsic factor affecting gene expression or fluorescence development, which is hardly feasible in living organism due to e.g. gene expression noise (Carey et al., 2013; Elowitz and Leibler, 2000; Keren et al., 2015; Sanchez et al., 2013). Beyond that, TF-based biosensors report on the intracellular metabolite level, which is a prerequisite for an application in FACS screenings. Most biotechnological applications, however, aim to maximize the amount of excreted product in the supernatant to reduce costs during downstream processing without an interest for intracellular metabolite levels (Delvigne et al., 2015). For this reason, a quantification of intracellular metabolites is negligible in most cases. Nevertheless, TF-based biosensors report on the relative intracellular metabolite concentration in a reliable way, which allows for the discrimination of cells or populations with different productivity during HT screening or monitoring of bioprocesses using FC/FACS or fluorescence microscopy.

Traditionally, the biosensor construct consists of the transcriptional regulator and the target promoter controlling the expression of an actuator gene encoded on a plasmid. During the development of the *mtr* biosensor for detecting L-phenylalanine in *E. coli*, different designs of the biosensor with and without the transcriptional regulator were found to drastically affect the biosensor's performance characteristics. On the one hand, the additional expression of the transcription factor avoids titration effects of the native regulator and allows for heterologous gene expression. On the other hand, the increased numbers of TF molecules can have a strong impact on the bacterial physiology by skewing the activity of the transcriptional network, especially in the case of global regulators controlling the expression of various target genes. This effect can even be multiplied by the amount of plasmid copies in the case of plasmid-based expression of sensor circuits (Delvigne et al., 2015). To avoid the interference with the native regulatory network, to prevent the multiplication of gene expression noise or to reliably study the dimensions of phenotypic heterogeneity, the use of low-copy number plasmids or chromosomal

integration have shown to be of great benefit (Freed et al., 2008; Mustafi et al., 2014; Silander et al., 2012). In addition, the different architectures of the *mtr* biosensor in this study (chapter 3.4) demonstrated that an additional copy of the regulator is often not necessary and may even lead to improved performance characteristics. For this reason, it might be advantageous to test different biosensor designs e.g. with and without the additional expression of a native regulator in advance. Further strategies to alter the performance characteristics of a biosensor are discussed in chapter 4.1.4 ("Engineering of biosensors for improved and desired characteristics").

For the visualization of intracellular metabolites, biosensors usually drive the production of an auto-fluorescent protein, e.g. green fluorescent protein (GFP) and derivatives. The drawback of GFP-derived fluorescent proteins, however, consists in the requirement of oxygen for the formation of the chromophore (Craggs, 2009), which excludes their reliable application during micro- and anaerobic cultivation. Alternatively, Drepper and co-workers developed a set of flavin mononucleotide (FMN)-based fluorescent proteins (FbFPs) based on the photoactive light oxygen voltage (LOV)-domain of blue-light photoreceptors from *Bacillus subtilis* and *Pseudomonas putida*, which enable fluorescent signaling in the absence of oxygen (Drepper et al., 2007; Drepper et al., 2010; Walter et al., 2012). Their low brightness, quantum yield and strongly reduced thermal or photostability in contrast to GFP derivatives have indeed been reported and addressed in different studies (Christie et al., 2012; Song et al., 2013; Wingen et al., 2014), however, the broad applicability of FbFP is still hampered (Mukherjee and Schroeder, 2015). Traditionally, GFP feature high stability with a half-life of more than 24 hours. Highly stable fluorescent proteins prevent dynamic measurements by the accumulation of reporter proteins within the cell. Engineered GFP derivatives already exhibit reduced photostability (Shaner et al., 2005). Additionally, the destabilization of auto-fluorescent proteins using variants of *ssrA* tags, which are recognized by cytoplasmic proteases, revealed further improvement of dynamic measurements of fluorescent signals in various microbes (Andersen et al., 1998; Hentschel et al., 2013; Triccas et al., 2002).

The application of biosensors for live cell imaging studies in microfluidic devices offers the possibility to study microbial population dynamics at the single cell level (Mustafi et al., 2014). The rate of iterative excitation should be kept a minimum – especially excitation light of the energy-rich short wavelength – to avoid phototoxic effects e.g. DNA damage by free radicals (Haselgrübler et al., 2014; Lipovsky et al., 2010; NPG-Editorial, 2013; Waters, 2013). Especially

the performance of multicolor experiments of different parameters in parallel using several fluorescent proteins can provide an immense physiological burden on the living cell (Schlüter et al., 2015; Shaner et al., 2005). To reduce the artifacts of exposed light, fluorescent proteins have to be carefully chosen according to their respective application and the organism under study.

4.1.4 Engineering of biosensors for improved and desired characteristics

The different designs of the *mtr* biosensor for L-phenylalanine detection revealed a significant influence of the architecture on the sensor's performance characteristics including the dynamic range, sensitivity and background signal (chapter 3.4). Extending beyond, diverse studies demonstrated that engineering of biosensors according to the respective purpose can become feasible due to the modular architecture of promoter regions (Blazeck and Alper, 2013) and transcriptional regulators (Galvao et al., 2007; Zhang et al., 2015b).

The *mtr* biosensor, which consists of the native promoter of *mtr* fused to the gene encoding the fluorescent protein Venus (Fig. 4.1.4.1 A), features a maximal fivefold increased fluorescent signal in response to L-phenylalanine (chapter 3.4). Other biosensors such as the pSenLys sensor for sensing L-lysine and the DcuR/DcuS-based or PcaR-based sensor for sensing dicarboxylic acids showed similar dynamic ranges of signal output (six- to 15-fold) in the presence of the respective effector molecule (Binder et al., 2012; Dietrich et al., 2013). The Lrp biosensor featured an about tenfold increased signal in response to L-isoleucine, twelvefold to L-valine, 22-fold to L-leucine and an even 78-fold dynamic range to L-methionine accumulation (Mustafi et al., 2012). A broad dynamic range as shown for L-methionine detection by the Lrp sensor is desired to reliably distinguish between different productive cells by FC or fluorescence microscopy. To enhance fatty acid sensing in *E. coli*, Zhang and coworkers introduced the TF-binding sites of the transcriptional regulator FadR into the strong phage promoters of lambda (P_L) and T7 (P_{A1}), thereby increasing the dynamic range up to 1000-fold (Zhang et al., 2012). Similarly, Lutz and Bujard engineered the tight regulation of the TetR/O system for sensing anhydrotetracycline over a 5000-fold range (Lutz and Bujard, 1997). A similar approach could also be considered for improving the dynamic range of the *mtr* biosensor in response to L-phenylalanine. This could be achieved by introducing one or two TyrR-binding sites up- and/or downstream of the -35 region of a strong phage promoter e.g. the well-studied lambda phage promoter (Fig. 4.1.4.1 B).

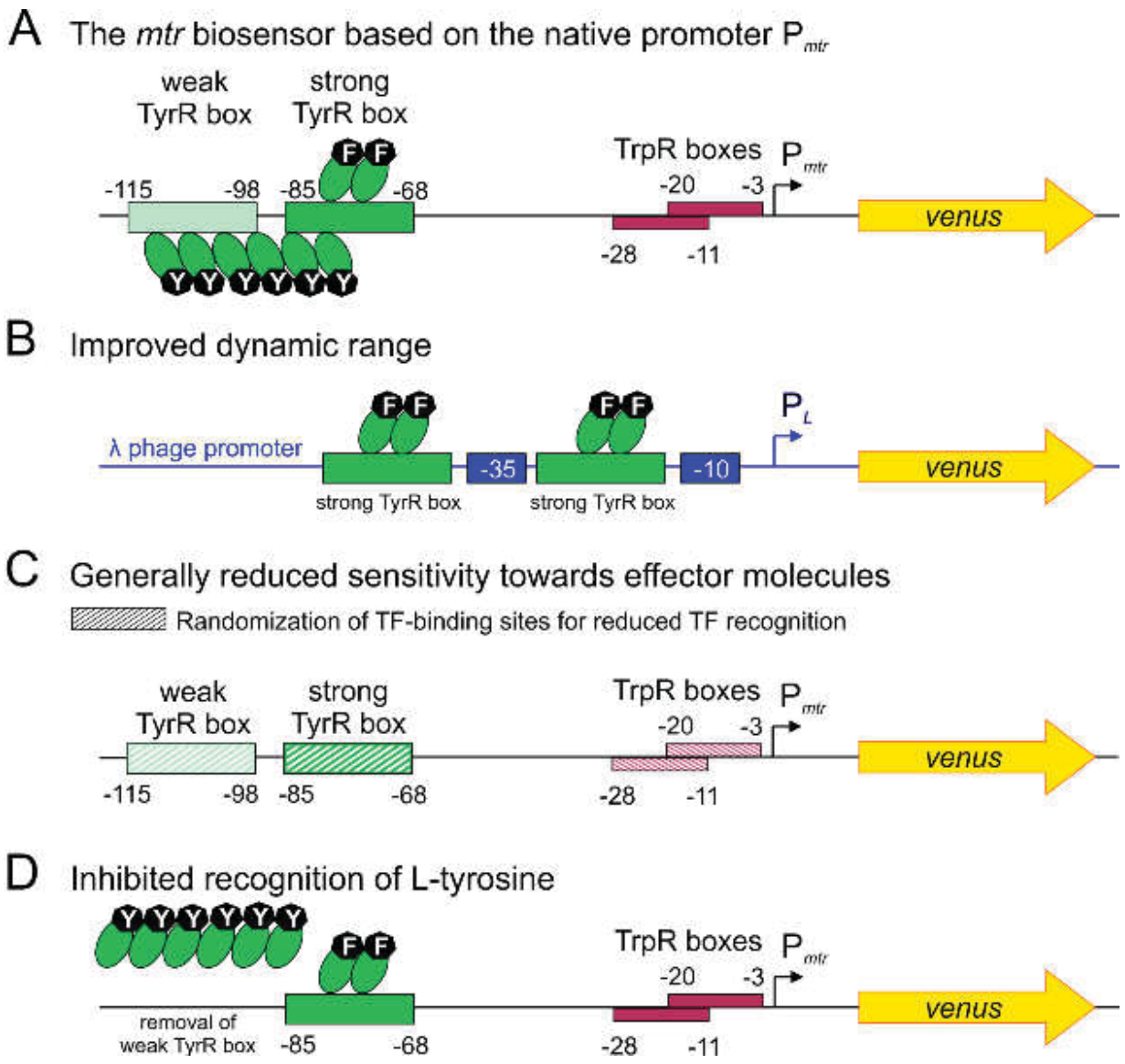

Fig. 4.1.4.1 The *mtr* biosensor and potential designs for improved and desired performance characteristics. A. The *mtr* biosensor is based on the native promoter P_{mtr} fused to the gene encoding the fluorescent protein Venus. The native promoter P_{mtr} consists of a weak and a strong TyrR box and two TrpR boxes. For L-phenylalanine (F)-mediated activation of gene expression, TyrR binds as dimer to the strong TyrR-binding site and recruits RNA-polymerase. L-tyrosine (Y)-mediated gene expression requires binding of TyrR as hexamer to the weak and strong TyrR boxes. B. Introduction of the strong TyrR box between the -10 and -35 region of the λ phage promoter P_L might improve the dynamic range and might likewise reduce the background noise. C. Randomization of TF-binding sites (shaded) by e.g. error-prone PCR results in a diversity of promoter derivatives of which *mtr* promoters with a K_d in the low mM range might be screened. D. The recognition of L-tyrosine as effector of the *mtr* promoter might be inhibited by removing or replacing the weak TyrR box.

Reporter systems with a dynamic response in the µM to mM range are of high value for biotechnological applications (Eggeling et al., 2015). For this reason, the sensitivity, which describes the rate of increase in reporter output to the amount of effector molecules, presents an important factor for the performance of the biosensor (Dietrich et al., 2010). To improve the sensitivity of the regulator BenR of *P. putida* KT2440 towards 3-methylbenzoate, Silva-Rocha and de Lorenzo successfully completed a second truncated operator motif within the P_b promoter (Silva-Rocha and de Lorenzo, 2012). Likewise, the addition of several additional operator motifs was proposed to increase the sensitivity (Tabor et al., 2009). The *mtr* biosensor, however, is already highly sensitive to L-phenylalanine in the µM range. The promoter of *mtr* contains TrpR-binding sites for L-tryptophan-mediated repression and upstream located TyrR-binding sites for L-phenylalanine- and L-tyrosine-mediated activation (Pittard et al., 2005). Engineering of TF-binding sites e.g. by error prone PCR, and screening for biosensors featuring a K_d in the low mM range might improve the biosensor's potential for the application in strains with industrially interesting L-phenylalanine or L-tyrosine production (Fig. 4.1.4.1 C).

The specificity of a biosensor for a defined effector molecule is important to reduce false-positive isolates during FACS HT screening or to avoid the misinterpretation of live cell imaging or bioprocess studies. As the *mtr* biosensor senses the aromatic amino acids L-phenylalanine and L-tyrosine, the isolation of L-tyrosine and L-phenylalanine producers is likely. The case of the *mtr* biosensor fortunately comprises an easy solution of this dilemma: L-tyrosine-mediated activation of the *mtr* promoter requires binding of TyrR as hexamer to the strong and the weak box (TF-binding site) in contrast to L-phenylalanine detection, which only requires binding to the strong box (Pittard et al., 2005; Sarsero and Pittard, 1991). By removing or replacing the weak box, the activation of gene expression upon L-tyrosine recognition may be eliminated (Fig. 4.1.4.1 D).

The diversity of biotechnologically produced metabolites challenges the expansion of biosensors for non-native and non-natural products (Schallmey et al., 2014). Theoretically, the modular architecture of transcriptional regulators (metabolite- and DNA-binding domains) enables engineering of the biosensor for improved, altered or novel specificities (Galvao and de Lorenzo, 2006). Different strategies proved successful to modify the ligand binding pockets of regulators by error-prone PCR (Wise and Kuske, 2000), chemical and saturation mutagenesis (Tang and Cirino, 2011; Tang et al., 2008; Tang et al., 2013) followed by HT screening of mutant libraries, or computational modelling based on crystal structures (Combs et al., 2013; Fry et al., 2010;

Looger et al., 2003; Mandell and Kortemme, 2009). A further approach relies on the artificial assembly of enzymatic metabolite-binding domains and the AraC DNA-binding domain e.g. for sensing isopentenyl diphosphate (Chou and Keasling, 2013). Furthermore, the orthogonality of biological functions still provides a bottleneck for metabolic engineering strategies, which often rely on heterologous pathways for the formation of non-native products (Mahr and Frunzke, 2016; Schallmey et al., 2014; Zhang et al., 2015b). For the functional transfer of biological parts between different host species, the expression from native promoters of the acceptor organisms as well as codon-optimization may be highly beneficial (Gopal and Kumar, 2013; Gustafsson et al., 2004; Sorensen and Mortensen, 2005). In addition, engineering the contact between the non-native regulator or promoter, and the native transcriptional or translational machinery (e.g. α-subunit of the RNA polymerase, DNA binding sites), which is necessary for metabolite recognition and signal transduction, might be interesting targets for improving orthogonality (Fig. 4.1.4.2).

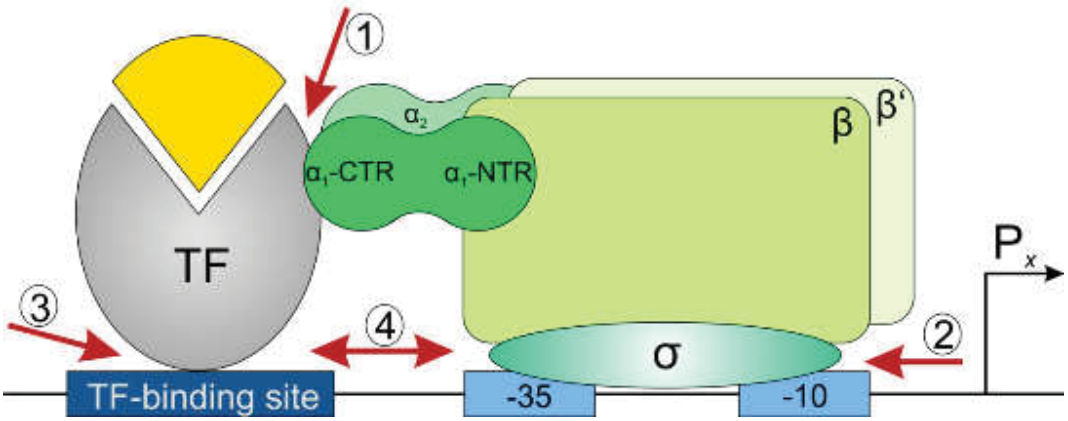

Fig. 4.1.4.2 The interaction between the transcription factor (TF, gray), the promoter P_x and the RNA polymerase (green). Potential targets for the improvement of the recognition of a non-native TF or native/non-native promoter P_x by the native transcription machinery: 1. The interaction between the α-subunit of the RNA-polymerase and the TF. 2. The recognition of the -10 and -35 region and the σ-factor. 3. The recognition between the TF and the TF-binding site (operator). 4. The distance between the -35 region and the TF-binding site.

In previous studies, the equipment with eukaryotic-specific signals (nuclear localization signal, transcriptional activation domain, etc.) proved successful to transfer bacterial regulators to yeast or mammalian cells allowing for S-adenosylmethionine, fatty acids or 2,4-diacetylphloroglucinol sensing (Ellis and Wolfgang, 2012; Stanton et al., 2014; Teo and Chang, 2014; Umeyama et al.,

2013). Nevertheless, efficient strategies are required to improve the orthogonality of transcriptional regulators and to understand the detailed interactions between the regulator, metabolite, operator and RNA polymerase (Charoensawan et al., 2015; Zhang et al., 2015b).

4.2 Novel strategies for engineering microbial cell factories

Rational metabolic engineering approaches mainly focus on the development of biosynthetic pathways, the sufficient supply with precursors, the import of substrates or the export of products as well as the degradation of those. A global and comprehensive consideration of the impact on microbial physiology is often neglected due to the high complexity of carbon and energy fluxes in living organisms. In addition, there are still many unknown and uncharacterized gene activities, regulatory mechanisms and metabolic fluxes, which obscure a systems-level insight into the global metabolic landscape. For this reason, novel metabolic engineering strategies and tools are in demand, which incorporate the entire physiology of the organism for improved production phenotypes. Here, adaptive laboratory evolution approaches as well as random mutagenesis of the entire genome followed by an elaborated screening strategy enabled the fast identification of non-intuitive targets for improving microbial cell factories (Atsumi et al., 2010; Baek et al., 2015; Fong et al., 2005; Mahr et al., 2015; Park et al., 2014; Sandberg et al., 2014; Xie et al., 2015). Further valuable contributions of both strategies for metabolic engineering purposes are highlighted in the following reviews (Abatemarco et al., 2013; Dietrich et al., 2010; Eggeling et al., 2015; Portnoy et al., 2011). Recently, the application of genetically-encoded biosensors revealed the expansion of the utility of these strategies to engineer biotechnological interesting, but inconspicuous metabolite production (Fig. 4.2).

4.2.1 Application of biosensors for high-throughput screening

Since the start of microbial engineering in the early last century, the diversification of genetic elements mimicking the processes of evolution and the consequential screening for desired functions have proven successful to develop novel and improved biotechnologically interesting phenotypes such as increased metabolite production (Becker and Wittmann, 2015; Dietrich et al., 2010; Parekh et al., 2000). The low-throughput ($<10^3$ individuals per day) of analytical techniques such as chromatography, mass or nuclear magnetic resonance spectroscopy, however, hamper screening of large mutant libraries. Here, the application of genetically-encoded biosensors visualizing intracellular metabolites, which allows for interfacing with FACS, revolutionized the HT screening of inconspicuous, small metabolites.

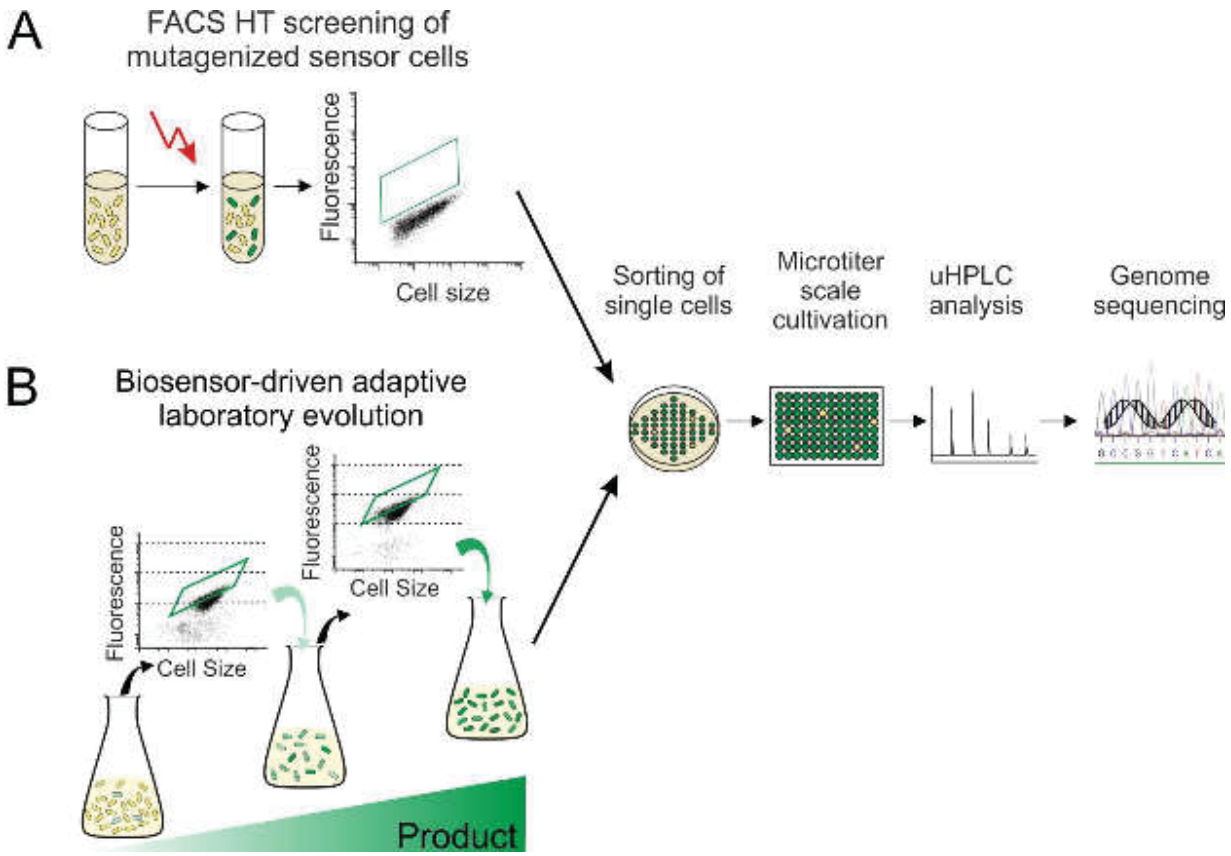

Fig. 4.2 Schematic of A. FACS HT screening of mutagenized sensor cells and B. biosensor-driven adaptive laboratory evolution. A. For FACS HT screening, sensor containing cells are randomly mutagenized by chemical mutagens such as MNNG. Cells are analyzed by FC and those with the highest fluorescent output are isolated by FACS as single clones on agar plates. B. For the biosensor-driven adaptive laboratory evolution, sensor cells with the top fluorescent output are iteratively isolated and re-cultivated. Then, high fluorescent sensor cells are spotted as single clones on agar plates. A. and B. Isolated single clones are re-cultivated in microtiter plates and analyzed for growth and fluorescence. The supernatant is assessed for the production by uHPLC. Subsequently, cells featuring desired characteristics are sequenced.

In a proof-of-principle study, the *mtr* biosensor for the detection of L-phenylalanine was used to screen a chemically mutagenized library of *E. coli* K-12 MG1655 cells using FACS (chapter 3.4). After mutagenesis, biosensor containing cells were screened by FACS, which allows for screening of about 80.000 cells per second and the possibility to isolate about 10.000 clones within the same time span (Fig. 4.2 A). Optionally, several enrichment steps with and without intermediate cultivation can be included to reduce false-positive clones. Following the isolation of single clones, a second screening step is of crucial importance as the increase of throughput is typically accompanied by reduced sensitivity and the neglect of small variations. Typically,

FACS-based screens are affected by the isolation of false-positive clones (22% this study; 77% (Mustafi et al., 2012)) due to the variance of the fluorescent signal for technical issues and noisy gene expression (Delvigne et al., 2015; Dietrich et al., 2010; Sanchez et al., 2013). In addition, the enrichment of exporter gene mutations improving or reducing the ability of metabolite secretion as well as the occurrence of modifications within the fluorescent reporter gene may likewise skew the picture of the actual production capacity of the organism, which can be revealed by re-analysis of isolated clones.

During screening for L-phenylalanine producers, about one third of 90 isolated mutant strains displayed at least two-fold up to 4.3-fold increased production titers (Fig. 4 in chapter 3.4). Similar studies featured a comparable fraction of positive clones (Binder et al., 2012; Mustafi et al., 2012). The top mutant clone excreted 160 µM L-phenylalanine into the supernatant. Compared to rationally engineered strains, which produce up to 300 mM (≈50 g L^{-1}) (Backman et al., 1990; Rüffer et al., 2004), the outcome appears quite low. Increased levels of L-phenylalanine can strongly impact the growth rate (Grinter, 1998). Polen and coworkers observed that the addition of 5 g L^{-1} L-phenylalanine reduced the growth rate by a factor of two (Polen et al., 2005). For this reason, the iterative enrichment by FACS, which was used to reduce the isolation of false-positive clones, might likewise select against slow growing cells impacted by increased L-phenylalanine production (chapter 3.4). Furthermore, the applied biosensor featured a highly sensitive response in the low µM range by approximating saturation in the mid-µM range. These performance characteristics of the biosensor consequently led to the isolation of clones with corresponding intracellular amino acid concentrations. Thereby, the identification of single clones with further increased production might be overlooked due to the high number of "low-performance" clones. Besides L-phenylalanine, the *mtr* biosensor responds additionally to increased L-tyrosine levels. Both aromatic amino acids share a great part of their biosynthetic route (Sprenger, 2007). Consequently, mutations increasing prephenic acid – a precursor of both amino acids – enhance the production of both. In this case, the fluorescent output of the biosensor would be composed of the response to L-phenylalanine and L-tyrosine. Interestingly, no clone with significantly increased L-tyrosine production was isolated (data not shown). Altogether, the design of the screening process (e.g. by implementation of several enrichment steps) as well as the performance of the biosensor may significantly impact the outcome of FACS HT screening. Here, the engineering of the biosensor for reduced sensitivity, improved specificity towards L-

phenylalanine or the increase of the dynamic range as described in chapter 4.1.4 (“Engineering of biosensors for improved and desired characteristics”) might be highly beneficial. For further limits and considerations for the application of biosensors, the reader is referred to chapter 4.1.3 (“Limitations of transcriptional regulator-based biosensors”).

For the establishment of the mutant *E. coli* library, the alkylating mutagen N-methyl-N’-nitro-N-nitrosoguanidine (MNNG) was chosen due to ability to generate genome-wide mutations as observed in a variety of previous studies (Binder et al., 2012; Harper and Lee, 2012; Ohnishi et al., 2008). The drawback of random mutagenesis is the emergence of several hundred small nucleotide polymorphisms (SNPs) throughout the entire genome, which hampers the identification of valuable, non-intuitive mutations. For example, the top five mutants isolated by FACS HT screening using the *mtr* biosensor revealed a total of 538 SNPs, of which 310 SNPs resulted in amino acid exchanges or stop codons (Tab. S4.2.1.1). Interestingly, amino acid exchanges were found in nine genes (*mtr, pheA, trpB, trpD, trpE, tyrA, tyrP, yedA, yddE*), which are associated with the biosynthesis or transport of aromatic amino acids. To verify beneficial SNPs for metabolite production, a high number of single mutations have to be re-introduced into a cured genomic background (Binder et al., 2012), which is laborious and time-consuming. Elaborated strategies like “Phenotype Sequencing” based on the computational sequence analysis of multiple independent mutants, or a recombineering strategy interfacing with biosensors based on FACS have been developed to improve the identification of valuable mutations (Binder et al., 2013; Harper et al., 2011). The interesting interplay of epistatic or synergistic mutations as observed during evolution-based studies (Cheng et al., 2014; Horinouchi et al., 2015; Oide et al., 2015; Sandberg et al., 2014; Tenaillon et al., 2012) might hardly be revealed by the abundance of mutations.

In addition, extensive studies using MNNG in *E. coli* and *C. glutamicum* demonstrated the preferential accumulation of GC to AT transitions (96.6%) and the dependency of the genomic context (Harper and Lee, 2012; Ohnishi et al., 2008), which strongly restricts the spectra of amino acid exchanges. In the *mtr* biosensor-based FACS HT screening of MNNG-mutagenized *E. coli* cells, for instance, 12% of all amino exchanges resulted in serine, 11% in isoleucine, and 10% in aspartic acid, asparagine or valine (Tab. S4.2.1.2). Exchanges to glycine, tyrosine, tryptophan, glutamine, proline or alanine were hardly or not identified. Furthermore, amino acids phenylalanine, tyrosine, isoleucine, asparagine or lysine were not found to be exchanged by

MNNG-mutagenesis (Tab. S4.2.1.2). This mutation spectra strongly limits the potential for the identification of ideal and desired protein functions e.g. enzymatic activities, feedback resistance, allosteric or DNA-binding capabilities, or protein-protein interactions. A broad range of alternative mutagens exists such as mutagenic chemicals including other alkylating agents, azides or base analogs (Benigni et al., 1992; Cai and Fix, 2002; Kodym and Afza, 2003; Pavlov et al., 1991; Richardson et al., 1988), or physical mutagens like ultra-violet (UV) and electromagnetic radiation (gamma rays or X rays) or atmospheric and room temperature plasma (ARTP) mutagenesis (Kodym and Afza, 2003; Zhang et al., 2015c; Zhang et al., 2014b). However, they all share rather one-sided mutation spectra. Here, the diversification of single, genetic fragments such as catalytic domains of interesting enzymes by error-prone PCR followed by FACS HT screening might contribute to the identification of desired phenotypical characteristics (Schendzielorz et al., 2014; Siedler et al., 2014a; Siedler et al., 2014b).

4.2.2 Biosensor-driven adaptive laboratory evolution

In contrast to random mutagenesis, adaptive laboratory evolution (ALE) approaches driven by mutation and selection profit from a strongly reduced number of mutations by promoting the establishment of beneficial traits and selecting against detrimental mutations at the same time (Abatemarco et al., 2013; Harper et al., 2011; Portnoy et al., 2011). Based on a natural mutation frequency of 10^{-10} to 10^{-9} mutations per base pair per replication cycle and short generation times (Barrick and Lenski, 2013), laboratory evolution experiments of microbes allow the selection of beneficial phenotypical traits from a natural diversity of phenotypic characteristics. So far, adaptive laboratory evolution has mostly been applied to easy selectable or fitness-linked phenotypes by iteratively increasing environmental stress (Eckdahl et al., 2015; Lee et al., 2013; Marietou et al., 2014; Oide et al., 2015; Reyes et al., 2014).

4.2.2.1 The establishment biosensor-driven adaptive laboratory evolution

In this study, the applicability of laboratory evolution was expanded to inconspicuous, small metabolites by imposing an artificial selective pressure on the fluorescent output of a biosensor using FACS. This novel approach was successfully applied to improve production of the basal L-valine producer strain *C. glutamicum* Δ*aceE* containing the Lrp biosensor (chapter 3.2, (Blombach et al., 2007; Mahr et al., 2015)). Cells with the top fluorescent output indicating increased L-valine production were iteratively isolated by FACS and (re-) cultivated (Fig. 4.2 B). As the Δ*aceE* strain displays a growth-decoupled L-valine production phenotype, cells were

iteratively sorted in the production phase after 28 hours of cultivation. Within five rounds of toggled sorting and cultivation, isolated evolved strains featured improved growth, on average about 25% increased L-valine production and three- to four-fold reduced by-product (L-alanine) formation. Sequencing of two isolated mutants revealed a total of seven SNPs, of which four (*ureD*-E188*, *glxR*-T93S, *prpD2*-T201I and *rpsP*-D30D(c90t)) were re-introduced and assessed in the non-evolved Δ*aceE* strain. All mutations featured about 15-20% increased biomass-specific L-valine yields ($Y_{P/X}$). The *ureD*-E188* mutation even resulted in a further increased L-valine yield of about 100%. Moreover, the reduction of L-alanine formation was attributed to a mutation in the cAMP-binding pocket of *glxR* (Mahr et al., 2015). To test the applicability of the biosensor-driven adaptive laboratory evolution approach to improve likewise the production of other metabolites, the L-leucine production strain *C. glutamicum* MV-Leu7 (Vogt et al., 2014) was additionally employed in a FACS-based evolution experiment using the Lrp biosensor (Fig. S4.2.2.1). In contrast to the Δ*aceE* strain for L-valine production, MV-Leu7 features a growth-coupled production phenotype, which requires an altered sorting strategy. Here, sorting of cells with the highest fluorescent output in the early exponential phase at an OD_{600} of 4 proved to be more efficient in contrast to sorting in the stationary phase after 28 hours, which was beneficial for the evolution of growth-decoupled L-valine production (data not shown). Within four iterative evolution steps, the biomass-specific L-leucine yield $Y_{P/X}$ increased from 0.55 to 0.81 mmol per g cell dry weight (CDW) by around 50% (Fig. S4.2.2.1). Interestingly, the growth rate dropped during the evolution experiment, which might result from the rerouting of carbon sources towards L-leucine production. Nevertheless, these results prove biosensor-driven adaptive laboratory evolution efficient and straightforward for improving production strains without a deep knowledge of the complex bacterial physiology.

4.2.2.2 “You get what you screen for”

Along with the statement “You get what you screen for” (Schmidt-Dannert and Arnold, 1999), the outcome of the biosensor-driven adaptive laboratory evolution approach strongly depends on several factors including i) the performance of the biosensor, ii) the growth- and production-phase selected for FC analysis and sorting, iii) the medium composition, iv) the scale of cultivation, v) the sorting strategy and accuracy of FACS and/or vi) cultivation conditions affecting the living cell.

First of all, the performance characteristics of the biosensor seem to be of high importance: During evolution, no further improvement of extracellular L-valine accumulation of the evolved culture was observed after the fifth sorting step (Fig. 1 in chapter 3.2, (Mahr et al., 2015)). This observation might indicate the saturation of the biosensor response, where an increase of intracellular amino acid concentration does not further result in an increase of the output of the biosensor due to reaching the highest rate of occupation of the promoter with transcription factors (Bintu et al., 2005a; Bintu et al., 2005b). For this reason, biosensor-driven evolution selecting cells with the top fluorescent output could not further improve L-valine production using the Lrp biosensor. Here, engineering of the biosensor is proposed to expand the operating range of the biosensor-driven adaptive laboratory evolution. While the sensitivity might be reduced by e.g. modifying the TF-binding site of the promoter or the DNA-binding domain within the TF itself, the dynamic range might be enhanced e.g. by the incorporation of the Lrp operator sequence in a strong phage promoter (as described in chapter 4.1.4 “Engineering of biosensors for improved and desired characteristics”).

The novel ALE approach proved highly successful to identify bottlenecks during the cultivation of the L-valine producer strain *C. glutamicum* Δ*aceE*. For instance, the identified *ureD*-E188* mutation generates a truncated, non-functional urease-accessory UreD protein. In a previous publication, UreD was categorized as protein of crucial importance for urease activity in order to degrade urea to ammonia and carbon dioxide (Nolden et al., 2000). Traditionally, urea serves as nitrogen source in the CGXII cultivation medium (Keilhauer et al., 1993). Interestingly, the lack of urea further increased L-valine production of the Δ*aceE* strain (Fig. 4 and 5 in chapter 3.2, (Mahr et al., 2015). Additional experiments within this study revealed that the degradation of urea strongly impacts the pH of a shake flask culture without pH maintenance by ammonia generation. This leads to improved growth, but strongly reduced L-valine production. Furthermore, the analyses indicated an increased activity of the anaplerotic enzymes phosphoenolpyruvate- and pyruvate carboxylase under elevated levels of CO_2/HCO_3^- (degradation product of urea) reducing the availability of the L-valine-precursor pyruvate by an enhanced efflux of glycolytic products via anaplerosis (chapter 3.3). The beneficial effect of urea deficiency on L-valine production, however, was more pronounced during shake flask cultivation (Fig. 5 and Fig. S4 in chapter 3.2 (Mahr et al., 2015)) – the method of choice during the performed evolution experiment. Obviously, the presence of urea in the CGXII minimal medium

provided a bottleneck for L-valine production. It remains a debatable point whether a similar urease inactivating mutation would have been found during altered cultivation and sorting conditions. Certainly, altered evolution strategies (e.g. sorting time, medium composition, etc.) may lead to completely different outcomes. The later application of the evolved strain has to be considered during the choice of cultivation conditions.

4.2.2.3 Beyond biosensor-driven adaptive laboratory evolution

Based on the natural mutation frequency, a total of seven mutations emerged during five rounds of biosensor-driven adaptive laboratory evolution (Tab. 2 in chapter 3.2, (Mahr et al., 2015)). Here, the implementation of a mutagenesis strategy, which only slightly increases the frequency of mutations, might be beneficial to allow selection from an increased genetic diversity. In contrast to random mutagenesis, the application of so-called mutator strains containing defective DNA repair systems might present an alternative option to increase diversity (Greener et al., 1997; Loh et al., 2010; Luan et al., 2013; Muteeb and Sen, 2010). For example, Oide and colleagues observed the emergence of an unexpected high number of mutations during ALE, which was proposed to result from the spontaneous development of a mutator phenotype in *C. glutamicum* cells (Oide et al., 2015). Furthermore, Chou and Keasling established the feedback-regulated evolution of phenotype (FREP) approach in *E. coli*, where the mutation rate is dynamically regulated by the target metabolite concentration controlling the expression of a mutator gene (*mutD5*) encoding a deficient proofreading exonuclease of DNA polymerase III (Chou and Keasling, 2013). However, FREP as well as the spontaneous development of mutator strains resulted in several hundred SNPs throughout the entire genome, which complicated the search for beneficial mutations. A strong reduction of the mutation rate by controlling a mutator gene from a weak, constitutive promoter might result in a decreased number of mutations and would allow interfacing with the biosensor-driven adaptive laboratory evolution approach. Here, a mutant *mutT* gene encoding oxoguanine-triphosphatase as part of the DNA mismatch repair machinery might be beneficial to increase the frequency of mutations in *C. glutamicum* (Nakamura et al., 2003; Resende et al., 2011).

An alternative strategy to FACS-based laboratory evolution of inconspicuous phenotypes provides the coupling of the biosensor output to growth (Dietrich et al., 2013; van Sint Fiet et al., 2006). By linking small-molecule production to an actuator mediating e.g. antibiotic or toxin resistance, for instance, bacterial growth in the presence of antibiotics or toxins is only possible,

if cells produce sufficient amounts of desired metabolites. Theoretically, a high selective pressure elicited by a high concentration of antibiotics or toxins should lead to the growth of cells with high metabolite production. One great limit of this strategy, however, is the evolution of antibiotic resistance not linked to product formation or the application of antibiotics, which are degraded over time. Furthermore, the system is limited at the point, where the detrimental effect of the antibiotic or toxin exceeds the potential for the development of resistance.

Beyond that, biosensor-driven adaptive laboratory evolution can be highly beneficial to balance metabolic fluxes upon vast metabolic engineering efforts such as the introduction of heterologous biosynthetic pathways or the deletion of central physiological reactions. Moreover, this strategy may also be applied to improve the tolerance of the engineered strain to detrimental or growth-inhibiting, inconspicuous end- and by-products such as aromatic amino acids (Polen et al., 2005). Altogether, biosensor-driven adaptive laboratory evolution approaches serve as excellent, complementary tools for metabolic engineering and may contribute to the identification of novel and non-intuitive targets to improve microbial cell factories.

4.3 Future prospects of biosensor applications

The present study demonstrates the enormous versatility of biosensors based on transcriptional regulators to reveal the formation of subpopulations in bioprocesses, to identify new and non-intuitive targets for strain engineering, and to improve fluxes of metabolites or energy for increased product formation. The broad biotechnological application of biosensors requires readily accessible sensor devices with appropriate and/or easy adjustable performance characteristics. Although efforts exist to generate libraries of standardized biological modules – so-called BioBricks (http://parts.igem.org/Catalog) (Endy, 2005; Voigt, 2006), the design of suitable, orthogonal biosensors is not yet like a Lego set. The efficient, easy and fast generation of custom-made sensor devices is still a bottleneck of the biosensor technology and has to be addressed in the future.

In the last years, increasing interest focused on the integration of regulatory circuits to dynamically control and balance metabolic fluxes upon diverse stimuli, and to overcome the natural barriers for metabolite overproduction (Dahl et al., 2013; Liu et al., 2015b; Xu et al., 2014; Zhang et al., 2012; Zhou and Zeng, 2015). To this end, elaborated *multiomic* strategies are required to identify metabolic bottlenecks. In addition, efficient workflows are in demand to

screen for biological bricks suitable to dynamically control pathways. For example, toggle switch designs proved successful to shift between different metabolic pathways upon intrinsic or extrinsic signals (Anesiadis et al., 2013; Soma et al., 2014; Tsuruno et al., 2015): L-valine production in *C. glutamicum* was engineered by increasing the supply with precursors *via* the inactivation of the PDHC (Δ*aceE*) (Blombach et al., 2007; Schreiner et al., 2005) or the downregulation of *aceE* (Buchholz et al., 2013). However, both strategies are inefficient as they require the addition of two expensive carbon sources or feature an impaired growth phenotype with a low substrate-specific yield (Blombach et al., 2007; Buchholz et al., 2013; Eikmanns and Blombach, 2014). Here, the incorporation of a toggle switch redirecting the flux from glycolysis towards L-valine biosynthesis upon reaching a high biomass formation might kill two birds with one stone – increased growth rates and biomass formation as well as improved metabolite production on a single carbon source. Furthermore, genetic circuits might also be interesting to control and coordinate the performance of synthetic communities of orthogonal microbes where organism A delivers precursors, carbon sources or energy to organism B producing the metabolite of interest (Bertrand et al., 2014; Hoelzle et al., 2014; Jagmann and Philipp, 2014; Pandhal and Noirel, 2014). For instance, Marchand and Collins established a quorum-sensing based system to allow communication of a synthetic community of *E. coli* and *B. subtilis* (Marchand and Collins, 2013). Genetic circuits may be beneficial e.g. to elicit growth or biosynthetic pathways of organism B upon a sufficient production of precursors by organism A. In the last years, biosensors were designed that likewise report on by-product formation, accumulation of toxic intermediates or the lack of oxygen or carbon sources – extrinsic and intrinsic factors that can influence bioprocesses (Constantinou and Polizzi, 2013). Linking the biosensor signal via electrodes to feed pumps or the aeration system, for instance, the intracellular requirements obscured by extracellular measurements may immediately be satisfied.

All these examples demonstrate the high potential of genetically-encoded biosensors to give new impetus to biotechnological strain and bioprocess development. Driven by the fascination and potential of microbial cells, the creativity for the implementation of biosensor circuits in microbial cell factories will certainly not arrest in the future.

5 REFERENCES

Abatemarco, J., Hill, A., Alper, H. S., 2013. Expanding the metabolic engineering toolbox with directed evolution. Biotechnol J. 8**,** 1397-410.

Aboul-Ela, F., Huang, W., Abd Elrahman, M., Boyapati, V., Li, P., 2015. Linking aptamer-ligand binding and expression platform folding in riboswitches: prospects for mechanistic modeling and design. Wiley Interdiscip Rev RNA. 6**,** 631-50.

Abreu-Goodger, C., Merino, E., 2005. RibEx: a web server for locating riboswitches and other conserved bacterial regulatory elements. Nucleic Acids Res. 33**,** W690-2.

Abreu, V. A., Almeida, S., Tiwari, S., Hassan, S. S., Mariano, D., Silva, A., Baumbach, J., Azevedo, V., Rottger, R., 2015. CMRegNet-An interspecies reference database for corynebacterial and mycobacterial regulatory networks. BMC Genomics. 16**,** 452.

Amantonico, A., Oh, J. Y., Sobek, J., Heinemann, M., Zenobi, R., 2008. Mass spectrometric method for analyzing metabolites in yeast with single cell sensitivity. Angew Chem. 47**,** 5382-5.

An, G. H., Bielich, J., Auerbach, R., Johnson, E. A., 1991. Isolation and characterization of carotenoid hyperproducing mutants of yeast by flow cytometry and cell sorting. Biotechnology (NY). 9**,** 70-3.

Andersen, J. B., Sternberg, C., Poulsen, L. K., Bjorn, S. P., Givskov, M., Molin, S., 1998. New unstable variants of green fluorescent protein for studies of transient gene expression in bacteria. Appl Environ Microbiol. 64**,** 2240-6.

Anesiadis, N., Kobayashi, H., Cluett, W. R., Mahadevan, R., 2013. Analysis and design of a genetic circuit for dynamic metabolic engineering. ACS Synth Biol. 2**,** 442-52.

Atsumi, S., Wu, T. Y., Machado, I. M., Huang, W. C., Chen, P. Y., Pellegrini, M., Liao, J. C., 2010. Evolution, genomic analysis, and reconstruction of isobutanol tolerance in *Escherichia coli*. Mol Syst Biol. 6**,** 449.

Backman, K., O'Connor, M. J., Maruya, A., Rudd, E., McKay, D., Balakrishnan, R., Radjai, M., DiPasquantonio, V., Shoda, D., Hatch, R., et al., 1990. Genetic engineering of metabolic pathways applied to the production of phenylalanine. Ann NY Acad Sci 589**,** 16-24.

Baek, S. H., Kwon, E. Y., Kim, Y. H., Hahn, J. S., 2015. Metabolic engineering and adaptive evolution for efficient production of D-lactic acid in *Saccharomyces cerevisiae*. Appl Microbiol Biotechnol.

Barrick, J. E., Lenski, R. E., 2013. Genome dynamics during experimental evolution. Nat Rev Genet. 14**,** 827-39.

Becker, J., Wittmann, C., 2012. Systems and synthetic metabolic engineering for amino acid production - the heartbeat of industrial strain development. Curr Opin Biotechnol. 23**,** 718-26.

Becker, J., Wittmann, C., 2015. Advanced biotechnology: metabolically engineered cells for the bio-based production of chemicals and fuels, materials, and health-care products. Angew Chem Int Ed Engl. 54**,** 3328-50.

Behjousiar, A., Kontoravdi, C., Polizzi, K. M., 2012. *In situ* monitoring of intracellular glucose and glutamine in CHO cell culture. PloS ONE. 7**,** e34512.

Beisel, C. L., Smolke, C. D., 2009. Design principles for riboswitch function. PLoS Comput Biol. 5**,** e1000363.

Bengert, P., Dandekar, T., 2004. Riboswitch finder--a tool for identification of riboswitch RNAs. Nucleic Acids Res. 32**,** W154-9.

Benigni, R., Palombo, F., Dogliotti, E., 1992. Multivariate statistical analysis of mutational spectra of alkylating agents. Mutat Res. 267**,** 77-88.

Berman, H. M., Westbrook, J., Feng, Z., Gilliland, G., Bhat, T. N., Weissig, H., Shindyalov, I. N., Bourne, P. E., 2000. The Protein Data Bank. Nucleic Acids Res. 28**,** 235-42.

Bermejo, C., Haerizadeh, F., Takanaga, H., Chermak, D., Frommer, W. B., 2011. Optical sensors for measuring dynamic changes of cytosolic metabolite levels in yeast. Nat Protoc. 6**,** 1806-17.

Bertrand, S., Bohni, N., Schnee, S., Schumpp, O., Gindro, K., Wolfender, J. L., 2014. Metabolite induction via microorganism co-culture: a potential way to enhance chemical diversity for drug discovery. Biotechnol Adv. 32**,** 1180-204.

Bilan, D. S., Pase, L., Joosen, L., Gorokhovatsky, A. Y., Ermakova, Y. G., Gadella, T. W., Grabher, C., Schultz, C., Lukyanov, S., Belousov, V. V., 2013. HyPer-3: a genetically encoded H_2O_2 probe with improved performance for ratiometric and fluorescence lifetime imaging. ACS Chem Biol. 8**,** 535-42.

Binder, D., Grünberger, A., Loeschcke, A., Probst, C., Bier, C., Pietruszka, J., Wiechert, W., Kohlheyer, D., Jaeger, K. E., Drepper, T., 2014. Light-responsive control of bacterial gene expression: precise triggering of the *lac* promoter activity using photocaged IPTG. Integr Biol (Camb). 6**,** 755-65.

Binder, S., Schendzielorz, G., Stabler, N., Krumbach, K., Hoffmann, K., Bott, M., Eggeling, L., 2012. A high-throughput approach to identify genomic variants of bacterial metabolite producers at the single-cell level. Genome Biol. 13**,** R40.

Binder, S., Siedler, S., Marienhagen, J., Bott, M., Eggeling, L., 2013. Recombineering in *Corynebacterium glutamicum* combined with optical nanosensors: a general strategy for fast producer strain generation. Nucleic Acids Res. 41**,** 6360-9.

Bintu, L., Buchler, N. E., Garcia, H. G., Gerland, U., Hwa, T., Kondev, J., Kuhlman, T., Phillips, R., 2005a. Transcriptional regulation by the numbers: applications. Curr Opin Genet Dev. 15**,** 125-35.

Bintu, L., Buchler, N. E., Garcia, H. G., Gerland, U., Hwa, T., Kondev, J., Phillips, R., 2005b. Transcriptional regulation by the numbers: models. Curr Opin Genet Dev. 15**,** 116-24.

Blazeck, J., Alper, H. S., 2013. Promoter engineering: recent advances in controlling transcription at the most fundamental level. Biotechnol J. 8**,** 46-58.

Blombach, B., Arndt, A., Auchter, M., Eikmanns, B. J., 2009. L-valine production during growth of pyruvate dehydrogenase complex-deficient *Corynebacterium glutamicum* in the presence of ethanol or by inactivation of the transcriptional regulator SugR. Appl Environ Microbiol. 75**,** 1197-200.

Blombach, B., Schreiner, M. E., Bartek, T., Oldiges, M., Eikmanns, B. J., 2008. *Corynebacterium glutamicum* tailored for high-yield L-valine production. Appl Microbiol Biotechnol. 79**,** 471-9.

Blombach, B., Schreiner, M. E., Holatko, J., Bartek, T., Oldiges, M., Eikmanns, B. J., 2007. L-valine production with pyruvate dehydrogenase complex-deficient *Corynebacterium glutamicum*. Appl Environ Microbiol. 73**,** 2079-84.

Bolten, C. J., Schröder, H., Dickschat, J., Wittmann, C., 2010. Towards methionine overproduction in *Corynebacterium glutamicum* - methanethiol and dimethyldisulfide as reduced sulfur sources. J Microbiol Biotechnol. 20**,** 1196-203.

Bonde, M. T., Klausen, M. S., Anderson, M. V., Wallin, A. I., Wang, H. H., Sommer, M. O., 2014. MODEST: a web-based design tool for oligonucleotide-mediated genome engineering and recombineering. Nucleic Acids Res. 42**,** W408-15.

Bongaerts, J., Kramer, M., Muller, U., Raeven, L., Wubbolts, M., 2001. Metabolic engineering for microbial production of aromatic amino acids and derived compounds. Metab Eng. 3**,** 289-300.

Buchholz, J., Schwentner, A., Brunnenkan, B., Gabris, C., Grimm, S., Gerstmeir, R., Takors, R., Eikmanns, B. J., Blombach, B., 2013. Platform engineering of *Corynebacterium glutamicum* with reduced pyruvate dehydrogenase complex activity for improved production of L-lysine, L-valine, and 2-ketoisovalerate. Appl Environ Microbiol. 79**,** 5566-75.

Cai, Z., Fix, D., 2002. Neighboring base identity affects N-ethyl-N-nitrosourea-induced mutagenesis in *Escherichia coli*. Mutat Res. 508**,** 71-81.

Carey, L. B., van Dijk, D., Sloot, P. M., Kaandorp, J. A., Segal, E., 2013. Promoter sequence determines the relationship between expression level and noise. PLoS Biol. 11**,** e1001528.

Charoensawan, V., Martinho, C., Wigge, P. A., 2015. "Hit-and-run": Transcription factors get caught in the act. Bioessays. 37**,** 748-54.

Chen, C., Li, Y., Hu, J., Dong, X., Wang, X., 2015. Metabolic engineering of *Corynebacterium glutamicum* ATCC13869 for L-valine production. Metab Eng. 29**,** 66-75.

Chen, X., Zhou, L., Tian, K., Kumar, A., Singh, S., Prior, B. A., Wang, Z., 2013. Metabolic engineering of *Escherichia coli*: a sustainable industrial platform for bio-based chemical production. Biotechnol Adv. 31**,** 1200-23.

Cheng, K. K., Lee, B. S., Masuda, T., Ito, T., Ikeda, K., Hirayama, A., Deng, L., Dong, J., Shimizu, K., Soga, T., Tomita, M., Palsson, B. O., Robert, M., 2014. Global metabolic network reorganization by adaptive mutations allows fast growth of *Escherichia coli* on glycerol. Nat Commun. 5**,** 3233.

Chou, H. H., Keasling, J. D., 2013. Programming adaptive control to evolve increased metabolite production. Nat Commun. 4**,** 2595.

Christie, J. M., Hitomi, K., Arvai, A. S., Hartfield, K. A., Mettlen, M., Pratt, A. J., Tainer, J. A., Getzoff, E. D., 2012. Structural tuning of the fluorescent protein iLOV for improved photostability. J Biol Chem. 287**,** 22295-304.

Church, G. M., Elowitz, M. B., Smolke, C. D., Voigt, C. A., Weiss, R., 2014. Realizing the potential of synthetic biology. Nat Rev Mol Cell Biol. 15**,** 289-94.

Combs, S. A., Deluca, S. L., Deluca, S. H., Lemmon, G. H., Nannemann, D. P., Nguyen, E. D., Willis, J. R., Sheehan, J. H., Meiler, J., 2013. Small-molecule ligand docking into comparative models with Rosetta. Nat Protoc. 8**,** 1277-98.

Constantinou, A., Polizzi, K. M., 2013. Opportunities for bioprocess monitoring using FRET biosensors. Biochem Soc Trans. 41**,** 1146-51.

Craggs, T. D., 2009. Green fluorescent protein: structure, folding and chromophore maturation. Chem Soc Rev. 38**,** 2865-75.

Cruz-Toledo, J., McKeague, M., Zhang, X., Giamberardino, A., McConnell, E., Francis, T., DeRosa, M. C., Dumontier, M., 2012. Aptamer Base: a collaborative knowledge base to describe aptamers and SELEX experiments. Database (Oxford). 2012**,** bas006.

Dahl, R. H., Zhang, F., Alonso-Gutierrez, J., Baidoo, E., Batth, T. S., Redding-Johanson, A. M., Petzold, C. J., Mukhopadhyay, A., Lee, T. S., Adams, P. D., Keasling, J. D., 2013. Engineering dynamic pathway regulation using stress-response promoters. Nat Biotechnol. 31**,** 1039-46.

Delvigne, F., Boxus, M., Ingels, S., Thonart, P., 2009. Bioreactor mixing efficiency modulates the activity of a prpoS::GFP reporter gene in *E. coli*. Microb Cell Factories. 8**,** 15.

Delvigne, F., Goffin, P., 2014. Microbial heterogeneity affects bioprocess robustness: dynamic single-cell analysis contributes to understanding of microbial populations. Biotechnol J. 9**,** 61-72.

Delvigne, F., Pecheux, H., Tarayre, C., 2015. Fluorescent Reporter Libraries as Useful Tools for Optimizing Microbial Cell Factories: A Review of the Current Methods and Applications. Front Bioeng Biotechnol. 3**,** 147.

Delvigne, F., Zune, Q., Lara, A. R., Al-Soud, W., Sorensen, S. J., 2014. Metabolic variability in bioprocessing: implications of microbial phenotypic heterogeneity. Trends Biotechnol. 32**,** 608-16.

Dennis, P. P., Bremer, H., 1974. Differential rate of ribosomal protein synthesis in *Escherichia coli* B/r. J Mol Biol. 84**,** 407-22.

Dietrich, J. A., McKee, A. E., Keasling, J. D., 2010. High-throughput metabolic engineering: advances in small-molecule screening and selection. Annu Rev Biochem. 79**,** 563-90.

Dietrich, J. A., Shis, D. L., Alikhani, A., Keasling, J. D., 2013. Transcription factor-based screens and synthetic selections for microbial small-molecule biosynthesis. ACS Synth Biol. 2**,** 47-58.

Drepper, T., Eggert, T., Circolone, F., Heck, A., Krauss, U., Guterl, J. K., Wendorff, M., Losi, A., Gärtner, W., Jaeger, K. E., 2007. Reporter proteins for *in vivo* fluorescence without oxygen. Nat Biotechnol. 25**,** 443-5.

Drepper, T., Huber, R., Heck, A., Circolone, F., Hillmer, A. K., Büchs, J., Jaeger, K. E., 2010. Flavin mononucleotide-based fluorescent reporter proteins outperform green fluorescent protein-like proteins as quantitative *in vivo* real-time reporters. Appl Environ Microbiol. 76**,** 5990-4.

Eckdahl, T. T., Campbell, A. M., Heyer, L. J., Poet, J. L., Blauch, D. N., Snyder, N. L., Atchley, D. T., Baker, E. J., Brown, M., Brunner, E. C., Callen, S. A., Campbell, J. S., Carr, C. J., Carr, D. R., Chadinha, S. A., Chester, G. I., Chester, J., Clarkson, B. R., Cochran, K. E., Doherty, S. E., Doyle, C., Dwyer, S., Edlin, L. M., Evans, R. A., Fluharty, T., Frederick, J., Galeota-Sprung, J.,

Gammon, B. L., Grieshaber, B., Gronniger, J., Gutteridge, K., Henningsen, J., Isom, B., Itell, H. L., Keffeler, E. C., Lantz, A. J., Lim, J. N., McGuire, E. P., Moore, A. K., Morton, J., Nakano, M., Pearson, S. A., Perkins, V., Parrish, P., Pierson, C. E., Polpityaarachchige, S., Quaney, M. J., Slattery, A., Smith, K. E., Spell, J., Spencer, M., Taye, T., Trueblood, K., Vrana, C. J., Whitesides, E. T., 2015. Programmed evolution for optimization of orthogonal metabolic output in bacteria. PloS ONE. 10**,** e0118322.

Eggeling, L., Bott, M., 2015. A giant market and a powerful metabolism: L-lysine provided by *Corynebacterium glutamicum*. Appl Microbiol Biotechnol. 99**,** 3387-94.

Eggeling, L., Bott, M., Marienhagen, J., 2015. Novel screening methods-biosensors. Curr Opin Biotechnol. 35**,** 30-6.

Eikmanns, B. J., Blombach, B., 2014. The pyruvate dehydrogenase complex of *Corynebacterium glutamicum*: an attractive target for metabolic engineering. J Biotechnol. 192 Pt B**,** 339-45.

Ellington, A. D., Szostak, J. W., 1990. *In vitro* selection of RNA molecules that bind specific ligands. Nature. 346**,** 818-22.

Ellis, J. M., Wolfgang, M. J., 2012. A genetically encoded metabolite sensor for malonyl-CoA. Chem Biol. 19**,** 1333-9.

Elowitz, M. B., Leibler, S., 2000. A synthetic oscillatory network of transcriptional regulators. Nature. 403**,** 335-8.

Endy, D., 2005. Foundations for engineering biology. Nature. 438**,** 449-53.

Engels, V., Wendisch, V. F., 2007. The DeoR-type regulator SugR represses expression of *ptsG* in *Corynebacterium glutamicum*. J Bacteriol. 189**,** 2955-66.

Erickson, B., Nelson, Winters, P., 2012. Perspective on opportunities in industrial biotechnology in renewable chemicals. Biotechnol J. 7**,** 176-85.

Fernandez-Lopez, R., Ruiz, R., de la Cruz, F., Moncalian, G., 2015. Transcription factor-based biosensors enlightened by the analyte. Front Microbiol. 6**,** 648.

Fong, S. S., Burgard, A. P., Herring, C. D., Knight, E. M., Blattner, F. R., Maranas, C. D., Palsson, B. O., 2005. *In silico* design and adaptive evolution of *Escherichia coli* for production of lactic acid. Biotechnol Bioeng. 91**,** 643-8.

Freed, N. E., Silander, O. K., Stecher, B., Böhm, A., Hardt, W. D., Ackermann, M., 2008. A simple screen to identify promoters conferring high levels of phenotypic noise. PLoS Genet. 4**,** e1000307.

Frommer, W. B., Davidson, M. W., Campbell, R. E., 2009. Genetically encoded biosensors based on engineered fluorescent proteins. Chem Soc Rev. 38**,** 2833-41.

Fry, H. C., Lehmann, A., Saven, J. G., DeGrado, W. F., Therien, M. J., 2010. Computational design and elaboration of a *de novo* heterotetrameric alpha-helical protein that selectively binds an emissive abiological (porphinato)zinc chromophore. J Am Chem Soc. 132**,** 3997-4005.

Furusawa, C., Horinouchi, T., Hirasawa, T., Shimizu, H., 2013. Systems metabolic engineering: the creation of microbial cell factories by rational metabolic design and evolution. Adv Biochem Eng Biotechnol. 131**,** 1-23.

Galvao, T. C., de Lorenzo, V., 2006. Transcriptional regulators à la carte: engineering new effector specificities in bacterial regulatory proteins. Curr Opin Biotechnol. 17**,** 34-42.

Galvao, T. C., Mencia, M., de Lorenzo, V., 2007. Emergence of novel functions in transcriptional regulators by regression to stem protein types. Mol Microbiol. 65**,** 907-19.

Ghribi, D., Zouari, N., Jaoua, S., 2004. Improvement of bioinsecticides production through mutagenesis of *Bacillus thuringiensis* by u.v. and nitrous acid affecting metabolic pathways and/or delta-endotoxin synthesis. J Appl Microbiol. 97**,** 338-46.

Global Industry Analysts Inc, 2015. The global amino acids market - trends, drivers & projections. http://www.strategyr.com/MarketResearch/Amino_Acids_Market_Trends.asp.

Gopal, G. J., Kumar, A., 2013. Strategies for the production of recombinant protein in Escherichia coli. Protein J. 32**,** 419-25.

Greener, A., Callahan, M., Jerpseth, B., 1997. An efficient random mutagenesis technique using an *E. coli* mutator strain. Mol Biotechnol. 7**,** 189-95.

Grinter, N. J., 1998. Developing an L-phenylalanine process. Chem Tech. 33-35.

Gruenwald, K., Holland, J. T., Stromberg, V., Ahmad, A., Watcharakichkorn, D., Okumoto, S., 2012. Visualization of glutamine transporter activities in living cells using genetically encoded glutamine sensors. PloS ONE. 7**,** e38591.

Grünberger, A., Paczia, N., Probst, C., Schendzielorz, G., Eggeling, L., Noack, S., Wiechert, W., Kohlheyer, D., 2012. A disposable picolitre bioreactor for cultivation and investigation of industrially relevant bacteria on the single cell level. Lab Chip. 12**,** 2060-8.

Grünberger, A., Probst, C., Helfrich, S., Nanda, A., Stute, B., Wiechert, W., von Lieres, E., Nöh, K., Frunzke, J., Kohlheyer, D., 2015. Spatiotemporal microbial single-cell analysis using a high-throughput microfluidics cultivation platform. Cytometry A. 87**,** 1101-15.

Grünberger, A., Wiechert, W., Kohlheyer, D., 2014. Single-cell microfluidics: opportunity for bioprocess development. Curr Opin Biotechnol. 29**,** 15-23.

Gustafsson, C., Govindarajan, S., Minshull, J., 2004. Codon bias and heterologous protein expression. Trends Biotechnol. 22**,** 346-53.

Harper, M., Lee, C. J., 2012. Genome-wide analysis of mutagenesis bias and context sensitivity of N-methyl-N'-nitro-N-nitrosoguanidine (NTG). Mutat Res. 731**,** 64-7.

Harper, M. A., Chen, Z., Toy, T., Machado, I. M., Nelson, S. F., Liao, J. C., Lee, C. J., 2011. Phenotype sequencing: identifying the genes that cause a phenotype directly from pooled sequencing of independent mutants. PloS ONE. 6**,** e16517.

Haselgrübler, T., Haider, M., Ji, B., Juhasz, K., Sonnleitner, A., Balogi, Z., Hesse, J., 2014. High-throughput, multiparameter analysis of single cells. Anal Bioanal Chem. 406**,** 3279-96.

Heider, S. A., Wendisch, V. F., 2015. Engineering microbial cell factories: Metabolic engineering of *Corynebacterium glutamicum* with a focus on non-natural products. Biotechnol J. 10**,** 1170-84.

Heinemann, M., Zenobi, R., 2011. Single cell metabolomics. Curr Opin Biotechnol. 22**,** 26-31.

Hentschel, E., Will, C., Mustafi, N., Burkovski, A., Rehm, N., Frunzke, J., 2013. Destabilized eYFP variants for dynamic gene expression studies in *Corynebacterium glutamicum*. Microb Biotechnol. 6**,** 196-201.

Hessels, A. M., Merkx, M., 2015. Genetically-encoded FRET-based sensors for monitoring Zn^{2+} in living cells. Metallomics 7**,** 258-66.

Hoelzle, R. D., Virdis, B., Batstone, D. J., 2014. Regulation mechanisms in mixed and pure culture microbial fermentation. Biotechnol Bioeng. 111**,** 2139-54.

Horinouchi, T., Suzuki, S., Hirasawa, T., Ono, N., Yomo, T., Shimizu, H., Furusawa, C., 2015. Phenotypic convergence in bacterial adaptive evolution to ethanol stress. BMC Evol Biol. 15**,** 180.

Hughes, S. R., Gibbons, W. R., Bang, S. S., Pinkelman, R., Bischoff, K. M., Slininger, P. J., Qureshi, N., Kurtzman, C. P., Liu, S., Saha, B. C., Jackson, J. S., Cotta, M. A., Rich, J. O., Javers, J. E., 2012. Random UV-C mutagenesis of *Scheffersomyces* (formerly *Pichia*) *stipitis* NRRL Y-7124 to improve anaerobic growth on lignocellulosic sugars. J Ind Microbiol Biotechnol. 39**,** 163-73.

Iizuka, R., Yamagishi-Shirasaki, M., Funatsu, T., 2011. Kinetic study of *de novo* chromophore maturation of fluorescent proteins. Anal Biochem. 414**,** 173-8.

Ikeda, M., 2006. Towards bacterial strains overproducing L-tryptophan and other aromatics by metabolic engineering. Appl Microbiol Biotechnol. 69**,** 615-26.

Ikeda, M., Katsumata, R., 1992. Metabolic engineering toproduce tyrosine or phenylalanine in a tryptophan-producing *Corynebacterium glutamicum* strain. Appl Environ Microbiol. 58**,** 781-5.

Jagmann, N., Philipp, B., 2014. Reprint of design of synthetic microbial communities for biotechnological production processes. J Biotechnol. 192 Pt B**,** 293-301.

Jahn, M., Seifert, J., von Bergen, M., Schmid, A., Buhler, B., Muller, S., 2013. Subpopulation-proteomics in prokaryotic populations. Curr Opin Biotechnol. 24**,** 79-87.

Jakociunas, T., Bonde, I., Herrgard, M., Harrison, S. J., Kristensen, M., Pedersen, L. E., Jensen, M. K., Keasling, J. D., 2015. Multiplex metabolic pathway engineering using CRISPR/Cas9 in *Saccharomyces cerevisiae*. Metab Eng. 28**,** 213-22.

Jang, S., Yang, J., Seo, S. W., Jung, G. Y., 2015. Riboselector: riboswitch-based synthetic selection device to expedite evolution of metabolite-producing microorganisms. Methods Enzymol. 550**,** 341-62.

Jehmlich, N., Hübschmann, T., Gesell Salazar, M., Volker, U., Benndorf, D., Müller, S., von Bergen, M., Schmidt, F., 2010. Advanced tool for characterization of microbial cultures by combining cytomics and proteomics. Appl Microbiol Biotechnol. 88**,** 575-84.

Keilhauer, C., Eggeling, L., Sahm, H., 1993. Isoleucine synthesis in *Corynebacterium glutamicum*: molecular analysis of the *ilvB-ilvN-ilvC* operon. J Bacteriol. 175**,** 5595-603.

Keren, L., van Dijk, D., Weingarten-Gabbay, S., Davidi, D., Jona, G., Weinberger, A., Milo, R., Segal, E., 2015. Noise in gene expression is coupled to growth rate. Genome Res. 25**,** 1893-902.

Kim, B., Kim, W. J., Kim, D. I., Lee, S. Y., 2015. Applications of genome-scale metabolic network model in metabolic engineering. J Ind Microbiol Biotechnol 42**,** 339-48.

Kiviet, D. J., Nghe, P., Walker, N., Boulineau, S., Sunderlikova, V., Tans, S. J., 2014. Stochasticity of metabolism and growth at the single-cell level. Nature. 514**,** 376-9.

Kodym, A., Afza, R., 2003. Physical and chemical mutagenesis. Methods Mol Biol. 236**,** 189-204.

Kopniczky, M. B., Moore, S. J., Freemont, P. S., 2015. Multilevel Regulation and Translational Switches in Synthetic Biology. IEEE Trans Biomed Circuits Syst.

Krömer, J. O., Wittmann, C., Schröder, H., Heinzle, E., 2006. Metabolic pathway analysis for rational design of L-methionine production by *Escherichia coli* and *Corynebacterium glutamicum*. Metab Eng. 8**,** 353-69.

Langemann, T., Mayr, U. B., Meitz, A., Lubitz, W., Herwig, C., 2016. Multi-parameter flow cytometry as a process analytical technology (PAT) approach for the assessment of bacterial ghost production. Appl Microbiol Biotechnol. 100**,** 409-18.

Lee, J. Y., Seo, J., Kim, E. S., Lee, H. S., Kim, P., 2013. Adaptive evolution of *Corynebacterium glutamicum* resistant to oxidative stress and its global gene expression profiling. Biotechnol Lett. 35**,** 709-17.

Lee, J. Y., Yang, K. S., Jang, S. A., Sung, B. H., Kim, S. C., 2011. Engineering butanol-tolerance in *Escherichia coli* with artificial transcription factor libraries. Biotechnol Bioeng. 108**,** 742-9.

Leuchtenberger, W., Huthmacher, K., Drauz, K., 2005. Biotechnological production of amino acids and derivatives: current status and prospects. Appl Microbiol Biotechnol. 69**,** 1-8.

Li, Y., Lin, Z., Huang, C., Zhang, Y., Wang, Z., Tang, Y. J., Chen, T., Zhao, X., 2015. Metabolic engineering of *Escherichia coli* using CRISPR-Cas9 meditated genome editing. Metab Eng. 31**,** 13-21.

Liang, J. C., Bloom, R. J., Smolke, C. D., 2011. Engineering biological systems with synthetic RNA molecules. Mol Cell. 43**,** 915-26.

Lieder, S., Jahn, M., Seifert, J., von Bergen, M., Muller, S., Takors, R., 2014. Subpopulation-proteomics reveal growth rate, but not cell cycling, as a major impact on protein composition in *Pseudomonas putida* KT2440. AMB Express. 4**,** 71.

Lipovsky, A., Nitzan, Y., Gedanken, A., Lubart, R., 2010. Visible light-induced killing of bacteria as a function of wavelength: implication for wound healing. Lasers Surg Med. 42**,** 467-72.

Liu, D., Evans, T., Zhang, F., 2015a. Applications and advances of metabolite biosensors for metabolic engineering. Metab Eng. 31**,** 35-43.

Liu, D., Xiao, Y., Evans, B. S., Zhang, F., 2015b. Negative feedback regulation of fatty acid production based on a malonyl-CoA sensor-actuator. ACS Synth Biol. 4**,** 132-40.

Liu, L., Redden, H., Alper, H. S., 2013. Frontiers of yeast metabolic engineering: diversifying beyond ethanol and *Saccharomyces*. Curr Opin Biotechnol. 24**,** 1023-30.

Liu, W., Jiang, R., 2015. Combinatorial and high-throughput screening approaches for strain engineering. Appl Microbiol Biotechnol. 99**,** 2093-104.

Loh, E., Salk, J. J., Loeb, L. A., 2010. Optimization of DNA polymerase mutation rates during bacterial evolution. Proc Natl Acad Sci U S A 107**,** 1154-9.

Looger, L. L., Dwyer, M. A., Smith, J. J., Hellinga, H. W., 2003. Computational design of receptor and sensor proteins with novel functions. Nature. 423**,** 185-90.

Luan, G., Cai, Z., Li, Y., Ma, Y., 2013. Genome replication engineering assisted continuous evolution (GREACE) to improve microbial tolerance for biofuels production. Biotechnol Biofuels. 6**,** 137.

Lutz, R., Bujard, H., 1997. Independent and tight regulation of transcriptional units in *Escherichia coli* via the LacR/O, the TetR/O and AraC/I1-I2 regulatory elements. Nucleic Acids Res. 25**,** 1203-10.

Mahr, R., Frunzke, J., 2016. Transcription factor-based biosensors in biotechnology: current state and future prospects. Appl Microbiol Biotechnol 100**,** 79-90.

Mahr, R., Gätgens, C., Gätgens, J., Polen, T., Kalinowski, J., Frunzke, J., 2015. Biosensor-driven adaptive laboratory evolution of l-valine production in *Corynebacterium glutamicum*. Metab Eng. 32**,** 184-94.

Mandell, D. J., Kortemme, T., 2009. Computer-aided design of functional protein interactions. Nat Chem Biol. 5**,** 797-807.

Mannironi, C., Scerch, C., Fruscoloni, P., Tocchini-Valentini, G. P., 2000. Molecular recognition of amino acids by RNA aptamers: the evolution into an L-tyrosine binder of a dopamine-binding RNA motif. RNA. 6**,** 520-7.

Marchand, N., Collins, C. H., 2013. Peptide-based communication system enables *Escherichia coli* to *Bacillus megaterium* interspecies signaling. Biotechnol Bioeng. 110**,** 3003-12.

Marietou, A., Nguyen, A. T., Allen, E. E., Bartlett, D. H., 2014. Adaptive laboratory evolution of *Escherichia coli* K-12 MG1655 for growth at high hydrostatic pressure. Front Microbiol. 5**,** 749.

Merulla, D., Buffi, N., Beggah, S., Truffer, F., Geiser, M., Renaud, P., van der Meer, J. R., 2013. Bioreporters and biosensors for arsenic detection. Biotechnological solutions for a world-wide pollution problem. Curr Opin Biotechnol. 24**,** 534-41.

Michener, J. K., Smolke, C. D., 2012. High-throughput enzyme evolution in *Saccharomyces cerevisiae* using a synthetic RNA switch. Metab Eng. 14**,** 306-16.

Michener, J. K., Thodey, K., Liang, J. C., Smolke, C. D., 2012. Applications of genetically-encoded biosensors for the construction and control of biosynthetic pathways. Metab Eng. 14**,** 212-22.

Mitsuhashi, S., 2014. Current topics in the biotechnological production of essential amino acids, functional amino acids, and dipeptides. Curr Opin Biotechnol. 26**,** 38-44.

Möglich, A., Hegemann, P., 2013. Biotechnology: Programming genomes with light. Nature. 500**,** 406-8.

Mohsin, M., Ahmad, A., 2014. Genetically-encoded nanosensor for quantitative monitoring of methionine in bacterial and yeast cells. Biosens Bioelectron. 59**,** 358-64.

Moussa, R., Baierl, A., Steffen, V., Kubitzki, T., Wiechert, W., Pohl, M., 2014. An evaluation of genetically encoded FRET-based biosensors for quantitative metabolite analyses *in vivo*. J Biotechnol. 191**,** 250-9.

Mukherjee, A., Schroeder, C. M., 2015. Flavin-based fluorescent proteins: emerging paradigms in biological imaging. Curr Opin Biotechnol. 31**,** 16-23.

Müller, S., Harms, H., Bley, T., 2010. Origin and analysis of microbial population heterogeneity in bioprocesses. Curr Opin Biotechnol. 21**,** 100-113.

Mustafi, N., Grünberger, A., Kohlheyer, D., Bott, M., Frunzke, J., 2012. The development and application of a single-cell biosensor for the detection of l-methionine and branched-chain amino acids. Metab Eng. 14**,** 449-57.

Mustafi, N., Grünberger, A., Mahr, R., Helfrich, S., Noh, K., Blombach, B., Kohlheyer, D., Frunzke, J., 2014. Application of a genetically encoded biosensor for live cell imaging of L-valine production in pyruvate dehydrogenase complex-deficient *Corynebacterium glutamicum* strains. PloS ONE. 9**,** e85731.

Muteeb, G., Sen, R., 2010. Random mutagenesis using a mutator strain. In: Braman, J., (Ed.), *In vitro* mutagenesis protocols. Springer Protocols, New York.

Nagai, T., Ibata, K., Park, E. S., Kubota, M., Mikoshiba, K., Miyawaki, A., 2002. A variant of yellow fluorescent protein with fast and efficient maturation for cell-biological applications. Nat Biotechnol. 20**,** 87-90.

Nahvi, A., Sudarsan, N., Ebert, M. S., Zou, X., Brown, K. L., Breaker, R. R., 2002. Genetic control by a metabolite binding mRNA. Chem Biol. 9**,** 1043.

Nakamura, Y., Nishio, Y., Ikeo, K., Gojobori, T., 2003. The genome stability in *Corynebacterium* species due to lack of the recombinational repair system. Gene. 317**,** 149-55.

Neumeyer, A., Hübschmann, T., Müller, S., Frunzke, J., 2013. Monitoring of population dynamics of *Corynebacterium glutamicum* by multiparameter flow cytometry. Microb Biotechnol. 6**,** 157-67.

Newman, J. R., Ghaemmaghami, S., Ihmels, J., Breslow, D. K., Noble, M., DeRisi, J. L., Weissman, J. S., 2006. Single-cell proteomic analysis of *S. cerevisiae* reveals the architecture of biological noise. Nature. 441**,** 840-6.

Ng, C. Y., Khodayari, A., Chowdhury, A., Maranas, C. D., 2015. Advances in *de novo* strain design using integrated systems and synthetic biology tools. Curr Opin Chem Biol. 28**,** 105-14.

Nielsen, J., Larsson, C., van Maris, A., Pronk, J., 2013. Metabolic engineering of yeast for production of fuels and chemicals. Curr Opin Biotechnol. 24**,** 398-404.

Nolden, L., Beckers, G., Mockel, B., Pfefferle, W., Nampoothiri, K. M., Kramera, R., Burkovskia, A., 2000. Urease of *Corynebacterium glutamicum*: organization of corresponding genes and investigation of activity. FEMS Microbiol Lett. 189**,** 305-10.

NPG-Editorial, 2013. Artifacts of light. Nat Methods. 10**,** 1135-1135.

Ohnishi, J., Mizoguchi, H., Takeno, S., Ikeda, M., 2008. Characterization of mutations induced by N-methyl-N'-nitro-N-nitrosoguanidine in an industrial *Corynebacterium glutamicum* strain. Mutat Res. 649**,** 239-44.

Oide, S., Gunji, W., Moteki, Y., Yamamoto, S., Suda, M., Jojima, T., Yukawa, H., Inui, M., 2015. Thermal and solvent stress cross-tolerance conferred to *Corynebacterium glutamicum* by adaptive laboratory evolution. Appl Environ Microbiol. 81**,** 2284-98.

Okada, S., Ota, K., Ito, T., 2009. Circular permutation of ligand-binding module improves dynamic range of genetically encoded FRET-based nanosensor. Protein Sci 18**,** 2518-27.

Okumoto, S., Jones, A., Frommer, W. B., 2012. Quantitative imaging with fluorescent biosensors. Annu Rev Plant Biol. 63**,** 663-706.

Paczia, N., Nilgen, A., Lehmann, T., Gatgens, J., Wiechert, W., Noack, S., 2012. Extensive exometabolome analysis reveals extended overflow metabolism in various microorganisms. Microb Cell Fact. 11**,** 122.

Paige, J. S., Nguyen-Duc, T., Song, W., Jaffrey, S. R., 2012. Fluorescence imaging of cellular metabolites with RNA. Science. 335**,** 1194.

Pandhal, J., Noirel, J., 2014. Synthetic microbial ecosystems for biotechnology. Biotechnol Lett. 36**,** 1141-51.

Parekh, S., Vinci, V. A., Strobel, R. J., 2000. Improvement of microbial strains and fermentation processes. Appl Microbiol Biotechnol. 54**,** 287-301.

Park, J. H., Jang, Y. S., Lee, J. W., Lee, S. Y., 2011. *Escherichia coli* W as a new platform strain for the enhanced production of L-valine by systems metabolic engineering. Biotechnol Bioeng. 108**,** 1140-7.

Park, S. H., Kim, H. U., Kim, T. Y., Park, J. S., Kim, S. S., Lee, S. Y., 2014. Metabolic engineering of *Corynebacterium glutamicum* for L-arginine production. Nat Commun. 5**,** 4618.

Pasteur, L., 1857. Memoire sur la fermentation appelee lactique Comptes rendus des seances de l'Academie des Sciences. 45.

Pauling, J., Rottger, R., Tauch, A., Azevedo, V., Baumbach, J., 2012. CoryneRegNet 6.0--Updated database content, new analysis methods and novel features focusing on community demands. Nucleic Acids Res. 40**,** D610-4.

Pavlov, Y. I., Noskov, V. N., Lange, E. K., Moiseeva, E. V., Pshenichnov, M. R., Khromov-Borisov, N. N., 1991. The genetic activity of N6-hydroxyadenine and 2-amino-N6-hydroxyadenine in *Escherichia coli*, *Salmonella typhimurium* and *Saccharomyces cerevisiae*. Mutat Res. 253**,** 33-46.

Petzold, C. J., Chan, L. J., Nhan, M., Adams, P. D., 2015. Analytics for metabolic engineering. Front Bioeng Biotechnol. 3**,** 135.

Pittard, J., Camakaris, H., Yang, J., 2005. The TyrR regulon. Mol Microbiol. 55**,** 16-26.

Polen, T., Krämer, M., Bongaerts, J., Wubbolts, M., Wendisch, V. F., 2005. The global gene expression response of *Escherichia coli* to L-phenylalanine. J Biotechnol. 115**,** 221-37.

Portnoy, V. A., Bezdan, D., Zengler, K., 2011. Adaptive laboratory evolution--harnessing the power of biology for metabolic engineering. Curr Opin Biotechnol. 22**,** 590-4.

Potzkei, J., Kunze, M., Drepper, T., Gensch, T., Jaeger, K. E., Buchs, J., 2012. Real-time determination of intracellular oxygen in bacteria using a genetically encoded FRET-based biosensor. BMC Biol 10**,** 28.

Radmacher, E., Vaitsikova, A., Burger, U., Krumbach, K., Sahm, H., Eggeling, L., 2002. Linking central metabolism with increased pathway flux: L-valine accumulation by *Corynebacterium* glutamicum. Appl Environ Microbiol. 68**,** 2246-50.

Raman, S., Rogers, J. K., Taylor, N. D., Church, G. M., 2014. Evolution-guided optimization of biosynthetic pathways. Proc Natl Acad Sci U S A. 111**,** 17803-8.

Resende, B. C., Rebelato, A. B., D'Afonseca, V., Santos, A. R., Stutzman, T., Azevedo, V. A., Santos, L. L., Miyoshi, A., Lopes, D. O., 2011. DNA repair in *Corynebacterium* model. Gene. 482**,** 1-7.

Reyes, L. H., Gomez, J. M., Kao, K. C., 2014. Improving carotenoids production in yeast via adaptive laboratory evolution. Metab Eng. 21**,** 26-33.

Richardson, K. K., Crosby, R. M., Skopek, T. R., 1988. Mutation spectra of N-ethyl-N'-nitro-N-nitrosoguanidine and 1-(2-hydroxyethyl)-1-nitrosourea in *Escherichia coli*. Mol Gen Genet MGG. 214**,** 460-6.

Ronda, C., Maury, J., Jakociunas, T., Jacobsen, S. A., Germann, S. M., Harrison, S. J., Borodina, I., Keasling, J. D., Jensen, M. K., Nielsen, A. T., 2015. CrEdit: CRISPR mediated multi-loci gene integration in *Saccharomyces cerevisiae*. Microb Cell Fact. 14**,** 97.

Rubakhin, S. S., Lanni, E. J., Sweedler, J. V., 2013. Progress toward single cell metabolomics. Curr Opin Biotechnol. 24**,** 95-104.

Rüffer, N., Heidersdorf, U., Kretzers, I., Sprenger, G. A., Raeven, L., Takors, R., 2004. Fully integrated L-phenylalanine separation and concentration using reactive-extraction with liquid-liquid centrifuges in a fed-batch process with *E. coli*. Bioprocess Biosyst Eng. 26**,** 239-48.

Sanchez, A., Choubey, S., Kondev, J., 2013. Regulation of noise in gene expression. Annu Rev Biophys. 42**,** 469-91.

Sandberg, T. E., Pedersen, M., LaCroix, R. A., Ebrahim, A., Bonde, M., Herrgard, M. J., Palsson, B. O., Sommer, M., Feist, A. M., 2014. Evolution of *Escherichia coli* to 42 degrees C and subsequent genetic engineering reveals adaptive mechanisms and novel mutations. Mol Biol Evol. 31**,** 2647-62.

Santos, C. N., Stephanopoulos, G., 2008. Melanin-based high-throughput screen for L-tyrosine production in *Escherichia coli*. Appl Environ Microbiol. 74**,** 1190-7.

Sariaslani, F. S., 2007. Development of a combined biological and chemical process for production of industrial aromatics from renewable resources. Annu Rev Microbiol. 61**,** 51-69.

Sarsero, J. P., Pittard, A. J., 1991. Molecular analysis of the TyrR protein-mediated activation of *mtr* gene expression in *Escherichia coli* K-12. J Bacteriol. 173**,** 7701-4.

Schallmey, M., Frunzke, J., Eggeling, L., Marienhagen, J., 2014. Looking for the pick of the bunch: high-throughput screening of producing microorganisms with biosensors. Curr Opin Biotechnol. 26**,** 148-54.

Schendzielorz, G., Dippong, M., Grunberger, A., Kohlheyer, D., Yoshida, A., Binder, S., Nishiyama, C., Nishiyama, M., Bott, M., Eggeling, L., 2014. Taking control over control: use of product sensing in single cells to remove flux control at key enzymes in biosynthesis pathways. ACS Synth Biol. 3**,** 21-9.

Schlüter, J. P., Czuppon, P., Schauer, O., Pfaffelhuber, P., McIntosh, M., Becker, A., 2015. Classification of phenotypic subpopulations in isogenic bacterial cultures by triple promoter probing at single cell level. J Biotechnol. 198**,** 3-14.

Schmidt-Dannert, C., Arnold, F. H., 1999. Directed evolution of industrial enzymes. Trends Biotechnol. 17**,** 135-6.

Schreiner, M. E., Fiur, D., Holatko, J., Patek, M., Eikmanns, B. J., 2005. E1 enzyme of the pyruvate dehydrogenase complex in *Corynebacterium glutamicum*: molecular analysis of the gene and phylogenetic aspects. J Bacteriol. 187**,** 6005-18.

Serganov, A., Nudler, E., 2013. A decade of riboswitches. Cell. 152**,** 17-24.

Shaner, N. C., Steinbach, P. A., Tsien, R. Y., 2005. A guide to choosing fluorescent proteins. Nat Methods. 2**,** 905-9.

Siedler, S., Schendzielorz, G., Binder, S., Eggeling, L., Bringer, S., Bott, M., 2014a. SoxR as a single-cell biosensor for NADPH-consuming enzymes in Escherichia coli. ACS Synth Biol. 3**,** 41-7.

Siedler, S., Stahlhut, S. G., Malla, S., Maury, J., Neves, A. R., 2014b. Novel biosensors based on flavonoid-responsive transcriptional regulators introduced into *Escherichia coli*. Metab Eng. 21**,** 2-8.

Silander, O. K., Nikolic, N., Zaslaver, A., Bren, A., Kikoin, I., Alon, U., Ackermann, M., 2012. A genome-wide analysis of promoter-mediated phenotypic noise in *Escherichia coli*. PLoS Genet. 8**,** e1002443.

Silva-Rocha, R., de Lorenzo, V., 2012. Broadening the signal specificity of prokaryotic promoters by modifying cis-regulatory elements associated with a single transcription factor. Mol BioSyst. 8**,** 1950-7.

Soma, Y., Tsuruno, K., Wada, M., Yokota, A., Hanai, T., 2014. Metabolic flux redirection from a central metabolic pathway toward a synthetic pathway using a metabolic toggle switch. Metab Eng. 23**,** 175-84.

Song, X., Wang, Y., Shu, Z., Hong, J., Li, T., Yao, L., 2013. Engineering a more thermostable blue light photo receptor *Bacillus subtilis* YtvA LOV domain by a computer aided rational design method. PLoS Comput Biol. 9**,** e1003129.

Sorensen, H. P., Mortensen, K. K., 2005. Advanced genetic strategies for recombinant protein expression in *Escherichia coli*. J Biotechnol. 115**,** 113-28.

Sprenger, G. A. (Ed.) 2006. Aromatic Amino Acids. Springer-Verlag, Berlin Heidelberg.

Sprenger, G. A., 2007. From scratch to value: engineering *Escherichia coli* wild type cells to the production of L-phenylalanine and other fine chemicals derived from chorismate. Appl Microbiol Biotechnol. 75**,** 739-49.

Stanton, B. C., Siciliano, V., Ghodasara, A., Wroblewska, L., Clancy, K., Trefzer, A. C., Chesnut, J. D., Weiss, R., Voigt, C. A., 2014. Systematic transfer of prokaryotic sensors and circuits to mammalian cells. ACS Synth Biol. 3**,** 880-91.

Stevens, N., Dyer, J., Marti, A. A., Solomon, M., Turro, N. J., 2007. FRETView: a computer program to simplify the process of obtaining fluorescence resonance energy transfer parameters. Photochem Photobiol Sci. 6**,** 909-11.

Tabor, J. J., Groban, E. S., Voigt, C. A., 2009. Performance characteristics for sensor and circuits used to program *E. coli*. In: Lee, S. Y., (Ed.), Systems Biology and Biotechnology of *Escherichia coli* Springer Science + Business Media B.V.

Tang, S. Y., Cirino, P. C., 2011. Design and application of a mevalonate-responsive regulatory protein. Angew Chem Int Ed. 50**,** 1084-6.

Tang, S. Y., Fazelinia, H., Cirino, P. C., 2008. AraC regulatory protein mutants with altered effector specificity. J Am Chem Soc. 130**,** 5267-71.

Tang, S. Y., Qian, S., Akinterinwa, O., Frei, C. S., Gredell, J. A., Cirino, P. C., 2013. Screening for enhanced triacetic acid lactone production by recombinant *Escherichia coli* expressing a designed triacetic acid lactone reporter. J Am Chem Soc. 135**,** 10099-103.

Tenaillon, O., Rodriguez-Verdugo, A., Gaut, R. L., McDonald, P., Bennett, A. F., Long, A. D., Gaut, B. S., 2012. The molecular diversity of adaptive convergence. Science. 335**,** 457-61.

Teo, W. S., Chang, M. W., 2014. Development and characterization of AND-gate dynamic controllers with a modular synthetic GAL1 core promoter in *Saccharomyces cerevisiae*. Biotechnol Bioeng. 111**,** 144-51.

Tosaka, O., Takanami, K., 1986. Biotechnology of amino acid production. Elsevier Science Ltd, Amsterdam, Oxford, New York, Tokyo.

Triccas, J. A., Pinto, R., Britton, W. J., 2002. Destabilized green fluorescent protein for monitoring transient changes in mycobacterial gene expression. Res Microbiol. 153**,** 379-83.

Tsuruno, K., Honjo, H., Hanai, T., 2015. Enhancement of 3-hydroxypropionic acid production from glycerol by using a metabolic toggle switch. Microb Cell Fact 14**,** 155.

Uchiyama, T., Miyazaki, K., 2010a. Product-induced gene expression, a product-responsive reporter assay used to screen metagenomic libraries for enzyme-encoding genes. Appl Environ Microbiol. 76**,** 7029-35.

Uchiyama, T., Miyazaki, K., 2010b. Substrate-induced gene expression screening: a method for high-throughput screening of metagenome libraries. Methods Mol Biol. 668**,** 153-68.

Uchiyama, T., Watanabe, K., 2008. Substrate-induced gene expression (SIGEX) screening of metagenome libraries. Nat Protoc. 3**,** 1202-12.

Ukibe, K., Katsuragi, T., Tani, Y., Takagi, H., 2008. Efficient screening for astaxanthin-overproducing mutants of the yeast *Xanthophyllomyces dendrorhous* by flow cytometry. FEMS Microbiol Lett. 286**,** 241-8.

Umeyama, T., Okada, S., Ito, T., 2013. Synthetic gene circuit-mediated monitoring of endogenous metabolites: identification of GAL11 as a novel multicopy enhancer of s-adenosylmethionine level in yeast. ACS Synth Biol. 2**,** 425-30.

van der Meer, J. R., Belkin, S., 2010. Where microbiology meets microengineering: design and applications of reporter bacteria. Nat Rev Microbiol. 8**,** 511-22.

van Sint Fiet, S., van Beilen, J. B., Witholt, B., 2006. Selection of biocatalysts for chemical synthesis. Proc Natl Acad Sci U S A. 103**,** 1693-8.

van Summeren-Wesenhagen, P. V., Marienhagen, J., 2015. Metabolic engineering of *Escherichia coli* for the synthesis of the plant polyphenol pinosylvin. Appl Environ Microbiol. 81**,** 840-9.

Vargas-Tah, A., Martinez, L. M., Hernandez-Chavez, G., Rocha, M., Martinez, A., Bolivar, F., Gosset, G., 2015. Production of cinnamic and p-hydroxycinnamic acid from sugar mixtures with engineered *Escherichia coli*. Microb Cell Fact. 14**,** 6.

Vasdekis, A. E., Stephanopoulos, G., 2015. Review of methods to probe single cell metabolism and bioenergetics. Metab Eng. 27**,** 115-35.

Vogt, M., Haas, S., Klaffl, S., Polen, T., Eggeling, L., van Ooyen, J., Bott, M., 2014. Pushing product formation to its limit: metabolic engineering of *Corynebacterium glutamicum* for L-leucine overproduction. Metab Eng. 22**,** 40-52.

Voigt, C. A., 2006. Genetic parts to program bacteria. Curr Opin Biotechnol. 17**,** 548-57.

Walter, J., Hausmann, S., Drepper, T., Puls, M., Eggert, T., Dihne, M., 2012. Flavin mononucleotide-based fluorescent proteins function in mammalian cells without oxygen requirement. PloS ONE. 7**,** e43921.

Wang, H. H., Isaacs, F. J., Carr, P. A., Sun, Z. Z., Xu, G., Forest, C. R., Church, G. M., 2009. Programming cells by multiplex genome engineering and accelerated evolution. Nature. 460**,** 894-8.

Waters, J. C., 2013. Live-cell fluorescence imaging. Methods Cell Biol. 114**,** 125-50.

Way, J. C., Collins, J. J., Keasling, J. D., Silver, P. A., 2014. Integrating biological redesign: where synthetic biology came from and where it needs to go. Cell. 157**,** 151-61.

Weiner, M., Albermann, C., Gottlieb, K., Sprenger, G. A., Weuster-Botz, D., 2014a. Fed-batch production of L-phenylalanine from glycerol and ammonia with recombinant *Escherichia coli*. Biochem Eng J. 83**,** 62-69.

Weiner, M., Tröndle, J., Albermann, C., Sprenger, G. A., Weuster-Botz, D., 2014b. Improvement of constraint-based flux estimation during L-phenylalanine production with *Escherichia coli* using targeted knock-out mutants. Biotechnol Bioeng. 111**,** 1406-16.

Wendisch, V. F., 2014. Microbial production of amino acids and derived chemicals: synthetic biology approaches to strain development. Curr Opin Biotechnol. 30**,** 51-8.

Wendisch, V. F., Bott, M., Eikmanns, B. J., 2006. Metabolic engineering of *Escherichia coli* and *Corynebacterium glutamicum* for biotechnological production of organic acids and amino acids. Curr Opin Microbiol. 9**,** 268-74.

Wiechert, W., Noack, S., 2011. Mechanistic pathway modeling for industrial biotechnology: challenging but worthwhile. Curr Opin Biotechnol. 22**,** 604-10.

Wieschalka, S., Blombach, B., Bott, M., Eikmanns, B. J., 2013. Bio-based production of organic acids with *Corynebacterium glutamicum*. Microb Biotechnol. 6**,** 87-102.

Wilson, D., Charoensawan, V., Kummerfeld, S. K., Teichmann, S. A., 2008. DBD--taxonomically broad transcription factor predictions: new content and functionality. Nucleic Acids Res. 36**,** D88-92.

Win, M. N., Smolke, C. D., 2007. A modular and extensible RNA-based gene-regulatory platform for engineering cellular function. Proc Natl Acad Sci U S A. 104**,** 14283-8.

Wingen, M., Potzkei, J., Endres, S., Casini, G., Rupprecht, C., Fahlke, C., Krauss, U., Jaeger, K. E., Drepper, T., Gensch, T., 2014. The photophysics of LOV-based fluorescent proteins--new tools for cell biology. Photochem Photobiol Sci. 13**,** 875-83.

Winkler, W., Nahvi, A., Breaker, R. R., 2002a. Thiamine derivatives bind messenger RNAs directly to regulate bacterial gene expression. Nature. 419**,** 952-6.

Winkler, W. C., Cohen-Chalamish, S., Breaker, R. R., 2002b. An mRNA structure that controls gene expression by binding FMN. Proc Natl Acad Sci U S A. 99**,** 15908-13.

Wise, A. A., Kuske, C. R., 2000. Generation of novel bacterial regulatory proteins that detect priority pollutant phenols. Appl Environ Microbiol. 66**,** 163-9.

Woo, H. M., Park, J. B., 2014. Recent progress in development of synthetic biology platforms and metabolic engineering of *Corynebacterium glutamicum*. J Biotechnol. 180**,** 43-51.

Woolston, B. M., Edgar, S., Stephanopoulos, G., 2013. Metabolic engineering: past and future. Annu Rev Chem Biomol Eng. 4**,** 259-88.

Xie, W., Lv, X., Ye, L., Zhou, P., Yu, H., 2015. Construction of lycopene-overproducing *Saccharomyces cerevisiae* by combining directed evolution and metabolic engineering. Metab Eng. 30**,** 69-78.

Xu, P., Wang, W., Li, L., Bhan, N., Zhang, F., Koffas, M. A., 2014. Design and kinetic analysis of a hybrid promoter-regulator system for malonyl-CoA sensing in *Escherichia coli*. ACS Chem Biol. 9**,** 451-8.

Yang, J., Seo, S. W., Jang, S., Shin, S. I., Lim, C. H., Roh, T. Y., Jung, G. Y., 2013. Synthetic RNA devices to expedite the evolution of metabolite-producing microbes. Nat Commun. 4**,** 1413.

Yano, T., Oku, M., Akeyama, N., Itoyama, A., Yurimoto, H., Kuge, S., Fujiki, Y., Sakai, Y., 2010. A novel fluorescent sensor protein for visualization of redox states in the cytoplasm and in peroxisomes. Mol Cell Biol. 30**,** 3758-66.

You, M., Litke, J. L., Jaffrey, S. R., 2015. Imaging metabolite dynamics in living cells using a Spinach-based riboswitch. Proc Natl Acad Sci U S A. 112**,** E2756-65.

Young, R., Bremer, H., 1976. Polypeptide-chain-elongation rate in *Escherichia coli* B/r as a function of growth rate. Biochem J. 160**,** 185-94.

Zaslaver, A., Bren, A., Ronen, M., Itzkovitz, S., Kikoin, I., Shavit, S., Liebermeister, W., Surette, M. G., Alon, U., 2006. A comprehensive library of fluorescent transcriptional reporters for *Escherichia coli*. Nat Methods. 3**,** 623-8.

Zhang, C., Kang, Z., Zhang, J., Du, G., Chen, J., Yu, X., 2014a. Construction and application of novel feedback-resistant 3-deoxy-d-arabino-heptulosonate-7-phosphate synthases by engineering the N-terminal domain for L-phenylalanine synthesis. FEMS Microbiol Lett. 353**,** 11-8.

Zhang, C., Zhang, J., Kang, Z., Du, G., Chen, J., 2015a. Rational engineering of multiple module pathways for the production of L-phenylalanine in *Corynebacterium glutamicum*. J Ind Microbiol Biotechnol. 42**,** 787-97.

Zhang, C., Zhang, J., Kang, Z., Du, G., Yu, X., Wang, T., Chen, J., 2013. Enhanced production of L-phenylalanine in *Corynebacterium glutamicum* due to the introduction of *Escherichia coli* wild-type gene *aroH*. J Ind Microbiol Biotechnol. 40**,** 643-51.

Zhang, F., Carothers, J. M., Keasling, J. D., 2012. Design of a dynamic sensor-regulator system for production of chemicals and fuels derived from fatty acids. Nat Biotechnol. 30**,** 354-9.

Zhang, J., Jensen, M. K., Keasling, J. D., 2015b. Development of biosensors and their application in metabolic engineering. Curr Opin Chem Biol. 28**,** 1-8.

Zhang, X., Zhang, C., Zhou, Q. Q., Zhang, X. F., Wang, L. Y., Chang, H. B., Li, H. P., Oda, Y., Xing, X. H., 2015c. Quantitative evaluation of DNA damage and mutation rate by atmospheric and room-temperature plasma (ARTP) and conventional mutagenesis. Appl Microbiol Biotechnol. 99**,** 5639-46.

Zhang, X., Zhang, X. F., Li, H. P., Wang, L. Y., Zhang, C., Xing, X. H., Bao, C. Y., 2014b. Atmospheric and room temperature plasma (ARTP) as a new powerful mutagenesis tool. Appl Microbiol Biotechnol. 98**,** 5387-96.

Zhou, L. B., Zeng, A. P., 2015. Engineering a lysine-ON riboswitch for metabolic control of lysine production in *Corynebacterium glutamicum*. ACS Synth Biol. 4**,** 1335-40.

6 APPENDIX

6.1 Supplemental information – Application of a genetically encoded biosensor for live cell imaging of L-valine production in pyruvate dehydrogenase complex-deficient *Corynebacterium glutamicum* strains

Nurije Mustafi[1•], Alexander Grünberger[1•], Regina Mahr[1], Stefan Helfrich[1], Katharina Nöh[1], Bastian Blombach[2], Dietrich Kohlheyer[1], Julia Frunzke[1*]

[1]IBG-1: Biotechnology, Forschungszentrum Jülich, Jülich, Germany

[2]Institute of Biochemical Engineering, University of Stuttgart, Stuttgart, Germany

[•]These authors contributed equally to this work.

*Corresponding author

Supporting Figures

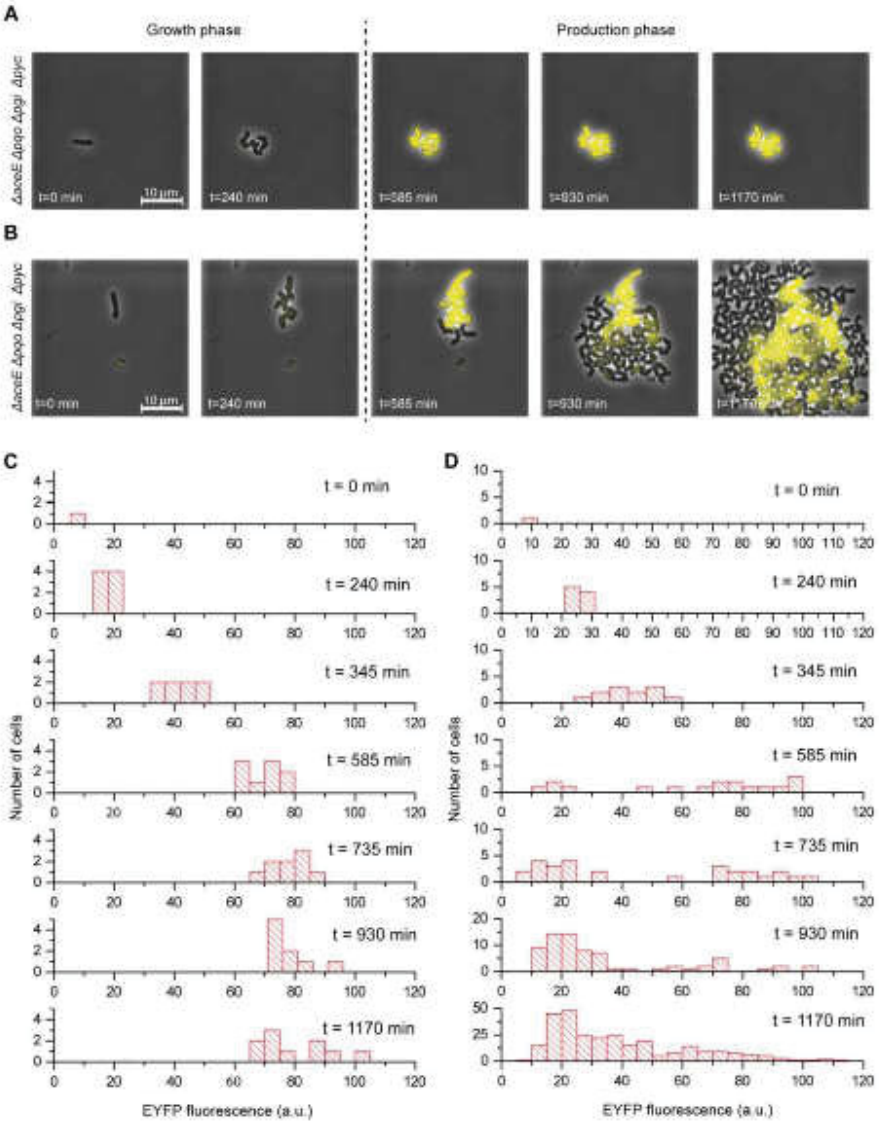

Figure S1. Phenotypic heterogeneity of the *ΔaceE Δpqo Δpgi Δpyc* sensor strain upon switch from growth to production phase. **(A)** Microcolony showing transition to producing cells or **(B)** a mixture of growing and producing cells after medium switch (initiated after 240 min). In approximately 50% of the recorded colonies one or several single cells continued growth after medium switch. **(C, D)** Fluorescence histograms depicting single cell fluorescence to selected times during growth (0-240 min) and production phase (0-1200 min) of the microcolonies shown in A **(C)** and B **(D)**. Cultivation was performed in CGXII minimal medium containing 154 mM acetate, 222 mM glucose and 0.5% BHI during growth phase or 222 mM glucose and 0.5% BHI during production phase, respectively.

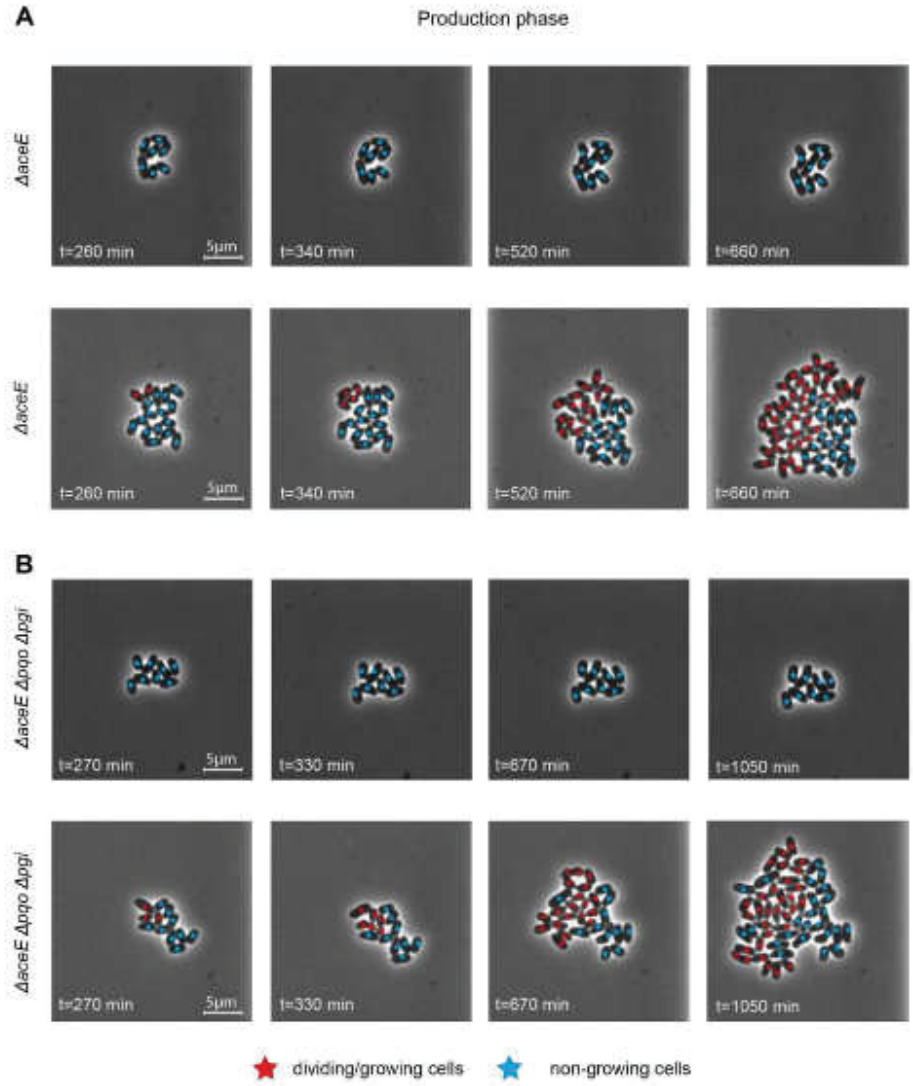

Figure S2. Phenotypic heterogeneity of *ΔaceE* and *ΔaceE Δpqo Δpgi* upon switch from growth to production phase. (A) *ΔaceE* microcolonies where all cells stopped growth (blue stars) upon transition to the production phase (upper row) or a mixture of growing (red stars) and non-growing cells (lower row) after initiation of the production phase. In approximately 50% of the recorded colonies one or several single cells continued growth after medium switch (initiated after 250 min). **(C)** *ΔaceE Δpqo Δpgi* microcolonies. In the upper row, all cells stopped growth whereas in the lower row a microcolony is shown were some cells continued growth after initiation of the production phase. In approximately 50% of the recorded colonies one or several single cells continued growth after medium switch (initiated after 250 min). These findings confirm that the phenotypic split shown in Figure 5 is not due to the presence of the Lrp-sensor. Cultivation was performed in CGXII minimal medium containing 154 mM acetate, 222 mM glucose and 0.5% BHI during growth phase or 222 mM glucose and 0.5% BHI during production phase, respectively.

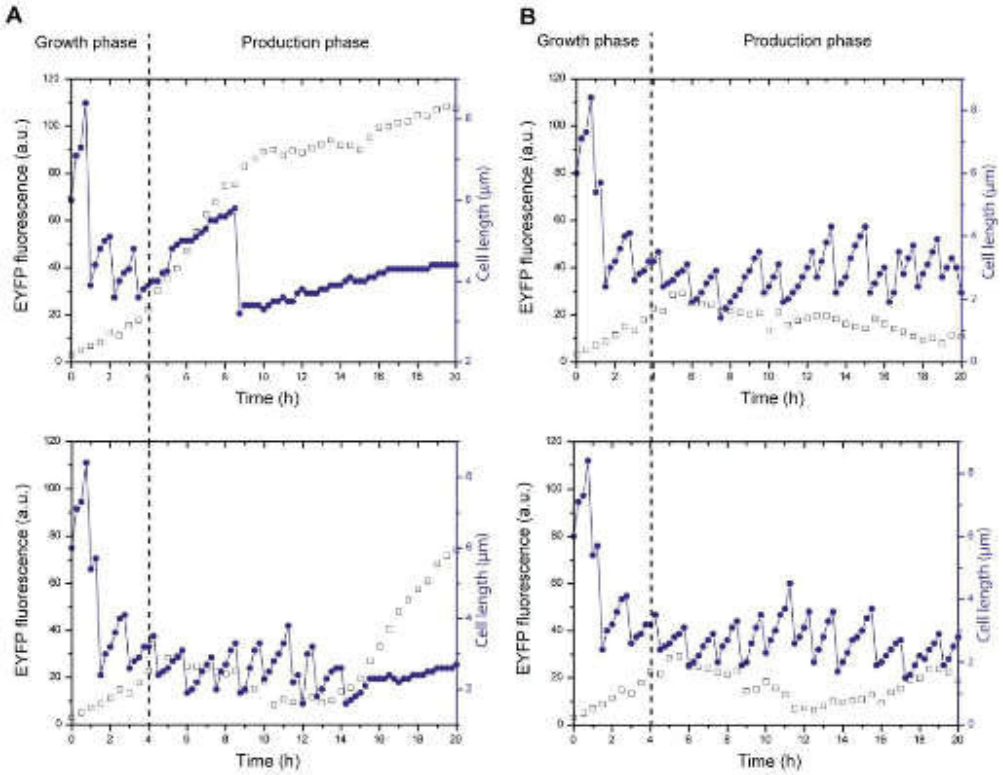

Figure S3. Single cell traces of the *ΔaceE Δpqo Δpgi Δpyc* sensor strain upon switch from growth to production phase. **(A)** Single cell traces showing the switch from growth (cell length=blue line) to production (fluorescence=squares) after several cell divisions during production phase (t=8.5 h, t=15.0 h). **(B)** Single cell traces showing no switch from growth to production. Single cell traces are taken from the cultivation of *ΔaceE Δpqo Δpgi Δpyc* sensor strain shown in Figure S1.

6.2 Supplemental information – Biosensor-driven adaptive laboratory evolution of L-valine production in *Corynebacterium glutamicum*

Regina Mahr[1], Cornelia Gätgens[1], Jochem Gätgens[1], Tino Polen[1], Jörn Kalinowski[2] and Julia Frunzke[1]*

Supporting Tables

Table S1 Comparative transcriptome analysis of mRNA levels of populations after the third versus after the second evolution step. Listed are all genes showing a ≥2-fold altered mRNA level. The relative mRNA level is given as average ratio ($3^{rd}/2^{nd}$) calculated from three independent biological replicates. Known transcriptional regulation of genes by transcriptional regulators is indicated by R (repression) and A (activation) (Pauling et al., 2012).

Locus	Gene	Annotation	R/A	Ratio $3^{rd}/2^{nd}$	*p* value
		GlxR regulon			
cg0344	*fabG1*	3-oxoacyl-acyl-carrier protein reductase	R^{GlxR}	2.937	0.043
cg0345	-	putative metal-dependent hydrolase of the TIM-barrel fold	R^{GlxR}	2.488	0.002
cg0346	*fadE*	glutaryl-CoA dehydrogenase	R^{GlxR}	2.415	0.045
cg0445	*sdhCD*	succinate:menaquinone oxidoreductase, cytochrome *b* subunit	R^{GlxR} R^{RamB} R^{RipA} A^{DtxR} A^{RamA}	0.459	0.036
cg0791	*pyc*	pyruvate carboxylase	R^{GlxR} R^{RamB}	0.405	0.049
cg0797	*prpB1*	2-methylisocitrate lyase	R^{GlxR}	0.355	0.011
cg0812	*dtsR1*	acetyl/propionyl-CoA carboxylase, beta subunit	R^{GlxR} R^{FasR}	0.308	0.006
cg0936	*rpf1*	resuscitation promoting factor	A^{GlxR}	0.267	0.011
cg0957	*fas-IB*	fatty acid synthase, Fas-I type	R^{GlxR} R^{FasR}	0.401	0.024
cg1037	*rpf2*	resuscitation promoting factor, secreted protein	A^{GlxR} A^{RamA} R^{RamB} R^{MtrA}	0.347	0.035
cg1314	*putP*	proline transport system	R^{GlxR} A^{LexA}	0.413	<0.001
cg1341	*narI*	nitrate reductase, gamma subunit	A^{GlxR} A^{RosR}	0.223	0.033

Locus	Gene	Annotation	R/A	Ratio $3^{rd}/2^{nd}$	*p* value
			R^{RipA} R^{ArnR}		
cg1342	*narJ*	nitrate reductase, delta subunit, assembly factor	A^{GlxR} A^{RosR} R^{RipA} R^{ArnR}	0.206	0.039
cg1343	*narH*	nitrate reductase, beta subunit, iron sulfur protein	A^{GlxR} A^{RosR} R^{RipA} R^{ArnR}	0.315	0.010
cg1344	*narG*	nitrate reductase, alpha subunit	A^{GlxR} A^{RosR} R^{RipA} R^{ArnR}	0.271	0.032
cg2119	*pfkB*	1-phosphofructokinase	R^{GlxR} R^{SugR} R^{FruR} R^{LldR}	0.471	<0.001
cg2403	*qcrB*	cytochrome bc_1 complex, cytochrome *b* subunit	A^{GlxR} A^{HrrA}	0.416	<0.001
cg2404	*qcrA*	cytochrome bc_1 complex, Rieske iron-sulfur protein	A^{GlxR} A^{HrrA}	0.385	<0.001
cg2406	*ctaE*	cytochrome aa_3 oxidase, subunit 3	A^{GlxR} A^{HrrA} R^{RamB}	0.467	<0.001
cg2559	*aceB*	malate synthase, part of glyoxylate shunt	R^{GlxR} R^{RamB} A^{RamA} A^{CspA2}	0.373	0.047
cg2840	*actA*	coenzyme A transferase acetate, propionate, succinate	A^{GlxR} R^{RamB}	0.427	0.009
		ArgR regulon			
cg1580	*argC*	N-acetyl-gamma-glutamyl-phosphate reductase	R^{ArgR} R^{FarR}	0.144	0.007
cg1582	*argB*	acetylglutamate kinase	R^{ArgR} R^{FarR}	0.345	0.003
cg1583	*argD*	acetylornithine aminotransferase	R^{ArgR} R^{FarR}	0.291	0.011
cg1584	*argF*	ornithine carbamoyltransferase	R^{ArgR} R^{FarR}	0.347	<0.001
cg1585	*argR*	transcriptional repressor of arginine biosynthesis, ArgR-family	R^{ArgR} R^{FarR}	0.410	0.001
cg1588	*argH*	argininosuccinate lyase	R^{ArgR}	0.453	<0.001
cg1814	*carA*	carbamoyl-phosphate synthase, small subunit	R^{ArgR}	0.383	0.005

Locus	Gene	Annotation	R/A	Ratio $3^{rd}/2^{nd}$	*p* value
		ArsR regulon			
cg1705	*arsB1*	arsenite permease, arsenical resistance-3 ACR3 family	R^{ArsR1} R^{ArsR2}	2.980	0.044
cg1706	*arsC1*	arsenate reductase, arsenical pump modifier	R^{ArsR1} R^{ArsR2}	2.555	0.018
		SufR regulon			
cg1760	*sufU*	cysteine desulfhydrase	R^{SufR} R^{OxyR} A^{SigM} A^{SigH}	3.175	0.032
cg1762	*sufC*	Fe-S cluster assembly ATPase	R^{SufR} R^{OxyR} A^{SigM} A^{SigH}	4.121	0.020
cg1763	*sufD*	Fe-S cluster assembly membrane protein	R^{SufR} R^{OxyR} A^{SigM} A^{SigH}	4.910	0.013
cg1764	*sufB*	Fe-S cluster assembly protein	R^{SufR} R^{OxyR} A^{SigM} A^{SigH}	5.956	0.016
cg1765	*sufR*	transcriptional regulator of *suf* operon	R^{SufR} R^{OxyR} A^{SigM} A^{SigH}	7.239	0.011
		Further interesting targets			
cg3149 *	*alaT*	aminotransferase, uses alanine, glutamate, 2-aminobutyrate and aspartate		0.660	0.089
cg2877 *	*avtA*	aminotransferase, uses alanine, keto-isovalerate and ketobutyrate		0.801	0.059
		SOS and stress response			
cg0831	*tusG*	trehalose uptake system, ABC-type, permease		0.379	0.005
cg0834	*tusE*	trehalose uptake system, ABC-type, bacterial extracellular solute-binding protein	A^{LexA}	0.353	0.024
cg0892	-	hypothetical protein		0.408	0.045
cg1362	*atpB*	F_1F_O-ATP synthase, α-subunit of F_O part	A^{SigH}	0.311	0.001
cg1364	*atpF*	F_1F_O-ATP synthase, β-subunit of F_O part	A^{SigH}	0.320	0.008
cg1553	*qor2*	quinone oxidoreductase	R^{QorR} R^{HrcA}	2.959	0.031

Locus	Gene	Annotation	R/A	Ratio $3^{rd}/2^{nd}$	*p* value
cg2106	-	hypothetical protein, conserved	A^{SigH}	2.846	0.042
cg3011	*groEL*	chaperonin GroEL	A^{SigH} R^{HrcA} R^{HspR}	2.538	0.004
cg3327	*dps*	starvation-induced DNA protecting protein	A^{DtxR} R^{OxyR}	2.220	<0.001
cg3330	-	putative secreted protein	A^{SigB}	3.147	0.012
		Others			
cg0061	*rodA*	putative FTSW/RODA/SPOVE family cell cycle protein		0.442	0.030
cg0177	-	hypothetical protein		0.443	0.021
cg0233		hypothetical protein, conserved		0.390	0.007
cg0238	-	putative L-gulonolactone oxidase, FAD/FMN-containing dehydrogenase		0.426	<0.001
cg0258	*moaE*	molybdopterin cofactor synthase, large subunit 2		0.476	0.013
cg0435	*udgA1*	UDP-glucose 6-dehydrogenase		0.445	<0.001
cg0593	*rpsJ*	30S ribosomal protein S10		2.373	0.009
cg0699	*guaB2*	inositol-5-monophosphate dehydrogenase	A^{SigH}	0.417	0.009
cg1076	*glmU*	putative UDP-N-acetylglucosamine pyrophosphorylase		0.447	0.019
cg1138	-	putative phosphinothricin acetyltransferase		0.417	0.005
cg1203	-	putative Mg^{2+} chelatase subunit ChlI		0.412	<0.001
cg1333	*argS*	arginyl-tRNA synthetase		0.425	0.001
cg1479	*malP*	maltodextrin phosphorylase		0.298	0.005
cg1730	-	putative secreted protease subunit, stomatin/prohibitin homolog		0.403	0.020
cg1793	-	hypothetical protein, conserved		0.412	0.008
cg1832		putative ABC-type iron-siderophore transporter, substrate-binding lipoprotein	R^{Cg1831}	0.425	0.050
cg1842	-	putative secreted metalloprotease		0.427	0.034
cg1905	-	hypothetical protein CGP3 region		0.314	0.018
cg2160	-	putative hydrolase of metallo-beta-lactamase superfamily		0.468	<0.001
cg2523	*malQ*	4-alpha-glucanotransferase		0.403	<0.001
cg2704	-	putative ABC-type putative sugar transporter, permease subunit		0.376	<0.001
cg2857	*purF*	amidophosphoribosyltransferase		0.395	0.001
cg3117	*cysX*	ferredoxin-like protein	A^{CysR} R^{DtxR} R^{McbR}	0.462	0.002
cg3179	*fadD2*	acyl-CoA synthase		0.459	0.002
cg3303	-	putative transcriptional regulator, PadR-like		2.336	0.003

Supporting Figures

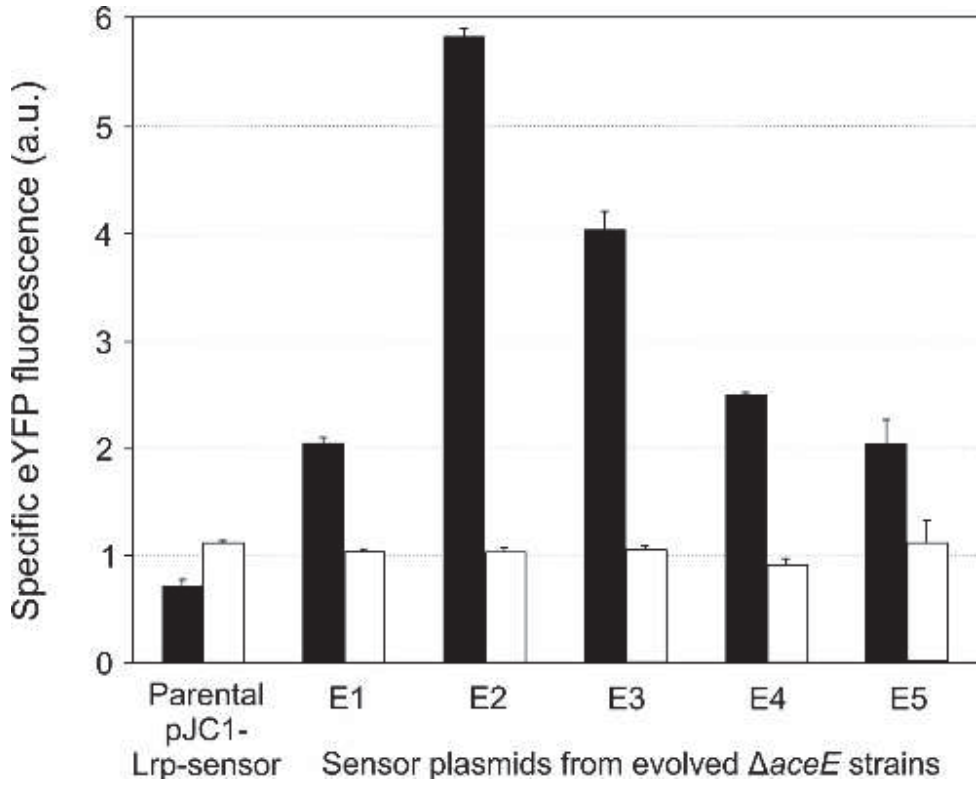

Fig. S1 The increased fluorescent output of evolved *C. glutamicum* Δ*aceE* strains does not derive from mutations within the sensor plasmids. Sensor plasmids (E1-E5) were isolated from evolved *C. glutamicum* Δ*aceE* strains (black) and were reintroduced into the non-evolved parental strain *C. glutamicum* Δ*aceE* (white). The specific eYFP fluorescent output of evolved strains and the non-evolved Δ*aceE* strains (containing the sensor of evolved strains) was recorded after 30 hours of cultivation in microtiter plates. The data represent average values from three independent cultivations including standard deviation.

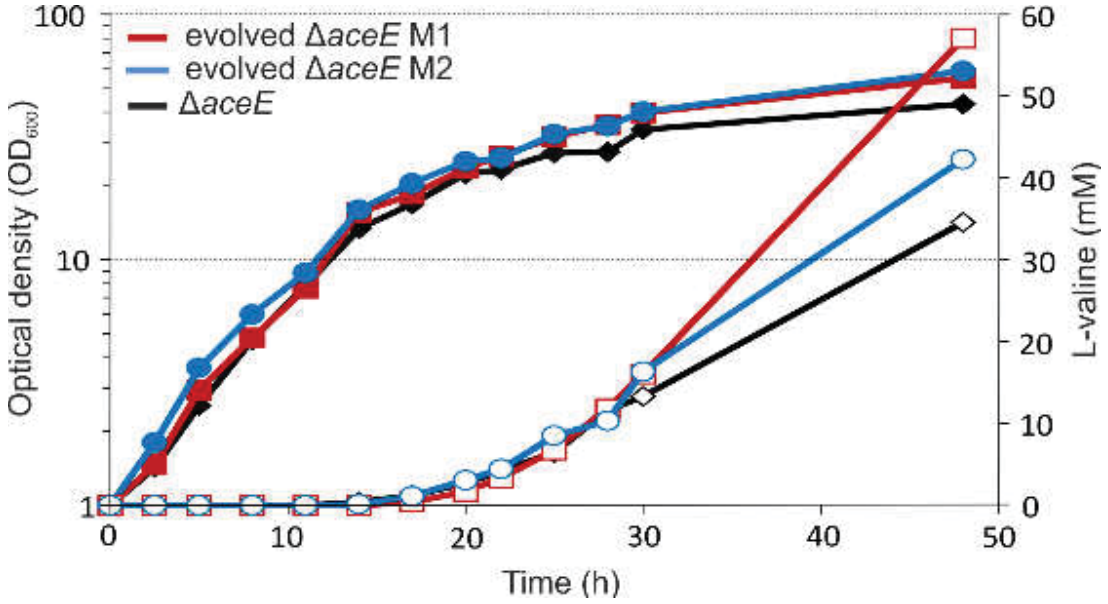

Fig. S2 Growth (filled symbols) and L-valine production (empty symbols) of *C. glutamicum* Δ*aceE* (black) and the evolved strains M1 (red) and M2 (blue) (Fig. 3, Tab. 2) during shake flask cultivation. First, cells were inoculated in 4 ml BHI medium containing 51 mM acetate and kanamycin (50 µg/ml), and incubated for eight hours at 30°C. Then, 1 ml of the preculture was used to inoculate a second preculture in 20 ml CGXII minimal medium containing 222 mM glucose, 254 mM acetate and kanamycin (50 µg/ml). After an overnight cultivation at 30°C, cells were inoculated to an OD_{600} of 1 in 50 ml CGXII minimal medium containing 222 mM glucose, 254 mM acetate and kanamycin (50 µg/ml).

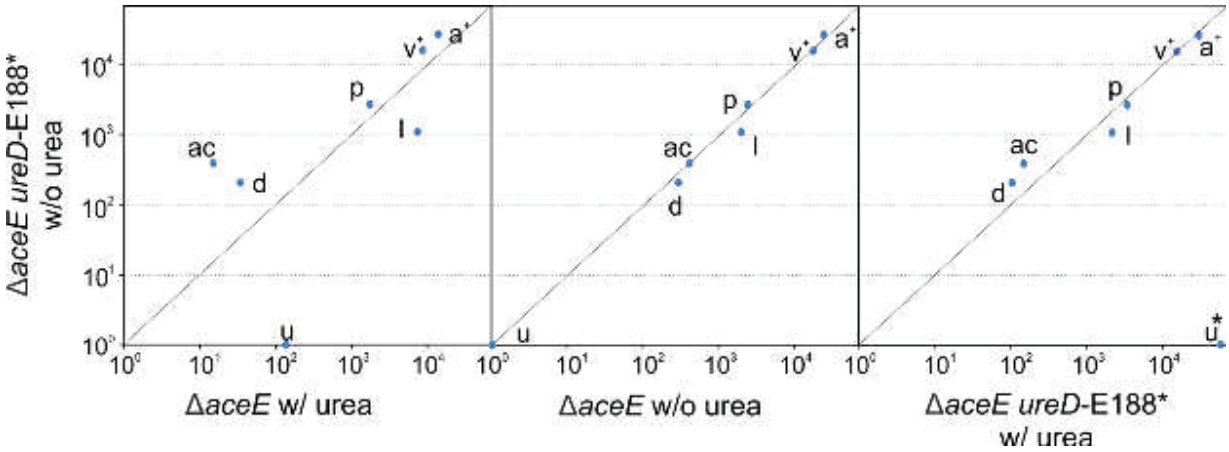

Fig. S3 GC-ToF-MS analysis of the influence of urea on the intracellular metabolite pool of *C. glutamicum* Δ*aceE* in comparison to Δ*aceE ureD*-E188* (Fig. 5). Peak areas of MS spectra are plotted against each other. The solid line marks the 45 degree angle line. Abbreviations: alanine (a), 2-aceto-lactate (ac), dihydroxyisovalerate (d), lactate (l), pyruvate (p), urea (u), valine (v).

Saturated peak areas are marked with an asterisk (*), while the plus (+) indicates the sum of peak areas of different trimethylsilyl (TMS) derivatives (L-valine 1TMS and L-valine 2TMS; L-alanine 2TMS and L-alanine 3TMS).

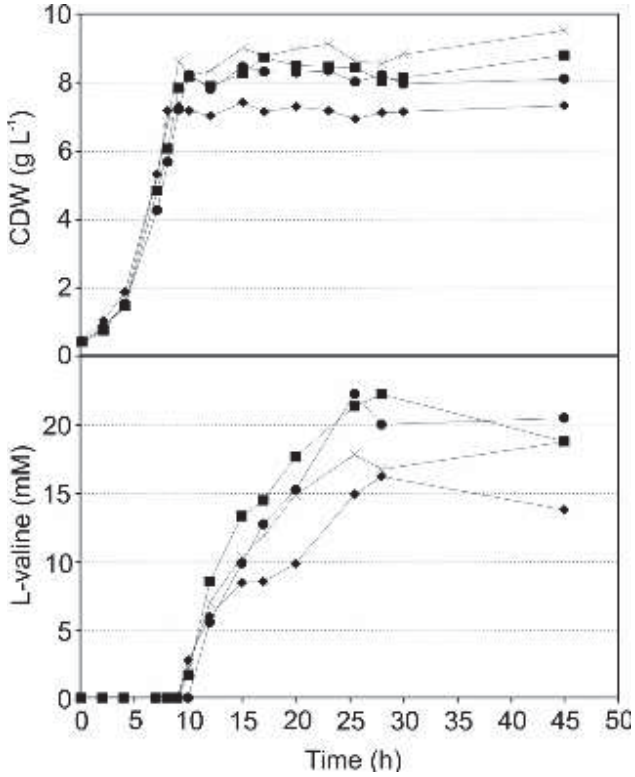

Fig. S4 Bioreactor batch fermentation of *C. glutamicum* Δ*aceE* in presence (♦) and without urea (■), and *C. glutamicum* Δ*aceE ureD*-E188* in presence (●) and without urea (×). Growth and L-valine production were monitored for 45 hours. Fermentations were performed at 30°C in a 1.4 L glass bioreactor (Multifors Multi-Fermenter System) with independently controllable bioreactors (Infors, Einsbach, Germany). Cells of a 50 ml overnight pre-culture in BHI medium containing 85 mM acetate were harvested, washed with 0.9% (w/v) saline and then inoculated to an OD_{600} of 1.5 in 500 ml CGXII minimal medium containing 0.5% BHI, 254 mM acetate and 222 mM glucose. The bioreactors were sparged with 0.9 l min^{-1} synthetic air, while dissolved oxygen was measured using a polarimetric oxygen electrode (Mettler Toledo, Gießen, Germany). The dissolved oxygen concentration was adjusted to 30% by a stirrer speed cascade from 600 to 1000 rpm. The pH was adjusted to pH 7 using 3 M potassium hydroxide and 3 M hydrochloric acid, while online pH measurements were done using a standard pH electrode (Mettler Toledo, Gießen, Germany). Foam development was suppressed by titration of 25% (v/v) silicon antifoam 204/water suspension (Sigma Aldrich, Steinheim, Germany).

References

Pauling, J., Röttger, R., Tauch, A., Azevedo, V., Baumbach, J., 2012. CoryneRegNet 6.0—Updated database content, new analysis methods and novel features focusing on community demands. Nucleic Acids Res. 40, D610-4.

6.3 Supplemental information – Urease inactivity increases L-valine production in *Corynebacterium glutamicum*

Supporting Tables

Table S1 Comparative transcriptome analysis of mRNA levels of *C. glutamicum* Δ*aceE* and Δ*aceE ureD*-E188* after 28 hours of shake flask cultivation in CGXII minimal medium containing 222 mM glucose and 254 mM acetate. Listed are all genes showing a ≥1.5-fold altered mRNA level and a *p* value of ≤0.20, with the exception of some interesting genes. The relative mRNA level is given as average ratio (Δ*aceE ureD*-E188*/Δ*aceE*) cultivated from three independent biological replicates.

Locus	Gene	Annotation	Ratio Δ*aceE ureD*-E188*/Δ*aceE*	*p* value
		GlxR regulon		
cg0566	*gabT*	4-aminobutyrate aminotransferase	2.13	0.195
cg0791	*pyc*	pyruvate carboxylase	0.17	0.281
cg0797	*prpB1*	2-methylisocitrate lyase	2.09	0.143
cg1143	-	putative transcriptional regulator	1.72	0.095
cg2403	*qcrB*	cytochrome *bc*1 complex, cytochrome *b* subunit	0.28	0.255
cg2410	*ltsA*	glutamine-dependent amidotransferase	1.67	0.001
cg2831	*ramA*	transcriptional regulator, acetate metabolism	0.20	0.299
cg3216	*gntP*	gluconate permease, gluconate:H+ symporter GntP family	2.20	0.055
cg3219	*ldhA*	NAD-dependent L-lactate dehydrogenase	0.24	0.300
cg3227	*lldD*	menaquinone-dependent L-lactate dehydrogenase	0.26	0.291
		AmtR regulon		
cg0115	*ureC*	urease alpha subunit	0.34	0.310
cg1064	*urtC*	ABC-type urea uptake system, permease subunit	1.60	0.200
cg1781	*soxA*	sarcosine oxidase- C-terminal fragment	1.66	0.002
		SOS and stress response		
cg0617	-	putative molybdopterin-guanine dinucleotide biosynthesis protein	0.37	0.160
cg1319	-	putative ATPase involved in DNA repair	1.58	0.070
cg1362	*atpB*	F_1F_O-ATP synthase, a-subunit of F_O part	1.63	0.001
cg1363	*atpE*	F_1F_O-ATP synthase, c-subunit of F_O part	0.34	0.324
cg1367	*atpG*	F_1F_O-ATP synthase, γ-subunit of F_1 part	0.19	0.287

Locus	Gene	Annotation	Ratio Δ*aceE ureD*-E188*/Δ*aceE*	*p* value
cg1696	-	putative antibiotic efflux permease of the major facilitator superfamily	9.00	0.167
cg1708	-	hypothetical protein, conserved	2.98	0.067
cg1765	*sufR*	transcriptional regulator of *suf* operon	0.24	0.142
cg2644	*clpP2*	ATP-dependent Clp protease proteolytic subunit	0.18	0.292
		RipA/DtxR regulon		
cg0310	*katA*	catalase	0.61	0.382
cg0445	*sdhC*	succinate:menaquinone oxidoreductase, cytochrome b subunit	0.69	0.498
cg0768	-	putative iron-siderophore ABC transporter	2.15	0.187
cg0769	-	putative iron-siderophore ABC transporter	2.87	0.152
cg1345	*narK*	nitrate/nitrite antiporter	0.39	0.311
		Specific biosynthesis pathways		
cg0977	-	putative ABC-type transport system	0.50	0.001
cg1218	*ndnR*	transcriptional repressor of NAD *de novo* biosynthesis genes	2.07	0.059
cg1588	*argH*	argininosuccinate lyase	0.07	0.224
cg2269	-	putative permease	1.78	0.153
cg2789	*mrx2*	mycoredoxin 2	0.44	0.248
cg3359	*trpE*	anthranilate synthase component I	0.17	0.343
		TCA		
cg2425	*sucE*	succinate exporter	1.54	0.063
cg0445	*sdhC*	succinate:menaquinone oxidoreductase, cytochrome b subunit	0.69	0.498
cg2613	*mdh*	malate dehydrogenase (EC:1.1.1.37)	0.58	0.393
		Others		
cg0074	-	putative sulfurtransferase	1.73	0.050
cg0181	*alkB*	alkylated DNA repair protein	1.63	0.077
cg0183	-	putative lyse type translocator	1.52	0.070
cg0208	-	hypothetical protein	0.14	0.169
cg0248	-	putative ABC-type polysaccharide/polyol phosphate export sytem	1.56	0.021
cg0356	-	putative serine protease	1.50	0.152
cg0368	-	putative secreted protein, conserved	1.88	0.145
cg0369	-	putative secreted protein, conserved	1.57	0.045
cg0385	*bglS'*	beta-glucosidase precursor-N-terminal domain	1.62	0.155
cg0401	*rmlA1*	TDP-glucose pyrophosphorylase	1.55	0.159
cg0525	-	hypothetical protein	3.07	0.174
cg0640	*fdxB*	ferredoxin no. 2, 2Fe-2S	1.64	0.138

Locus	Gene	Annotation	Ratio Δ*aceE ureD*-E188*/Δ*aceE*	*p* value
cg0658	*rptA*	terminal rhamnopyranosyltransferase	1.72	0.096
cg0672	-	hypothetical protein, conserved	1.95	0.080
cg0733	-	putative ABC transporter ATP-binding protein	1.78	0.087
cg0752	-	putative secreted or membrane protein	0.25	0.140
cg0765	-	putative secreted protein	2.05	0.130
cg0784	-	putative cell wall-associated hydrolase	1.69	0.050
cg0794	*yciC*	putative P-loop GTPase	2.03	0.046
cg0852	-	hypothetical protein, conserved	1.51	0.033
cg0866	-	putative purine/pyrimidine phosphoribosyl transferase	1.64	0.070
cg0872	-	putative GTPase	0.40	0.199
cg0919	*tnp18a*	transposase	1.67	0.001
cg0973	*pgi*	glucose-6-phosphate isomerase	0.28	0.274
cg1111	*eno*	enolase, phosphopyruvate hydratase	0.26	0.260
cg1118	-	putative pyrimidine reductase	1.59	0.001
cg1133	*glyA*	serine hydroxymethyltransferase	0.33	0.198
cg1149	-	hypothetical protein	1.58	0.135
cg1236	*tpx*	thiol peroxidase	0.03	0.088
cg1302	-	putative HKD family nuclease	1.58	0.165
cg1354	*rho*	transcription termination factor Rho	1.86	0.005
cg1355	*prfA*	peptide chain release factor 1 RF-1	2.11	0.059
cg1360	-	putative membrane protein	1.95	0.025
cg1413	*rbsB*	ribose/xylose transport	0.04	0.263
cg1457	*dnaQ2*	putative DNA polymerase III, epsilon subunit	1.59	0.124
cg1467	-	putative transcriptional regulator	1.69	0.119
cg1501	*coaD*	phosphopantetheine adenylyltransferase	1.63	0.085
cg1754	-	hypothetical protein	1.77	0.088
cg1807	*dfp*	phosphopantothenoylcysteine synthase/decarboxylase	1.71	0.146
cg1827	*aroB*	3-dehydroquinate synthase	1.61	0.073
cg1829	*aroC*	chorismate synthase	2.01	0.084
cg1922	-	hypothetical protein CGP3 region	2.10	0.109
cg1950	*tnp14b*	transposase fragment CGP3 region	1.60	0.018
cg1978	-	hypothetical protein CGP3 region	1.54	0.067
cg1984	-	hypothetical protein CGP3 region	2.03	0.079
cg1993	-	hypothetical protein CGP3 region	1.94	0.145
cg2072	-	putative di-and tricarboxylate transporter	1.55	0.075
cg2088	-	hypothetical protein	1.53	0.003
cg2092	*sigA*	RNA polymerase sigma factor	0.37	0.320
cg2102	*sigB*	RNA polymerase sigma factor	0.23	0.315
cg2104	*galE*	UDP-glucose 4-epimerase	0.20	0.314

Locus	Gene	Annotation	Ratio Δ*aceE ureD*-E188*/Δ*aceE*	*p* value
cg2340	-	putative ABC-type amino acid transport system	1.67	0.001
cg2382	-	putative GCN5-related N-acetyltransferase	1.62	0.037
cg2389	-	putative membrane protein	1.57	0.101
cg2446	*glnE*	glutamate-ammonia-ligase adenylyltransferase	0.74	0.182
cg2483	-	hypothetical protein	1.98	0.101
cg2490	-	putative secreted guanine-specific ribonuclease	1.77	0.029
cg2494	*dgt*	deoxyguanosinetriphosphate triphosphohydrolase-like protein	1.55	0.009
cg2568	*dctM*	C4-dicarboxylate transport system permease large protein	6.58	0.177
cg2574	-	putative threonine efflux transporter	1.51	0.075
cg2673	-	putative permease of the major facilitator superfamily	1.63	0.035
cg2757	*tnp15a*	transposase	1.67	0.021
cg2772	*clpS*	ATP-dependent Clp protease adaptor protein	0.46	0.312
cg2797	-	hypothetical protein, conserved	2.26	0.121
cg2799	*pknE*	putative secreted protein	0.37	0.201
cg2868	*nuc*	putative extracellular nuclease	1.95	0.064
cg2888	*phoR*	two component response regulator	0.08	0.185
cg2900	*ddh*	meso-diaminopimelate dehydrogenase	1.70	0.023
cg2918	-	putative dehydrogenase or related protein	1.94	0.157
cg2919	-	putative oxidoreductase	1.54	0.015
cg2940	-	putative ATPase components of ABC-type transport system	1.97	0.133
cg3016	-	hypothetical protein	2.03	0.083
cg3049	*fprA*	putative ferredoxin/ferredoxin-NADP reductase	0.24	0.293
cg3060	*cgtS6*	two component sensor kinase	2.11	0.086
cg3065	-	hypothetical protein, conserved	1.56	0.168
cg3146	*bglY'*	beta-glucosidase-fragment	1.51	0.057
cg3148	*'fepC'*	putative ABC transporter	1.57	0.129
cg3185	-	hypothetical protein, conserved	1.53	0.161
cg3199	-	putative hydrolase of the HAD superfamily	1.61	0.195
cg3231	-	hypothetical protein	1.77	0.162
cg3284	*copS*	two component sensor kinase	1.51	0.050
cg3349	*nagL*	maleylpyruvate isomerase	3.21	0.186
cgr10	-	5S ribosomal RNA	1.54	0.106
cgtRNA_3542	-	Tyr tRNA	1.55	0.164
cgtRNA_3570	-	Met tRNA	1.52	0.020

Supporting Figures

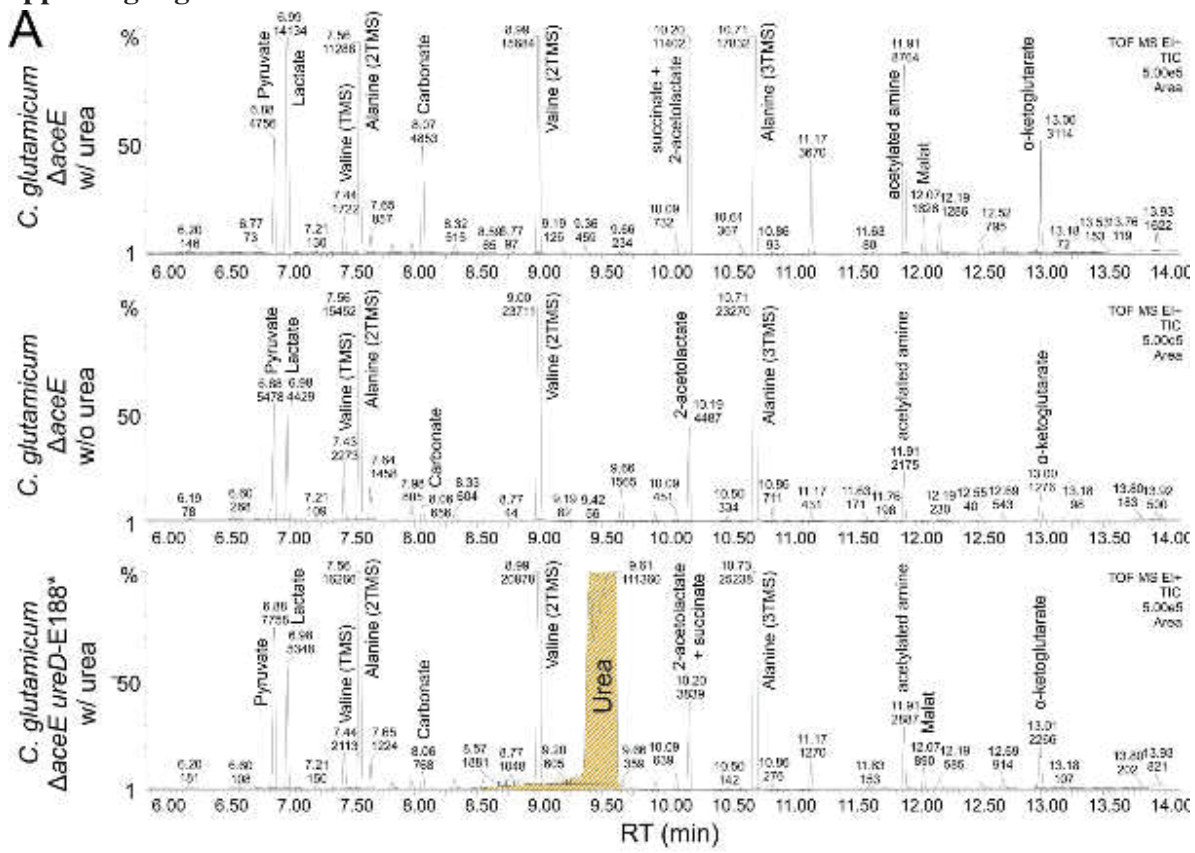

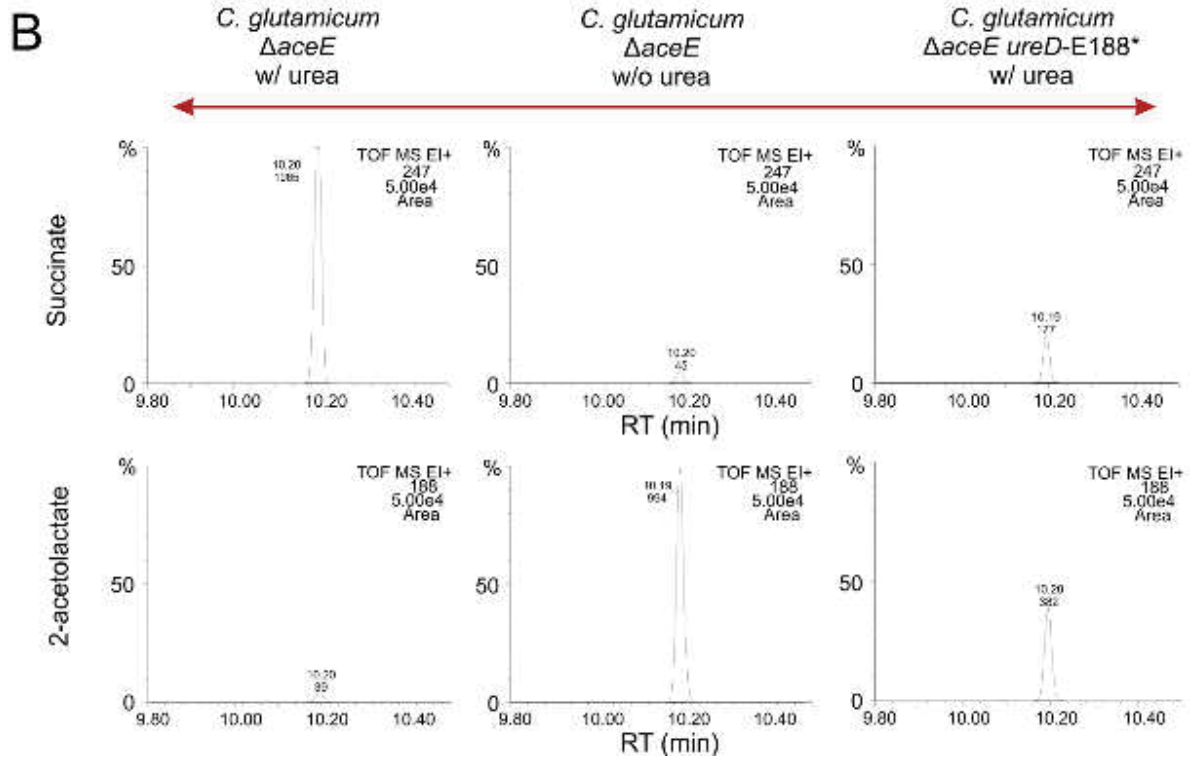

Fig. S1 GC-ToF-MS analysis of the supernatant after cultivating *C. glutamicum* Δ*aceE* with and without urea and Δ*aceE ureD*-E188* with urea for 30 hours. A. Overview of MS spectra. B. MS spectra of succinate and 2-acetolactate. The red arrow indicates the reading direction (succinate and 2-acetolactate peaks are comparable among themselves, but not both molecules with each other). Metabolome analyses of supernatants were performed on a 6890N gas chromatograph (Agilent, Santa Clara, USA) coupled to a Micromass GCT Premier high-resolution time-of-flight mass spectrometer (Waters, Milford, USA). Sample preparation, derivatization, MS operation and peak identification were performed as described previously (Paczia et al., 2012). Abbreviation: trimethylsilyl (TMS) derivatives.

References

Paczia, N., Nilgen, A., Lehmann, T., Gätgens, J., Wiechert, W., Noack, S. (2012). Extensive exometabolome analysis reveals extended overflow metabolism in various microorganisms. Microb Cell Fact. 11, 122.

6.4 Supplemental information – Screening of an *Escherichia coli* promoter library for a phenylalanine biosensor

Supporting Figures

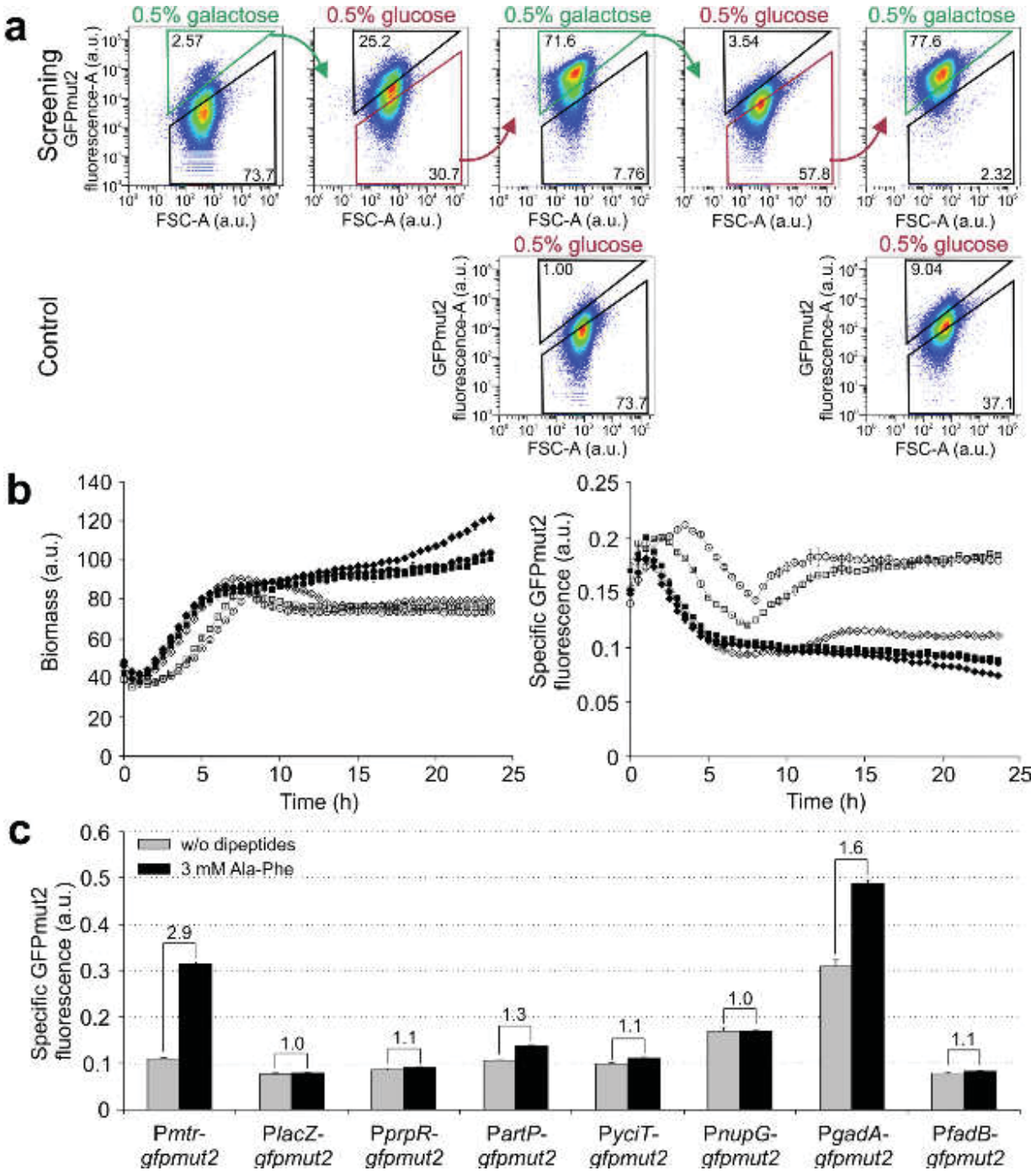

Fig. S1 Screening of galactose and L-phenylalanine responsive promoters. **a** Initially, the pooled strains containing of the Alon promoter library were incubated in 20 ml M9 minimal medium without effector

molecules and split in fractions of low and high fluorescence to reduce the fraction of constitutively active or inactive promoters (not shown). Subsequently, cells with low fluorescence were re-incubated in 20 ml M9 minimal medium containing 0.5% (w/v) of the effector molecule galactose for six hours at 37°C and 120 rpm. One million cells from the green gate were sorted on filter plates and incubated overnight at 37°C and 170 rpm in 4 ml LB with kanamycin. To separate constitutive "ON" promoters from responsive promoters, counter-selection was performed by subsequently incubating the isolated cells in 20 ml M9 minimal medium containing 0.5% (w/v) glucose for six hours. This time, cells from the red gate ("OFF" promoters) were sorted on filter plates and incubated overnight in 4 ml LB with kanamycin. To reduce the fraction of false positive clones, one further round of toggled screening was performed. The green and red arrows indicate the gate chosen for cell sorting throughout the screening procedure. A culture grown in glucose minimal medium served as reference. The numbers indicate the percentage of the entire population covered by the respective gate. **b** Biomass formation and specific GFPmut2 fluorescence of *E. coli* K-12 MG1655 containing plasmids pUA66 (♦), pUA66_P$_{gals}$-*gfpmut2* (●) and pUA66_P$_{lacZ}$-*gfpmut2* (■). The strains were cultivated in the BioLector microbioreactor system at 37°C and 1200 rpm in M9 minimal medium containing 0.5% (w/v) glucose as negative control (filled symbols) or 0.5% (w/v) galactose as inductor (empty symbols). **c** Specific Venus fluorescence of selected clones from the Alon library containing promoter-*gfpmut2* fusions that were enriched during the screening for L-phenylalanine responsive promoters. Cells were cultivated in the presence (black bar) or without (gray bar) 3 mM L-alanyl-L-phenylalanine (Ala-Phe). Numbers above bars indicate the minimal dynamic range (fold-change induced *versus* non-induced). **b** and **c** Data represent average values of three independent biological replicates.

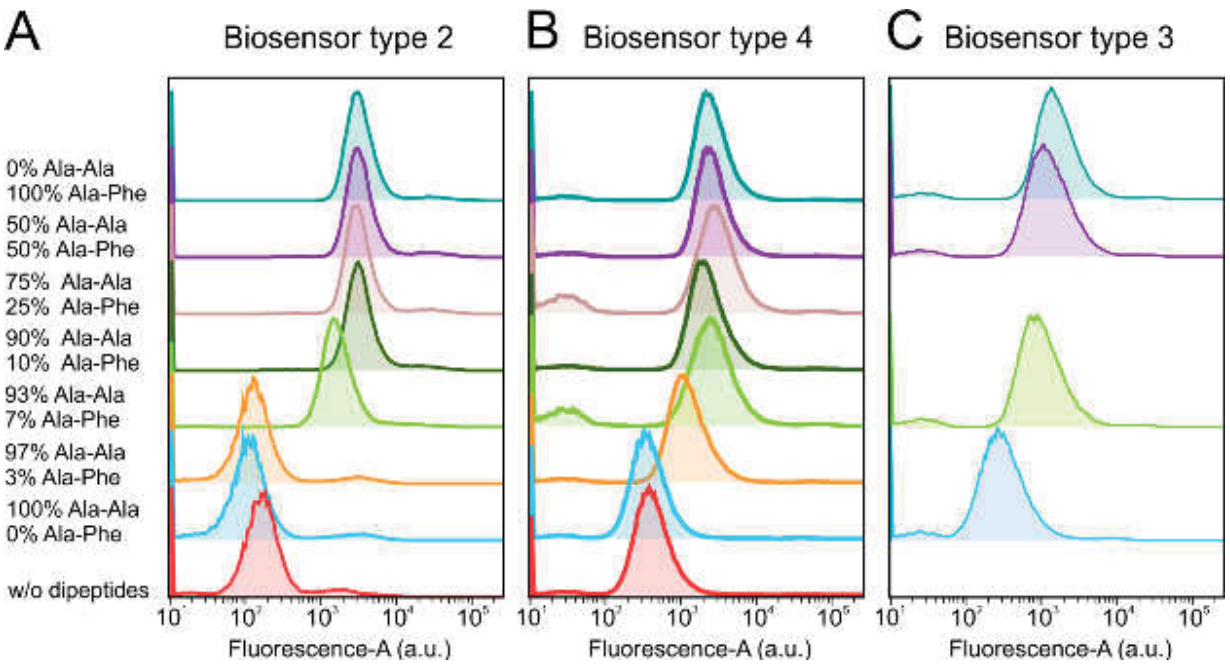

Fig. S2 Flow cytometric (FC) analyses of different biosensor designs **a** type two, **b** type four and **c** type three in presence of different ratios of Ala-Ala and Ala-Phe (overall concentration 3 mM) showing histograms of the Venus fluorescence. Cells were cultivated in microtiter plates in M9 minimal medium

containing 0.5% (w/v) glucose and kanamycin in the presence of different Ala-Phe/Ala-Ala ratios. After seven hours of incubation, the sensor output was analyzed by FC.

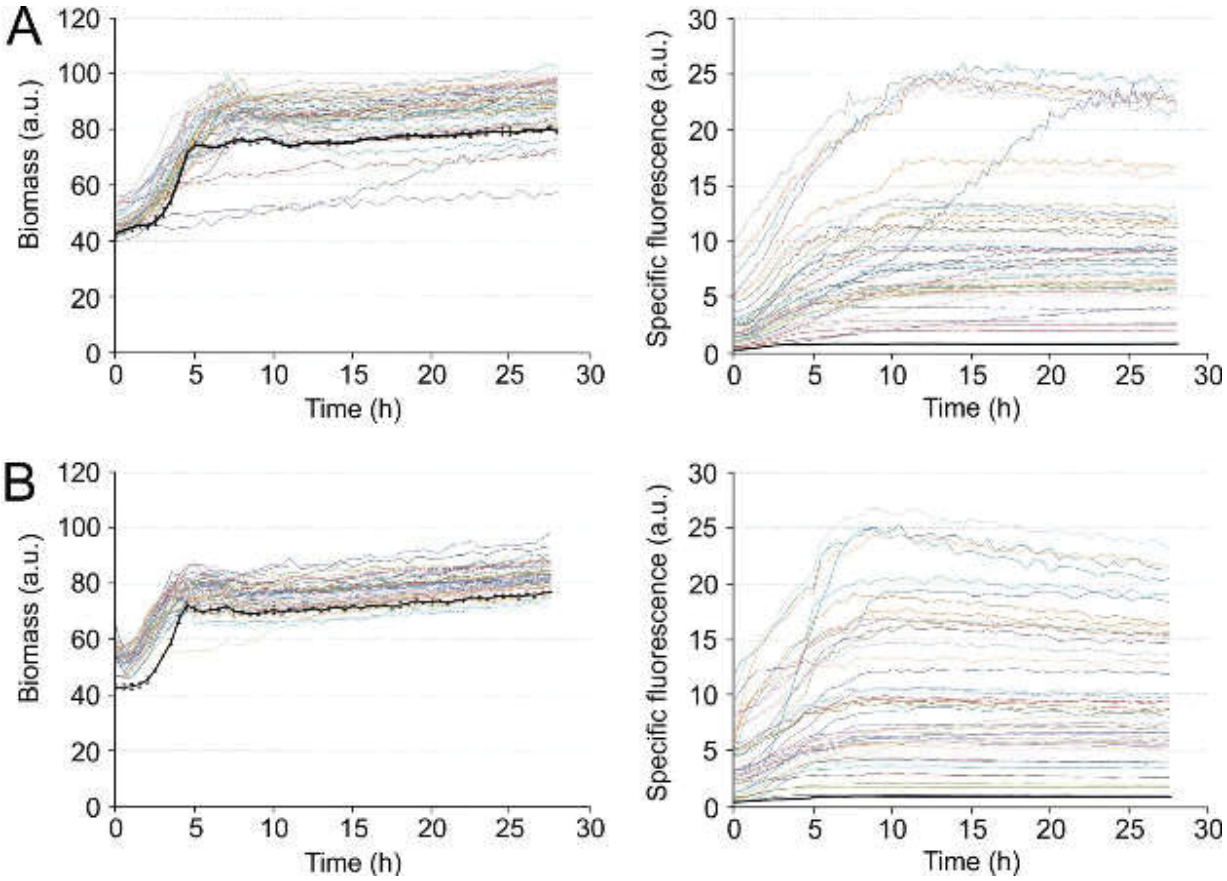

Fig. S3 Growth and specific Venus fluorescence of isolated mutants. **a** and **b** 90 isolated mutants (each 45 mutants depicted in a and b) were analyzed by cultivation at microtiter scale in phenylalanine production medium containing 0.5% (w/v) glucose and kanamycin for 28 hours (colored lines). Growth and fluorescence of the non-mutagenized *E. coli* K-12 MG1655/pJC1-*mtr* sensor-type1 strain is indicated by the black line. Data shown for isolated mutant clones represent single measurements; the data shown for the non-mutagenized wild type-strain represent average data of three biological replicates.

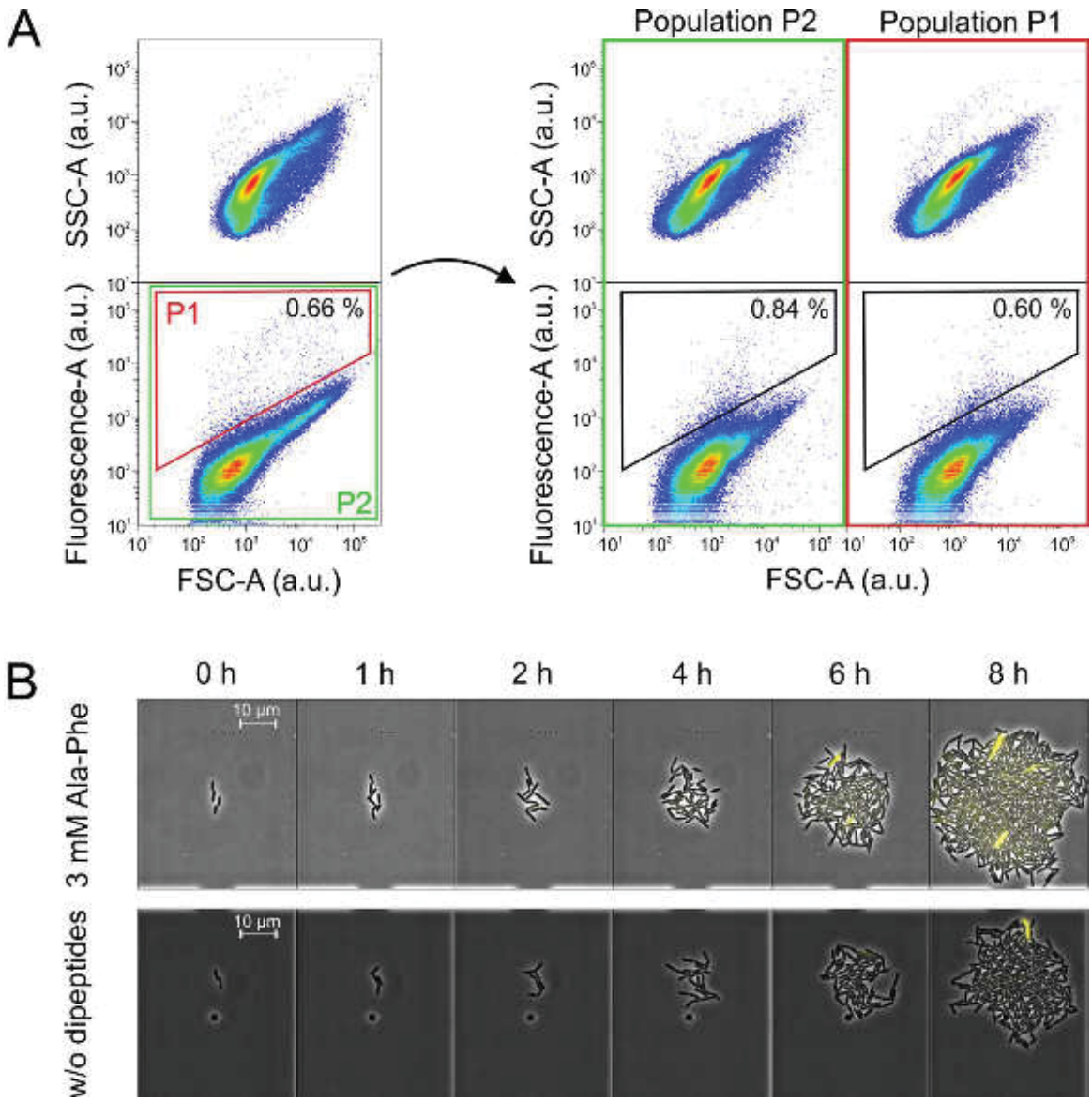

Fig. S4 Biosensor-based single-cell analysis reveals cell-to-cell variability of *E. coli* K-12 MG1655. **a** FC analysis of *E. coli* K-12 MG1655 pJC1-*mtr* sensor-type1 cells after eight hours of cultivation in 20 ml phenylalanine production medium containing 0.5% (w/v) glucose and kanamycin at 37°C and 120 rpm. Dot plots display the side scatter (SSC), forward scatter (FSC) and Venus fluorescence of single cells. 2 x 10^5 cells were sorted from gate P1 (red) and P2 (green) in 4 ml LB with kanamycin and incubated overnight at 37°C and 170 rpm. The following day, cells were inoculated in 20 ml phenylalanine production medium, incubated for eight hours and re-analyzed by FC (P1, red and P2, green). The numbers in the gates indicate the percentage of cells showing spontaneously increased fluorescent outputs. **b** Live cell imaging of isogenic microcolonies of *E. coli* K-12 MG1655 cells containing the sensor plasmid pJC1-*mtr* sensor-type1 in presence of 3 mM (upper row) and without (lower row) the dipeptide L-alanyl-L-phenylalanine (Ala-Phe). The cells were cultivated for eight hours in L-phenylalanine production medium in microfluidic monolayer cultivation chambers as previously described (Grünberger et al., 2012; Grünberger et al., 2015). (Grünberger et al., 2012; Grünberger et al., 2015).

Supporting references

Grünberger, A., Paczia, N., Probst, C., Schendzielorz, G., Eggeling, L., Noack, S., Wiechert, W., Kohlheyer, D., 2012. A disposable picolitre bioreactor for cultivation and investigation of industrially relevant bacteria on the single cell level. Lab Chip. 12, 2060-8.

Grünberger, A., Probst, C., Helfrich, S., Nanda, A., Stute, B., Wiechert, W., von Lieres, E., Nöh, K., Frunzke, J., Kohlheyer, D., 2015. Spatiotemporal microbial single-cell analysis using a high-throughput microfluidics cultivation platform. Cytometry A. 87, 1101-15.

6.5 Supplemental information – Discussion

Supporting Tables

Table S4.2.1: Overview of mutations identified in five mutants (1-5) isolated by FACS HT screening of an MNNG-mutagenized *E. coli* K-12 MG1655 library using the *mtr* biosensor encoded on the plasmid pJC1-*mtr* biosensor type1. Sequencing and comparative analysis were performed as previously described (Mahr et al., 2015). Reads were mapped using accession NC_000913 as the reference genome. Mutations in genes associated with the biosynthesis or transport of aromatic amino acids are highlighted with an asterisk. Abbreviation: Original strain *E. coli* K-12 MG1655 pJC1-*mtr* biosensor type1 (parental strain).

Gene	Gene name	Mutein	Parental strain	Mutant 1	Mutant 2	Mutant 3	Mutant 4	Mutant 5
b0040	*caiT*	A203V	-	x	-	-	-	-
b0043	*fixC*	G316S	-	x	-	-	-	-
b0068	*thiB*	T160I	-	x	-	-	-	-
b0073	*leuB*	A270V	-	x	-	-	-	-
b0084	*ftsI*	V453I	-	-	-	-	x	-
b0085	*murE*	G378D	-	x	-	-	-	-
b0088	*murD*	A109T	-	x	-	-	-	-
b0219	*yafV*	A82T	-	-	-	-	x	-
b0463	*acrA*	A355T	-	-	-	-	x	-
b0532	*sfmD*	A388V	-	-	-	-	x	-
b0621	*dcuC*	D100N	-	-	-	-	x	-
b0841	*ybjG*	R139C	-	-	-	-	-	x
b0844	*ybjI*	P56S	-	-	-	-	-	x
b0847	*ybjL*	A428V	-	-	-	-	-	x
b0847	*ybjL*	L298F	-	-	-	-	-	x
b0876	*ybjD*	P332S	-	-	-	x	-	-
b0974	*hyaC*	T216I	-	-	-	-	-	x
b0984	*gfcD*	G264D	-	-	-	-	-	x
b0997	*torA*	R592H	-	-	-	-	-	x
b0998	*torD*	A96T	-	-	-	-	-	x
b0999	*cbpM*	G29D	-	-	-	-	-	x
b1018	*efeO*	E80K	-	-	-	-	-	x
b1022	*pgaC*	R293C	-	-	-	-	-	x
b1023	*pgaB*	P126S	-	-	-	-	-	x
b1159	*mcrA*	P249S	-	-	x	-	-	-
b1177	*ycgJ*	G15R	-	x	-	-	-	-
b1180	*ycgM*	E86K	-	x	-	-	-	-
b1184	*umuC*	A178T	-	x	-	-	-	-
b1192	*ldcA*	S232N	-	-	-	x	-	-

Gene	Gene name	Mutein	Parental strain	Mutant 1	Mutant 2	Mutant 3	Mutant 4	Mutant 5
b1194	*ycgR*	A170T	-	-	-	x	-	-
b1194	*ycgR*	S2N	-	-	-	x	-	-
b1195	*ymgE*	M21I	-	x	-	-	-	-
b1198	*dhaM*	G103D	-	-	-	x	-	-
b1201	*dhaR*	G111E	-	x	-	-	-	-
b1201	*dhaR*	A122T	-	x	-	-	-	-
b1202	*ycgV*	P653L	-	x	-	-	-	-
b1207	*prs*	G294D	-	-	-	x	-	-
b1220	*ychO*	P280S	-	-	-	x	-	-
b1224	*narG*	H706R	-	-	-	x	-	-
b1224	*narG*	T791I	-	-	-	x	-	-
b1247	*oppF*	G85D	-	x	-	-	-	-
b1255	*yciC*	G38R	-	-	x	-	-	-
b1261	*trpB**	R363H	-	-	-	x	-	-
b1261	*trpB**	E155K	-	-	-	x	-	-
b1263	*trpD**	A130T	-	-	-	x	-	-
b1264	*trpE**	C377Y	-	-	x	-	-	-
b1276	*acnA*	V766M	-	-	x	-	-	-
b1315	*ycjS*	D301N	-	-	x	-	-	-
b1320	*ycjW*	T88I	-	-	x	-	-	-
b1372	*stfR*	G859E	-	-	x	-	-	-
b1378	*pfo*	A920V	-	-	x	-	-	-
b1386	*tynA*	T717I	-	-	x	-	-	-
b1387	*paaZ*	H525Y	-	-	x	-	-	-
b1392	*paaE*	V72M	-	-	x	-	-	-
b1394	*paaG*	L209F	-	-	-	-	x	-
b1397	*paaJ*	E219K	-	-	x	-	-	-
b1407	*ydbD*	G396D	-	-	x	-	-	-
b1407	*ydbD*	A531T	-	-	x	-	-	-
b1407	*ydbD*	A697T	-	-	x	-	-	-
b1411	*ynbD*	W235*	-	-	x	-	-	-
b1411	*ynbD*	W236*	-	-	x	-	-	-
b1413	*hrpA*	A347T	-	-	x	-	-	-
b1421	*trg*	G295D	-	-	x	-	-	-
b1431	*ydcL*	G188D	-	-	x	-	-	-
b1450	*mcbR*	E76K	-	-	x	-	-	-
b1459	*yncI*	G197D	-	-	x	-	-	-
b1463	*nhoA*	W119*	-	-	x	-	-	-
b1464	*yddE*	P150S	-	-	x	-	-	-
b1468	*narZ*	P90S	-	-	x	-	-	-
b1483	*ddpF*	P265S	-	-	x	-	-	-
b1486	*ddpB*	A107V	-	-	x	-	-	-

Gene	Gene name	Mutein	Parental strain	Mutant 1	Mutant 2	Mutant 3	Mutant 4	Mutant 5
b1487	*ddpA*	A297V	-	-	x	-	-	-
b1487	*ddpA*	T96S	-	-	-	-	x	-
b1492	*gadC*	P481S	-	-	x	-	-	-
b1493	*gadB*	P191S	-	-	x	-	-	-
b1501	*ydeP*	P564L	-	-	x	-	-	-
b1612	*fumA*	P5S	-	-	-	-	x	-
b1623	*add*	A201V	-	-	-	x	-	-
b1711	*btuC*	G153E	-	-	-	x	-	-
b1750	*ydjX*	L12F	-	-	-	x	-	-
b1753	*ynjA*	A120V	-	-	-	x	-	-
b1754	*ynjB*	S264L	-	-	-	x	-	-
b1764	*selD*	G181E	-	-	-	x	-	-
b1774	*ydjJ*	G148R	-	-	-	x	-	-
b1790	*yeaM*	A239T	-	-	-	x	-	-
b1808	*yoaA*	A62T	-	-	-	x	-	-
b1808	*yoaA*	P7L	-	-	x	-	-	-
b1809	*yoaB*	P90S	-	-	-	x	-	-
b1833	*yebS*	S119L	-	-	-	x	-	-
b1849	*purT*	R68H	-	-	-	-	x	-
b1864	*yebC*	T174I	-	-	x	-	-	-
b1864	*yebC*	T126I	-	-	x	-	-	-
b1868	*yecE*	G128D	-	-	x	-	-	-
b1876	*argS*	G297D	-	-	-	-	-	x
b1876	*argS*	V574I	-	-	x	-	-	-
b1886	*tar*	P539S	-	-	-	-	-	x
b1896	*otsA*	Q444*	-	-	x	-	-	-
b1907	*tyrP**	D280N	-	-	x	-	-	-
b1916	*sdiA*	V211I	-	-	-	-	-	x
b1919	*dcyD*	A143V	-	-	x	-	-	-
b1924	*fliD*	G8R	-	-	x	-	-	-
b1929	*yedE*	V21I	-	-	x	-	-	-
b1938	*fliF*	G101D	-	-	x	-	-	-
b1943	*fliK*	D142G	-	-	x	-	-	-
b1952	*dsrB*	A23T	-	-	x	-	-	-
b1957	*yodC*	V11I	-	-	x	-	-	-
b1959	*yedA**	A303V	-	-	x	-	-	-
b1967	*hchA*	S34F	-	-	x	-	-	-
b1976	*mtfA*	P232L	-	-	x	-	-	-
b1978	*yeeJ*	V1431I	-	-	-	-	-	x
b1988	*nac*	G170E	-	-	x	-	-	-
b1992	*cobS*	G228S	-	-	x	-	-	-
b2000	*flu*	T87I	-	-	x	-	-	-

Gene	Gene name	Mutein	Parental strain	Mutant 1	Mutant 2	Mutant 3	Mutant 4	Mutant 5
b2000	*flu*	G484S	-	-	-	-	-	x
b2000	*flu*	G751D	-	-	-	-	-	x
b2000	*flu*	G826S	-	-	-	-	-	x
b2006	*yeeW*	D15N	-	-	-	-	-	x
b2025	*hisF*	D182N	-	-	-	-	-	x
b2042	*wcaN*	P202S	-	-	x	-	-	-
b2043	*wcaM*	R278C	-	-	-	-	-	x
b2046	*wzxC*	P167S	-	-	-	-	-	x
b2049	*cpsB*	A407V	-	-	-	-	-	x
b2049	*cpsB*	S282F	-	-	-	-	-	x
b2064	*asmA*	Q384*	-	-	-	-	-	x
b2069	*yegD*	G272D	-	-	x	-	-	-
b2071	*yegJ*	D114N	-	-	x	-	-	-
b2076	*mdtC*	G251D	-	-	-	-	-	x
b2078	*baeS*	G59S	-	-	-	-	-	x
b2078	*baeS*	G137D	-	-	x	-	-	-
b2079	*baeR*	R51H	-	-	-	-	-	x
b2086	*yegS*	D244N	-	-	-	-	-	x
b2091	*gatD*	R304W	-	-	x	-	-	-
b2095	*gatZ*	A413V	-	-	-	-	-	x
b2095	*gatZ*	A32T	-	-	-	-	-	x
b2096	*gatY*	G139D	-	-	-	-	-	x
b2097	*fbaB*	P24S	-	-	x	-	-	-
b2100	*yegV*	G53D	-	-	x	-	-	-
b2100	*yegV*	A62T	-	-	x	-	-	-
b2103	*thiD*	R197W	-	-	-	-	-	x
b2124	*yehS*	A77V	-	-	x	-	-	-
b2131	*osmF*	A8V	-	-	x	-	-	-
b2132	*bglX*	R486C	-	-	-	-	-	x
b2134	*pbpG*	R274C	-	-	-	-	-	x
b2134	*pbpG*	R104C	-	-	x	-	-	-
b2139	*mdtQ*	P359L	-	-	-	-	-	x
b2139	*mdtQ*	P141S	-	-	x	-	-	-
b2142	*yohK*	V160I	-	-	x	-	-	-
b2144	*sanA*	E228K	-	-	x	-	-	-
b2146	*preT*	E295K	-	-	x	-	-	-
b2151	*galS*	P291L	-	-	x	-	-	-
b2151	*galS*	P47S	-	-	-	-	-	x
b2154	*yeiG*	D92N	-	-	x	-	-	-
b2158	*yeiH*	D130N	-	-	-	-	-	x
b2159	*nfo*	V174I	-	-	-	-	-	x
b2163	*yeiL*	V85M	-	-	x	-	-	-

Gene	Gene name	Mutein	Parental strain	Mutant 1	Mutant 2	Mutant 3	Mutant 4	Mutant 5
b2176	*rtn*	P326S	-	-	x	-	-	-
b2176	*rtn*	G494D	-	-	x	-	-	-
b2178	*yejB*	S351N	-	-	-	-	-	x
b2180	*yejF*	E503K	-	-	-	-	-	x
b2206	*napA*	S618S	-	-	x	-	-	-
b2206	*napA*	T297M	-	-	x	-	-	-
b2214	*apbE*	A192V	-	-	-	-	-	x
b2241	*glpA*	P123L	-	x	-	-	-	-
b2332	*yfcO*	G183D	-	-	-	-	x	-
b2368	*emrK*	A202V	-	-	-	-	x	-
b2464	*talA*	G138E	-	-	-	-	x	-
b2479	*gcvR*	D38N	-	-	-	-	x	-
b2482	*hyfB*	R380Q	-	-	-	-	x	-
b2491	*hyfR*	A285T	-	-	-	-	x	-
b2493	*yfgO*	A154V	-	-	-	-	x	-
b2538	*hcaE*	G318D	-	-	-	-	x	-
b2574	*nadB*	V41I	-	-	-	x	-	-
b2599	*pheA**	D18N	-	-	-	-	x	-
b2600	*tyrA**	G90E	-	x	-	-	-	-
b2642	*yfjW*	T227I	-	-	x	-	-	-
b2661	*gabD*	G459D	-	-	-	-	x	-
b2677	*proV*	A194T	-	-	-	-	x	-
b2678	*proW*	R181H	-	-	-	-	x	-
b2681	*ygaY*	A131T	-	-	-	-	x	-
b2698	*recX*	W161*	-	x	-	-	-	-
b2703	*srlE*	G73D	-	-	-	-	x	-
b2705	*srlD*	D209N	-	-	-	-	x	-
b2710	*norV*	D73N	-	-	-	-	x	-
b2710	*norV*	W119*	-	-	-	-	x	-
b2730	*hypE*	G241D	-	-	-	-	x	-
b2750	*cysC*	A153V	-	-	-	-	x	-
b2764	*cysJ*	A194V	-	-	-	-	x	-
b2764	*cysJ*	T25M	-	-	-	-	x	-
b2764	*cysJ*	P6S	-	-	-	-	x	-
b2766	*ygcN*	E277K	-	-	-	-	x	-
b2775	*yqcE*	G328E	-	-	-	-	x	-
b2784	*relA*	P253S	-	-	-	-	x	-
b2784	*relA*	A247V	-	-	-	-	x	-
b2785	*rlmD*	T241I	-	-	-	-	x	-
b2786	*barA*	V375I	-	-	-	-	x	-
b2786	*barA*	P797S	-	x	-	-	-	-
b2803	*fucK*	A412V	-	-	-	-	-	x

Gene	Gene name	Mutein	Parental strain	Mutant 1	Mutant 2	Mutant 3	Mutant 4	Mutant 5
b2810	*csdA*	A198V	-	x	-	-	-	-
b2822	*recC*	D906N	-	x	-	-	-	-
b2834	*tas*	T342I	-	-	-	-	x	-
b2835	*lplT*	R395H	-	-	-	-	x	-
b2838	*lysA*	E202K	-	x	-	-	-	-
b2873	*hyuA*	A46V	-	x	-	-	-	-
b2874	*yqeA*	V184M	-	-	-	-	x	-
b2879	*ssnA*	D207N	-	-	-	-	x	-
b2882	*xanQ*	D466N	-	-	-	-	x	-
b2933	*cmtA*	G109E	-	-	-	-	x	-
b2938	*speA*	V365M	-	-	-	-	x	-
b2942	*metK*	T44I	-	-	-	-	x	-
b2943	*galP*	Q147*	-	-	-	-	x	-
b2955	*yggW*	A377V	-	-	-	-	x	-
b2976	*glcB*	E630K	-	-	-	-	x	-
b2979	*glcD*	E288K	-	-	-	-	x	-
b2981	*yghO*	W22*	-	x	-	-	-	-
b2983	*yghQ*	A321T	-	-	-	-	x	-
b2988	*gss*	W305*	-	x	-	-	-	-
b2988	*gss*	E37K	-	x	-	-	-	-
b2993	*hybD*	T87I	-	-	-	-	x	-
b2995	*hybB*	G235S	-	x	-	-	-	-
b2996	*hybA*	S122F	-	-	-	-	x	-
b2996	*hybA*	D43N	-	x	-	-	-	-
b2997	*hybO*	P220S	-	-	-	-	x	-
b3006	*exbB*	V237I	-	x	-	-	-	-
b3008	*metC*	A91V	-	x	-	-	-	-
b3009	*yghB*	G129E	-	-	-	-	x	-
b3013	*yqhG*	S195F	-	x	-	-	-	-
b3017	*ftsP*	A158V	-	x	-	-	-	-
b3019	*parC*	G53S	-	x	-	-	-	-
b3020	*ygiS*	W84*	-	x	-	-	-	-
b3020	*ygiS*	V76M	-	x	-	-	-	-
b3046	*yqiG*	A573V	-	x	-	-	-	-
b3046	*yqiG*	G1191D	-	-	-	-	x	-
b3049	*glgS*	T34I	-	-	-	-	x	-
b3051	*yqiK*	V53I	-	-	-	-	x	-
b3051	*yqiK*	G176D	-	-	-	-	x	-
b3056	*cca*	G16E	-	x	-	-	-	-
b3056	*cca*	G149D	-	x	-	-	-	-
b3067	*rpoD*	D193N	-	-	x	-	-	-
b3093	*exuT*	Q431*	-	-	-	-	x	-

Gene	Gene name	Mutein	Parental strain	Mutant 1	Mutant 2	Mutant 3	Mutant 4	Mutant 5
b3095	*yqjA*	A143V	-	-	-	-	x	-
b3102	*yqjG*	R275C	-	-	-	-	x	-
b3104	*yhaI*	P49L	-	-	-	-	x	-
b3110	*yhaO*	G183D	-	-	-	-	x	-
b3114	*tdcE*	R67H	-	-	-	-	x	-
b3124	*garK*	S343N	-	-	-	-	x	-
b3124	*garK*	A51V	-	-	-	-	x	-
b3128	*garD*	E71K	-	-	-	-	x	-
b3142	*yraH*	G11S	-	-	-	-	x	-
b3142	*yraH*	G18D	-	-	-	-	x	-
b3151	*yraQ*	A9T	-	-	-	-	x	-
b3158	*yhbU*	L13F	-	-	-	-	x	-
b3160	*yhbW*	A220V	-	-	-	-	x	-
b3161	*mtr**	D317N	-	-	-	-	x	-
b3162	*deaD*	G459D	-	-	-	-	x	-
b3162	*deaD*	V208M	-	-	-	-	x	-
b3163	*nlpI*	E290K	-	-	-	-	x	-
b3163	*nlpI*	A155T	-	-	-	-	x	-
b3164	*pnp*	E646K	-	-	-	-	x	-
b3165	*rpsO*	D74N	-	-	-	-	x	-
b3168	*infB*	T344I	-	-	-	-	x	-
b3178	*ftsH*	V86I	-	-	-	-	x	-
b3182	*dacB*	W153*	-	-	-	-	x	-
b3194	*mlaE*	T227M	-	-	-	-	x	-
b3225	*nanA*	P182L	-	-	x	-	-	-
b3482	*rhsB*	R772K	-	-	-	-	x	-
b3591	*selA*	A373T	-	-	-	-	x	-
b3638	*yicR*	G82E	-	-	-	-	x	-
b3671	*ilvB*	D126N	-	-	-x	-	-	-
b3725	*pstB*	L177F	-	-	-	-	-	x
b3744	*asnA*	E244K	-	-	-	-	-	x
b3745	*viaA*	S397N	-	-	-	x	-	-
b3971	*rrfB*	P24S	-	-	-	-	x	-
b4239	*treC*	A344T	-	-	-	-	x	-
b4241	*treR*	R117C	-	-	-	-	x	-
b4279	*yjhB*	R63K	-	-	-	-	x	-
b4295	*yjhU*	M156I	-	-	-	-	x	-
b4296	*yjhF*	W427*	-	-	-	-	x	-
b4301	*sgcE*	G171R	-	-	-	-	x	-
b4305	*sgcX*	D193N	-	-	-	-	x	-
b4305	*sgcX*	G90D	-	-	-	-	x	-
b4308	*yjhR*	T373I	-	-	-	-	x	-

Gene	Gene name	Mutein	Parental strain	Mutant 1	Mutant 2	Mutant 3	Mutant 4	Mutant 5
b4312	*fimB*	T177I	-	-	-	-	x	-
b4319	*fimG*	S55F	-	-	-	-	x	-
b4320	*fimH*	S93F	-	-	-	-	x	-
b4324	*uxuR*	P26S	-	-	-	-	x	-
b4325	*yjiC*	A248T	-	-	-	-	x	-
b4326	*iraD*	P78S	-	-	-	-	x	-
b4332	*yjiJ*	A160T	-	-	-	-	x	-
b4356	*lgoT*	A287V	-	x	-	-	-	-
b4379	*yjjW*	P239S	-	x	-	-	-	-
b4392	*slt*	V51M	-	x	-	-	-	-
b4393	*trpR**	G85E	-	x	-	-	-	-
b4423	*ldrC*	S29G	-	-	-	-	x	-
b4462	*ygaQ*	T598I	-	x	-	-	-	-
b4463	*ygcU*	L432F	-	-	-	-	x	-
b4466	*sslE*	G1484S	-	-	-	-	x	-
b4466	*sslE*	D619N	-	-	-	-	x	-
b4466	*sslE*	R146C	-	-	-	-	x	-
b4467	*glcF*	V156M	-	-	-	-	x	-
b4467	*glcF*	D96N	-	-	-	-	x	-
b4492	*ydbA*	E52K	-	-	x	-	-	-
b4492	*ydbA*	S641N	-	-	x	-	-	-
b4498	*gatR*	L576F	-	-	-	-	-	x
b4498	*gatR*	P83L	-	-	-	-	-	x
b4537	*yecJ*	T77I	-	-	-	-	-	x
b4565	*sgcB*	C47Y	-	-	-	-	x	-
b4582	*yoeA*	G302S	-	-	-	-	-	x
b4639	*yeeH*	S20N	-	-	x	-	-	-
b4661	*yfcU*	D603N	-	x	-	-	-	-
b4696	*yneO*	A1023T	-	-	x	-	-	-

Table S4.2.1.2: Summary of identified amino acid exchanges or stop codons (stop) in isolated clones by the *mtr* biosensor-based FACS HT screening of an *E. coli* K-12 MG1655 library mutagenized by MNNG.

Amino acid	Exchanged to...	Amount	Amino acid	Exchanged to...	Amount
Alanine	Threonine	27	**Glutamine**	Stop	3
Alanine	Valine	32	**Arginine**	Cysteine	9
Cysteine	Tyrosine	2	**Arginine**	Tryptophan	2
Aspartate	Asparagine	25	**Arginine**	Histidine	7

Amino acid	Exchanged to...	Amount	Amino acid	Exchanged to...	Amount
Aspartate	Glycine	1	**Arginine**	Glutamine	1
Glutamate	Lysine	18	**Arginine**	Lysine	2
Glycine	Aspartate	32	**Serine**	Leucine	2
Glycine	Glutamate	13	**Serine**	Phenylalanine	6
Glycine	Serine	9	**Serine**	Asparagine	7
Glycine	Arginine	5	**Serine**	Glycine	1
Histidine	Tyrosine	1	**Threonine**	Methionine	2
Histidine	Arginine	1	**Threonine**	Isoleucine	19
Leucine	Phenylalanine	7	**Threonine**	Serine	1
Methionine	Isoleucine	2	**Valine**	Methionine	9
Proline	Leucine	10	**Valine**	Isoleucine	13
Proline	Serine	27	**Tryptophan**	Stop	10

Supporting Figures

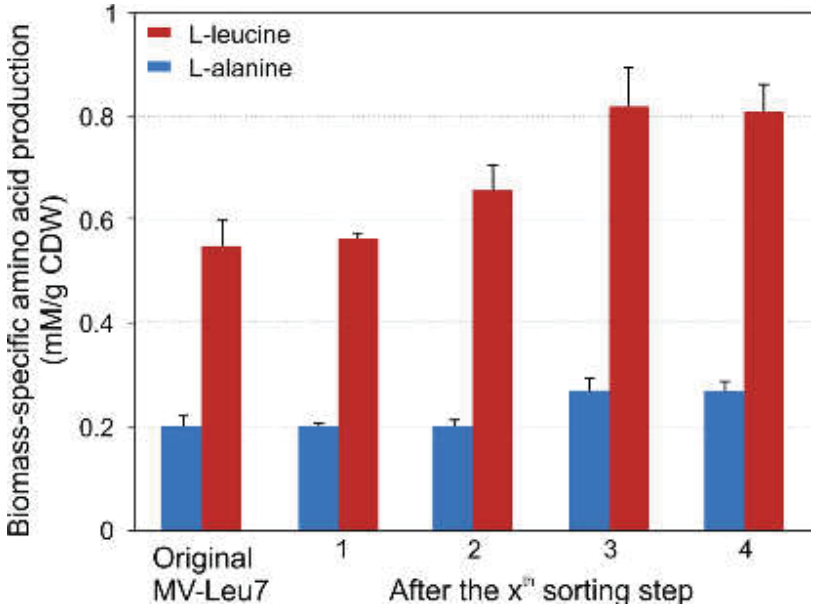

Fig. S4.2.2.1 The development of the biomass-specific L-leucine and L-alanine production during biosensor-driven adaptive laboratory evolution of the growth-coupled L-leucine production strain *C. glutamicum* MV-Leu7. The MV-Leu7 strain containing the plasmid-encoded Lrp biosensor was cultivated in CGXII minimal medium until reaching an OD_{600} of 4. Subsequently, the cells with the top 10% fluorescent output were isolated by FACS and re-

cultivated. The procedure of iterative sorting and re-cultivation was modified from Mahr et al. (2015).

References

Mahr, R., Gätgens, C., Gätgens, J., Polen, T., Kalinowski, J., Frunzke, J., 2015. Biosensor-driven adaptive laboratory evolution of L-valine production in *Corynebacterium glutamicum*. Metab Eng. 32, 184-94.

6.6 Transcriptional regulators in the service of biotechnology

“Transcriptionsregulatoren im Dienste der Biotechnologie”

Regina Mahr, Julia Frunzke*

IBG-1: Biotechnology, Forschungszentrum Jülich, Jülich, Germany

*Corresponding author

Name of Journal: BIOspektrum

Impact Factor: 0.00

Author contributions

Own contribution to the work: 80%

	Name	Contribution
Draft of the manuscript	***Mahr, R.***	50%
	Frunzke, J.	50%
Writing		
"Mikroorganismen als Zellfabriken"	***Mahr, R.***	80%
	Frunzke, J.	20%
"Die natürliche Sensorik der Zelle nutzen"	***Mahr, R.***	80%
	Frunzke, J.	20%
"Biosensor-basiertes Hochdurchsatz-Screening"	***Mahr, R.***	80%
	Frunzke, J.	20%
"Phänotypische Heterogenität in industriellen Mikroorganismen"	***Mahr, R.***	80%
	Frunzke, J.	20%
"Eine erleuchtete Zukunft"	***Mahr, R.***	80%
	Frunzke, J.	20%
Figures		
Figure 1	***Mahr, R.***	90%
	Frunzke, J.	10%
Figure 2	***Mahr, R.***	90%
	Frunzke, J.	10%
Figure 3	***Mahr, R.***	90%
	Frunzke, J.	10%

Biosensoren

Transkriptionsregulatoren im Dienste der Biotechnologie

REGINA MAHR, JULIA FRUNZKE
INSTITUT FÜR BIO- UND GEOWISSENSCHAFTEN, IBG-1: BIOTECHNOLOGIE, FORSCHUNGSZENTRUM JÜLICH

Microbes have evolved a variety of sensor devices for the intracellular detection of small molecules. This capability was recently harnessed for the construction of transcription factor-based biosensors translating the intracellular amino acid accumulation in *Corynebacterium glutamicum* into a fluorescent readout. These systems were successfully implemented in FACS high throughput screening approaches and allow the study of microbial populations at the single cell level.

DOI: 10.1007/s12268-013-0385-y

■ Mikroorganismen besitzen eine enorme Vielfalt an metabolischen Syntheseleistungen und verfügen somit über das Potenzial, ein breites Spektrum biotechnologisch interessanter Moleküle aus einfachen, regenerativen Substraten herzustellen. Die mikrobielle Produktion von Aminosäuren, organischen Säuren, Polymer-Vorstufen oder Bioethanol stellt daher eine attraktive Alternative zur energieintensiven chemischen Synthese, basierend auf Rohöl, dar. Neben *Escherichia coli* ist heute *Corynebacterium glutamicum* mit einer jährlichen Produktion von 2,6 Millionen Tonnen L-Glutamat und 1,5 Millionen Tonnen L-Lysin einer der bedeutendsten Mikroorganismen in der industriellen Biotechnologie [1].

Bei der Entwicklung und Verbesserung von Produktionsstämmen spielt neben rationalen Ansätzen (*Metabolic Engineering*) die klassische Zufallsmutagenese eine zentrale Rolle. Dabei entstehen auf einfachem Wege Stammbibliotheken großer Diversität. Jedoch ist die individuelle Analyse von Wachstum und Produktion ausgewählter Mutanten zeit- und kostenintensiv. Der Großteil industriell relevanter Metabolite ist durch einfache optische Methoden nicht detektierbar; aufwendige chromatografische Analysen verhindern häufig die Hochdurchsatz-Analyse von Produktionsstämmen. In diesem Zusammenhang sind genetische Schaltkreise von Nutzen, die aus einem Sensor (Protein oder RNA) und einem Reportergen bestehen, dessen Expression durch den Sensor reguliert wird, und welche die intrazelluläre Produktbildung an ein optisches Signal (z. B. Fluoreszenz) koppeln. Dieser Ansatz ermöglicht die Etablierung von effizienten Hochdurchsatz-Verfahren und realisiert zudem die Analyse auf Einzelzellebene (**Abb. 1**).

Die natürliche Sensorik der Zelle nutzen

Um physiologische Prozesse optimal an wechselhafte Umweltbedingungen anzupassen, verfügen Mikroorganismen über ein breites Spektrum an regulatorischen Proteinen oder kleinen RNAs. In Prokaryoten spielt die Kontrolle der Transkription durch Transkriptionsregulatoren eine zentrale Rolle. Die Kontrolle der Genexpression in Abhängigkeit von der Bildung metabolischer Intermediate oder Endprodukte ist ein universales Prinzip, und

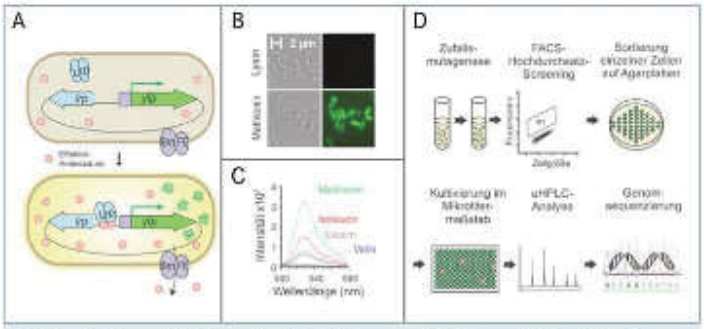

▲ **Abb. 1:** Design und Funktionsweise des Lrp-Biosensors. **A.** Der Sensor basiert auf dem Transkriptionsregulator Lrp aus *Corynebacterium glutamicum* und dem Zielpromotor *brnFE*, der die Expression des *eyfp*-Gens kontrolliert. Bringt man diesen Sensor in *C. glutamicum* ein, so zeigen Wildtyp-Sensorzellen (oben) nur Hintergrundfluoreszenz. Zellen mit erhöhtem intrazellulärem Level der Effektoraminosäuren (unten) fluoreszieren grün. **B.** Nach Zugabe von drei Millimol Methionin fluoreszieren *C. glutamicum*-Sensorzellen. **C.** Die Fluoreszenzspektrometrie induzierter *C. glutamicum*-Sensorzellen zeigt, dass der Sensor die spezifische Detektion von Methionin und verzweigtkettigen Aminosäuren ermöglicht. **D.** Transkriptionsregulator-basierte Sensoren ermöglichen die spezifische Sortierung einzelner Zellen mit erhöhtem Aminosäurelevel (Sensorsignal) mittels FACS (Fluoreszenz-aktivierte Zellsortierung). Aus Mutanten- oder Enzymbibliotheken werden einzelne Zellen mit erhöhtem eYFP-Signal auf Agarplatten sortiert. Mittels uHPLC (*ultra high-performance liquid chromatography*) wird die Aminosäureexkretion der Mutanten im Kulturüberstand überprüft. Die Genomsequenzierung ausgewählter Produktionsstämme dient der Identifizierung neuer Targets für die biotechnologische Stammentwicklung. Adaptiert nach [2].

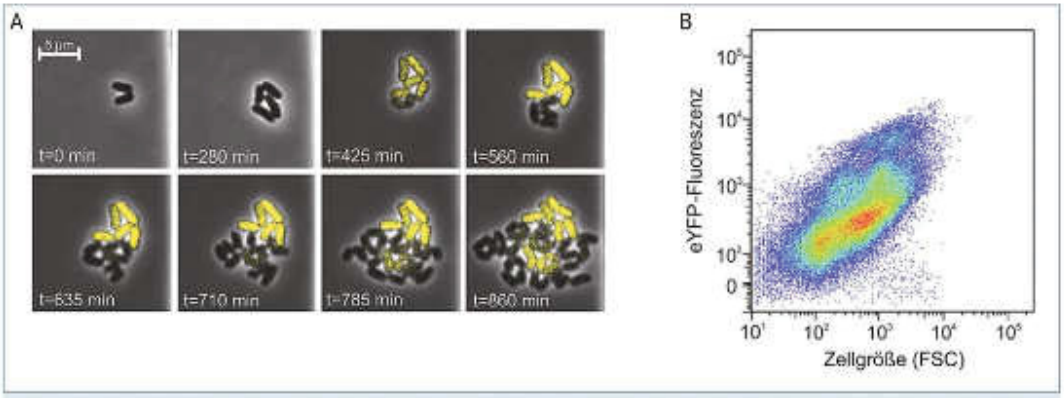

▲ **Abb. 2:** Biosensor-basierte Analyse der Populationsheterogenität. Biosensoren ermöglichen die Analyse mikrobieller Produktionsstämme auf Einzelzellniveau. In diesem Beispiel wurde der Lrp-Sensor genomisch in den *Corynebacterium glutamicum* L-Valin-Produzenten Δ*aceE* integriert. **A**, *Live cell imaging*-Analysen zeigen unter bestimmten Bedingungen eine signifikante Heterogenität des Stammes: L-Valin-produzierende Zellen weisen ein Sensorsignal auf (gelb), andere zeigen uneingeschränktes Wachstum und keine erhöhten L-Valin-Level. **B**, Auch für die L-Valin-Produktion im Bioreaktor zeigt die durchflusszytometrische Analyse des L-Valin-Produzenten Δ*aceE* eine signifikante phänotypische Heterogenität. Der Sensor hilft, das Auftreten von unproduktiven Subpopulationen im Prozess zu visualisieren. FSC: *forward scatter* (indikativ für die Zellgröße).

in der Literatur ist bereits eine Vielzahl derartiger Regulatoren beschrieben. Setzt man die Produktion eines Autofluoreszenzproteins unter Kontrolle eines solchen Sensors, ermöglicht dies die spezifische, intrazelluläre Detektion bestimmter Metabolite.

Nach diesem Prinzip wurde kürzlich ein Biosensor zur intrazellulären Visualisierung von L-Methionin und den verzweigtkettigen Aminosäuren L-Leucin, L-Isoleucin und L-Valin für *C. glutamicum* entwickelt [2]. Dieser Sensor basiert auf dem Transkriptionsregulator Lrp (*leucine-responsive protein*), der in Abhängigkeit von der Effektormolekülkonzentration die Expression des *brnFE*-Operons aktiviert, das für ein Aminosäure-Exportsystem codiert [3]. Durch eine transkriptionelle Fusion des *brnFE*-Promotors an das *eyfp*-Gen (*enhanced yellow fluorescent protein*) wird die intrazelluläre Konzentration von L-Methionin und verzweigtkettigen Aminosäuren in ein optisches Signal umgewandelt (**Abb. 2**). Nach einem ähnlichem Prinzip wurde auch der pSenLys-Biosensor für *C. glutamicum* konstruiert, der die intrazelluläre Akkumulation von L-Lysin, L-Histidin und L-Arginin detektiert [4]. Dieser Sensor basiert auf dem Transkriptionsregulator LysG, ein Aktivator des Aminosäure-Exporters LysE in *C. glutamicum* [5]. Beide Sensoren ermöglichen die spezifische Detektion der Effektoraminosäuren in einzelnen Zellen und zeigen einen linearen Detektionsbereich im niedrigen bis mittleren millimolaren Bereich – eine optimale Voraussetzung für die Analyse und Entwicklung mikrobieller Produktionsstämme.

Biosensor-basiertes Hochdurchsatz-Screening

Moderne durchflusszytometrische Verfahren ermöglichen die Analyse einzelner mikrobieller Zellen hinsichtlich phänotypischer Parameter wie Größe, Granularität und Fluoreszenz. Mittels Fluoreszenz-aktivierter Zellsortierung (FACS) können einzelne Zellen mit gewünschten Eigenschaften ausgewählt und auf Agar- oder in Mikrotiterplatten isoliert werden. Ein hoher Durchsatz von 10^4 Klonen pro Sekunde bietet hierbei ideale Bedingungen für die Analyse großer Mutantenbibliotheken.

Die Kombination von genetisch codierten Biosensoren und FACS ebnet den Weg für die Etablierung von Hochdurchsatz Screenings zur Isolation von mikrobiellen Metabolitproduzenten (**Abb. 1D**). Aus Stammbibliotheken können mittels FACS einzelne Zellen, die ein erhöhtes Sensorsignal zeigen, aussortiert werden. In einem Sekundär Screening identifiziert die chromatografische Analyse des Kulturüberstandes Stämme, die das gewünschte Produkt effizient sekretieren, und reduziert gleichzeitig die Selektion von Mutanten mit evolviertem Fluoreszenzreporter oder defekten Exportsystemen. Durch Genomsequenzierung können schließlich wertvolle Erkenntnisse über neue, bisher unbekannte Targets für die Entwicklung von Produktionsstämmen gewonnen werden.

Sowohl der Biosensor pSenLys als auch der Lrp-Sensor wurden erfolgreich im FACS-Hochdurchsatz-Screening eingesetzt [2, 4]. Das Screening von chemisch mutagenisierten *C. glutamicum*-Wildtypzellen mit pSenLys führte neben bereits bekannten Targets zur Isolierung der noch unbekannten Mutation G81E im *murE*-Gen, das für die UDP-N-Acetylmuramyl-Tripeptid-Synthetase codiert. Diese Mutation steigert die Produktion in einem bereits etablierten Lysinproduzenten (DM1933) um 27 Prozent. Die genannten Ergebnisse verdeutlichen das Potenzial dieser neuen Hochdurchsatz-Methode für die Isolierung von Stämmen mit verbesserter Produktion und die Identifizierung neuer Targets für die Stammentwicklung.

Phänotypische Heterogenität in industriellen Mikroorganismen

Seit Jahrzehnten beobachten Mikrobiologen, dass selbst klonale Populationen, also Zellen des gleichen Genotyps, häufig eine bemerkenswerte Variabilität hinsichtlich phänotypischer Parameter wie Zellgröße, Wachstum und/oder Metabolitproduktion aufweisen. Im Bioprozess kann sich das Auftreten von ineffizient produzierenden Subpopulationen signifikant auf Ertrag und Stabilität des Prozesses auswirken. Die Anwendung von genetisch codierten Biosensoren bietet neue Einblicke in Populationen mikrobieller Produk-

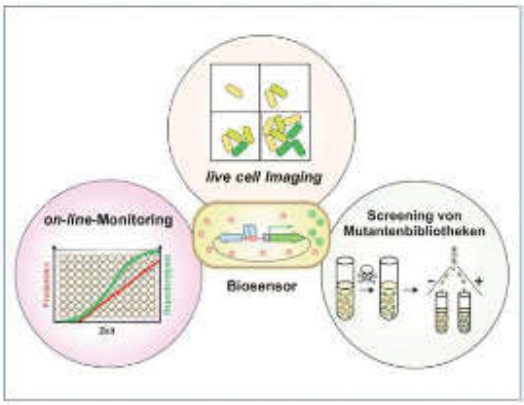

◀ **Abb. 3:** Anwendungsmöglichkeiten von Biosensoren. Biosensoren unterstützen die Evaluierung und Überwachung von biotechnologischen Produktionsprozessen im *on-line*-Monitoring-Verfahren auf Populationsebene oder mittels *live cell imaging* auf Einzelzellniveau. Zudem ermöglichen Biosensoren die Etablierung von FACS-Hochdurchsatz-Screenings.

tionsstämme auf Einzelzellebene; dies ermöglicht eine frühzeitige Erkennung produktionslimitierender Faktoren und die Optimierung von Kultivierungsbedingungen.

In neuartigen mikrofluidischen Chipsystemen kann mittels *live cell imaging* das Wachstum und die Fluoreszenzeigenschaften einzelner Zellen in Echtzeit verfolgt werden. Die Kultivierung in mikrofluidischen Bioreaktoren bietet zudem den großen Vorteil, dass Nährstoff- und Sauerstoffversorgung aufgrund eines kontinuierlichen Zuflusses von frischem Medium optimal eingestellt werden können [6, 7]. Die Untersuchung des L-Valin-produzierenden Stamms *C. glutamicum* Δ*aceE*, in dessen Genom der Lrp-Sensor integriert wurde, zeigte nicht nur Unterschiede zwischen den Zellen bezüglich der Verdopplungsrate und Zellgröße, sondern auch im Fluoreszenzverhalten, was letztlich auf eine heterogene L-Valin-Produktion hindeutet (**Abb. 2**, [8]).

Zusätzlich erlaubt der Einsatz von Fluoreszenzfarbstoffen (wie z. B. DAPI, PI, Syto 9) die Untersuchung weiterer Parameter in einzelnen Zellen, etwa die Messung des DNA-Gehalts, des Membranpotenzials oder der Membranintegrität (Viabilität). DAPI-Färbung von *C. glutamicum*-Populationen offenbarte charakteristische Muster der Chromosomen-Äquivalente einzelner Zellen, abhängig von der Wachstumsphase und den Kultivierungsbedingungen [9].

Eine erleuchtete Zukunft

Die Natur selbst stellt eine Vielzahl geeigneter Sensoren in Form von Proteinen oder RNA-Aptameren für die Detektion weiterer biotechnologisch relevanter Metabolite bereit. Die Synthetische Biologie sowie das *Protein Engineering* ermöglichen darüber hinaus das Design neuartiger Schaltkreise für die spezifische Visualisierung natürlicher oder auch nicht-natürlicher Moleküle (z. B. Polymer-Vorstufen oder Feinchemikalien). Der Einsatz von Biosensoren öffnet neue Wege zur Analyse und Entwicklung von biotechnologischen Produktionsstämmen. Anwendungsgebiete erstrecken sich über effiziente Verfahren zum *on-line*-Monitoring von Bioprozessen und dem *live cell imaging* der Metabolitproduktion auf Einzelzellebene bis hin zur Etablierung von Hochdurchsatz-Screenings von Stamm- oder Enzymbibliotheken (**Abb. 3**). In den folgenden Jahren gilt es nun, die Anwendungsbreite, das Potenzial, aber auch die Grenzen derartiger Systeme für die biotechnologische Stammentwicklung und Einzelzellanalyse eingehend zu bewerten.

Danksagung

Wir bedanken uns bei allen Mitgliedern der AG Frunzke und Kohlheyer, insbesondere bei Nurije Mustafi und Alexander Grünberger. Der Helmholtz-Gemeinschaft und dem Bundesministerium für Forschung und Bildung (BMBF) danken wir für die finanzielle Unterstützung. ■

Literatur

[1] Eggeling L, Bott M (2005) Handbook of *Corynebacterium glutamicum*. CRC Press, Boca Raton, FL, USA
[2] Mustafi N, Grünberger A, Kohlheyer D et al. (2012) The development and application of a single-cell biosensor for the detection of L-methionine and branched-chain amino acids. Metab Eng 14:449–457
[3] Lange C, Mustafi N, Frunzke J et al. (2012) Lrp of *Corynebacterium glutamicum* controls expression of the *brnFE* operon encoding the export system for L-methionine and branched-chain amino acids. J Biotechnol 158:231–241
[4] Binder S, Schendzielorz G, Stäbler N et al. (2012) A high-throughput approach to identify genomic variants of bacterial metabolite producers at the single-cell level. Genome Biology 13:R40
[5] Bellmann A, Vrljic M, Patek M et al. (2001) Expression control and specificity of the basic amino acid exporter LysE of *Corynebacterium glutamicum*. Microbiology 147:1765–1774
[6] Grünberger A, Paczia N, Probst C et al. (2012) A disposable picoliter bioreactor for cultivation and investigation of industrially relevant bacteria on the single cell level. Lab Chip 12:2060–2068
[7] Grünberger A, Probst C, Heyer A et al. (2013) Microfluidic picoliter bioreactor for microbial single-cell analysis: fabrication, system setup and operation. J Vis Exp, doi: 10.3791/50600
[8] Mustafi N, Grünberger A, Mahr R et al. (2014) Application of a genetically encoded biosensor for live cell imaging of L-valine production in pyruvate dehydrogenase complex-deficient *Corynebacterium glutamicum* strains. Plos One (in Revision)
[9] Neumeyer A, Lüttschwager C, Müller S et al. (2013) Monitoring of population dynamics of *Corynebacterium glutamicum* by multiparameter flow cytometry. Microb Biotechnol 6:157–167

Korrespondenzadresse:
Juniorprof. Dr. Julia Frunzke
Institut für Bio- und Geowissenschaften
IBG1: Biotechnologie
Forschungszentrum Jülich
D-52425 Jülich
Tel.: 02461-61-5430
Fax: 02461-61-2710
j.frunzke@fz-juelich.de

AUTORINNEN

Regina Mahr
Jahrgang 1988. 2007–2012 Biologiestudium an der Universität Würzburg und der University of Leeds, UK. Masterarbeit am Institut für Molekulare Infektionsbiologie, Würzburg. Seit 2012 Doktorarbeit am Forschungszentrum Jülich, Institut für Bio- und Geowissenschaften.

Julia Frunzke
Jahrgang 1980. 1999–2004 Biologiestudium an der Universität Marburg. 2004–2007 Doktorarbeit am Forschungszentrum Jülich, Institut für Biotechnologie. 2008–2009 Postdoc an der ETH Zürich, Schweiz. Seit 2009 Gruppenleiterin am Institut für Bio- und Geowissenschaften am Forschungszentrum Jülich; dort seit 2011 Leiterin einer Helmholtz-Nachwuchsgruppe und seit 2013 Juniorprofessorin an der Universität Düsseldorf.

Danksagung

Ein ganz besonderer Dank gilt meiner Betreuerin Juniorprof. Dr. Julia Frunzke, die mir die Möglichkeit gab an meinem favorisierten Thema zu arbeiten. Ich danke Ihr für die vielen inspirierenden Diskussionen, das entgegengebrachte Interesse, und Ihre Unterstützung und Motivation in herausfordernden Zeiten. Bemerkenswert sind Ihre stete Verfügbarkeit und ein offenes Ohr in jeder Lebenssituation. Ich danke Ihr für die Möglichkeit an renommierten, internationalen Tagungen teilnehmen und die Organisation von unvergesslichen Retreats.

Bei Herrn Prof. Dr. Johannes Hegemann möchte ich mich ganz herzlich für die Übernahme der Aufgaben als Zweitgutachter und Mentor bedanken. Über die vielen Tipps und Anregungen bin ich sehr dankbar!

Prof. Dr. Michael Bott und allen Gruppenleitern danke ich für die kritische Auseinandersetzung mit meiner Arbeit. Die Anregungen haben mich stets inspiriert.

Dem IBG-1 danke ich für die tolle Arbeitsatmosphäre und die Hilfsbereitschaft in den letzten Jahren.

Allen Mitgliedern des OptoSys Projekt danke ich für den regen Austausch und die gute Zusammenarbeit.

Ein großes Dankeschön geht an alle ehemaligen und jetzigen AG-Mitglieder (Toni, Nurije, Arun, Eva, Andrea, Meike, Dominik, Eugen, Raphael, Marc, Max, Isabel, Johanna, Sabrina, Simon und Conni) für die sehr gute Atmosphäre, die tolle Gruppendynamik und die Hilfsbereitschaft.

Besonderer Dank geht an meine beiden fleißigen Masterstudenten Raphael und Johanna. Ich danke Ihnen für das Interesse an der Thematik, die Diskussionen und die tolle Arbeitsatmosphäre. Vielen Dank für Eure ausdauernde Unterstützung!

Für die technische Unterstützung im Labor bedanke ich mich herzlich bei Conni, Dominik und Simon. Michael Vogt danke ich für den Tausch von technischer Expertise bezüglich HPLC oder Fermenter, und so manche Überstunde.

Der Sensoren-Front bestehend aus Stephan, Georg, Nurije, Michael, Lothar und Jan danke ich für den offenen Austausch und die vielen Inspirationen. Sense up! Bei Alex bedanke ich mich für die regen wissenschaftlichen Diskussionen bei einem Kaffee oder einem Spaziergang ums FZ.

Ein großer Dank geht an meine fleißigen Korrekturleser Eva, Alex, Elisabeth und Raphael für die kritische Durchsicht dieser Arbeit.

Ein besonderer Dank geht an meine Eltern und meine Familie, die immer an mich geglaubt und mich durch das Studium und die Doktorarbeit stets unterstützt haben. Auch wenn die Entfernung noch so groß ist, weiß ich dennoch wo „Dahaam“ ist.

Meinem Tom danke ich herzlichst für den liebevollen Rückhalt zu Hause, die ausdauernde Unterstützung und die kulinarischen Hochgenüsse während der letzten Jahre. Vielen lieben Dank!

Erklärung

Ich versichere an Eides Statt, dass die Dissertation von mir selbständig und ohne unzulässige fremde Hilfe unter Beachtung der „Grundsätze zur Sicherung guter wissenschaftlicher Praxis an der Heinrich-Heine Universität Düsseldorf“ erstellt worden ist. Die Dissertation wurde in der vorgelegten oder in ähnlicher Form noch bei keiner anderen Institution eingereicht. Ich habe bisher keine erfolglosen Promotionsversuche unternommen.

Düsseldorf, den 27.01.2016